To the Graduate Council:

I am submitting herewith a dissertation written by April D. Pyle entitled "Analysis of Aneuploidy During Mouse Spermatogenesis." I have examined the final electronic copy of this dissertation for form and content and recommend that it be accepted in partial fulfillment of the requirements for the degree of Doctor of Philosophy, with a major in Biochemistry, Cellular and Molecular Biology.

Mary Ann Handel
Major Professor

We have read this dissertation
and recommend its acceptance:

Jeffrey M. Becker

Bruce D. McKee

Eugene M. Rinchik

Liane B. Russell

Accepted for the Council:

Dr. Anne Mayhew
Vice Provost and
Dean of Graduate Studies

(Original signatures are on file in the Graduate Student Services Office.)

ANALYSIS OF ANEUPLOIDY DURING MOUSE SPERMATOGENESIS

A Dissertation

Presented for the

Doctor of Philosophy

Degree

The University of Tennessee, Knoxville

April Dawn Pyle

May 2002

DEDICATION

For Mom, Dad, and Kim

ACKNOWLEDGEMENTS

My time at the University of Tennessee has been both a rewarding and challenging experience. I am forever in debt to my family and wish to thank my parents Walter and Kathy Pyle for their continuous support and for always being there. Thanks for always believing in me! In addition, my sister Kim has always been a true inspiration and I want to thank you for your strength, kindness and encouragement. Thanks also to Jorge, Sebastian and Seth from Tia April. Thank you to the rest of my family for a lifetime of support.

Words cannot express how grateful I am to my advisor Dr. Mary Ann Handel. She is truly an amazing woman, scientist, teacher and friend. Thank you for always listening, challenging me and molding me into a scientist. Thanks to the past and present members of the Handel lab. In particular, thanks to Dr. Shannon Eaker for all your support, laughter and encouragement. I will always think fondly about my time in the Handel lab and sharing the scientific experiences with you. Thanks to John Cobb, for his wisdom, kindness and support. Thanks to Amy Inselman for always listening. Thanks to Tim Wiltshire, Cynthia Park, Debbie Andreadis, Laura Richardson, Trish Smith, Shannon Matulis, Brent Bowker, Stefan Kirov and Laurie Kellam for all their technical experience and intellectual help throughout the years.

Outside of the lab, I would like to thank my committee members Dr. McKee, Dr. Becker, Dr. Rinchik, and Dr. Russell for their wisdom and support. Thanks for being an inspiration as a scientist and teacher. In addition, I would like to thank Dr. Koontz, Dr. Ganguly, Dr. Roberts, Dr. Wicks and Dr. Pinnaduwage for always being instructive and

helpful during my time as a graduate student at UT. Thanks also to other graduate students for their support, including Dr. David Barnes, Dr. Keith Henry and Dr. Jennifer Cobb.

I would also like to thank Bob Clouse for his continuous support, understanding, amazing design and troubleshooting skills, and of course his friendship. Thank you to my best friend, Leigh Ann Boutwell, for your encouragement, always listening, and fun times. Also, thanks to Shelly Moore and Jennifer Castor Tiller for their friendship. Lastly, thanks to everyone in Knoxville for making my experience during school a memorable one.

ABSTRACT

Successful transition through meiosis is required for production of chromosomally-balanced gametes. When chromosome segregation goes awry during meiosis, aneuploidy can occur. Unfortunately, the mechanisms behind this nondisjunction are not well understood. Therefore, this dissertation has focused on learning more about the causative factors associated with aneuploidy during spermatogenesis. Are there factors that are always associated with leading to production of aneuploid sperm? One of the main goals of this dissertation is to find mouse models to study what factors may be involved in chromosome malsegregation; such as pairing, recombination, and transition through the division phases of meiosis.

The first part of the dissertation will be an introduction into what is known about gamete aneuploidy. This section will review what is known about how meiotic error may arise in both humans and the mouse. The introduction will discuss links between factors that are thought to be associated with aneuploidy, and this dissertation will extend this information into new directions in analysis of predisposing factors of gamete aneuploidy.

Part II focuses on a novel mouse model for gamete aneuploidy. PL/J males were found to be an important mouse model for both gamete aneuploidy and abnormal sperm-head morphology. In addition, it was found that PL/J males exhibit both genetic and phenotypic complexity in regard to the traits of aneuploidy and abnormal sperm-head morphology.

Parts III-VII discuss other useful mouse models for study of gamete aneuploidy. Robertsonian heterozygous (Rb/+) translocation mice and *Mlh1* $^{-/-}$ mice were both used to

examine what happens when meiosis goes awry. For example, both Rb/+ and *Mlh1* $^{-/-}$ mice were found to have a checkpoint that most likely detects unaligned or abnormal chromosome configurations. High percentages of MI spermatocytes in these mice were found to be apoptotic. In Part V, *Brca2* $^{-/-}$ mice were rescued with the human *BRCA2* transgene. These mice survive, but are sterile. Analysis was performed to determine the point of arrest in these mice and if they have features of a normal progression through meiosis.

The last two chapters focus on different approaches for the study of aneuploidy. Part VI examines whether the topoisomerase-II inhibitor, etoposide, can induce meiotic nondisjunction. It was shown by sperm FISH that etoposide does induce meiotic nondisjunction, with the highest frequency of nondisjunction occurring at MII. The next part of this section discusses use of a novel screen for detection of new meiotic mutations. A sperm FISH screen was used in this study to detect dominant mutations. This study showed that although screening by sperm FISH is feasible, it is not a practical screen when large numbers of gametes need to be scored.

The last section, Part VIII, is a summary of what we have learned and what directions should be taken to increase our understanding of how meiotic error arises leading to nondisjunction. This section will compare and contrast what we have learned from each mouse model and what factors may contribute to production of aneuploid sperm. The discovery of factors associated with aneuploidy will be essential in learning how to prevent the deleterious effects that occur as a result of malsegregation of chromosomes.

TABLE OF CONTENTS

CHAPTER		PAGE
	PART I: INTRODUCTION	
I	GAMETIC ANEUPLOIDY: AN INTRODUCTION……..	2
	LIST OF REFERENCES……...	23
	PART II: SPERMATOGENESIS IN PL/J MICE: A GENETIC MODEL GAMETIC ANEUPLOIDY	
	ABSTRACT……	33
I	INTRODUCTION……..	34
II	MATERIALS AND METHODS……	41
III	RESULTS……...	46
IV	DISCUSSION…….	94
	LIST OF REFERENCES……	103
	PART III: EVIDENCE FOR MEIOTIC SPINDLE CHECKPOINT FROM ANALYSIS OF SPERMATOCYTES FROM ROBERTSONIAN-CHROMOSOME HETEROZYGOUS MICE	
	ABSTRACT……	112
I	INTRODUCTION…….	114
II	MATERIALS AND METHODS……	121
III	RESULTS…….	127

CHAPTER PAGE

IV DISCUSSION…… 159

LIST OF REFERENCES…… 171

PART IV: MEIOTIC PROPHASE ABNORMALITIES AND METAPHASE CELL DEATH IN MLH1-DEFICIENT SPERMATOCYTES: INSIGHTS INTO REGULATION OF SPERMATOGENIC PROCESS

ABSTRACT……... 180

I INTRODUCTION……..... 182

II MATERIALS AND METHODS……... 185

III RESULTS……..……..…… 189

IV DISCUSSION……... . 206

LIST OF REFERENCES…….. 213

PART V: PARTIAL COMPLEMENTATION OF *Brca2* MUTATION IN MICE BY THE HUMAN *BRCA2* GENE SHOWS A SEXUALLY DIMORPHIC MEIOTIC PHENOTYPE

ABSTRACT…….. 221

I INTRODUCTION……. 223

II MATERIALS AND METHODS……. 225

III RESULTS……. 227

IV DISCUSSION……... 242

CHAPTER PAGE

LIST OF REFERENCES…….. 245

PART VI: ETOPOSIDE: ENVIRONMENTAL INDUCTION OF GAMETIC ANEUPLOIDY

I INTRODUCTION……..249

II MATERIALS AND METHODS……253

III RESULTS……255

IV DISCUSSION……. 263

LIST OF REFERENCES…… 267

PART VII: MUTAGENESIS AND A PHENOTYPE SCREEN FOR GAMETIC ANEUPLOIDY

I INTRODUCTION……..273

II MATERIALS AND METHODS……278

III RESULTS……281

IV DISCUSSION…….291

LIST OF REFERENCES……295

PART VIII: CONCLUSION

I SUMMARY…….302

LIST OF REFERENCES…….315

VITA……319

LIST OF TABLES

TABLE PAGE

PART II: SPERMATOGENESIS IN PL/J MICE: A GENETIC MODEL GAMETIC ANEUPLOIDY

1 Analysis of the frequency of abnormal sperm-head morphology and hyperhaploidy in PL/J, B6 and F1progeny……52

2 Analysis of the frequency of abnormal sperm-head morphology and hyperhaploidy in the F1 X PL/J backcross mice……55

3 Analysis of FISH signal domains in MI spermatocytes from PL/J males……79

PART III: EVIDENCE FOR MEIOTIC SPINDLE CHECKPOINT FROM ANALYSIS OF SPERMATOCYTES FROM ROBERTSONIAN-CHROMOSOME HETEROZYGOUS MICE

1 Sperm FISH analysis of frequencies of aneuploid sperm from B6 and Rb-heterozygous mice……131

2 Frequencies of unpaired chromosomes in MI spermatocytes Rb-heterozygous mice……136

3 Frequencies of apoptosis and chromosome misalignment in metaphase spermatocytes……152

TABLE PAGE

PART VI: ETOPOSIDE: ENVIRONMENTAL INDUCTION OF GAMETIC ANEUPLOIDY

1 Analysis of the frequency of hyperhaploidy by sperm FISH (experiment one) in etoposide-treated and control males…….258

2 Analysis of the frequency of hyperhaploidy by sperm FISH (experiment two) in etoposide-treated and control males…….262

PART VII: MUTAGENESIS AND A PHENOTYPE SCREEN FOR GAMETIC ANEUPLOIDY

1 Analysis of the frequency of hyperhaploidy by sperm FISH in control males (no ENU)…….284

2 Analysis of the frequency of hyperhaploidy by sperm FISH in sons (G1) of ENU treated ales……...288

3 Analysis of the frequency of hyperhaploidy by sperm FISH in sons (G2) of ENU treated males…….……...290

LIST OF FIGURES

FIGURE PAGE

PART I: INTRODUCTION

1 Diagram of meiotic chromosome segregation……3

2 Diagram of sperm FISH with DNA probes specific for chromosomes 8, X, and Y…….….16

PART II: SPERMATOGENESIS IN PL/J MICE: A GENETIC MODEL GAMETIC ANEUPLOIDY

1 Types of abnormal sperm-head morphology in PL/J…..……..48

2 Illustration of three-color sperm FISH in PL/J and B6…….50

3 Scatter plot illustration of the frequency of hyperhaploidy and abnormal sperm-head morphology…….57

4 Immunofluorescence analysis of MLH1 foci in PL/J and B6 spermatocytes……61

5 Statistically lower numbers of MLH1 foci in PL/J spermatocytes compared to B6 spermatocytes……..64

6 Reduction in chiasmata in PL/J MI spermatocytes……66

7 Illustration of asynapsis in PL/J spermatocytes stained with SYCP3……..……69

8 Statistically significant numbers of asynapsis compared to B6 spermatocytes…….……..71

FIGURE PAGE

9 Air-dried chromosome preparations of B6 and PL/J chromosomes after treatment with okadaic acid……74

10 Paint-probe analysis of chromosome pairing in PL/J MI spermatocytes……77

11 Immunofluorescence analysis of spindle defects and unaligned chromosomes in PL/J MI spermatocytes…….81

12 Frequency of unaligned chromosomes and abnormal spindles in B6 and PL/J…….83

13 Immunofluorescence analysis of abnormal pericentrin foci in PL/J compared to B6……..86

14 Apoptosis of spermatids in PL/J testes……..90

15 Frequency of apoptosis in PL/J compared to B6 spermatids……..92

PART III: EVIDENCE FOR MEIOTIC SPINDLE CHECKPOINT FROM ANALYSIS OF SPERMATOCYTES FROM ROBERTSONIAN-CHROMOSOME HETEROZYGOUS MICE

1 Diagrammatic representation of a Rb chromosome meiotic pairing configuration involving chromosomes 2 (green) and 8 (yellow)……118

2 Illustrations of sperm stained by the three-color FISH method ……129

FIGURE PAGE

3 Air-dried meiotic metaphase I (MI) chromosome spreads labeled with chromosome paint probes (2: green, 8: red)……..134

4 Pairing abnormalities in surface-spread spermatocytes from Rb/+ mice……139

5 Confocal imaging of MI chromosomes and spindles from B6 and Rb/+ spermatocytes…….141

6 The frequencies of spermatogenic cell stages from B6 (white bars) and Rb/+ (black bars) adult mice……..144

7 Frequencies of seminiferous tubules at indicated stages and of apoptotic tubules (red bar) in B6 (white bars) and Rb/+ (black bars) adult mice…….147

8 Apoptotic cells in stage-XII tubule sections of B6 (A) and Rb/+ (B) 23-day old mice…….149

9 CENP-E staining in prometaphase and metaphase spermatocytes from B6 and Rb/+ mice……155

10 CENP-F staining in prometaphase and metaphase spermatocytes from B6 and Rb/+ mice……157

FIGURE PAGE

PART IV: MEIOTIC PROPHASE ABNORMALITIES AND METAPHASE CELL DEATH IN MLH1-DEFICIENT SPERMATOCYTES: INSIGHTS INTO REGULATION OF SPERMATOGENIC PROCESS

1 Defective chromosome pairing in *Mlh1* $^{-/-}$ spermatocytes revealed by paint-probe analysis…….191

2 Pachytene spermatocytes from *Mlh1* $^{-/-}$ mice are competent to condense chromosomes in response to OA treatment……194

3 Analysis of the G2/M transition in *Mlh1*$^{-/-}$ spermatocytes with immunofluorescence staining with MPM-2 and the phosphorylated form of histone H3-Ser 10 (A and B); staining with SYCP3 and the phosphorylated form of histone H3-Ser 10 (C and D)……...……196

4 Abnormalities during chromosome alignment and segregation in *Mlh1* $^{-/-}$ spermatocytes seen by microscopy……..199

5 Frequency of tubules with apoptotic cells in *Mlh1* $^{-/-}$ mice increases dramatically at 22 days of age……...……..202

6 Apoptosis of *Mlh1* $^{-/-}$ spermatocytes occurs at MI…….…….204

FIGURE PAGE

PART V: PARTIAL COMPLEMENTATION OF *Brca2* MUTATION IN MICE BY THE HUMAN *BRCA2* GENE SHOWS A SEXUALLY DIMORPHIC MEIOTIC PHENOTYPE

1 Localization pattern of BRCA2 during spermatogenesis…….230

2 Immunofluorescence analysis of stage of arrest in BRCA2 KO/KO, tg+ spermatocytes with SYCP3 and H1t……233

3 Absence of RAD51 foci in BRCA2 KO/KO, tg+ spermatocytes……..…235

4 Overall % of L/Z spermatocytes with reduced numbers of RAD51 foci in BRCA2 KO/KO, tg/+ compared to KO/+, tg/+…….…….237

5 Number of RAD51 foci in BRCA2 KO/KO, tg/+ compared to KO/+, tg/+……..239

6 Gamma-H2AX staining reveals the presence of double-strand breaks in BRCA2 KO/KO, tg/+ mice……..241

PART VII: ETOPOSIDE: ENVIRONMENTAL INDUCTION OF GAMETIC ANEUPLOIDY

1 Representative sperm FISH images from etoposide-

FIGURE PAGE

treated mice……..260

PART VII: MUTAGENESIS AND A PHENOTYPE SCREEN FOR GAMETIC ANEUPLOIDY

1 Representative sperm FISH images from sons of ENU treated males…….….286

PART VIII: CONCLUSION

1 Comparison of abnormalities seen in four mouse models for aneuploidy: Rb/+, *Mlh1* $^{-/-}$, PL/J, and *Brca2* $^{-/-}$……304

PART I

GAMETIC ANEUPLOIDY: AN INTRODUCTION

CHAPTER I

EXAMINATION OF GAMETE ANEUPLOIDY

Successful completion of meiosis is essential for production of euploid gametes. Errors arising in meiosis can result in nondisjunction of chromosomes leading to aneuploidy (sperm or eggs with an extra copy of a chromosome or deficiency of a copy). The consequences of nondisjunction are often lethal and no less than 0.3% of all newborns are trisomic or monosomic (Hassold, 1998). Down syndrome and Kleinfelter syndrome (XXY) are examples of consequences of aneuploid conceptuses. Since the outcome of nondisjunction can be devastating, it is unfortunate that the mechanisms leading to failure of proper chromosome segregation are largely unknown. The experiments in this dissertation will analyze spermatogenesis as a model system to uncover mechanisms and processes associated with gametic aneuploidy.

Spermatogenesis consists of both mitotic and meiotic divisions. The initial stages of spermatogenesis involve proliferation of spermatogonia, which then differentiate into meiotic cells. Meiosis is a unique division that produces haploid gametes from diploid parental cells, when a single round of DNA replication is followed by two rounds of chromosome segregation (Roeder, 1997). The first of two divisions is a reductional division in which homologous chromosomes are separated, and the second is an equational division where separation of sister chromatids occurs (Fig.1). During the first meiotic prophase, an extended sequence of events occurs that is essential for proper segregation of chromosomes. During leptonema, the axial elements of the developing

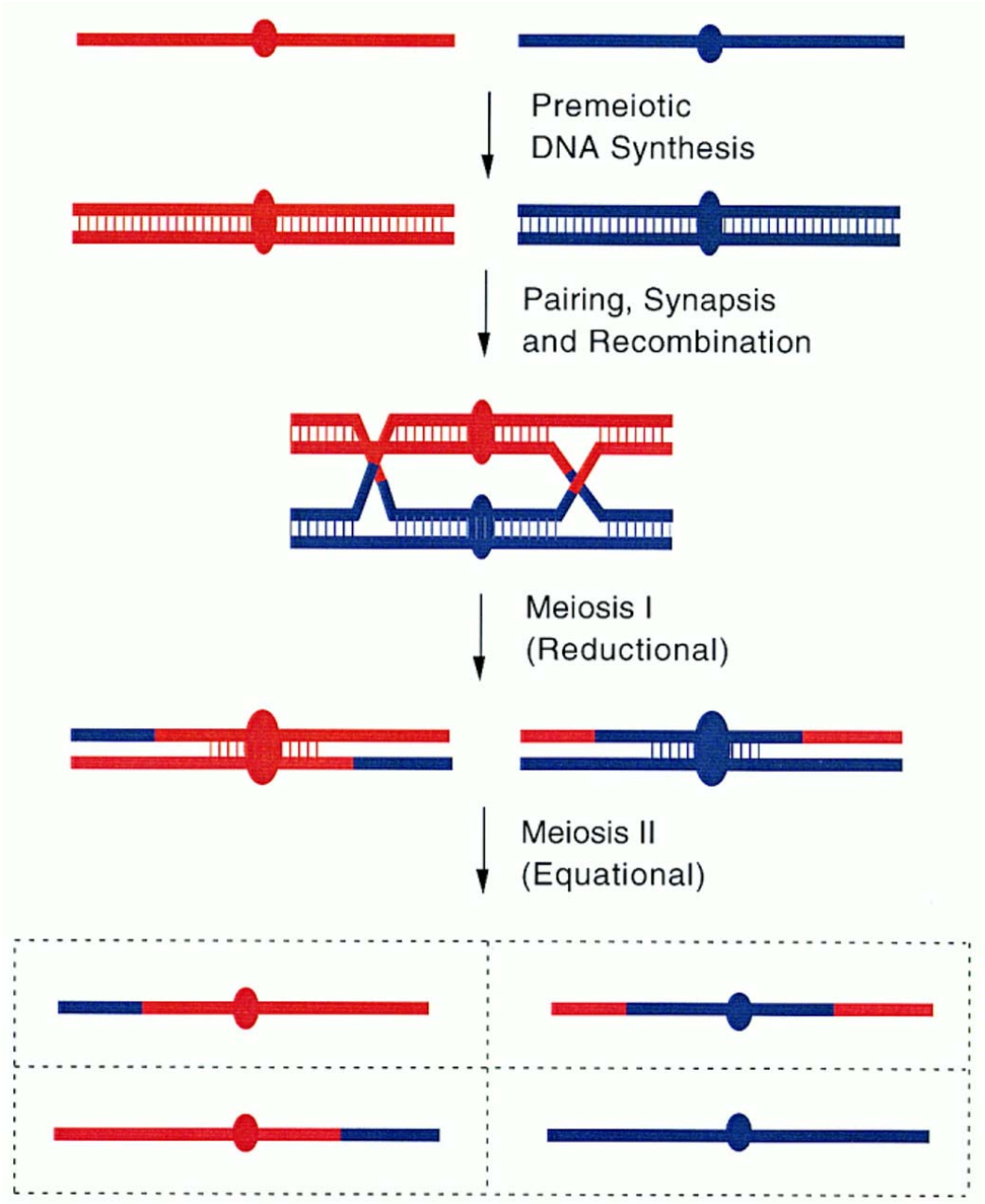


Fig. 1. Diagram of meiotic chromosome segregation, as depicted in (Roeder, 1997). Homologous chromosomes are shown in red or blue. Each solid line represents a sister chromatid, and the hatched lines indicate sister chromatid cohesion.

synaptonemal complex (SC) begin to form, and double strand breaks (DSBs) are thought to occur at this time. The synaptonemal complex is a proteinaceous structure that is thought to mediate association of homologous chromosomes during prophase of meiosis I (Moses et al., 1984). In the next stage of meiosis, zygonema, chromosome synapsis is first initiated, Holliday junctions are formed and DSBs begin to disappear. During pachynema, chromosomes become fully synapsed. In diplonema the synaptonemal complex is disassembled, chromosomes begin to condense, and chiasmata, manifestations of meiotic crossover, are visible (Roeder, 1997). In diakinesis/metaphase there is further chromosome compaction, and alignment of chromosomes onto the metaphase I spindle assists in proper chromosome segregation. The homologous chromosomes are then separated during anaphase I. The second division phase of meiosis, MII, is similar to mitosis in that separation of sister chromatids occurs. Errors arising during either MI or MII divisions can result in nondisjunction leading to aneuploidy.

What is the incidence and origin of aneuploidy?

Aneuploidy occurs in approximately 50% of all spontaneous abortions. Trisomy is the most commonly identified chromosome abnormality in human and occurs in 4% of all clinically recognized pregnancies (Hassold, 1998). The detrimental effect of aneuploidy derives from the changes in gene doses and genetic imbalances, which arise from the change in chromosome number. For the autosomes, this genetic imbalance typically results in early termination of the pregnancy. In humans, monosomic autosomal conceptuses die at an early stage, but XO conceptuses survive. In the case of XO monosomy, it appears that 70-80 % of these have a single maternal X and loss of the

paternal X or Y chromosome; therefore the error is paternal in origin. For autosomal trisomies, there are chromosome-specific variations in the frequency of nondisjunction, but it is known that maternal MI errors predominate among most trisomies (Hassold and Hunt, 2001). For example, DNA polymorphism analysis has showed that most trisomy 21 conceptuses are a result of maternal MI error. In one study, five families with trisomy 21 offspring were examined for parental origin. Four of the five studied were maternal in origin (Stewart et al., 1988).

Compared to human data, the spontaneous occurrence of aneuploidy in mice is lower. It has been concluded that only 2% of early mouse embryos are aneuploid (Bond and Chandley, 1983). However, mating schemes have been developed involving mice with chromosomal rearrangements to generate large numbers of aneuploid conceptuses for studies of the phenotypic effect of monosomy and trisomy. Complete trisomies for all 19 of the autosomes have been generated and studied, and none are compatible with survival for more than a few weeks after birth (reviewed in Gearhart et al., 1986). In fact, the only complete monosomy and trisomies that are compatible with survival to adulthood involve the sex chromosomes and are XO, XXY, and XYY, reviewed in (Russell, 1976). There are considerable data on the origin of aneuploidy, but much less is known about the underlying non-disjunctional mechanisms. The next few sections will review what is known about mechanisms that could lead to nondisjunction of chromosomes.

Altered recombination can lead to gamete aneuploidy

Although the mechanisms are still not well understood, recent studies have focused on altered recombination as a factor contributing to gamete aneuploidy. There is a well-established correlation between recombination and human nondisjunction (Henderson and Edwards, 1968; Stewart et al., 1988). Evidence for a connection between abnormal recombination and nondisjunction has come from using genetic mapping techniques to study the inheritance of DNA polymorphisms in human trisomic conceptuses. Significant decrease in recombination frequency is a feature of most MI-derived trisomies. One of the most pronounced reductions in recombination is observed for paternally derived XXY's in which the genetic map of the XY pairing region is decreased four- to fivefold, from ~50 cM normally to ~10-15 cM in trisomy generating meioses (Hassold et al., 1991). Recombination and chromosome nondisjunction also seem to vary depending on which chromosome is involved in the nondisjunction event. For example, recombination is significantly reduced in chromosomes 15,16,18,21 and X trisomies when MI in origin. Therefore, altered recombination can be associated with abnormal chromosome segregation.

Since an association has been shown between altered recombination and nondisjunction, it is important to understand why abnormal recombination is so detrimental. One of the reasons could be that meiotic exchange or recombination is the primary mechanism by which segregation of homologous chromosomes at meiosis I is ensured. This is because the mechanism of disjunction is mediated by chiasmata (physical manifestations of recombination), which are formed at the sites of exchange. Chiasmata serve to link homologous chromosomes together forming a bivalent. The

bivalent then attaches to the spindle and once proper orientation is achieved, disjunction can occur (Hawley, 1988). In contrast, achiasmate systems of segregation have also been identified in several species. Most of our understanding of recombination has come from studies of lower eukaryotes, such as *Saccharomyces cerevisiae* and *Drosophila*. Meiosis in *Drosophila melanogaster* males is completely achiasmate and does not seem to be particularly error prone. However, there is evidence for repeated sequences used as pairing sites in the XY bivalent and scattered sites in the autosomal chromosomes (McKee, 1998). These pairing sites are an alternative to recombination and may help to ensure proper segregation. Interestingly, a substantial proportion of MI nondisjunction in *Drosophila* females is attributable to homologous chromosome pairs that have failed to undergo meiotic exchange, and similar numbers have been found in maternal MI nondisjunction in humans (Koehler et al., 1996). In both flies and humans, nonexchange bivalents and bivalents with single, distal exchanges are more susceptible to meiotic nondisjunction than those with more proximally localized chiasmata (Koehler and Hassold, 1998).

In addition to studies of lower eukaryotes, identification of mammalian homologs of recombination proteins has helped to increase knowledge of recombination-based disjunction. For example, knockout mice for both PMS2 and MLH1, proteins involved in DNA repair and recombination, have uncovered possible roles for each of these proteins in nondisjunction. PMS2-deficient males are infertile, producing only abnormal spermatozoa. Analysis of the axial element and synaptonemal complex formation during prophase of meiosis I in the *Pms2* knockout indicates abnormalities in chromosome synapsis (Baker et al., 1995). In addition, in the *Mlh1* knockout mouse, the role that this

protein plays during recombination and DNA repair is being elucidated. Mice that are deficient for *Mlh1* exhibit increased levels of prematurely separated chromosomes and arrest in meiosis I. In the *Mlh1* knockout, crossover is virtually eliminated causing the formation of univalents (Baker et al., 1996). There is also strong evidence that localization of the MLH1 protein on mouse pachytene-stage synaptonemal complexes (SCs) identifies sites of crossover (Anderson et al., 1999; Hassold et al., 2000). The frequency and distribution of MLH1 foci corresponds to previous cytogenetic analysis of chiasmata. This allows accurate assessment of the number of crossovers that occur during pachytene of meiosis I. These studies are helping to further our understanding of the role altered recombination may play during nondisjunction.

The synaptonemal complex: pairing and maintenance of homologous chromosomes

In order for proper chiasmata to be formed, homologs must be brought into intimate association with one another. This process is mediated by a structure known as the synaptonemal complex, which consists of two lateral elements, a central element and transverse filaments. The three main protein components of the SC are SYCP1, 2 and 3. SYCP1 localizes to the central region helping to link the lateral elements together. SYCP 2 and 3 form components of the lateral/axial elements and are first detected in leptotene and persist through diplotene (Moens et al., 1998). Recently, *Sycp3* was knocked out in mice, and the phenotype was male sterility with spermatogenic failure in early meiotic prophase (Yuan et al., 2000). In the *Sycp3* knockout, spermatogenesis is disrupted at the zygotene stage of meiosis and at this point, most of the cells undergo apoptosis. In these mice, the axial elements are absent, synapsis does not occur and the chromosomes are

present as univalents. Therefore, SYCP3 is required for normal meiotic progression. Studies are inconclusive as to whether the SC is required for efficient recombination to occur. The meiotic mutant c(3)G (crossover suppressor on 3 of Gowen) abolishes both synaptonemal complex (SC) formation and meiotic recombination, whereas mutations in the mei-W68 and mei-P22 genes prevent recombination but allow normal SC to form. It has been shown that meiotic recombination between homologous chromosomes in Drosophila females requires synapsis and SC formation, and also that the synaptic defect correlates with the exchange defects (Page and Hawley, 2001). There are several organisms with achiasmate meiosis that require a synaptonemal complex to link homologous chromosomes prior to the division phase, however others (e.g., S.*pombe*) do not seem to require an SC for exchange to occur efficiently and to progress to MI. Therefore, it is not clear if SC formation is required for recombination or if abnormalities in the SC can alter recombination.

Requirement for metaphase alignment and checkpoint control in the metaphase to anaphase transition

Even if the synaptonemal complex is formed correctly and recombination ensues, the chromosomes still must align properly at the metaphase plate. Metaphase arrest can result from misbalance of kinetochore forces. The kinetochore is the point at which each chromatid is attached to the spindle. Control of the metaphase to anaphase transition is believed to be a factor of kinetochore tension. It has been shown in praying mantis' spermatocytes that the absence of tension on even a single kinetochore is sufficient to signal a meiotic error and result in cell death (Li and Nicklas, 1997). This is important

because the triggering of a metaphase arrest by unaligned chromosomes may be able to prevent production of aneuploid sperm.

In the presence of unaligned chromosomes, the "spindle checkpoint" is activated which blocks proteolytic events required for the onset of anaphase (Gorbsky et al., 1999). The checkpoint functions by preventing a ubiquitin ligase called the anaphase-promoting complex/cyclosome (APC/C) from ubiquitinylating proteins whose destruction is required for anaphase onset. Several proteins (ex. MADs, BUBs) are believed to be involved, primarily by transient association with the kinetochores of unaligned chromosomes. Since, signaling of the spindle checkpoint originates from the kinetochores that lack proper attachment to the spindle, once all of the kinetochores are attached, the checkpoint is abrogated and the metaphase-anaphase transition can be completed. Therefore, to ensure transition into anaphase, chromosomes must align properly at the metaphase plate. A checkpoint system monitors this and halts progression into anaphase until tension is sufficient to ensure proper disjunction.

Aberrant spindle formation and its role in nondisjunction

As discussed previously, a spindle checkpoint is activated due to misalignment of chromosomes at the metaphase plate. Part of this checkpoint involves attachment of the chromosomes to the meiotic spindle. The spindle, composed of a microtubule-based structure, plays a role in accurate chromosome segregation. Proper segregation of chromosomes is ensured by stable MI connections between the chromosomes and opposite poles of the spindle, also called bipolar orientation. If the spindle is not formed completely, then its role in proper disjunction could be lost, leading to aneuploidy. The

formation of the spindle is essential in providing connections through microtubules to the kinetochores and also act as a site for binding of spindle-associated motor proteins (ex., CENPs). One example, is CENP-C, that has been shown to be necessary for kinetochore assembly and for establishing a stable attachment of chromosomes to the mitotic spindle (Sullivan et al., 1996). If the spindle is not formed properly, this attachment of the kinetochores to the spindle could be lost.

The direct role that abnormal spindles play in nondisjunction is not well understood. There is evidence that abnormal spindles are present in Robertsonian (Rb) translocation mice that have an increased rate of nondisjunction in both oocytes and spermatocytes (Eichenlaub-Ritter and Winking, 1990); (Eaker et al., 2001). The abnormalities in spindle morphology in spermatocytes will be discussed in Parts II and III of this dissertation. In the case of Robertsonian oocytes, the presence of unequal numbers of kinetochores facing opposite spindle poles affected spindle structure and may have been associated with the increased nondisjunction. In Robertsonian oocytes, the spindle was often asymmetrical, with one long and one short spindle half. It has also been shown that chromosomes do in fact influence meiotic spindle assembly. This was demonstrated in oocytes from mice with a targeted disruption in the MLH1 protein. In this mouse model, chromosomes are often seen as univalents and their abnormal orientation during prometaphase may have resulted in formation of non-stable MI spindles. The spindle poles often continued to elongate and abnormalities were seen in organization in the midzone microtubules. This work suggests that the chromosomes are involved in helping to form a stable bipolar spindle (Woods et al., 1999). Abnormal

chromosome configurations could then lead to abnormalities in spindle formation, which could contribute to nondisjunction.

There have also been studies correlating nondisjunction to spindle aberrations after exposure to chemicals such as trichlorfon. In one study, mouse oocytes were exposed to trichlorfon, a common pesticide. Treatment with trichlorfon caused aberrant spindle morphology and abnormal chromosome behavior, especially in meiosis II (Yin et al., 1998). Specifically, if treatment was performed during meiosis I resumption in oocytes, formation of a spindle was disturbed. However, despite spindle abnormalities and failure of bivalents to align properly, oocytes still progressed to metaphase II. At this stage, spindles were highly abnormal. Characteristically, the spindles were bipolar but did not consist of two similarly shaped halves. Many spindles were asymmetric with one small and one broad spindle pole. The density of microtubules in the central part of the spindle also appeared to be reduced. These abnormalities suggest that a stable bipolar spindle is important is assisting in proper segregation of chromosomes. Therefore, studying spindle dynamics may help in understanding the role of the bipolar spindle during meiosis and how abnormalities in spindle structure could lead to gamete aneuploidy.

Centrosomes may play a role in control of the bipolar spindle

The microtubule organizing center (MTOC), or centrosome, is an organelle whose function is important in organization of the spindle poles during mitosis and meiosis. The role of the centrosome is not well characterized in meiosis, but is a little better studied in mitosis. The centrosome duplicates exactly once per cell cycle, but the precise molecular

mechanisms are still unclear. The daughter centrosomes form two poles of the spindle after nuclear envelope breakdown. If the centrosome fails to duplicate before the onset of mitosis, most somatic cells will return to interphase without dividing, causing polyploidy. If the centrosome duplicates more than once in a cell cycle, then a multipolar spindle may be assembled and the chromosomes may be unequally distributed to the daughter cells (Hinchcliffe and Sluder, 2001). This can lead to cellular imbalance and instability. In fact, there have been several reports of abnormal centrosome number in correlation with aneuploidy (Levine et al., 1991) and (Lingle et al., 1998). It is believed that multipolar and monopolar mitoses are a direct consequence of centrosomal defects. For example, multipolar and monopolar mitoses result from extra centrosome duplication or lack of centrosome duplication or separation prior to mitosis. Cells also are believed not to have a checkpoint that aborts mitosis in response to extra spindle poles (Sluder et al., 1997). Therefore proper centrosome number and formation is essential for preventing genetic instability. Since this cellular imbalance can be a causative factor associated with aneuploid cells, it will be essential to characterize further the role of the centrosome in proper chromosome segregation during meiosis.

Methods for detection of aneuploidy

Since the consequences of malsegregation of chromosomes can be detrimental to survival, studies of mechanisms are important, and new methods for detection of aneuploidy continue to be explored. Traditional indicators of nondisjunction include asynaptic axes, hyperhaploid complements, supernumerary sex bodies and fetal death (Russell, 1985). Two approaches have traditionally been used in diagnosing

malsegregation: direct chromosomal examination and genetic detection systems. Direct chromosome examination is often the fastest method and includes evaluation of meiotic prophase, metaphase II counts, pronuclear chromosomes at first cleavage, and analysis of embryos. Some of the indicators of nondisjunction during prophase include synaptonemal complex abnormalities, lowered chiasmata frequency, and occurrence of univalents at diakinesis-metaphase (Polani and Jagiello, 1976). In addition, analysis of MII cells by chromosome counts or C-banding is a direct way of detecting malsegregation that had occurred in MI (Polani, 1972). Alternatively, since paternal and maternal chromosome contributions remain separate in the pronuclei of the zygote and chromosome morphology is easier to count than at MII; the analysis of chromosome constitution in pronuclei has often been used to detect malsegregation events. Analysis of aneuploidy can also be examined in preimplantation and postimplantation stages but is often laborious and availability of large numbers for study is often a limiting factor.

Since autosomal monosomies are often lethal by the time of birth, aneuploidy-detection methods that use genetic markers or screens have been used. These genetic screens for detection of malsegregation often include complementation with tester stocks (such as translocation mice) and trisomy marker or numerical sex-chromosome anomaly (NSA) tests. Complementation is used to achieve chromosomally balanced survivors. The tester stock is chosen to provide a high frequency of nullisomic or disomic gametes. These can be complemented with chromosomally normal mice to produce gametes for study of nondisjunction. A good example is the use of Robertsonian tester stocks mated to produce heterozygous viable mice. NSA tests use markers for the sex-chromosomes

that can be detected in offspring. This allows for detection of supernumerary sex chromosomes as well as sex-chromosome loss (Russell, 1968).

More recently, DNA polymorphisms have been used to study the parent of origin of the nondisjunction event and to examine the stage of the abnormality in trisomic fetuses (Hassold, 1998). In addition, analysis of sperm cells through fluorescence *in situ* hybridization (FISH) with chromosome-specific probes can be used; see Fig. 2 (Williams et al., 1993). This technique has proved advantageous in screening for aneuploidy due to the large number of cells able to be scored and chromosome-specific probes that allow for determination of disomic or diploid sperm and if the sex-chromosome disomy is a result of failure at MI or MII. The primary methods for detection of aneuploidy that will be used in this dissertation are: 1) fluorescence *in situ* hybridization to determine the frequency of aneuploidy for chromosomes 8, X, and Y (for which we have centromeric-specific point probes); also paint probes spanning chromosomes 8 and 2 will be used, 2) air-dried chromosome preparations that allow for visualization of chromosome number, chromosome condensation and chiasmata , and 3) indirect immunofluorescence to localize proteins within the seminiferous tubules or to specific locations within spermatogenic cells.

Gamete aneuploidy in mammals: contrasts between males and females

Trisomy in humans appears to be predominantly associated with maternal age, however paternal errors can also account for nondisjunction events. Therefore, knowledge can be gained from studying nondisjunction in spermatogenesis and

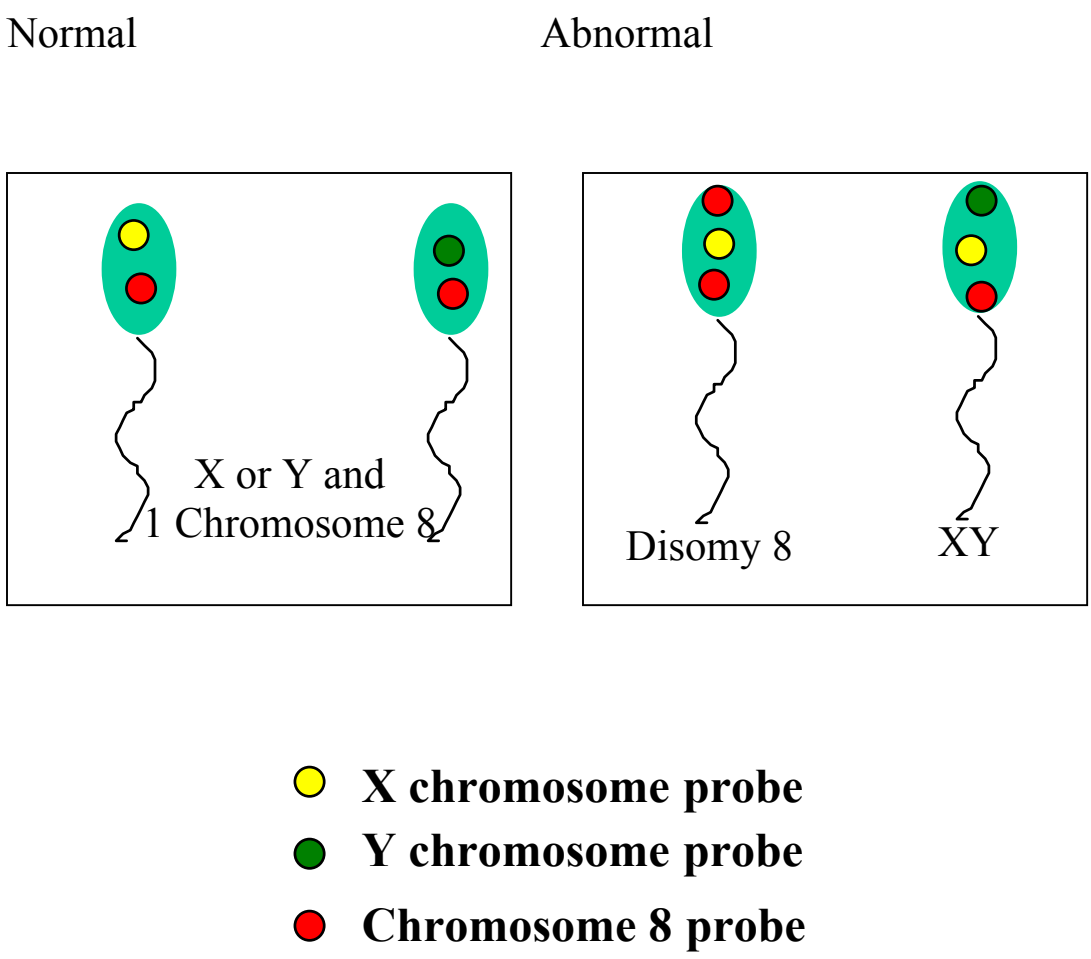


Figure 2. This diagram shows how FISH can be used to detect aneuploidy in sperm. A sperm head will normally have an X or Y signal plus one 8 signal. However if nondisjunction has occurred then additional signals will be detected (e.g., two chromosome 8 signals or both an X and a Y signal).

comparing this with mechanisms of malsegregation in females. There is considerable variability in the chromosome-specific rates of aneuploidy and where segregation errors occur (MI or MII) between males and females. The paternal-age effect is smaller than the maternal-age effect, and is thought to primarily involve errors during MII sex-chromosome segregation, whereas the maternal-age effect is more likely to arise from MI errors producing autosomal trisomies (Wyrobek et al., 1996). Only 10-30% of autosomal trisomies (chromosomes 13, 14, 15, 21, and 22) originate in paternal meiosis, with the majority of these arising in paternal meiosis II (Hassold et al., 1996). Overall, 5% of trisomy 21 is of paternal meiotic origin, with 40% arising at paternal MI and 60% at MII (Yoon et al., 1996). The paternal contribution to aneuploidy is greater from the sex chromosomes, with 100% of XYY-error paternal in origin (MII or post-fertilization error) and 50% of XXY are due to paternal MI error (Lorda-Sanchez et al., 1992).

DNA polymorphism analysis used to investigate the parent and meiotic stage of origin demonstrate that greater than 95% of human aneuploidy is attributable to errors in female meiosis (Hassold et al., 1993). In contrast to males, females are characterized by a protracted arrest at prophase of MI and a subsequent arrest at metaphase of MII. All oocytes enter meiosis during fetal development and remain in prophase of MI until just prior to ovulation. The completion of the first meiotic division could take 40 years or longer (Hunt and LeMaire-Adkins, 1998). Therefore much research has been focused on the speculation that the age-related increase in nondisjunction may be a result of damage accrued during the arrest period, but this is still under investigation. The incidence of trisomy among clinically recognized pregnancies stays fairly constant until later stages of

the reproductive life span of the human female, when the incidence of trisomy sharply increases (Hassold and Jacobs, 1984).

In addition to the speculation that damage occurring during the protracted arrest phase of female meiosis can lead to aneuploid conceptuses; it is also thought that females are error-prone and may lack checkpoint control mechanisms (LeMaire-Adkins et al., 1997). The fidelity of chromosome segregation is ensured by cell cycle control mechanisms that regulate transition points in the cell cycle. Checkpoints function to detect mistakes and inhibit cell cycle progression until the mistakes are corrected or eliminated. Studies have shown that there is a pachytene checkpoint in mammals that detects disturbances in synapsis and/or recombination of even a single pair of homologues (Tepperberg et al., 1997; Odorisio et al., 1998). In contrast to males, female carriers of structural chromosome abnormalities produce viable gametes, although some progeny are unbalanced (Hunt et al., 1995). Thus, female meiosis may lack stringent checkpoint controls. Part III in this dissertation will discuss evidence from Robertsonian and *Mlh1* $^{-/-}$ spermatocytes that suggests there may be a checkpoint that detects misaligned or abnormal chromosome configurations at MI. There also may be some sex-chromosome specific variations in checkpoint control (Hunt and LeMaire-Adkins, 1998). Studies with XO oocytes have shown that even though the X chromosome does not align properly at metaphase in a significant proportion of oocytes, there does not seem to be a delay in anaphase onset (LeMaire-Adkins et al., 1997). This suggests that females may lack a stringent checkpoint control mechanism and lends support to why females are error prone with increased levels of nondisjunction compared to males.

Mouse models can be used to gain a greater understanding of gamete aneuploidy

In order to accurately characterize what may be causing meiotic nondisjunction, it is essential to examine mouse models for aneuploidy. Many causative factors have been examined in respect to nondisjunction, as discussed in earlier sections, however mouse models for nondisjunction are needed to verify if these factors associated with nondisjunction are present. The focus of this dissertation is to examine new mouse models for aneuploidy in males to gain a greater understanding of both genetic and phenotypic mechanisms associated with aneuploidy.

The majority of my research has involved examination of a new genetic model for aneuploidy, PL/J males. **The specific aim for Part II** is to examine PL/J mice as a model for both gamete aneuploidy and abnormal sperm-head morphology. This work tests the hypothesis that the abnormal traits of aneuploidy and abnormal sperm-head morphology seen in PL/J mice are complex genetically and phenotypically. The phenotypic complexity involves abnormalities during prophase, spindle assembly and metaphase alignment. This chapter will bring new insight into the role complexity can play in leading to nondisjunction both genetically and phenotypically.

Other genetic models will be discussed in this dissertation and include Robertsonian heterozygous (Rb/+) translocation and *Mlh1* knockout mice. These models have also proven useful in understanding the requirements for successful division during meiosis. Previous studies involving Robertsonian translocation mice have shown that aneuploid gametes are produced and also disturbances are caused in both spindle structure, pairing abnormalities and increased germ cell death, most of which will be discussed in Part III (Eaker et al., 2001); (Everett et al., 1996); (Eichenlaub-Ritter and

Winking, 1990). **The specific aim of Parts III-VII** is to study meiotic abnormalities in four other mouse models. Part III tests the hypothesis that Robertsonian-heterozygous mice have increased levels of sperm aneuploidy. Meiotic abnormalities seen in Rb mice are predicted to lead to activation of a spindle assembly checkpoint and programmed cell death. In addition, as discussed earlier the *Mlh1* knockout model has proven essential in dissecting the function of genes that are involved in proper segregation of meiotic chromosomes. Part IV tests the hypothesis that the DNA mismatch repair protein MLH1 is required for proper progression through the meiotic division phase, and cell death occurs as a result of failure of proper chromosome alignment on the metaphase plate. The next mouse model, in Part V tests the hypothesis that Brca2 $^{-/-}$ mice that have been rescued by a BAC containing the human BRCA2 protein, which is poorly expressed in the gonads, have abnormal meiotic progression, leading to spermatogenic arrest. These and other genetic models, as discussed in this dissertation, will certainly prove useful in dissecting the complexity behind the mechanisms leading to aneuploid offspring.

Previous mouse models have involved chemically-induced aneuploidy. This is important due to the concern that chemicals and environmental factors may increase the frequency of aneuploidy and could having negative effects on human health. Examples include chemicals such as taxol and trichlorfon, exposure to which has been shown to induce spindle aberrations and aneuploidy in mouse oocytes and zygotes (Mailhes et al., 1999)and (Yin et al., 1998). In addition to chemicals that interact directly with cellular organelles responsible for chromosome movement (such as spindle fibers, centromeres or kinetochores), other types of damaging agents have been used in studies of nondisjunction. One example, etoposide, a common cancer chemotherapeutic agent, is a

topoisomerase-II inhibitor and has been shown to have its main effect during prophase of meiosis and to decrease recombination (Russell et al., 1998; Russell et al., 2000). Etoposide has also been shown to induce acentric fragments, deletions and aneuploidy in MI, MII and zygotes. One study showed that treatment of spermatocytes with etoposide induced the highest level of aneuploidy in MII (Marchetti et al., 2001). Part VI tests the hypothesis that the chemotherapeutic agent etoposide is a potent inducer of sperm aneuploidy.

With the aid of the mouse models for aneuploidy, a greater understanding of the mechanisms of pairing, recombination, alignment and proper segregation of chromosomes can be achieved. However, this understanding is based on phenotypic analysis, mostly using genes known to be involved in proper segregation of chromosomes. It is also important to find new approaches to use for dissection of meiotic abnormalities leading to aneuploidy. In this respect, new genes will be essential in uncovering new roles during meiosis. Part VII focuses on a novel approach for obtaining new meiotic mutants, through ENU mutagenesis and using sperm FISH as a screen for dominant mutations leading to gamete aneuploidy.

In conclusion, since aneuploidy can cause birth defects and is often lethal, the origins of chromosome nondisjunction leading to aneuploidy need to be better characterized. This dissertation focuses on the etiology of gamete aneuploidy and will take several approaches to increase knowledge about factors associated with nondisjunction. Several genetic models will be examined as well as a chemically-induced model for induction of gamete aneuploidy. There will also be discussion on ways to detect new genes associated with aneuploidy. The final summary in the last

chapter will discuss what we have learned and what direction to go from here, with the hope of finding new ways to prevent birth defects and embryonic lethality associated with aneuploid conceptuses.

LIST OF REFERENCES

Anderson LK, Reeves A, Webb LM, Ashley T. 1999. Distribution of crossing over on mouse synaptonemal complexes using immunofluorescent localization of MLH1 protein. Genetics 151:1569-1579.

Baker SM, Bronner CE, Zhang L, Plug AW, Robatzek M, Warren G, Elliott EA, Yu JA, Ashley T, Arnheim N, Flavell RA, Liskay RM. 1995. Male mice defective in the DNA mismatch repair gene *PMS2* exhibit abnormal chromosome synapsis in meiosis. Cell 82:309-319.

Baker SM, Plug AW, Prolla TA, Bronner CE, Harris AC, Yao X, Christie DM, Monell C, Arnheim N, Bradley A, Ashley T, Liskay RM. 1996. Involvement of mouse *Mlh1* in DNA mismatch repair and meiotic crossing over. Nat Genet 13:336-342.

Bond DJ, Chandley AC. 1983. The origins and causes of aneuploidy in experimental organisms. In DJ Bond and AC Chandley (ed): "Aneuploidy," Oxford: Oxford University Press, pp 27-54.

Eaker S, Pyle A, Cobb J, Handel MA. 2001. Evidence for meiotic spindle checkpoint from analysis of spermatocytes from Robertsonian-chromosome heterozygous mice. J Cell Sci 114:2953-2965.

Eichenlaub-Ritter U, Winking H. 1990. Nondisjunction, disturbances in spindle structure, and characteristics of chromosome alignment in maturing oocytes of mice heterozygous for Robertsonian translocations. Cytogenet Cell Genet 54:47-54.

Everett CA, Searle JB, Wallace BMN. 1996. A study of meiotic pairing, nondisjunction and germ cell death in laboratory mice carrying Robertsonian translocations. Genet Res 67:239-247.

Gearhart JD, Davisson MT, Oster-Granite ML. 1986. Autosomal aneuploidy in mice: generation and developmental consequences. Brain Research Bulletin 16:789-801.

Gorbsky GJ, Kallio M, Daum JR, Topper LM. 1999. Protein dynamics at the kinetochore: cell cycle regulation of the metaphase to anaphase transition. FASEB J 13:S231-S234.

Hassold T, Abruzzo M, Adkins K, Griffin D, Merrill M, Millie E, Saker D, Shen J, Zaragoza M. 1996. Human aneuploidy: incidence, origin, and etiology. Environ Mol Mutagen 28:167-175.

Hassold T, Hunt P. 2001. To ERR (Meiotically) is human: The genesis of human aneuploidy. Nat Rev Genet 2:280-291.

Hassold T, Hunt PA, Sherman S. 1993. Trisomy in humans: incidence, origin, and etiology. Curr Opinion Genet Devel 3:398-403.

Hassold T, Sherman S, Hunt P. 2000. Counting cross-overs: characterizing meiotic recombination in mammals. Hum Mol Genet 9:2409-2419.

Hassold TJ. 1998. Nondisjunction in the human male. In MA Handel (ed): "Meiosis and Gametogenesis," 37. 525 B Street, Suite 1900, San Diego, CA 92101-4495: Academic Press Inc, pp 383-406.

Hassold TJ, Jacobs PA. 1984. Trisomy in man. Ann Rev Genet 18:69-97.

Hassold TJ, Sherman SL, Pettay D, Page DC, Jacobs PA. 1991. XY chromosome nondisjunction in man is associated with diminished recombination in the pseudoautosomal region. Am J Hum Genet 49:253-260.

Hawley RS. 1988. Exchange and chromosomal segregation in eucaryotes. In R Kucherlapati and GR Smith (ed): "Genetic Recombination," Washington, DC 20006: Amer Soc Microbiol, pp 497- 527.

Henderson SA, Edwards RG. 1968. Chiasma frequency and maternal age in mammals. Nature 217:22-28.

Hinchcliffe EH, Sluder G. 2001. "It takes two to tango": understanding how centrosome duplication is regulated throughout the cell cycle. Gene Develop 15:1167-1181.

Hunt P, Lemaire R, Embury P, Sheean L, Mroz K. 1995. Analysis of chromosome behavior in intact mammalian oocytes: monitoring the segregation of a univalent chromosome during female meiosis. Hum Mol Genet 4:2007-2012.

Hunt PA, LeMaire-Adkins R. 1998. Genetic control of mammalian female meiosis. In MA Handel (ed): "Meiosis and Gametogenesis," 37. 525 B Street, Suite 1900, San Diego, CA 92101-4495: Academic Press Inc, pp 359-381.

Koehler KE, Hassold TJ. 1998. Human aneuploidy: lessons from achiasmate segregation in *Drosophila melanogaster*. Ann Hum Genet 62:467-479.

Koehler KE, Hawley RS, Sherman S, Hassold T. 1996. Recombination and nondisjunction in humans and flies. Hum Molec Genet 5:1495-1504.

LeMaire-Adkins R, Radke K, Hunt PA. 1997. Lack of checkpoint control at the metaphase/anaphase transition: A mechanism of meiotic nondisjunction in mammalian females. J Cell Biol 139:1611-1619.

Levine DS, Sanchez CA, Rabinovitch PS, Reid BJ. 1991. Formation of the tetraploid intermediate is associated with the development of cells with more than four centrioles in

the elastase-simian virus 40 tumor antigen transgenic mouse model of pancreatic cancer. Proceedings of the National Academy of Sciences of the United States of America 88:6427-6431.

Li XT, Nicklas RB. 1997. Tension-sensitive kinetochore phosphorylation and the chromosome distribution checkpoint in praying mantid spermatocytes. J Cell Sci 110:537-545.

Lingle WL, Lutz WH, Ingle JN, Maihle NJ, Salisbury JL. 1998. Centrosome hypertrophy in human breast tumors: Implications for genomic stability and cell polarity. Proc Natl Acad Sci USA 95:2950-2955.

Lorda-Sanchez I, Binkert F, Maechler M, Robinson WP, Schinzel AA. 1992. Reduced recombination and paternal age effect in Kleinfelter syndrome. Human Genetics 89:524-530.

Mailhes JB, Carabatsos MJ, Young D, London SN, Bell M, Albertini DF. 1999. Taxol-induced meiotic maturation delay, spindle defects, and aneuploidy in mouse oocytes and zygotes. Mutat Res 423:79-90.

Marchetti F, Bishop JB, Lowe X, Generoso WM, Hozier J, Wyrobek AJ. 2001. Etoposide induces heritable chromosomal aberrations and aneuploidy during male meiosis in the mouse. Proc Nat Acad Sci Usa 98:3952-3957.

McKee BD. 1998. Pairing sites and the role of chromosome pairing in meiosis and spermatogenesis in male Drosophila. In MA Handel (ed): "Meiosis and Gametogenesis," 37. 525 B Street, Suite 1900, San Diego, CA 92101-4495: Academic Press Inc, pp 77-115.

Moens PB, Pearlman RE, Heng HHQ, Traut W. 1998. Chromosome cores and chromatin at meiotic prophase. In MA Handel (ed): "Meiosis and Gametogenesis," 37. 525 B Street, Suite 1900, San Diego, CA 92101-4495: Academic Press Inc, pp 241-262.

Moses MJ, Dresser ME, Poorman PA. 1984. Composition and role of the synaptonemal complex. Soc Exp Biol 246-270.

Odorisio T, Rodriguez TA, Evans EP, Clarke AR, Burgoyne PS. 1998. The meiotic checkpoint monitoring synapsis eliminates spermatocytes via p53-independent apoptosis. Nat Genet 18:257-261.

Page SL and Hawley RS. 2001. c(3)G encodes a Drosophila synaptonemal complex protein. Genes Dev 15(23):3130-43.

Polani PE. 1972. Centromere localization at meiosis and the position of chiasmata in the male and female mouse. Chromosoma 36:343-374.

Polani PE, Jagiello GM. 1976. Chiasmata, meiotic univalents, and age in relation to aneuploid imbalance in mice. Cytogenetics and Cell Genetics 16:505-529.

Roeder GS. 1997. Meiotic chromosomes: it takes two to tango. Gene Develop 11:2600-2621.

Russell LB. 1968. The use of sex-chromosome anomalies for measuring radiation effects in different germ-cell stages of the mouse. In (ed): "Effects of radiation in meiotic systeme," Vienna: IAEA, pp 27-41.

Russell LB. 1976. Numerical sex-chromosome anomalies in mammals: their spontaneous occurrence and use in mutagenesis studies. In A Hollaender (ed): "Chemical Mutagens," Chapter 37. New York: Plenum Publishing Corporation, pp 55-91.

Russell LB. 1985. Experimental approaches for the detection of chromosomal malsegregation occuring in the germline of mammals. In VL Dellarco, Voytek, P.E., Hollaender, A. (ed): "Aneuploidy: Etiology and Mechanisms," 36. New York: Plenum Press, pp 377-396.

Russell LB, Hunsicker PR, Hack AM, Ashley T. 2000. Effect of the topoisomerase-II inhibitor etoposide on meiotic recombination in male mice. Mutat Res Genet Toxicol E M 464:201-212.

Russell LB, Hunsicker PR, Johnson DK, Shelby MD. 1998. Unlike other chemicals, etoposide (a topoisomerase-II inhibitor) produces peak mutagenicity in primary spermatocytes of the mouse. Mutat Res Fundam Mol Mech Mut 400:279-286.

Sluder G, Thompson EA, Miller FJ, Hayes J, Rieder CL. 1997. The checkpoint control for anaphase onset does not monitor excess numbers of spindle poles or bipolar spindle symmetry. J Cell Sci 110:421-429.

Stewart GD, Hassold TJ, Berg A, Watkins P, Tanzi R, Kurnit D. 1988. Trisomy 21 (Down Syndrome): studying nondisjunction and meiotic recombination by using cytogenetic and molecular polymorphisms that span chromosome 21. Am J Hum Genet 42:227-236.

Sullivan BA, Schwartz S, Willard HF. 1996. Centromeres of human chromosomes. Environ Mol Mutagen 28:182-191.

Tepperberg JH, Moses MJ, Nath J. 1997. Colchicine effects on meiosis in the male mouse .1. Meiotic prophase: synaptic arrest, univalents, loss of damaged spermatocytes and a possible checkpoint at pachytene. Chromosoma 106:183-192.

Williams BJ, Ballenger CA, Malter HE, Bishop F, Tucker M, Zwingman TA, Hassold TJ. 1993. Non-disjunction in human sperm: Results of fluorescence *in situ* hybridization studies using two and three probes. Hum Mol Genet 11:1929-1936.

Woods LM, Hodges CA, Baart E, Baker SM, Liskay M, Hunt PA. 1999. Chromosomal influence on meiotic spindle assembly: Abnormal meiosis I in female *Mlh1* mutant mice. J Cell Biol 145:1395-1406.

Wyrobek AJ, Aardema M, Eichenlaub-Ritter U, Ferguson L, Marchetti F. 1996. Mechanisms and targets involved in maternal and paternal age effects on numerical aneuploidy. Environ Mol Mutagen 28:254-264.

Yin H, Cukurcam S, Betzendahl I, Adler ID, Eichenlaub-Ritter U. 1998. Trichlorfon exposure, spindle aberrations and nondisjunction in mammalian oocytes. Chromosoma 107:514-522.

Yoon PW, Freeman SB, Sherman SL, Taft LF, Gu YC, Pettay D, Flanders WD, Khoury MJ, Hassold TJ. 1996. Advanced maternal age and the risk of Down Syndrome characterized by the meiotic stage of the chromosomal error: a population-based study. Am J Hum Genet 58:628-633.

Yuan L, Liu JG, Zhao J, Brundell E, Daneholt B, Hoog C. 2000. The murine *SCP3* gene is required for synaptonemal complex assembly, chromosome synapsis, and male fertility. Mol Cell 5:73-83.

PART II

SPERMATOGENESIS IN PL/J MICE: A GENETIC MODEL FOR GAMETIC ANEUPLOIDY

ABSTRACT

It was previously shown that sperm from mice of the PL/J strain have an increased frequency of sperm-head morphology abnormalities. Application of the technique of sperm fluorescence in situ hybridization (FISH) revealed that PL/J sperm are also characterized by an elevated frequency of aneuploidy compared to sperm from C57BL/6J males. The traits of abnormal sperm-head morphology and aneuploidy are complex phenotypically. During prophase, spermatocytes of PL/J mice exhibit chromosome asynapsis. At meiotic metaphase, it is apparent that there is reduced crossing over in PL/J spermatocytes. Additionally, during the first meiotic division, 34.7% of the PL/J spermatocytes exhibit aberrant spindle morphology (compared to 5.7% for C57BL/6J spermatocytes). Spindle abnormalities include monopolar spindles, split spindle poles and incomplete spindle formation. Staining with antibody to pericentrin reveals abnormal numbers of centrosomes in PL/J spermatocytes. Thus increased frequency of sperm aneuploidy in PL/J males is associated with, and may be caused by, aberrant centrosome and spindle formation. The traits of sperm aneuploidy and aberrant head morphology are also complex genetically. F1 progeny of a cross between PL/J and C57BL/6J do not exhibit a higher frequency of either sperm aneuploidy or sperm-head morphology aberrations, as would be expected for a dominant trait. Among progeny of a backcross of the F1 to PL/J, none of 16 males assessed exhibited elevated frequencies of either sperm aneuploidy or sperm-head morphology abnormalities. Thus the aberrant PL/J traits are apparently inherited in a complex manner, with several genes and/or modifiers affecting the generation of sperm aneuploidy and abnormal sperm-head morphology.

CHAPTER I

INTRODUCTION

Among human conceptuses, aneuploidy is the most prevalent chromosome abnormality and accounts for both a significant proportion of all spontaneous abortions and mental retardation among live births (e.g., Down syndrome). Thus meiotic nondisjunction of chromosomes presents a significant clinical problem. Most aneuploidy of human conceptuses is thought to arise from errors in maternal meiosis; however, errors during paternal meiosis can also give rise to aneuploid gametes (Hassold, 1998). This paper will address issues of concern in meiosis that can lead to production of aneuploid sperm.

Mechanisms contributing to meiotic nondisjunction and gametic aneuploidy are largely unknown, which is unfortunate, given the clinical significance and societal burden of aneuploidy. Factors implicated include meiotic pairing and recombination, behavior of chromosomes during the meiotic division phases and morphology and function of the spindle and associated centrosomes. The possible role that each of these factors could have in gamete aneuploidy will be addressed using a mouse model for sperm aneuploidy and abnormal sperm-head morphology.

One factor associated with nondisjunction is altered recombination. Early evidence for altered recombination as a causative factor contributing to gamete aneuploidy (Koehler et al., 1996) has been amply substantiated by evidence from analyses of human Trisomy 21 fetuses (Hassold and Sherman, 2000; Hassold et al., 2000; Lamb et al., 1997; Savage et al., 1998). Specifically, genetic mapping techniques have been used to study the inheritance of DNA polymorphisms in trisomic conceptuses. This

approach allows for study of the relationship between recombination and human nondisjunction by comparing the frequency and distribution of meiotic exchanges in trisomy-generating meioses (Hassold and Hunt, 2001). In one example, paternal nondisjunction of chromosome 21 was studied in 67 trisomy-21 conceptuses. It was found that a 1:1 ratio existed between MI to MII errors, but that reduced recombination was found along the chromosome 21 involved in paternal MI nondisjunction (Savage et al., 1998). Significant reductions in recombination are a feature of most MI-derived trisomies examined thus far. Maintenance of contact between homologous chromosomes through recombination is thought to ensure proper bipolar orientation of bivalents at metaphase I (MI). Thus, both decreased recombination and aberrantly situated recombination events are risk factors for meiotic nondisjunction; in both flies and humans, nonexchange bivalents and bivalents with single, distal exchanges are more susceptible to meiotic nondisjunction than those with more proximally localized chiasmata (Koehler et al., 1996).

In order to gain a greater understanding of how location of meiotic exchange events can predispose to nondisjunction, tools for analysis of recombination sites are needed. Importantly, identification of proteins implicated in recombination and technology for *in situ* localization of these proteins has made it now possible to analyze genome-wide exchange patterns in individual meiosis. For example, there is strong evidence that localization of the mammalian MLH1 protein on mouse pachytene-stage synaptonemal complexes (SCs) identifies sites of crossover (Anderson et al., 1999; Hassold et al., 2000). The frequency and distribution of MLH1 foci corresponds to previous cytogenetic analysis of chiasmata. The MLH1 protein can then be used to

analyze meiotic exchange patterns. It has been shown that on average, there are ~23 MLH1 foci per set of autosomal SCs (synaptonemal complexes or proteinacious structures that localize to pairing regions between homologous chromosomes, reviewed in (Moses et al., 1984)) in normal mouse spermatocytes. Most mouse SCs have 1 or 2 MLH1 foci, at the most 3, depending on the length of the SC. This technology allows for accurate assessment of the number of crossovers that occur during pachytene of meiosis I.

In addition to recombination, the assembly of the meiotic spindle, the alignment of chromosomes onto it, and the polar centrosomal regions are all likely to be important in ensuring proper segregation of chromosomes in the meiotic divisions; however the roles of these structures are not yet clearly defined. There is evidence that abnormal spindles may be associated with nondisjunction. Gametocytes of mice bearing heterozygous configurations of Robertsonian (Rb) translocation chromosomes and their acrocentric counterparts are prone to nondisjunction and abnormal spindles are frequently observed. Rb chromosomes are metacentric, or nearly metacentric, chromosomes formed by the centric fusion of two acrocentric chromosomes (Robertson, 1916). During the first meiotic prophase in individuals heterozygous for Rb chromosomes, the Rb participates in a trivalent with the two homologous acrocentric chromosomes. Pairing defects (as represented in Fig. 1, Chap. III A) in this unusual configuration could give rise to the potential for error in either chromosome alignment at metaphase I (MI) or unbalanced segregation at anaphase I. Specifically, in Rb heterozygous oocytes, complete spindle formation is disturbed (Eichenlaub-Ritter and Winking, 1990). In this study, Rb oocytes had several translocations and chromosomes in the multivalent that did not align properly

at the equator. The centromeres of neighboring chromosomes in the multivalent remained maloriented, and pronounced lagging of chromosomes was observed at telophase I (Eichenlaub-Ritter and Winking, 1990). Therefore, disturbance in spindle structure and chromosome behavior appear to correlate with the chromosomal constitution in these oocytes and, ultimately, with failures in proper chromosome separation.

There is additional evidence that chromosome configuration and behavior can directly influence meiotic spindle assembly in mouse oocytes. For example, oocytes from *Mlh1* knockout mice, are characterized by univalent chromosomes with abnormal orientation, leading to aberrant spindle formation (Woods et al., 1999). In this example, the spindle poles often continued to elongate and abnormalities were seen in organization in the midzone microtubules. Further studies are needed to determine whether spindle abnormalities are involved or are a direct consequence of nondisjunction. In addition, the spindle structure involved in leading to abnormal spindle formation and segregation of chromosomes needs to be better characterized.

One such spindle structure is the centrosome, a microtubule-organizing center (MTOC). The centrosome determines the number and polarity of cytoplasmic microtubules. The role of the centrosome in meiosis is not well understood. In mitosis the centrosome duplicates once per cell cycle, with daughter centrosomes forming two poles of the spindle after nuclear envelope breakdown. The consequence of failure in centrosome duplication is a return to interphase without division, causing polyploidy; and the consequence of multiple centrosome duplication is assembly of a multipolar spindle, with unequal distribution of chromosomes (Hinchcliffe and Sluder, 2001). Thus

abnormal centrosome behavior can be correlated with aneuploidy, especially in tumor cells. The idea is that the extra centrosomes lead to chromosome missorting and damage, thus causing aneuploidy. Aneuploidy, in turn, may result in the loss of tumor suppressor genes or the gain or activation of cancer-causing oncogenes. In fact, one study found that cells lacking the critical tumor suppressor gene, *p53*, have multiple centrosomes instead of the normal one or two. Experiments have shown in cell culture, that centrosome amplification disturbs mitotic fidelity, causing the cells to end up with abnormal chromosome complements. Because *p53*'s loss or inactivation is thought to contribute to the development of many human cancers, these findings suggested a new way that lack of a functional *p53* gene might lead to cancer: by disturbing centrosome function and thereby generating aneuploidy (Fukasawa K et al., 1996). Abnormal centrosome numbers are also seen in several human cancers such as breast, prostate, lung, colon, and brain (Marx, 2001). The centrosomes role in mitosis leading to cancer is beginning to be revealed, but its role in meiosis and connection to aneuploidy is still not well understood. Centrosome requirements are different between oogenesis and spermatogenesis. For example, in contrast to spermatogenesis, meiosis I in *Drosophila* oogenesis is accomplished in the absence of centrosomes (Megraw and Kaufman, 2000). Therefore, it will be important to learn more about centrosomal differences in gametogenesis and the role of centrosomes during meiosis.

Since there are several factors that could be associated with nondisjunction, elucidation of the mechanisms associated with aneuploidy will require efficient means of detecting nondisjunction. In the past decade, much of our knowledge of the contribution of sperm aneuploidy has derived from extensive use of sperm fluorescence *in situ*

hybridization (FISH) with chromosome-specific probes (Hassold, 1998). This technique is advantageous for determination of the frequency of gamete aneuploidy since large numbers of gametes can be scored. For this reason it is now possible to use FISH as a screening technique to detect animal models for gametic aneuploidy. This is important, for in order to understand the etiology of mammalian meiotic nondisjunction, mouse models of aneuploidy will be essential. To date, most examples of mouse models prone to gametic aneuploidy have involved either chromosomes aberrations, such as Robertsonian translocation heterozygosity (Eichenlaub-Ritter and Winking, 1990), or chemical treatment that causes gametic aneuploidy. For example, one study showed by sperm FISH that aneuploidy was induced after treatment of mice *in vivo* with acrylamide, colchicines, diazepam or thiabendazole (Schmid et al., 1999). However, of even more utility for probing mechanisms leading to gametic aneuploidy would be a genetic model.

The PL/J mouse, an inbred strain, has proven to be a mouse model for both aneuploidy and abnormal sperm-head morphology. PL/J mice were previously shown to have a high frequency (42%) of sperm with abnormal-head morphology (Burkhart and Malling, 1981). Our present study shows that PL/J males also exhibit an increased frequency of sperm aneuploidy. This study demonstrates that these abnormalities are complex, both phenotypically and genetically. Meiotic abnormalities include asynapsis, reduced recombination, as well as abnormalities in chromosome condensation and alignment, and spindle structure. Genetically, inheritance of the abnormal traits is complex, suggesting multi-genic determination of the phenotypic traits. Therefore, this study examines the genetic and phenotypic complexity associated with aneuploidy using PL/J as a mouse model.

CHAPTER II

MATERIALS AND METHODS

Animals and Crosses

PL/J mice were obtained from The Jackson Laboratory, Bar Harbor, ME. For genetic analysis, they were crossed to C57BL/6J (B6) mice (The Jackson Laboratory, Bar Harbor, ME). F1 males and females were backcrossed to PL/J mice. All mice were maintained with food and water provided *ad libitum* on a 14 hr light/10 hr dark schedule**.**

Three-color Fluorescence in Situ Hybridization (FISH)

For sperm FISH analysis, males were killed by cervical dislocation and sperm from epididymides were collected in 2.2% citrate. Sperm were spread onto a slide and dried. The slides were soaked in 10 mM dithithreitol (DTT) on ice for 30 min and placed immediately into 4 mM diiodosalicyclic acid (LIS) for 1 hr. The slides were air dried and dehydrated in ethanol. Slides and probes were denatured at 78°C in formamide, then dehydrated and air-dried. Probes specific for chromosomes 8, X and Y were a generous gift from Dr.Terry Hassold, Case Western University, Cleveland, Ohio. Biotin was used to label 1 µg of the Y probe pERS-532 (Eicher et al., 1991); the Chr. 8 probe, which was a mixture (2 µg total) of four subclones (Boyle and Ward, 1992), was labeled with digoxygenin; and 1 µg of the X chromosome-specific probe DXWas (Disteche et al., 1987) was labeled with both biotin and digoxygenin separately. Probes were labeled using a nick translation kit (Roche Pharmaceutical) and purified over a Sephadex- G50 column. The probe mix was added to each slide; which was then incubated at 37°C

overnight. The next day, slides were washed in 50% formamide/2X SSC, in 2X SSC, and then in PN Buffer (0.1M NaH_2PO_4, 0.1M Na_2HPO_4, 0.05% NP-40, pH 8). Slides were incubated in a BSA-blocking buffer and the appropriate fluorochrome-conjugated detector, also in BSA, at 37°C for 30 min, then washed in PN buffer twice. After adding DAPI/Antifade (Molecular Probes), slides were viewed with an Olympus epifluorescent microscope at 100X. Estimates of sperm aneuploidy were deliberately conservative. Only hyperhaploidy, and not hypohaploidy, was scored; the aneuploidy frequency represents twice the hyperhaploidy frequency. Additionally, sperm were deemed suitable for scoring only when the following criteria were met: fluorescent signals were clearly within and not on the edge of the sperm nucleus, fluorescent signals were all in the same plane of focus, and any two signals scored as separate were separated by a distance equal or greater than one signal domain.

Chromosome painting was performed on testicular cells fixed in 3:1 ethanol:acetic acid and then air-dried onto slides (Evans et al., 1964). The slides were air-dried overnight and dehydrated in a 70%, 90%, 90% and 100% ethanol series, then air-dried again. The DNA of the cells was denatured by incubation in 70% formamide/2X SSC at 65°C for 2 min. The slides were then quenched in the ethanol series above and air-dried. Chromosome paint probes, for Chrs. 2 and 8 (Cambio Inc, Cambridge, UK), were warmed to 37°C, and denatured at 65°C for 10 min, then at 37°C for 60-90 min. Subsequently, 15 µl of each chromosome paint probe was added to each slide and the cells were coverslipped, sealed and incubated overnight at 37°C in a humidified chamber. The slides were washed twice for 5 min at 45˚C in 50% formamide/2X SSC and then twice in 0.1X SSC. Detection reagents 1 and 2, provided by

the manufacturer (Cambio, Inc.) for the Chr. 2 probe, which required amplification, were made in a 3% BSA/4X SSC blocking solution and slides were incubated with the appropriate detection reagent for 40 min in a humidified chamber at 37˚C. The slides were then processed for visualization as above.

Testis Fixation and In Situ Apoptosis Detection

Mice were killed by cervical dislocation, testes removed, and fixed in 4% paraformaldehyde overnight at 4^{o}C. Testes from 3 PL/J mice and 3 B6 mice were fixed in this manner. The testes were dehydrated through an ethanol series and toluene, then embedded in paraffin. The tissue was sectioned at 3-6 μM, and the sections placed on slides to dry. After deparaffination in xylene and rehydration in a decreasing ethanol series, the slides were subjected to the TUNEL reaction for assessment of apoptosis. Apoptosis assays were performed using the In Situ Cell Death Detection Kit (Roche/Boehringer Mannheim), employing the TUNEL reaction following the manufacturer's protocol, with the exception that the enzyme incubation was for 15 min. Tubule cross-sections were scored as apoptotic when three or more apoptotic meiotic cells were observed per tubule cross-section.

Fixation and Immunofluorescent Labeling of Tubule Segments and Isolated Germ Cells

To obtain cytological preparations enriched in meiotically dividing spermatocytes (stage XII of the mouse seminiferous epithelium) a variation of the transillumination procedure (Parvinen et al., 1993) was used. Testes from adult mice (3 B6 males and 3

PL/J males) were detunicated, then digested with collagenase for 8 min at 33°C in Krebs-Ringer bicarbonate (KRB) buffered media. Transillumination patterns were observed using a dissecting microscope and the desired stage XII segments (visualized as 3 mm beyond the site of transition from optically dense to light) were excised and transferred onto a microscope slide in KRB. For fixation, a coverslip was placed on top of the segment, then the entire slide was frozen in liquid N_2 for 25 sec. The coverslip was removed, and the slide was fixed in 3:1 ethanol/acetic acid. Prior to incubation with antibody, the slide was placed in PBS/0.2% Triton X-100 (Sigma) for 5 min, then placed in blocking solution (PBS/10% goat serum) for 30 min.

Cell preparations enriched in germ cells were prepared as previously described (Cobb et al., 1999b). Briefly, testes were detunicated and digested in 0.5 mg/ml collagenase (Sigma) in Krebs-Ringer buffer for 20 min at 32°C and then in 0.5 mg/ml trypsin (Sigma) for 13 min, followed by filtering through 80 μm mesh and washing in buffer. To induce meiotic chromosome condensation, germ cells were cultured for 2 hrs to allow stabilization in culture and then treated with 5 μM okadaic acid (OA) or ethanol for 6 hrs as previously described (Wiltshire et al., 1995). Chromosome condensation was evaluated after making air-dried chromosome preparations as described above. Surface-spread preparations were used to visualize nuclei; cells were fixed in 2% paraformaldehyde with 0.03% SDS (Cobb et al., 1999a). Spermatocytes from germ cell preparations were also embedded in a fibrin clot using modifications to a previously published protocol (LeMaire-Adkins et al., 1997). Germ cells were isolated as above, and brought to a concentration of 25 X 10^6 cells/ml. 3 μl of fibrinogen (Calbiochem, 10mg/ml fresh) and 1.5 μl of the cell suspension were mixed on a slide. Then 2.5 μl of

thrombin (Sigma, 250 units) was added, and allowed to clot for 5 min. The slide was fixed in 4% paraformaldehyde, washed in 0.2% Triton X-100, then processed for immunofluorescence.

Antisera used were polyclonal anti-SYCP3 (Eaker et al., 2001), anti-β-tubulin (Amersham), anti-phosphorylated histone H3-Ser10 (Upstate Biotech), anti-pericentrin (Covance), anti-MLH1 (Becton Dickinson Co/PharMingen), anti- SynD1 (gift from C. Hoog at the Karolinske Institute, Stockholm). Following overnight incubation in primary antibody, slides were incubated with rhodamine- or fluorescein-conjugated secondary antibodies (Pierce), followed by mounting with Prolong Antifade (Molecular Probes) containing DAPI (Molecular Probes) to stain DNA. Control slides were stained with either secondary antibodies only, or pre-immune sera as a primary antibody. Staining was observed with an Olympus epifluorescence microscope and images were captured and transferred to Adobe PhotoShop with a Hamamatsu color 3CCD camera. Confocal imaging was performed using a Leica TC SP2 laser-scanning confocal microscope.

CHAPTER III

RESULTS

PL/J males exhibit abnormal sperm-head morphology and an increased frequency of hyperhaploid sperm

Our analysis confirmed previous reports that PL/J (PL) mice exhibit abnormalities in sperm-head morphology. For PL/J males (n=4, 1000 sperm ea.), the mean frequency of abnormal sperm-head morphology was 30.03% (Table 1), while for control C57BL/6J (B6) males (n=4, 1000 sperm ea.), the mean frequency of abnormal sperm was 1.3%. The types of abnormalities seen included enlarged head shape, no head (mitochondrial drop), and narrow/elongated sperm (Fig. 1). Since PL/J sperm-head morphology is abnormal, determination of sperm chromosome content is also important. Sperm FISH was used to determine if PL/J also have aneuploid sperm. Centromeric point probes specific for chromosomes 8, X, and Y were used to determine the percentage of sperm aneuploidy for these three chromosomes. This analysis revealed that PL/J males do produce aneuploid sperm. Fig. 2 illustrates examples of some of the types of hyperhaploidy seen in PL/J sperm. The frequency of hyperhaploidy (Table 1) for PL/J is 3.4% +/- 0.80 and is statistically significant ($p < 0.0001$), compared to control B6 at 0.35% +/- 0.19 (n=4, 1000 sperm ea). PL/J males exhibit both abnormal sperm-head morphology and hyperhaploidy. The next important question is how are these traits inherited? Determination of the inheritance pattern of sperm aneuploidy and abnormal-sperm head morphology will reveal if the transmission of the traits is due to a mendelian or complex pattern of inheritance.

Figure 1. Sperm morphology. A. This panel shows the normal morphology of sperm from B6 males. B. This panel shows representative examples of aberrant morphology of sperm from P/J males, including enlarged head (E), small head (S), and no head (N). Bar = 10 μm.


A

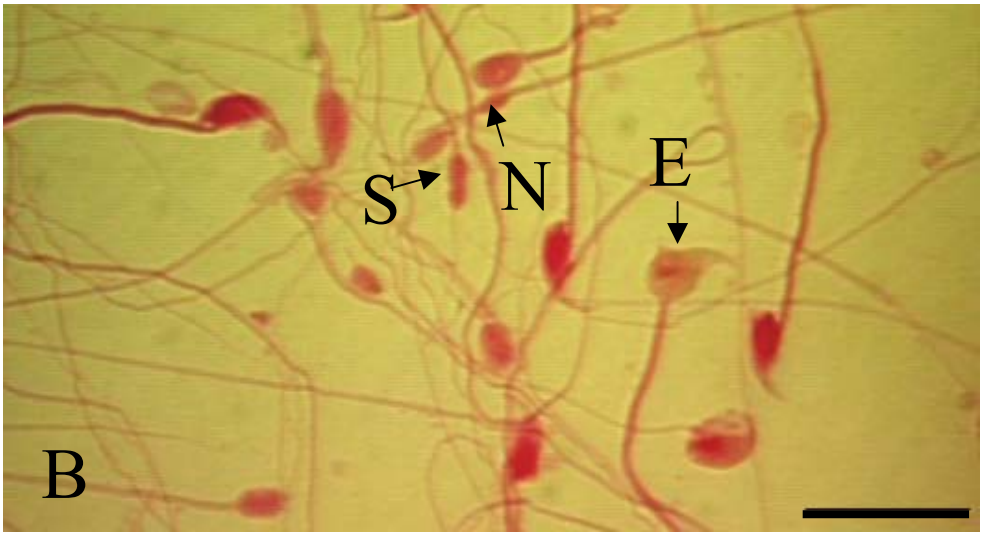

S
N
E
B

Figure 2. Representative images from sperm FISH analysis. A and B. Normal sperm from B6 males. C and D. Sperm from PL/J males exhibiting hyperhaploidy. Spot signals are Chr. 8 detected with rhodamine (red), Chr. Y detected with FITC (green), and Chr. X detected with both rhodamine and FITC (yellow).

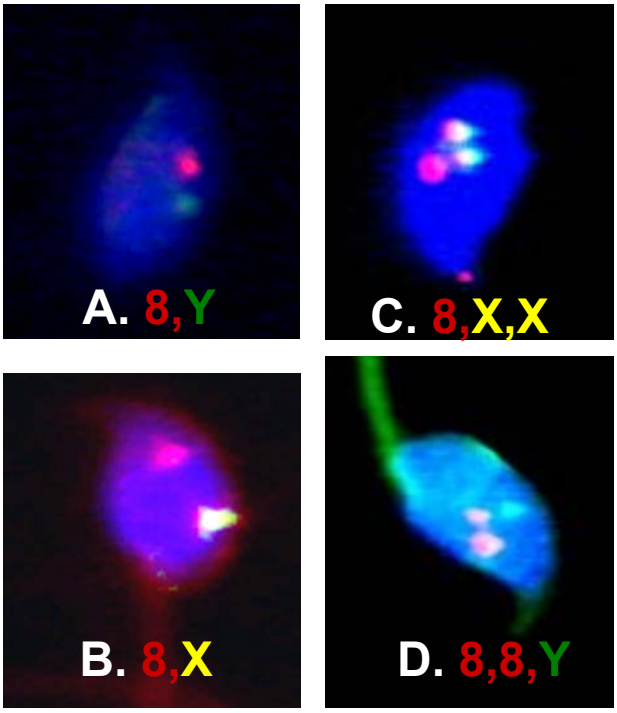

A. 8,Y
C. 8,X,X
B. 8,X
D. 8,8,Y

Table 1. Frequency of hyperhaploidy and abnormal sperm-head morphology (SHM) in PL/J, C57BL/6J and F1 progeny. The mean frequency of hyperhaploidy in PL/J of 3.4% (**) is statistically higher than the frequencies of hyperhaploidy in both C57BL/6J and F1 progeny.

Genetic Background	Mouse #	% Hyperhaploidy	% Abnormal Sperm Head Morphology
A. Parental and F1's			
PL/J	1	3.1	30.1
	2	2.9	35.6
	3	4.6	25.3
	4	3.0	29.1
	Mean	**3.4 ****	**30.03**
C57BL/6J	1	0.6	0.8
	2	0.2	1.1
	3	0.4	0.8
	4	0.2	1.1
	Mean	**0.35**	**1.3**
PL X B6	1	1.1	2.0
	2	0.8	1.3
	3	0.99	1.0
	4	0.9	0.9
	Mean	**0.95**	**1.3**
B6 X PL	1	1.3	1.0
	2	0.7	1.5
	3	0.8	0.9
	4	0.7	1.0
	Mean	**0.88**	**1.10**

Sperm aneuploidy and abnormal sperm-head morphology are inherited in a complex manner

Genetic crosses were performed to determine the mode of inheritance of both abnormal sperm-head morphology and hyperhaploidy. PL/J and B6 mice were crossed to determine if the trait of abnormal sperm-head morphology is inherited in a dominant manner. Both parental combinations (PL/J X B6 and B6 X PL/J) were crossed; in each instance the female is denoted first. Analysis of the F1 progeny showed that there was no increase in abnormal sperm-head morphology over the control B6 males, with an average of 1.3 and 1.10, respectively (Table 1). The F1 progeny had a large reduction in the frequency of sperm with abnormal-head morphology as compared to PL/J (30% vs. 1.3/1.1%), and differences in paternal/maternal transmission was not statistically significant.

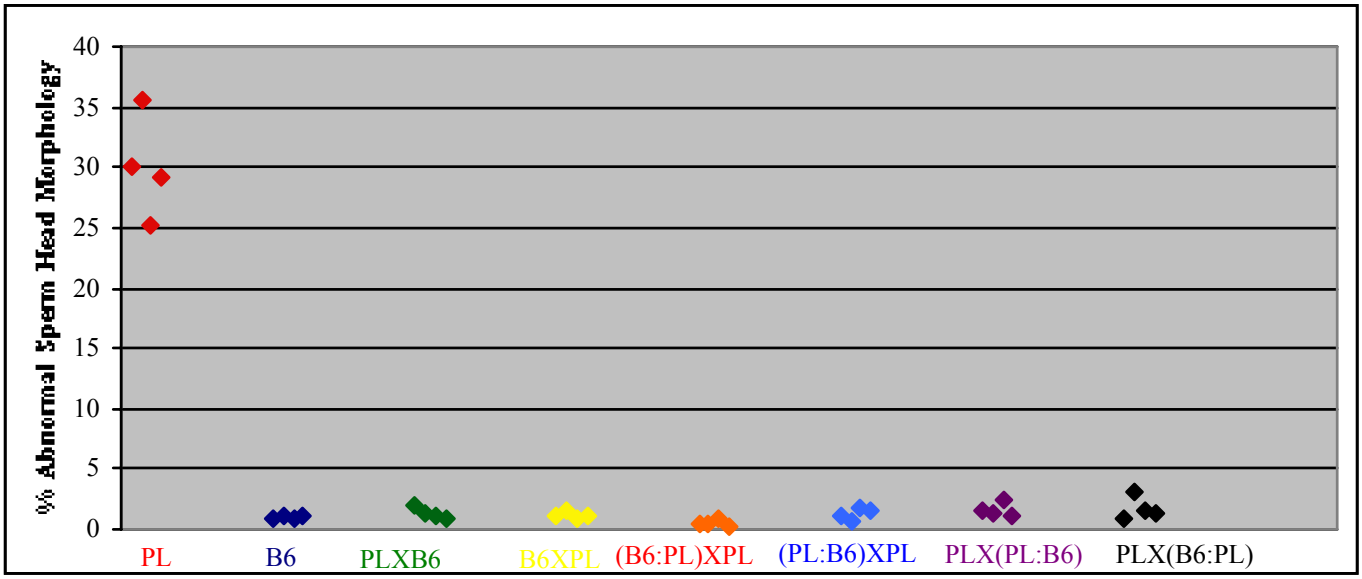
The trait of abnormal sperm-head morphology was then examined by backcross of the F1 to PL/J (in backcrosses, denoted as PL) and B6, to see if abnormal sperm-head morphology is inherited in a recessive manner due to one gene. Four mice of each backcross were scored (B6 : PL F1) X PL male, (PL : B6 F1) X PL male, PL female X (PL : B6 F1), and PL female X (B6 : PL F1). The mean frequencies of head-shape abnormalities for the backcross progeny are 0.50, 1.20, 1.65, and 1.68, respectively (Table 2). F1 by B6 backcross analysis did not reveal an increased frequency of abnormal sperm-head morphology in any individuals (data not shown). The male with the lowest frequency (.3%) of abnormal sperm-head morphology was from the (B6:PL F1) X PL male cross and the male with the highest (3.0%) was from the PL female X (B6:PL) cross (Fig 3A). The progeny (B6:PL/J)F1 X PL backcross class had an overall

Table 2. Frequency of hyperhaploidy and abnormal sperm-head morphology (SHM) in the F1 X PL/J backcross mice. ** indicates the highest value, * is the lowest value in each column.

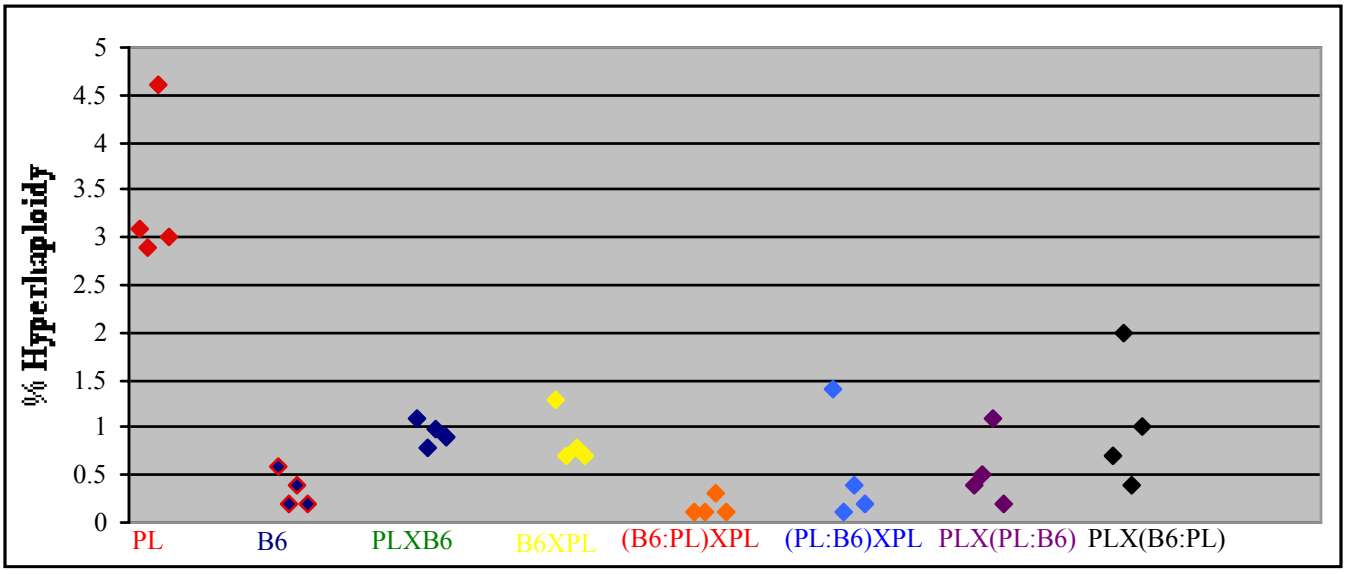
Genetic Background	Mouse #	% Hyperhaploidy	% Abnormal Sperm Head Morphology
B. Backcrosses			
(B6:PL)X PL	1	0.1	0.4
	2	0.1	0.5
	3	0.3	0.8
	4	0.1*	0.3*
(PL:B6)X PL	1	1.4	1.0
	2	0.1	0.6
	3	0.4	1.7
	4	0.2	1.5
PL X (PL:B6)	1	0.4	1.6
	2	0.5	1.3
	3	1.1	2.5
	4	0.2	1.2
PL X (B6:PL)	1	0.7	0.8
	2	2.0*	3.0*
	3	0.4	1.6
	4	1.0	1.3

Figure 3. Frequency of hyperhaploidy and abnormal sperm-head morphology (SHM) in all crosses represented in scatter plots. Part A shows the abnormal-sperm head morphology frequency in each mouse. Part B shows the hyperhaploidy frequency in each mouse.

A


% Abnormal Sperm Head Morphology
40
35
30
25
20
15
10
5
0
PL
B6
PLXB6
B6XPL
(B6:PL)XPL
(PL:B6)XPL
PLX(PL:B6)
PLX(B6:PL)

B


% Hyperhaploidy
5
4.5
4
3.5
3
2.5
2
1.5
1
0.5
0
PL
B6
PLXB6
B6XPL
(B6:PL)XPL
(PL:B6)XPL
PLX(PL:B6)
PLX(B6:PL)

frequency of abnormal sperm-head morphology (0.5% +/- .9 SD) that was statistically ($p < .05$) lower than the frequencies for all the other backcross progeny.

The inheritance pattern of hyperhaploidy was examined in the same genetic crosses described above. The F1 progeny show that hyperhaploidy is not inherited in a dominant manner, since none exhibits hyperhaploidy frequency as high as PL/J. However, there is a statistically significant ($p < .001$) increase in the percentage of hyperhaploidy in the F1 (.91% +/- .21 SD) in comparison to B6 (.35% +/- .19 SD). The PL X B6 average frequency is 0.95% and for B6 X PL is 0.88%. This may represent a semi-dominant pattern of inheritance of aneuploidy in the F1 progeny (although not abnormal sperm-head morphology; see Table 1). Analysis of backcross progeny showed that there were no individuals with as high a frequency of gamete aneuploidy as seen in PL/J with respect to hyperhaploidy, (Table 2 and Fig 3B). Although one male (from PL female X (B6:PL) cross), with a sperm aneuploidy frequency of 2.0% was close to the mean frequency of hyperhaploidy in PL/J. Possible correlations were examined in each cross between abnormal sperm-head morphology and abnormal chromosome constitution of sperm. In most instances where there is an increase in abnormal sperm-head morphology there is also an increase in the percent hyperhaploidy. For example, the individuals with the highest frequency (3.0%) of abnormal sperm-head morphology (from the PL X (B6:PL) cross) also had the highest frequency (2.0%) of hyperhaploidy. A direct correlation between aneuploidy and sperm morphology was impossible to determine, since the swelling procedure in sperm FISH precludes scoring sperm-head morphology. Our analysis reveals that the inheritance of both abnormal sperm-head

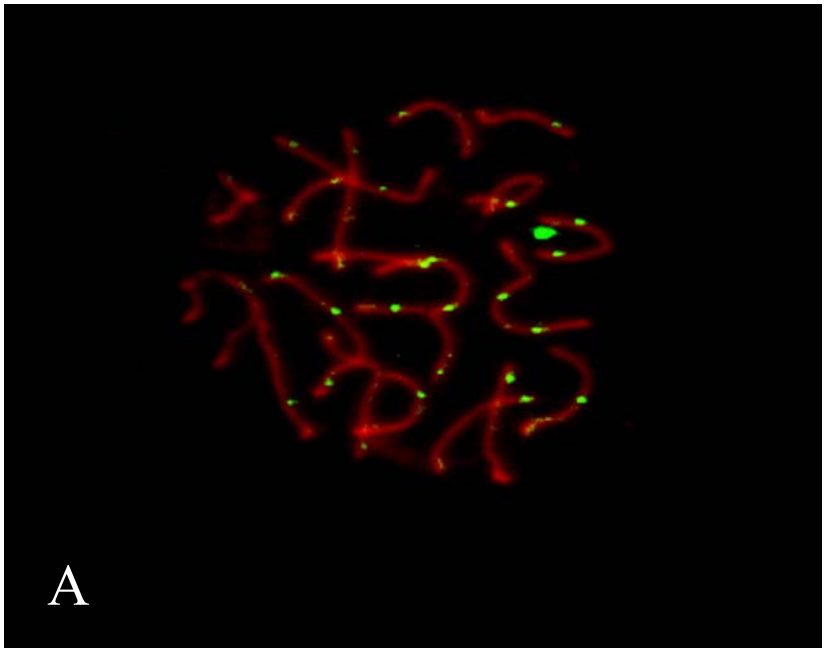
morphology and hyperhaploidy is inherited in a quantitative manner, perhaps due to more than one gene.

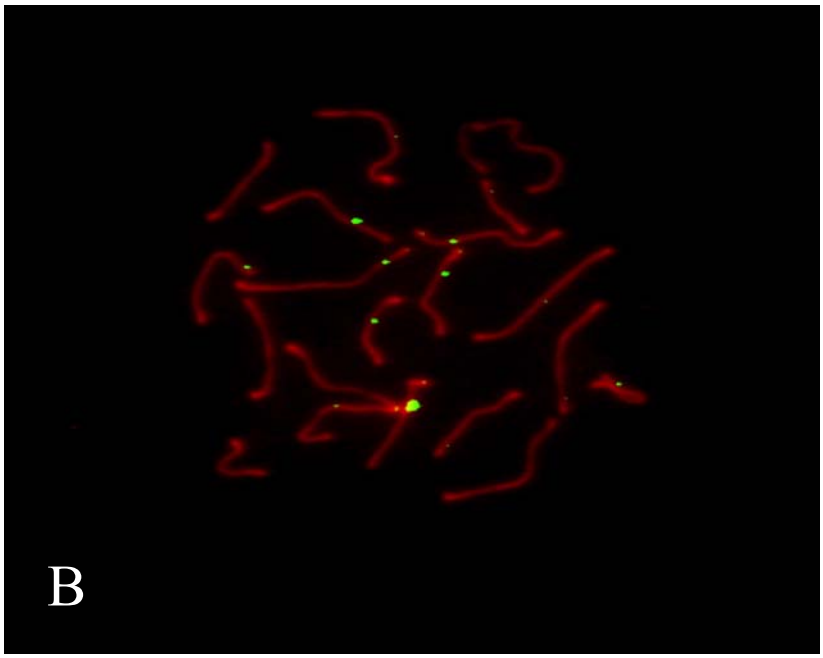
Since the inheritance pattern is complex, how aneuploidy might arise in PL/J was examined using phenotypic analysis. Several factors can be associated with nondisjunction, as discussed previously, such as a decrease in recombination/chiasmata frequency and spindle-associated abnormalities. Each of these was assessed in PL/J males. The following phenotype analysis will help in understanding the genetic complexity in PL/J mice, as well as players that may be associated with causing nondisjunction.

Spermatocytes in PL/J males exhibit prophase abnormalities including reduced MLH1 foci and chiasmata frequency, and asynapsis

In order to examine features that could be associated with an increase in malsegregation of chromosomes in PL/J male mice, recombination frequency was assessed cytologically. This experiment was performed to determine if there is a significant difference between recombination in PL/J compared to B6 spermatocytes, since a decrease in recombination has been shown to be associated with nondisjunction (Hassold and Sherman, 2000). The recombination frequency was determined by counting MLH1 foci, since the MLH1 protein has been shown to correlate with previous studies on chiasmata number and to be representative of sites of recombination in spermatocytes (Anderson et al., 1999). A decrease in MLH1 foci was found in PL/J spermatocytes compared to B6 spermatocytes (Fig. 4). Spermatocytes from PL/J mice

Figure 4. PL/J males exhibit lower numbers of MLH1 foci than do B6 males. A shows SC axes from a B6 spermatocyte with 26 MLH1 foci and B shows SC axes from a PL/J spermatocyte with 19 MLH1 foci.


A


B

(n=3, 30 spermatocytes ea.) have statistically lower number ($p<.05$) of MLH1 foci, with a mean of 19.8 +/- 1.8, compared to control B6 males, where the mean is 22.45 +/- 1.6 foci (Fig. 5). The range of foci number in PL/J is from 17-23, whereas in B6 the range is from 20-26, further evidence for a decrease.

Chiasmata counts were examined in PL/J, since chiasmata represent visual manifestations of crossover. This was done to determine if there is also a decrease in the number of chiasmata in PL/J and if the chiasmata counts correlated with the decrease in recombination as was measured by staining with an antibody against MLH1. Chiasmata number was determined by examining air-dried chromosome preparations (Fig. 6). Fewer chiasmata were scored on chromosomes from PL/J males, with a range of 12-21 compared to a range of 19-23 chiasmata on chromosomes from B6 spermatocytes. Interestingly, the number of chiasmata scored is less than the number of MLH1 foci scored. This could be because chromosomes from PL/J males were often in a MII-like configuration. Instead of appearing as tight bivalents, the chromatin looks "loose" and the regions that are forming chiasmata are not "tight" chiasmata and therefore not easily scoreable. Since the chiasmata are not easily visible and the chromosomes are not forming complete bivalents, they instead appear similar to sister chromatids, with absent chiasmata.

Often when recombination does not occur properly or chromosomes do not appear as complete bivalents, other abnormalities may be present, such as the inability to completely pair prior to initiation of recombination in prophase. To test this, PL/J spermatocytes were examined for characteristics of synapsis such as complete synaptonemal complex (SC) formation during prophase of meiosis. The SC is involved

Figure 5. PL/J spermatocytes have statistically lower numbers of MLH1 foci per spermatocyte than do B6 spermatocytes. The difference is significant at $p < 0.05$ (n=3, 30 spermatocytes scored from each). Error bars represent standard error and data were tested for significance using students t-test analysis.

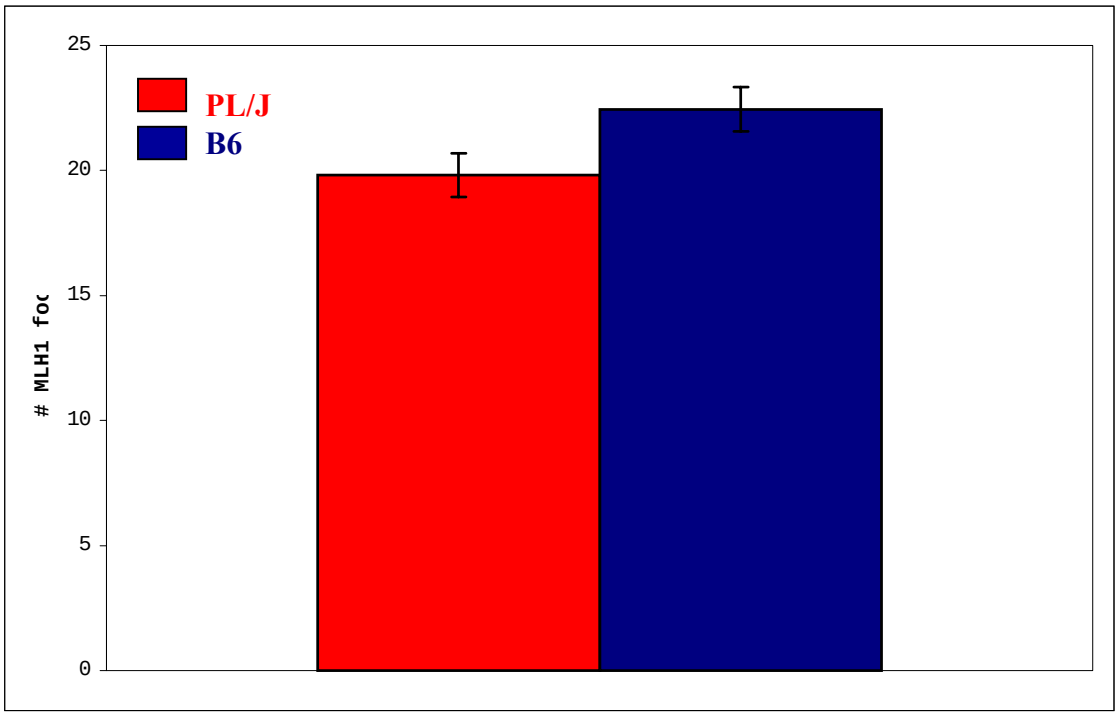
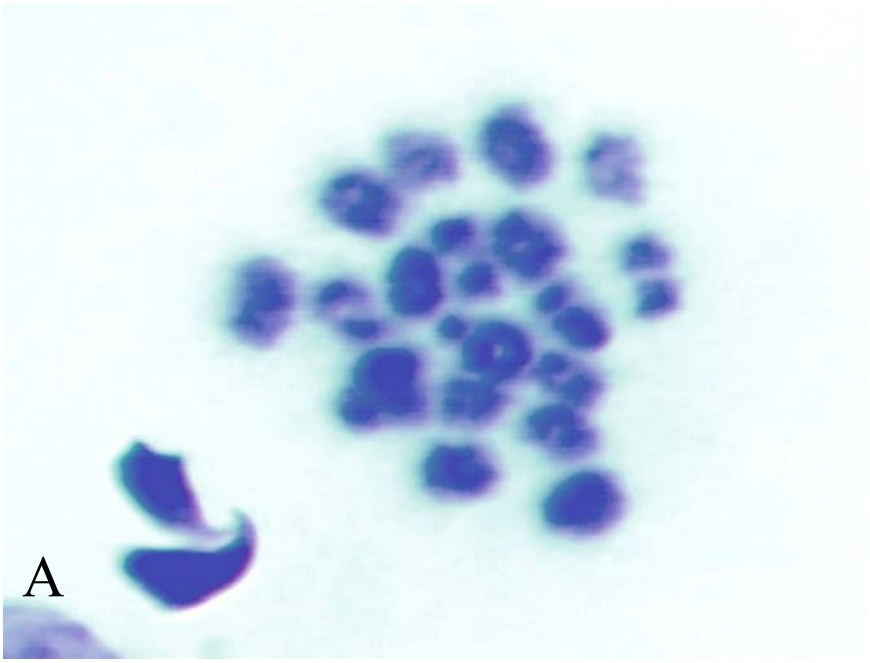
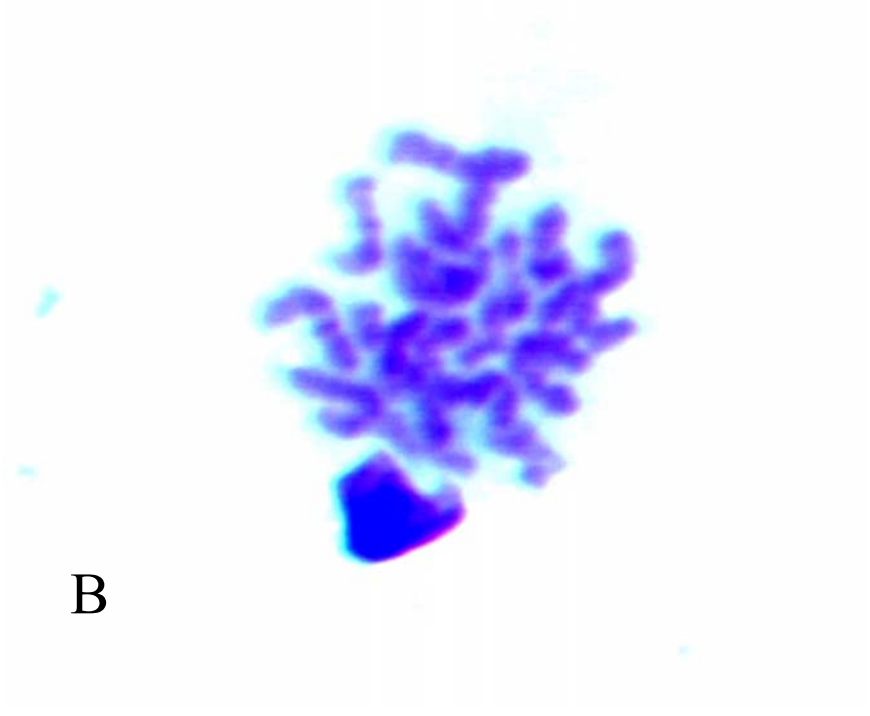

25
20
15
10
5
0
MLH1 foc
PL/J
B6

Figure 6. Air-dried chromosome preparations revealed a decrease in chiasmata in metaphase I PL/J spermatocytes compared to B6 spermatocytes. In A, B6 chromosomes have a normal chiasmata count (21), as compared to B, where PL/J chromosomes have a reduction in the number of chiasmata (16). Note also in B, that the chromosomes are not normally condensed, appearing more like metaphase-II chromosomes, with chiasmata not as easily visible.


A


B

in ensuring complete association of homologous chromosomes during prophase. Analysis of the SC was accomplished using antibodies against SYCP3 and SYCP1, proteins of the synaptonemal complex. Fig. 7 shows spermatocytes from PL/J males stained with an antibody against SYCP3, revealing regions of autosomal asynapsis (regions that do not pair properly between homologous chromosomes). The SC antibody, SYND1, is useful because its staining is only present in regions of synapsis, therefore where asynapsis occurs SYND1 staining disappears (data not shown). Overlay of the two antibodies revealed regions of asynapsis in PL/J spermatocytes. In order to determine the timing of asynapsis, spermatocytes were stained with antibodies against H1t and SYCP3. H1t is a testis-specific histone that first appears at mid-pachytene, and is therefore a good marker for staging pachytene spermatocytes. 91% of spermatocytes with regions of asynapsis did not stain with the antibody against H1t. Cells with complete synapsis stained with H1t. Since appearance of H1t starts in mid-pachytene, it is most likely that asynapsis rather than desynapsis is occurring in PL/J spermatocytes. This would indicate a problem in finding/pairing with the correct homologous partner. Control spermatocytes revealed complete pairing during prophase as expected. However, PL/J spermatocytes had an average of 19.3% spermatocytes with asynapsis as compared to 2.15% for B6 spermatocytes (Fig. 8). Only pachytene spermatocytes were examined to ensure no confusion with the normal desynapsis (unpairing regions) that occurs in diplotene spermatocytes.

Figure 7. PL/J spermatocytes exhibit small regions of asynapsis (arrows), as shown with staining with an antibody to SYCP3.

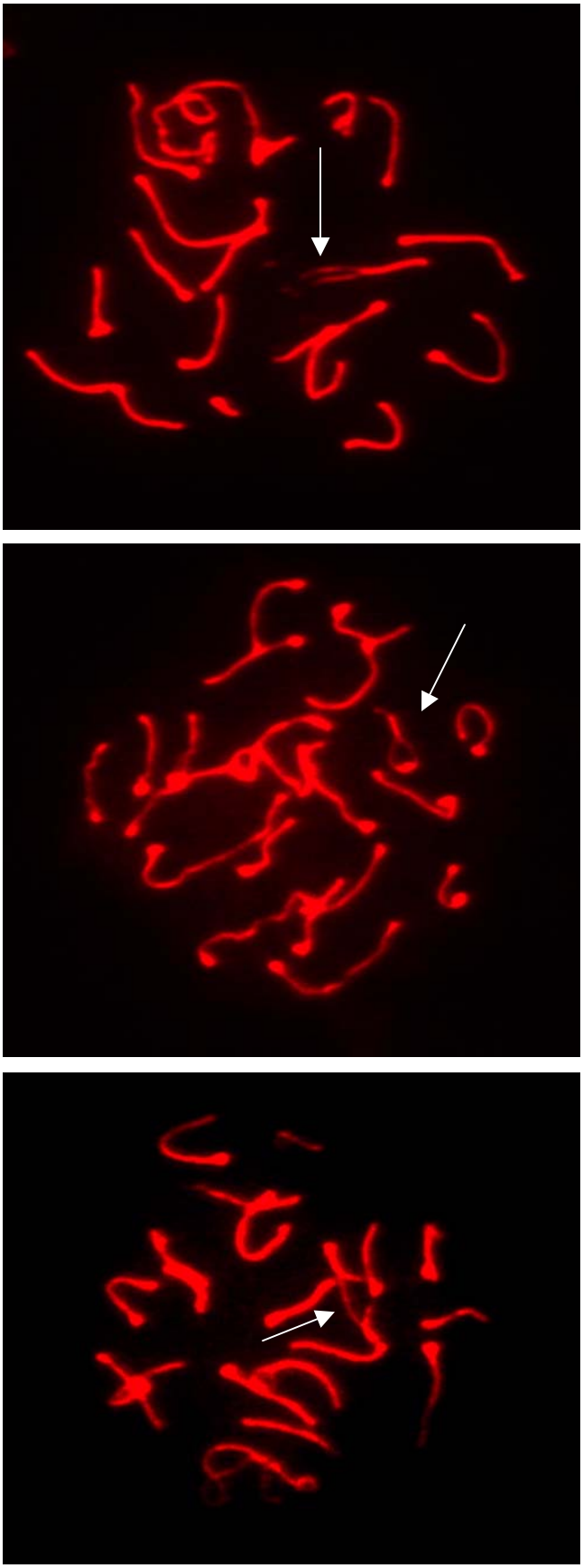
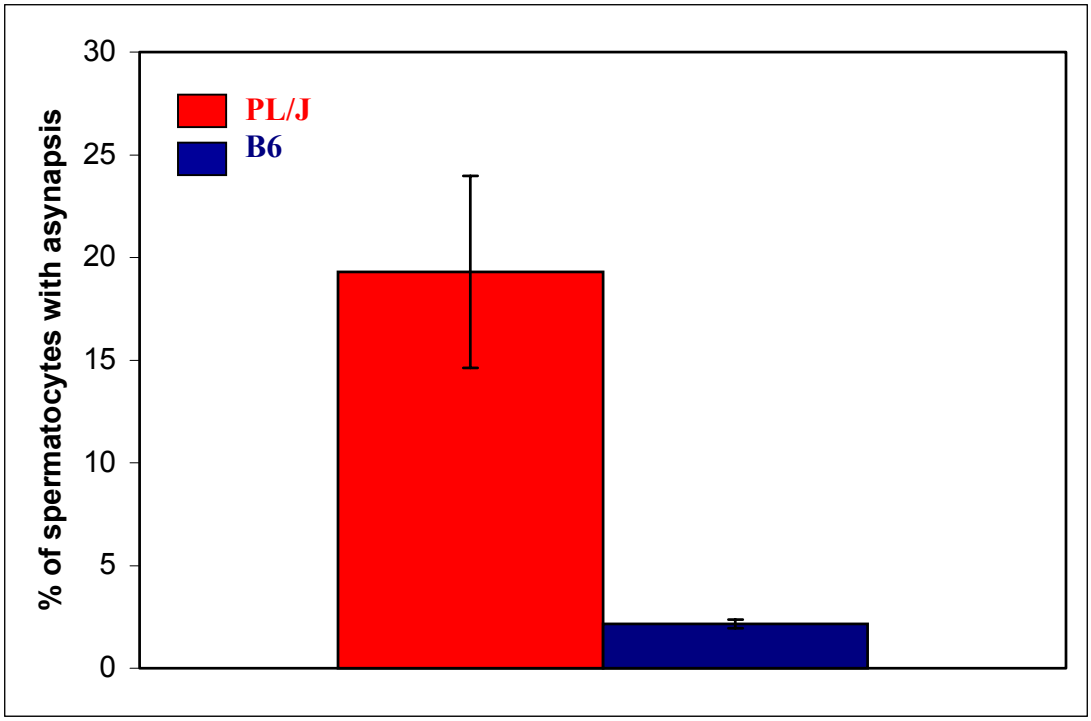


Figure 8. More PL/J spermatocytes exhibit regions of asynapsis than do B6 spermatocytes. PL/J spermatocytes have an average of 19.3% spermatocytes with asynapsis as compared to 2.15% for C57 spermatocytes (n=3 mice, 50 spermatocytes scored for each). Error bars represent standard deviation and data were tested for significance using students t-test analysis.

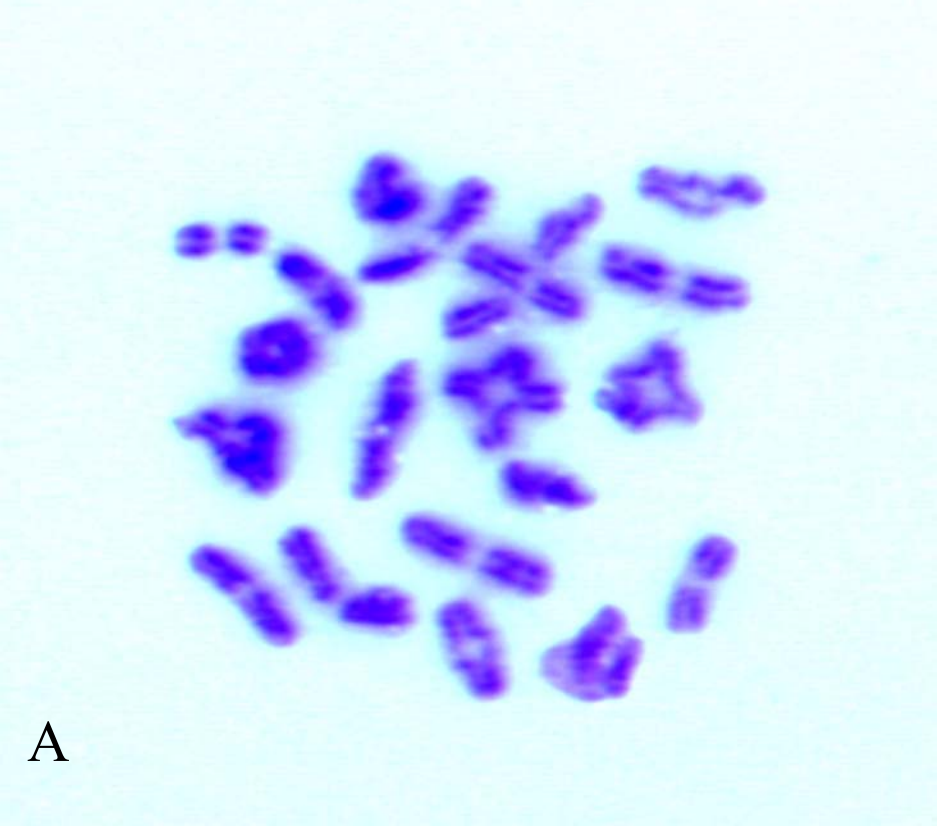

30
25
20
15
10
5
0
% of spermatocytes with asynapsis
PL/J
B6

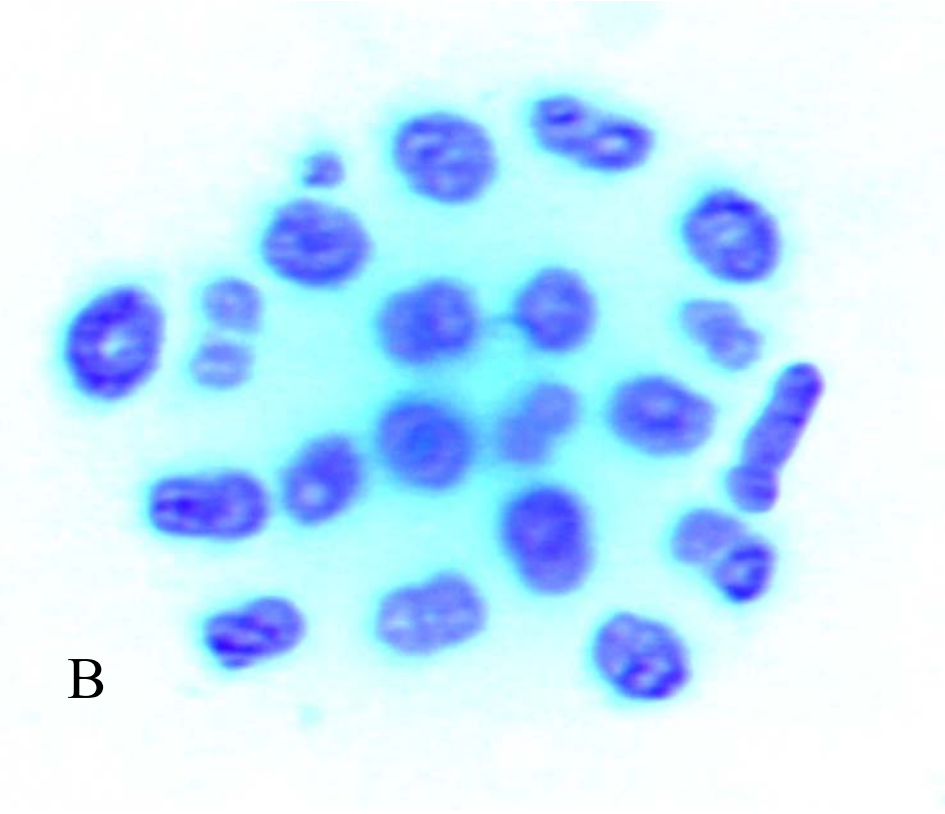
PL/J metaphase chromosomes are not competent to properly condense after treatment with okadaic acid and are present as univalents

Previous results from our laboratory have established an assay for spermatocyte meiotic competence (Cobb et al., 1999a). We have used this assay to answer whether PL/J spermatocytes have reached the point of meiotic competence to condense to bivalent chromosomes and also if the correct chromosome configuration can be achieved. Briefly, isolated mixed germ cells from control B6 and PL/J males were treated with the protein phosphatase inhibitor okadaic acid in order to determine if chromosomes from PL/J are able to condense to a MI configuration after treatment with the inhibitor. Chromosomes from PL/J are not fully competent to condense to proper metaphase bivalents as compared to B6 (Fig 9). The chromosomes appear as if they are beginning to condense since chromosomes are visible, but neither the chiasmata nor the chromosomes are in a "tight" configuration. Therefore, chiasmata are not readily visible in chromosomes from PL/J compared to B6. PL/J chromosomes appear to have "loose" chromatin instead of forming tight, condensed chromosomes with proper chiasmata. Therefore, PL/J spermatocytes are not completely meiotically competent after treatment with okadaic acid, and do not condense to proper metaphase bivalents.

Since the presence of univalents is associated with nondisjunction, PL/J metaphase chromosomes were analyzed for the presence of univalents (testicular not OA induced MI's). Paint probe analysis for chromosomes 8 and 2 was used to determine if chromosomes can be found as univalents at MI. PL/J MI chromosomes were shown to have an elevated frequency of univalents. Univalents are easily visible, since signals are joined in a bivalent and separated if a univalent is formed. Chromosomes were only

Figure 9. Air-dried chromosome preparations revealed that chromosomes from PL/J spermatocytes after treatment with the protein phosphatase inhibitor okadaic acid are not completely competent to condense metaphase chromosomes, as are control C57 metaphases. A represents chromosomes from a C57 MI spermatocyte and B represents chromosomes from a PL/J MI spermatocyte after treatment with OA.


A


B

scored as univalents if the signals were separated by at least one domain (one signal can fit in between each signal). In Fig. 10, an example is shown of abnormal chromosome configuration during MI. In A, the chromosomes are pairing correctly, whereas in B, chromosomes 8 and 2 are not pairing correctly forming univalents. Thirty-two percent of MI chromosomes in PL/J males (n=2) are not pairing correctly and are forming univalents (Table 3).

PL/J spermatocytes exhibit many division-phase and spindle abnormalities

Since 3.4% of PL/J sperm are aneuploid for chromosomes 8 or X and Y, attachment of the chromosomes to the spindle in PL/J was examined. This was monitored because previous results have shown that a characteristic of aneuploidy is failure of proper attachment of chromosomes to the spindle (Eaker et al., 2001). Immunofluorescence and confocal studies, using an antibody against phosphorylated histone H3, revealed that a high percentage of chromosomes are unaligned or are not properly positioned at MI. In Fig. 11, examples are shown of PL/J MI spermatocytes with unaligned chromosomes as compared to control MI spermatocytes from B6. One example, in Fig.10B, the chromosomes are seen lagging behind a spindle pole. 13% of PL/J spermatocytes (n=3, 1000 ea.) have one or more unaligned chromosomes at MI (Fig. 12). The unaligned chromosomes can be seen off the spindle apparatus or lagging behind a spindle pole, measured by H3 staining.

In addition to unaligned chromosomes, MI spermatocytes of PL/J also exhibit markedly different spindle structures than do B6 MI spermatocytes. Spindle

Figure 10. Chromosome pairing in PL/J MI spermatocytes are shown in A and B. These images represent MI spermatocytes stained with paint probes for chromosomes 8 and 2. In A, chromosomes 8 and 2 are pairing correctly. In B, chromosomes 8 and 2 are not pairing correctly, forming univalents.

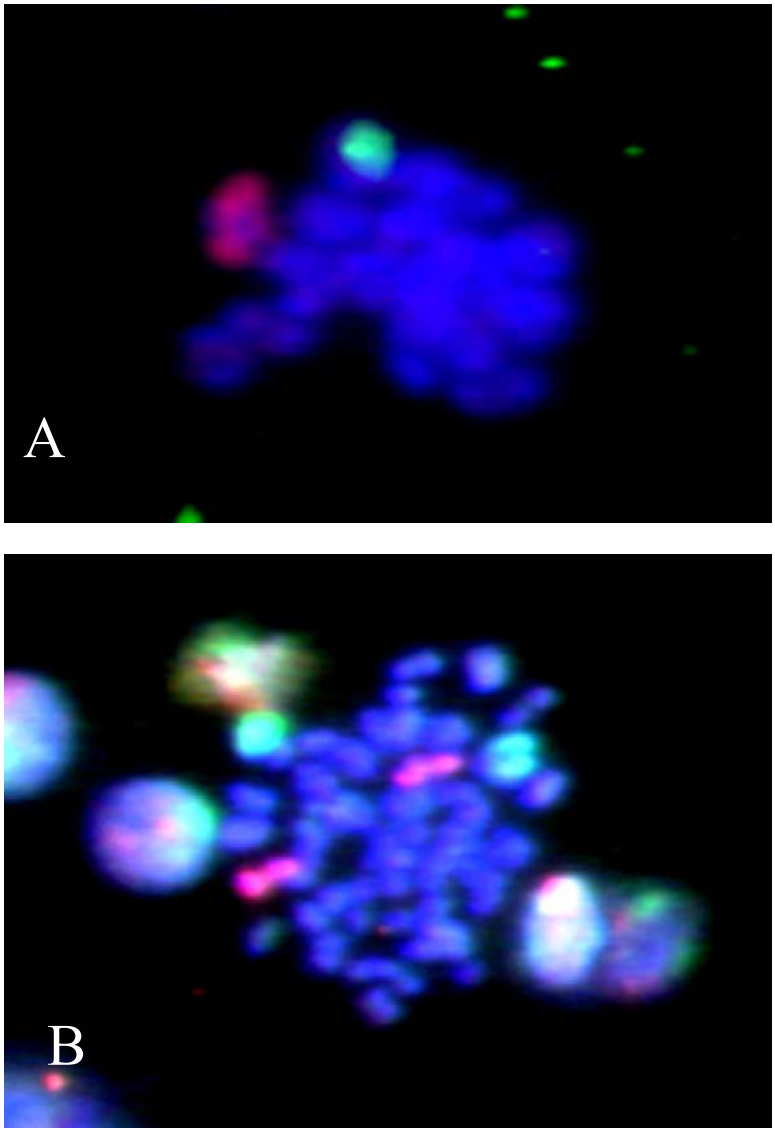
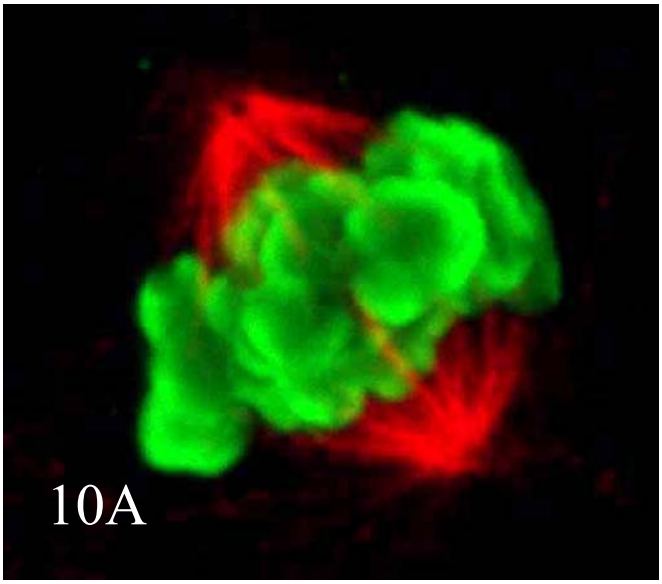
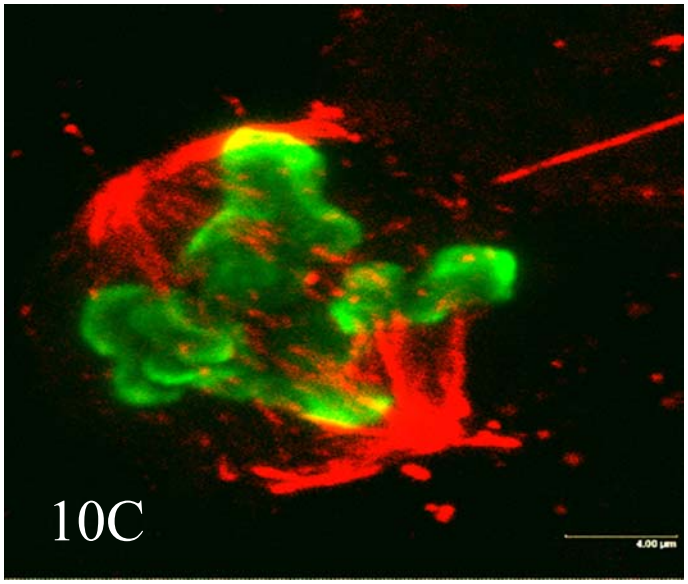

A
B

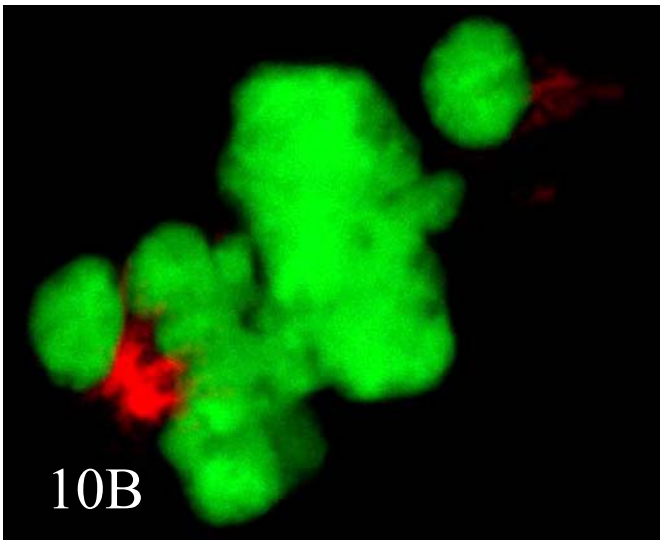
Table 3. A summary of FISH signal domains after paint probe analysis in MI spermatocytes from PL/J males (n=2).

Domain Description	Total # of cells
1 signal for each	21
2 close signals for chromosome 8 and two separated signals for chromosome 2	5
2 close signals for chromosome 2 and two separated signals for chromosome 8	2
All signals separated by more than one signal domain	3
Total # chr pairs scored	62
Total # abnormal chr. Pairs	13
Frequency of abnormal chr. pairs	21.00%

Figure 11. PL/J spermatocytes exhibit abnormalities in chromosome alignment on the spindle as well as defects in the spindle, as shown with antibodies against ß-tubulin (red) and phosphorylated histone H3 (green). The first confocal image illustrates a spindle from a C57BL/6J spermatocyte with a normal bipolar spindle and precise chromosomal alignment on the metaphase plate (11A). Examples of PL/J abnormal spindles include: a PL/J spindle with only one pole (11B); both abnormal alignment of chromosomes and irregular, dispersed spindle fibers (11C); and abnormal polar organization (11D), creating a "split" pole (arrow).


10A


10C


10B

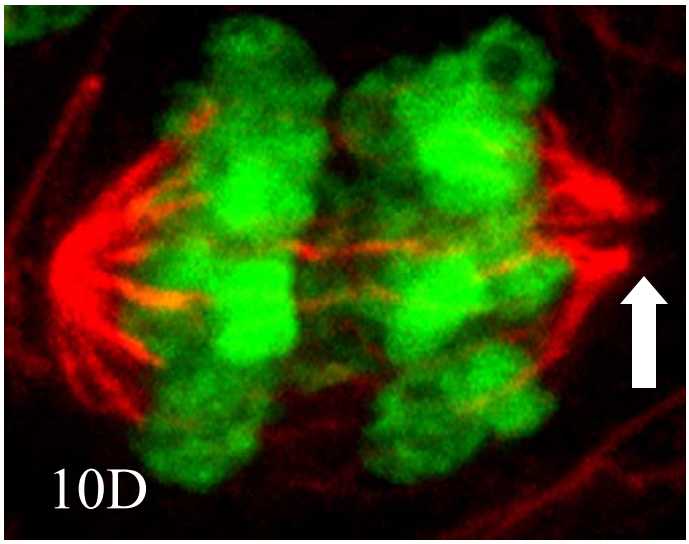
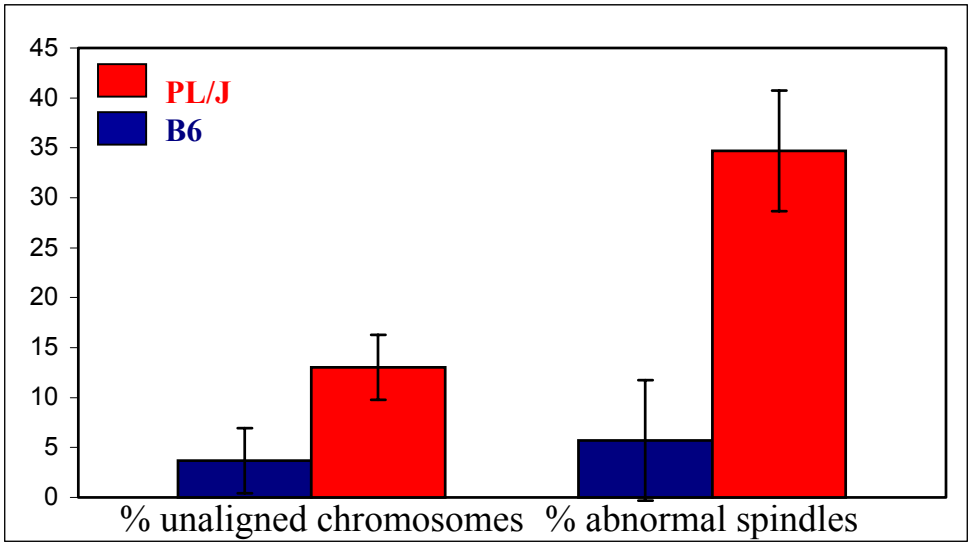

10D

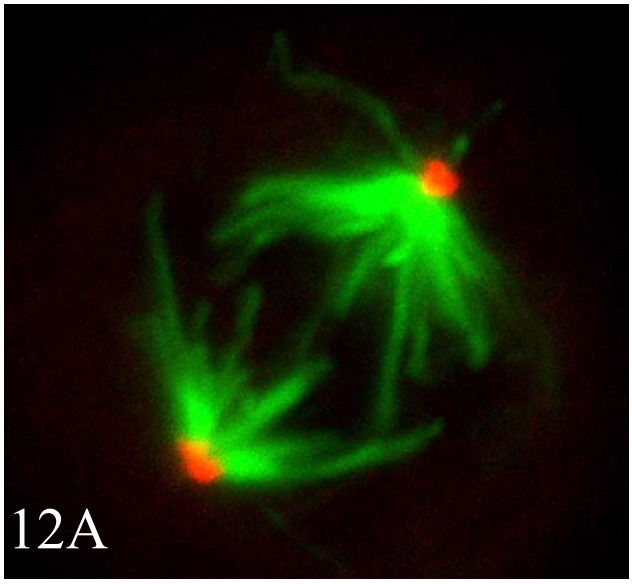
Figure 12. The frequency of unaligned chromosomes and abnormal spindles is significantly higher in PL/J MI spermatocytes than among C57BL/6J MI spermatocytes.

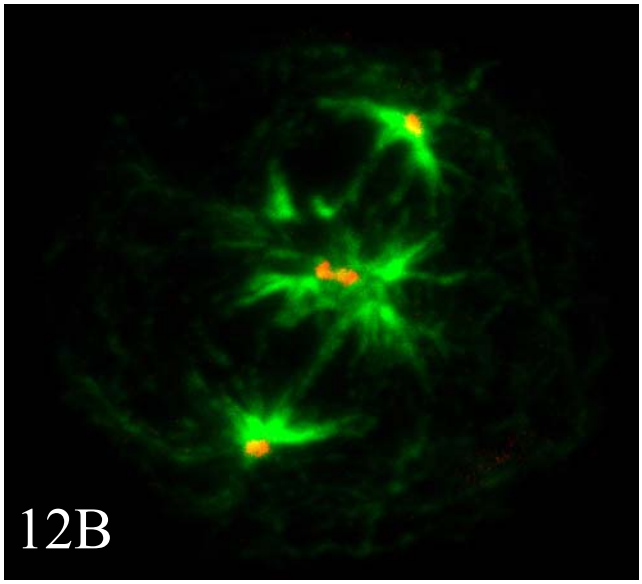

45
40
35
30
25
20
15
10
5
0
PL/J
B6
% unaligned chromosomes
% abnormal spindles

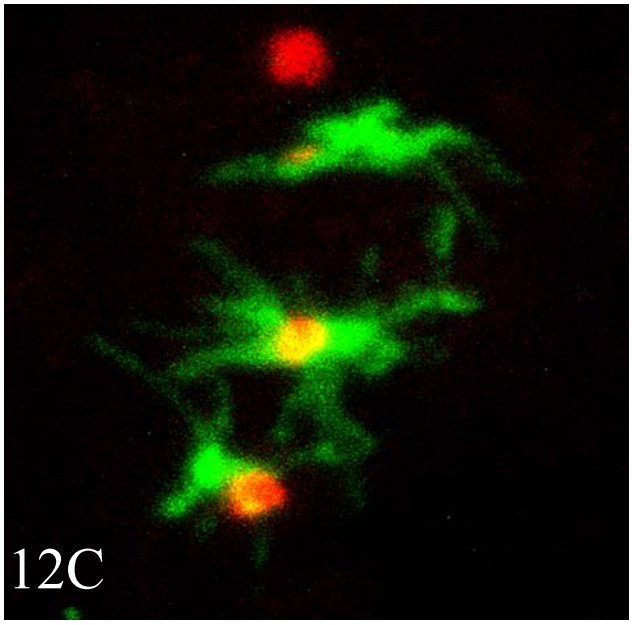
abnormalities were examined by confocal and immunofluorescence staining with antibodies against spindles seen in PL/J MI spermatocytes is microtubules not completely formed on one side or monopolar spindles. This is shown in Fig. 11B where one pole is present, although abnormal, and the other pole is not present. The abnormal spindles also usually have "choppy" microtubules that look as if they have not been formed completely (Fig. 11C). The abnormalities in spindle structure also include splitting or abnormal polar organization. An example is depicted in Fig. 11D, where an anaphase cell is shown with normal chromosome alignment, but abnormal polar organization as depicted by the arrow. 34% of PL/J (n=3, 1000 ea.) MI spermatocytes were found to have abnormal spindles (Fig. 12). To further examine characteristics of spindles in PL/J males, spindle poles were examined as a measure of spindle pole formation.

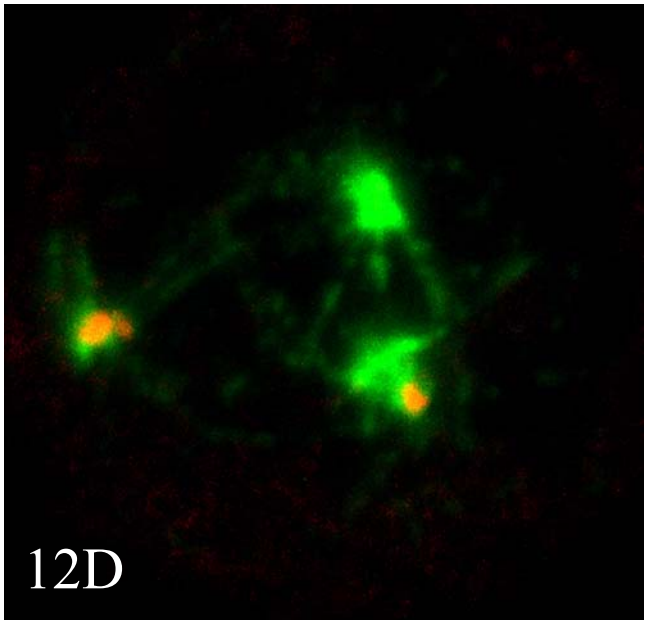
Spindle poles were observed by using an antibody against the centrosome (pericentrin). This is valuable, because increased amounts of pericentrin have been shown to be associated with genetic instability and aneuploidy in cancer cells. Specifically, one group found that concentrations of pericentrin are higher than normal in prostate and other cancers (Pihan et al., 2001). Therefore, it was of interest to determine if abnormal centrosome numbers were also present in PL/J spermatocytes. Fig. 13 represents confocal images from MI PL/J and B6 spermatocytes stained with antibodies against ß-tubulin and pericentrin. In Fig. 13A, the B6 control spermatocyte is normal with two pericentrin foci and spindle fibers. Fig. 13 B-D represent PL/J MI spermatocytes with abnormal pericentrin staining. In Fig. 13 B, there are four pericentrin foci and four spindles (two spindles with pericentrin foci are connected). In Fig. 13 C,

Figure 13. These confocal images of metaphase I spindles from both C57BL/6J and PL/J spermatocytes show spindle pole abnormalities revealed by staining with antibodies against pericentrin (red) and ß-tubulin (green). In 13A, the C57BL/6J spermatocyte is normal with two pericentrin foci and aligned spindle fibers. The remaining images are of PL/J spermatocytes, where abnormalities include supernumerary pericentrin foci and spindles (13B), pericentrin foci not associated with a spindle pole (13C), a spindle pole without a pericentrin focus (13D), and multiple pericentrin foci and spindle poles (13E). Although only 0.63% of C57BL/6J spermatocytes have more than 2 pericentrin foci, 9.75% of PL/J MI spermatocytes have greater than two pericentrin foci.

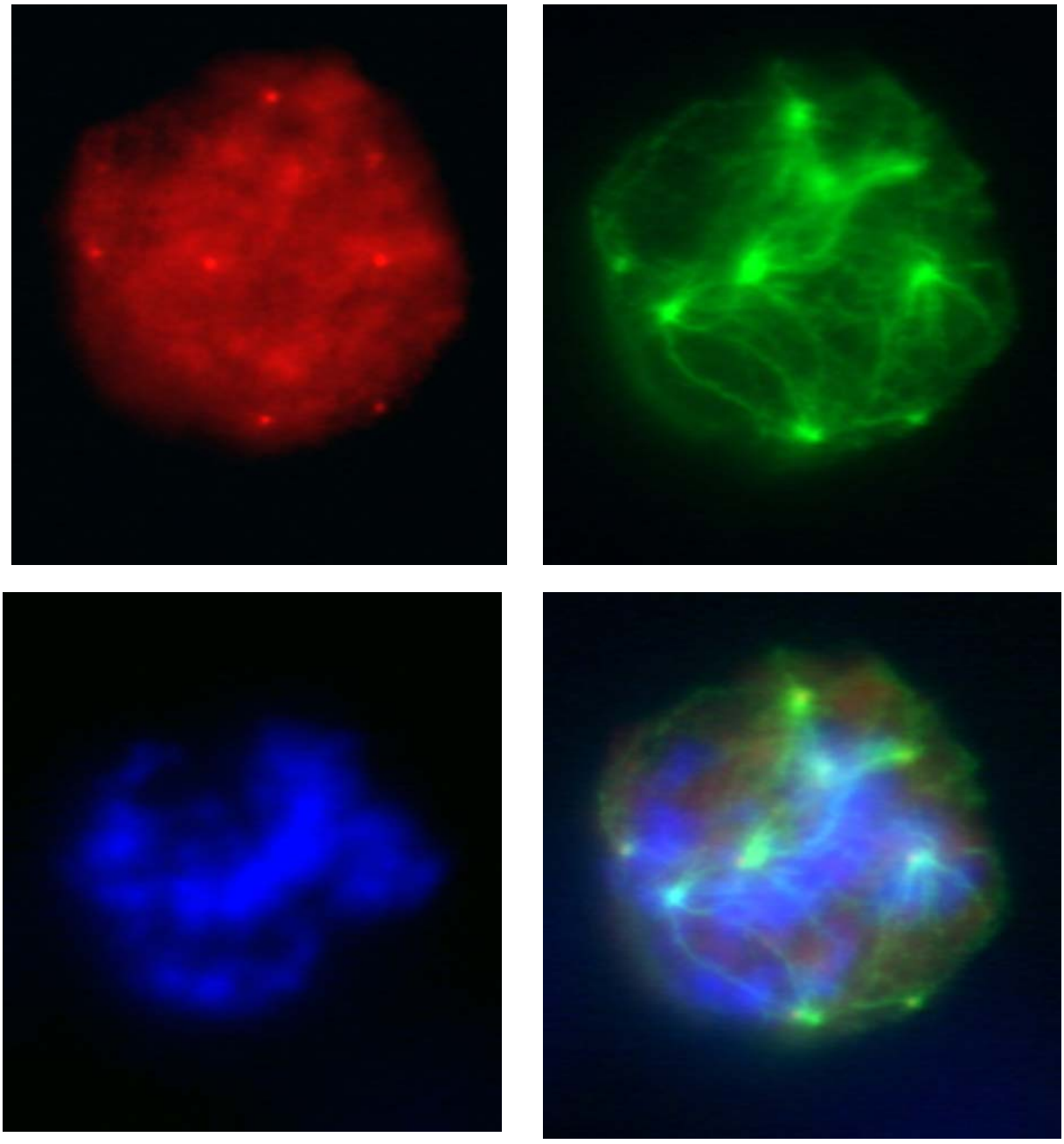

12A


12B


12C


12D

12E



there are three pericentrin foci and three spindles, but one pericentrin focus is not associated with a spindle pole. In Fig. 13 D, there are three spindle poles and two pericentrin foci. In Fig. 13E, there are multiple spindles and pericentrin foci (~8). In this spermatocyte, the DNA (as shown by staining with DAPI) is being pulled to several different poles. This is a characteristic often present in abnormal cancer cell lines with aneuploidy. A total of 9.75% of MI spermatocytes from PL/J (n=3) have greater than the normal two pericentrin foci as compared to 0.625% for C57 MI spermatocytes. The abnormalities seen with pericentrin staining could then be an indicator of genetic instability in PL/J spermatocytes. The increased numbers of centrosomes may also be associated with abnormalities seen in spindle morphology.

PL/J spermatids are apoptotic as revealed by the TUNEL assay

Since there are so many phenotypic abnormalities in PL/J, it was reasoned that there could be a mechanism of elimination of abnormal spermatocytes. The TUNEL method was used to stain tubule sections for apoptosis. Surprisingly, neither division stage cells (stage 12) nor MI cells stained positive for apoptosis. However, a significant number of spermatids were found to be apoptotic. Fig. 14 depicts apoptotic spermatids from PL/J with an increased FITC signal seen only on spermatids. Tubule sections were scored as apoptotic if the tubule section had >3 apoptotic spermatids per tubule cross section. The frequency of tubules with apoptotic spermatids is 11% in PL/J, but only 5% in control B6 testes(n=3, 500 sections each), Fig. 15. Therefore, one method of elimination for abnormalities seen in PL/J is possibly at the spermatid stage of spermiogenesis (differentiation of round spermatids to sperm), however complete

Figure 14. Apoptosis of spermatids in PL/J testes. This image represents a sectioned testis from PL/J mice. The tubule section is stained with FITC-dUTP, which recognizes apoptotic cells and DAPI, a general DNA stain. Spermatids in PL/J testes have increased FITC signals (arrow) revealing that they are apoptotic.

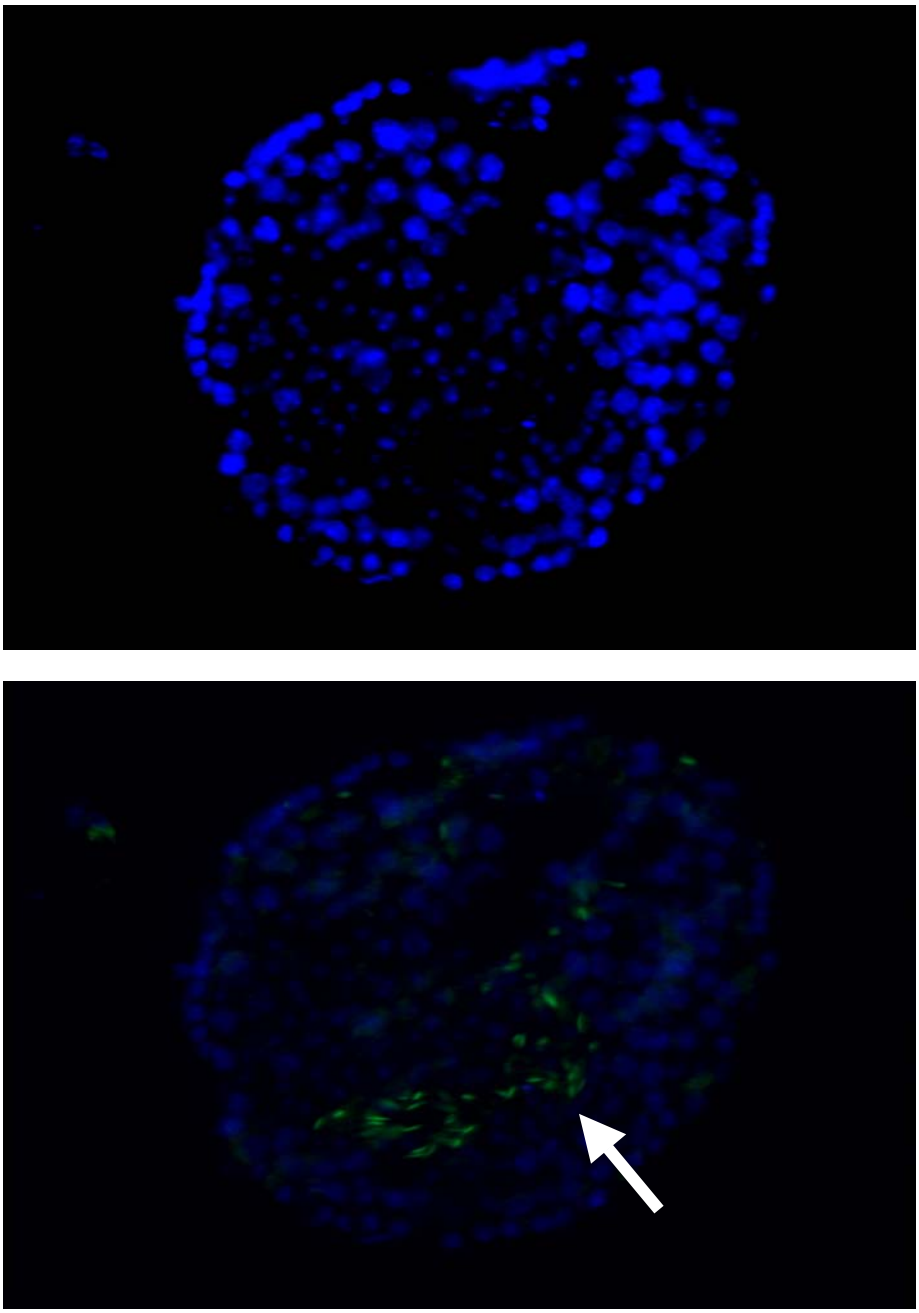
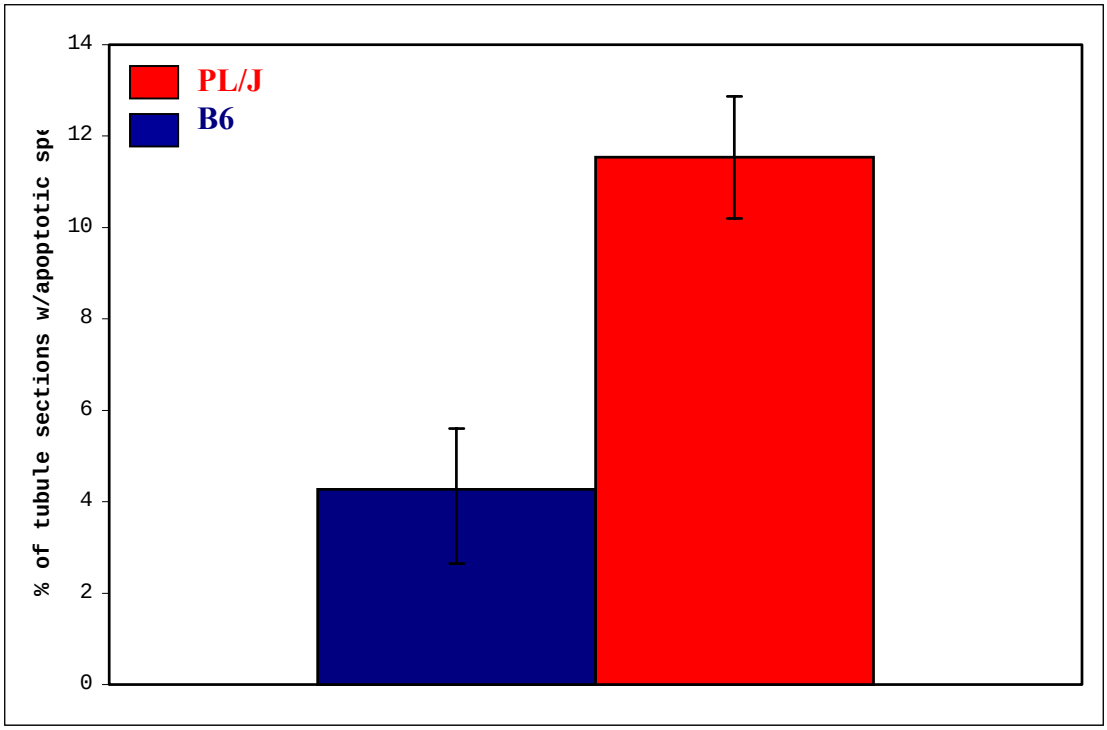


Figure 15. Frequency of apoptosis in PL/J spermatids. Spermatids from PL/J (n=3 mice) have an increase in apoptosis of 10.85%, compared to C57 with 5% apoptotic spermatids.


PL/J
B6
% of tubule sections w/apoptotic sp
14
12
10
8
6
4
2
0

elimination of aneuploid or abnormal sperm does not occur since both types of sperm are still produced.

CHAPTER IV

DISCUSSION

Complex inheritance of sperm aneuploidy and abnormal sperm-head morphology

In this study, we have validated PL/J males as a model for both gamete aneuploidy and abnormal sperm-head morphology. Abnormalities seen in PL/J males are complex both genetically and phenotypically. We have documented abnormal sperm-head morphology and increased nondisjunction in the sperm of PL/J mice. Genetically the dissection of these abnormalities is complex. We performed crosses to C57BL/6J mice to determine the mode of inheritance of the traits of abnormal sperm-head morphology and nondisjunction. We expected that the traits would be inherited in a simple mendelian pattern of inheritance due to analysis of transmission of other meiotic abnormalities studied in infertility research. For example, in one human family with asynapsis and spermatogenic abnormalities, the trait of asynapsis was inherited as autosomal recessive (Chaganti et al., 1980). However in PL/J males, analysis of the F1 and backcross progeny show that the inheritance of sperm aneuploidy and abnormal sperm-head morphology is not a simple matter; i.e. there is no clear dominant or recessive pattern of inheritance. One possibility is that the traits are due to more than one gene in a quantitative manner, although we have not seen any mice with an increase in abnormal sperm head morphology or aneuploidy like that of PL/J males. The backcross analysis shows that there is not an increase in the frequency of abnormal sperm-head morphology as compared to the increases seen in aneuploidy frequency. This may be due to more than one gene controlling the expression of the trait/s of abnormal sperm-head

morphology separate from the gene/s involved in aneuploidy. There also might be a small semi-dominant effect in the F1s as seen by a slight increase over control B6 males in the percentage of hyperhaploidy. This would again indicate that separate gene/s were controlling aneuploidy, since this is not seen in the F1 analysis of abnormal sperm-head morphology. The genetic analysis thus shows that inheritance of the traits for sperm aneuploidy and abnormal sperm-head morphology are inherited in a complex manner.

Pachytene abnormalities: decreased recombination and chiasmata, asynapsis

In addition to the genetic complexity, this study has shown that there are numerous abnormalities during meiosis in PL/J males. PL/J spermatocytes have difficulties in proper segregation of chromosomes. What could be causing nondisjunction in PL/J? This could be attributable to both the asynaptic defects and decreased recombination seen in PL/J spermatocytes. Numerous studies have correlated a decrease in recombination with nondisjunction (Hassold and Sherman, 2000; Hassold et al., 1991), and for review see (Hassold et al., 2000). PL/J males have a statistically significant ($p<.05$) decrease in recombination as measured by MLH1 foci, with a mean of 19.8 +/- 1.8, compared to control B6 males, where the mean is 22.45 +/- 1.6 foci (Fig. 4). The range of foci number in PL/J is from 17-23, whereas in B6 the range is from 20-26. The range is especially interesting, since B6 spermatocytes never have below 20 MLH1 foci, further suggesting that PL/J males have altered recombination. Chiasmata counts are also less than the MLH1 foci. This could be due to the difficulties in counting chiasmata in PL/J since the chromosomes do not appear as tight bivalents. Also in the study by (Anderson et al., 1999), it was suggested that the increased length of the synaptonemal complex over the diakinesis bivalent makes MLH1 focus analysis a more

accurate method of estimating exchange frequency than chiasmata counts. Therefore, the MLH1 foci analysis may be more accurate in representing the reduction in recombination found in PL/J spermatocytes.

There may also be a connection between asynapsis and inability to recombine properly. Since homologous chromosomes in mice pair and recombine, it is possible that if pairing is not complete, initiation and completion of proper crossover may not occur. One study showed that homologous pairing is reduced in asynaptic mutants of yeast, but how this affects recombination is not well understood (Loidl et al., 1994). Chemical induction of damage has also been shown to result in aneuploidy by producing abnormal pairing and recombination. For example, colcemid was administered to gestational day 13 female mice to test effects on homologue pairing, synapsis and recombination of fetal oogenesis. Pairing abnormalities were detected in pachytene oocytes by light and electron microscopy examination of bivalents and synaptonemal complexes. There was also a reduction in the total chiasmata per treated diplotene oocyte (22.74) compared to controls (31.07) (Jagiello et al., 1989). Another study showed that with addition of colchicine to mouse spermatocytes, asynapsis occurred and resulted in aneuploidy (Tepperberg et al., 1999). It is therefore possible that the lack of proper synapsis could lead to the decrease seen in recombination and subsequent aneuploidy in PL/J males.

Chromosome condensation is altered in PL/J chromosomes

Defects in recombination or synapsis could lead to improper chromosome condensation and segregation of chromosomes during meiosis. PL/J males exhibit difficulties in proper chromosome condensation after treatment with okadaic acid.

Normally okadaic acid induces premature metaphase-I condensation of pachytene spermatocytes (Cobb et al., 1999a). It has also been shown that one of the requirements for successful division in mouse spermatocytes is proper chromosome condensation prior to alignment on the metaphase plate (Handel et al., 1999). Chromosome condensation is thought to occur after the spermatocytes have completed essential requirements in prophase of meiosis I, such as pairing and recombination. PL/J males are not competent as compared to control C57 males to condense proper metaphase bivalents, therefore the timing of condensation could be altered. Since asynapsis and recombination abnormalities are occurring in PL/J, the spermatocytes may not be ready or "competent" to condense properly since the requirements have not been completed correctly in prophase.

In addition, there could be mutations in genes required for successful condensation of chromosomes. An example could be a mutation in a topoisomerase-type I or II protein that is involved in removing torsional stress in DNA. If topoisomerase function is altered, then chromosomes may not be able to condense properly. For example, treatment of pachytene spermatocytes with teniposide, which inhibits topoisomerase II after the generation of DNA double strand breaks by the enzyme, results in little or no chromosome condensation (Cobb et al., 1997). Therefore, incompetence or inability to condense to proper metaphase bivalents could lead to the observed meiotic abnormalities in PL/J, possibly due to mutations in genes involved in ensuring proper chromosome condensation.

Division phase and spindle-associated abnormalities

Abnormal spindles are present in a high frequency (34%) in PL/J MI spermatocytes. There are multiple spindle abnormalities seen, including monopolar, incomplete formation of spindles, "choppy" microtubules, and split-spindle poles. There have been several studies in which abnormal spindles are present, chemically-induced or spontaneously formed, however the role of abnormal spindles during meiosis is not well understood (Yin et al., 1998; Eichenlaub-Ritter and Winking, 1990). It is possible that the abnormal spindles are formed as a result of unaligned chromosomes. A similar situation occurred in *Mlh1* knockout mice, in which the spindles were highly abnormal as a result of improper congression of chromosome at the metaphase I plate. In the absence of the MLH1 protein, meiotic recombination was dramatically reduced, and as a result, the vast majority of chromosomes were present as unpaired univalents at the first meiotic division (Baker et al., 1996). The orientation of these univalent chromosomes at prometaphase suggested that they were unable to establish stable bipolar spindle attachments, presumably due to the inability to differentiate functional kinetochore domains on individual sister chromatids. In the presence of this aberrant chromosome behavior a stable first meiotic spindle was not formed, the spindle poles continued to elongate, and the vast majority of cells never initiated anaphase. These results suggested that, in female meiotic systems in which spindle formation is based on the action of multiple microtubule organizing centers, the chromosomes not only promote microtubule polymerization and organization but their attachment to opposite spindle poles acts to stabilize the forming spindle poles (Woods et al., 1999). Therefore one possibility is that the abnormal spindles found in PL/J MI spermatocytes could also form as a result of

abnormal chromosome orientation, which was present in PL/J MI spermatocytes at a frequency of 13%.

Several spindle-associated abnormalities are also seen in PL/J spermatocytes. We have documented abnormal numbers of the centrosomal-associated protein pericentrin in metaphase I PL/J spermatocytes. There are several systems in which there is a direct relationship between an abnormal number of centrosomes and development of aneuploidy in mitotic systems leading to tumor formation (Levine et al., 1991; Lingle et al., 1998). In fact, centrosome-associated kinases such as members of the aurora kinase and polo-like kinase families are thought to be likely candidates for increased activity at tumor centrosomes. These kinases are involved in regulating centrosome function and duplication, and their over expression is associated with the development of aneuploidy (Bischoff et al., 1998). Therefore abnormal expression of centrosomal proteins or pathways could lead to aneuploidy and possibly tumor formation. However, over expression of centrosome-associated kinases would most likely lead to dominant phenotypes and is therefore not likely to be the only factor associated with PL/J abnormal spindles. The centrosome may also play a role in maintenance and proper formation of spindle microtubules. It is possible that abnormal centrosome numbers seen in PL/J spermatocytes could then lead to abnormal or incomplete spindle formation in PL/J males.

Mechanism of elimination for abnormal spermatids

PL/J males do not seem to possess a checkpoint that monitors abnormal segregation of chromosomes occurring during meiosis. Evidence of a checkpoint would be the presence of apoptotic spermatocytes, most likely MI spermatocytes or division

phase spermatocytes (stage 12). We did not observe apoptosis in the spermatocytes of PL/J mice. However, we did see an increase in the percentage of apoptotic spermatids. This could be due to the abnormalities seen in abnormal sperm-head morphology in PL/J males. Since approximately 30% of sperm in PL/J are abnormal as measured by the sperm collected from the epididymides, there could be an even greater amount that are abnormal but eliminated at the spermatid stage of spermiogenesis by apoptosis. This checkpoint is faulty, since sperm with abnormal-head morphology are still produced. However, this may suggest that there are multiple checkpoints, in both meiosis and spermiogenesis. If that is the case, then why are the abnormal spermatocytes not getting eliminated during meiosis? There are many possible explanations, some of these being mutations in checkpoint proteins or apoptotic machinery as well as mutations in prominent biochemical pathway players. Some of these possibilities might help to explain the complexity we see genetically and phenotypically in PL/J males leading to sperm aneuploidy.

Conclusions on phenotypic and genetic complexity

PL/J males are a model for both abnormal sperm-head morphology and aneuploid sperm. It is clear that multiple abnormalities are seen phenotypically in PL/J males. During prophase, spermatocytes of PL/J mice exhibit chromosome asynapsis. At meiotic metaphase, there is reduced crossing over in PL/J spermatocytes. Additionally, during the first meiotic division, PL/J spermatocytes exhibit aberrant spindle morphology including monopolar spindles, split spindle poles and incomplete spindle formation. PL/J MI spermatocytes also exhibit abnormal numbers of centrosomes. It is not yet clear how

each of these abnormalities is related. The genetic analysis further shows complexity of inheritance of the traits of sperm aneuploidy and abnormal sperm-head morphology. Therefore there may be several genes or modifiers that contribute to the phenotypic complexity seen in PL/J males. Further studies are needed to determine how each abnormal trait is inherited and if each is inherited separately or independently.

Possible connections between autoimmune, leukemic, and spermatogenic disorders

PL/J mice were developed by Lynch from 200 non-inbred "Princeton" stocks, purchased in 1922, and developed as a high leukemia strain (Albert et al., 1965). PL/J males have also been found to show susceptibility to immunodeficiency and autoimmune disorders, particularly experimental allergic encephalomyelitis (EAE) (Lindsey, 1996). Since PL/J mice are often used as leukemic and autoimmune mouse models, the connection between these abnormalities and the spermatogenic defects observed are not clear. One possibility is that there is a larger genetic deficiency such as mutations in genes involved in converging biochemical pathways that may lead to abnormalities in gene expression or hormone levels that affect both spermatogenesis and immune regulation. Testicular cells can be regulated by factors such as growth hormones, neuropeptides and steroids. Several agents able to affect steroid production and spermatogenesis can also affect leukocytes, and many of the testis-regulating factors are produced by immune cells, suggesting that testicular cells and leukocytes may interact. The possibility that leukocytes may produce substances able to affect the testicular functions suggests that inhibition of immune system activation in the testis may be important also for reasons other than protection of auto antigenic germ cells from an

autoimmune attack (Maddocks et al., 1990). Therefore, regulation of immune and germ cells could be compromised in PL/J males leading to both spermatogenic and immune abnormalities or the two may be independently controlled.

An interesting recent development has shown that mice deficient for the p53-induced phosphatase gene, *Wip1*, exhibit defects in the testis, immune function and cell cycle control. *Wip1* message is expressed at high levels in the testes and the null mice show male reproductive atrophy, reduced fertility and diminished T and B cell function. Fibroblasts from *Wip1* null embryos have decreased proliferation and are compromised entering mitosis (Choi et al., 2002). Since a gene such as *Wip1* plays a role in spermatogenesis, lymphoid cell function, and cell cycle regulation it is possible that mutations in similar genes could lead to abnormalities seen in PL/J males. Whatever the connection between leukemia and spermatogenic abnormalities seen, it is clear that PL/J mice are complex both phenotypically and genetically. Therefore, it will continue to be a challenge to dissect the many phenotypes seen in PL/J males to help expand our knowledge of the mechanisms leading to meiotic aneuploidy.

LIST OF REFERENCES

Albert S, Wolf PL, Pryjma I, Moore W. 1965. Thymus development in high and low-leukemic mice. J Reticuloendothel Soc 2:218-237.

Anderson LK, Reeves A, Webb LM, Ashley T. 1999. Distribution of crossing over on mouse synaptonemal complexes using immunofluorescent localization of MLH1 protein. Genetics 151:1569-1579.

Baker SM, Plug AW, Prolla TA, Bronner CE, Harris AC, Yao X, Christie DM, Monell C, Arnheim N, Bradley A, Ashley T, Liskay RM. 1996. Involvement of mouse *Mlh1* in DNA mismatch repair and meiotic crossing over. Nat Genet 13:336-342.

Bischoff JR, Anderson L, Zhu YF, Mossie K, NG L, Souza B, Schryver B, Flanagan P, Clairvoyant F, Ginther C, Chan CM, Novotny M, Slamon DJ, Plowman GD. 1998. A homologue of Drosophila aurora kinase is oncogenic and amplified in human colorectal cancers. EMBO Journal 17:3052-3065.

Boyle AL, Ward DC. 1992. Isolation and initial characterization of a large repeat sequence element specific to mouse chromosome 8. Genomics 12:517-525.

Brown CR, Doxsey SJ, White E, Welch WJ. 1994. Both viral (adenovirus) and cellular (hsp 70, p53) components interact with centrosomes. Journal of Cellular Physiology 160:47-60.

Burkhart JG, Malling HV. 1981. Sperm abnormalities in the PL/J strain: A description and proposed mechanism for malformation. Gam Res 4:171-183.

Chaganti RSK, Jhanwar SC, Ehrenbard LT, Kourides IA, Williams JJ. 1980. Genetically determined asynapsis, spermatogenic degeneration, and infertility in men. Am J Hum Genet 32:833-848.

Choi J, Nannenga B, Demidov ON, Bulavin DV, Cooney A, Brayton C, Zhang Y, Mbawuike IN, Bradley A, Appella E, Donehower LA. 2002. Mice deficient for the wild-type p53-induced phosphatase gene (Wip1) exhibit defects in reproductive organs, immune function, and cell cycle control. Molecular and Cellular Biology 22:1094-1105.

Cobb J, Cargile B, Handel MA. 1999a. Acquisition of competence to condense metaphase I chromosomes during spermatogenesis. Develop Biol 205:49-64.

Cobb J, Miyaike M, Kikuchi A, Handel MA. 1999b. Meiotic events at the centromeric heterochromatin: histone H3 phosphorylation, topoisomerase II alpha localization and chromosome condensation. Chromosoma 108:412-425.

Cobb J, Reddy RK, Park C, Handel MA. 1997. Analysis of expression and function of topoisomerase I and II during meiosis in male mice. Mol Reprod Dev 46:489-498.

Disteche CM, Gandy SL, Adler DA. 1987. Translocation and amplification of an X-chromosome DNA repeat in inbred strains of mice. Nucl Acids Res 15:4393-4401.

Eaker S, Pyle A, Cobb J, Handel MA. 2001. Evidence for meiotic spindle checkpoint from analysis of spermatocytes from Robertsonian-chromosome heterozygous mice. J Cell Sci 114:2953-2965.

Eichenlaub-Ritter U, Winking H. 1990. Nondisjunction, disturbances in spindle structure, and characteristics of chromosome alignment in maturing oocytes of mice heterozygous for Robertsonian translocations. Cytogenet Cell Genet 54:47-54.

Eicher EM, Hale DW, Hunt PA, Lee BK, Tucker PK, King TR, Eppig JT, Washburn LL. 1991. The mouse Y* chromosome involves a complex rearrangement, including interstitial positioning of the pseudoautosomal region. Cytogenet Cell Genet 57:221-230.

Evans EP, Breckon G, Ford CE. 1964. An air-drying method for meiotic preparations from mammalian testes. Cytogenetics 3:289-294.

Fukasawa K, Choi T, Kuriyama R, Rulong S, GF VW. 1996. Abnormal centrosome amplification in the absence of p53. Science 271:1744-7.

Handel MA, Cobb J, Eaker S. 1999. What are the spermatocyte's requirements for successful meiotic division? J Exp Zool 285:243-250.

Hassold T, Hunt P. 2001. To ERR (Meiotically) is human: The genesis of human aneuploidy. Nat Rev Genet 2:280-291.

Hassold T, Sherman S. 2000. Down syndrome: genetic recombination and the origin of the extra chromosome 21. Clin Genet 57:95-100.

Hassold T, Sherman S, Hunt P. 2000. Counting cross-overs: characterizing meiotic recombination in mammals. Hum Mol Genet 9:2409-2419.

Hassold TJ. 1998. Nondisjunction in the human male. In MA Handel (ed): "Meiosis and Gametogenesis," 37. 525 B Street, Suite 1900, San Diego, CA 92101-4495: Academic Press Inc, pp 383-406.

Hassold TJ, Sherman SL, Pettay D, Page DC, Jacobs PA. 1991. XY chromosome nondisjunction in man is associated with diminished recombination in the pseudoautosomal region. Am J Hum Genet 49:253-260.

Hinchcliffe EH, Sluder G. 2001. "It takes two to tango": understanding how centrosome duplication is regulated throughout the cell cycle. Gene Develop 15:1167-1181.

Hsu LC, White RL. 1998. BRCA1 is associated with the centrosome during mitosis. Proc Natl Acad Sci USA 95:12983-12988.

Jagiello GM, Sung WK, Fang JS, Ducayen MB. 1989. Colcemid effects on homologue pairing and crossing over during fetal mouse oogenesis. Experientia 45:

Koehler KE, Hawley RS, Sherman S, Hassold T. 1996. Recombination and nondisjunction in humans and flies. Hum Molec Genet 5:1495-1504.

Lamb NE, Feingold E, Savage A, Avramopoulos D, Freeman S, Gu Y, Hallberg A, Hersey J, Karadima G, Pettay D, Saker D, Shen J, Taft L, Mikkelsen M, Petersen MB, Hassold T, Sherman SL. 1997. Characterization of susceptible chiasma configurations that increase the risk for maternal nondisjunction of chromosome 21. Hum Mol Genet 6:1391-1399.

LeMaire-Adkins R, Radke K, Hunt PA. 1997. Lack of checkpoint control at the metaphase/anaphase transition: A mechanism of meiotic nondisjunction in mammalian females. J Cell Biol 139:1611-1619.

Levine DS, Sanchez CA, Rabinovitch PS, Reid BJ. 1991. Formation of the tetraploid intermediate is associated with the development of cells with more than four centrioles in the elastase-simian virus 40 tumor antigen transgenic mouse model of pancreatic cancer. Proceedings of the National Academy of Sciences of the United States of America 88:6427-6431.

Lindsey JW. 1996. Characteristics of initial and reinduced experimental autoimmune encephalomyelitis. Immunogenetics 44:292-297.

Lingle WL, Lutz WH, Ingle JN, Maihle NJ, Salisbury JL. 1998. Centrosome hypertrophy in human breast tumors: Implications for genomic stability and cell polarity. Proc Natl Acad Sci USA 95:2950-2955.

Loidl J, Klein F, Scherthan H. 1994. Homologous pairing is reduced but not abolished in asynaptic mutants of yeast. J Cell Biol 125:1191-1200.

Maddocks S, Parvinen M, Soder O, Punnonen J, Pollanen P. 1990. Regulation of the testis. J Reprod Immunol 18:33-50.

Marx J. 2001. Cell biology. Do centrosome abnormalities lead to cancer? Science 292:426-9.

Megraw TL, Kaufman TC. 2000. The centrosome in Drosophila oocyte development. Curr Top Dev Biol 49:385-407.

Moses MJ, Dresser ME, Poorman PA. 1984. Composition and role of the synaptonemal complex. Soc Exp Biol 246-270.

Parvinen M, Toppari J, Lahdetie J. 1993. Transillumination phase contrast microscope techniques for evaluation of male germ cell toxicity and mutagenicity. In RE Chapin and JJ Heindel (ed): "Methods in Toxicology," 3, part A. San Diego: Academic Press, pp 142-165.

Pihan GA, Purohit A, Wallace J, Malhotra R, Liotta L, Doxsey SJ. 2001. Centrosome defects can account for cellular and genetic changes that characterize prostate cancer progression. Cancer Research 61:2212-9.

Robertson WRB. 1916. Chromosome studies I. Taxonomic relationships shown in the chromosomes of *Tettigidae* and *Acrididae*: V-shaped chromosomes and their significance in *Acrididae*, *Locustidae*, and *Gryllidae*: Chromosomes and variation. J Morphol 27:179-331.

Savage AR, Petersen MB, Pettay D, Taft L, Allran K, Freeman SB, Karadima G, Avramopoulos D, Torfs C, Mikkelsen M, Hassold TJ, Sherman SL. 1998. Elucidating the mechanisms of paternal non-disjunction of chromosome 21 in humans. Hum Mol Genet 7:1221-1227.

Schmid TE, Xu W, Adler ID. 1999. Detection of aneuploidy by multicolor FISH in mouse sperm after in vivo treatment with acrylamide, colchicine, diazepam or thiabendazole. Mutagenesis 14:173-179.

Tepperberg JH, Moses MJ, Nath J. 1999. Colchicine effects on meiosis in the male mouse - II. Inhibition of synapsis and induction of nondisjunction. Mutat Res Fundam Mol Mech Mut 429:93-105.

Wiltshire T, Park C, Caldwell KA, Handel MA. 1995. Induced premature G2/M transition in pachytene spermatocytes includes events unique to meiosis. Dev Biol 169:557-567.

Woods LM, Hodges CA, Baart E, Baker SM, Liskay M, Hunt PA. 1999. Chromosomal influence on meiotic spindle assembly: Abnormal meiosis I in female *Mlh1* mutant mice. J Cell Biol 145:1395-1406.

Yin H, Cukurcam S, Betzendahl I, Adler ID, Eichenlaub-Ritter U. 1998. Trichlorfon exposure, spindle aberrations and nondisjunction in mammalian oocytes. Chromosoma 107:514-522.

PART III

EVIDENCE FOR MEIOTIC SPINDLE CHECKPOINT FROM ANALYSIS OF SPERMATOCYTES FROM ROBERTSONIAN-CHROMOSOME HETEROZYGOUS MICE*

*The work for this part was accomplished by efforts of April Pyle, Shannon Eaker, John Cobb and Mary Ann Handel. Part III was published in its entirety as Eaker S, Pyle A, Cobb J, Handel MA (2001): Evidence for meiotic spindle checkpoint from analysis of spermatocytes from Robertsonian-chromosome heterozygous mice. J Cell Sci 114:2953-2965. Part III also appeared in the Ph.D. dissertation of Dr. Shannon Eaker.

ABSTRACT

Mice heterozygous for Robertsonian centric fusion chromosomal translocations frequently produce aneuploid sperm. In this study RBJ/Dn X C57BL/6J F1 males, heterozygous for four Robertsonian translocations (2N = 36), were analyzed to determine effects on germ cells of error during meiosis. Analysis of sperm by three color fluorescence *in situ* hybridization revealed significantly elevated aneuploidy, thus validating Robertsonian heterozygous mice as a model for production of chromosomally abnormal gametes. Primary spermatocytes from heterozygous males exhibited abnormalities of chromosome pairing in meiotic prophase and metaphase. Despite prophase abnormalities, the prophase/metaphase transition occurred. However, an increased frequency of cells with misaligned condensed chromosomes was observed. Cytological analysis of both young and adult heterozygous mice revealed increased apoptosis in spermatocytes during meiotic metaphase I. Metaphase spermatocytes with misaligned chromosomes accounted for a significant proportion of the apoptotic spermatocytes, suggesting that a checkpoint process identifies aberrant meioses. Immunofluorescence staining revealed that kinetochores of chromosomes that failed to align on the spindle stained more intensely for kinetochore antigens CENP-E and CENP-F than did aligned chromosomes. Taken together, these observations are consistent with

detection of malattached chromosomes by a meiotic spindle checkpoint mechanism that monitors attachment and/or congression of homologous chromosome pairs. However, the relatively high frequency of gametic aneuploidy suggests that the checkpoint mechanism does not efficiently eliminate all germ cells with chromosomal abnormalities.

CHAPTER I

INTRODUCTION

Accurate meiotic segregation of chromosomes is essential for normal reproduction and a major determinant of gamete quality. Errors in chromosome segregation in either of the two meiotic divisions can lead to gametic loss, reduced fertility, or aneuploidy in offspring. Understanding the mechanisms that ensure normal chromosome segregation and of checkpoints that come into play in cases of chromosomal meiotic abnormalities could provide insights into the origin of aneuploidy, such as trisomy 21 (Down syndrome), in our own species. However, little is known of the mechanisms that determine gamete genetic quality.

Mitotic checkpoints govern functional assembly of the mitotic spindle apparatus and bipolar attachment of chromosomes (Burke, 2000; Gardner and Burke, 2000). These mechanisms respond to malattachment of chromosomes by delaying exit from mitosis. Tension developed as chromosomes achieve bipolar attachment appears to be critical to the mechanism (Li and Nicklas, 1995; Nicklas et al., 1995). Tension can be assessed by changes in phosphorylation of kinetochore proteins (Gorbsky et al., 1999; Li and Nicklas, 1997; Waters et al., 1999), and these proteins appear to monitor both spindle assembly and chromosome attachment, signaling the onset (or delay) of anaphase. For example, centromeric protein CENP-E is a kinesin-like motor protein whose activity at kinetochores is thought to be monitored by the spindle assembly checkpoint (Yen et al., 1992). CENP-E is essential for microtubule/kinetochore attachment, as chromosomes from HeLa cells lacking the CENP-E gene or injected with antibodies against the CENP-

E protein do not align properly on the metaphase plate, and subsequently do not proceed through division (Schaar et al., 1997). hCENP-E is thought to be involved in checkpoint signaling as it associates with the checkpoint protein hBUBR1 (Chan et al., 1999). The association of the checkpoint protein MAD2 with the kinetochore has recently been shown to be dependent on the presence of CENP-E, thus linking CENP-E to another component of the spindle assembly checkpoint mechanism (Abrieu et al., 2000).

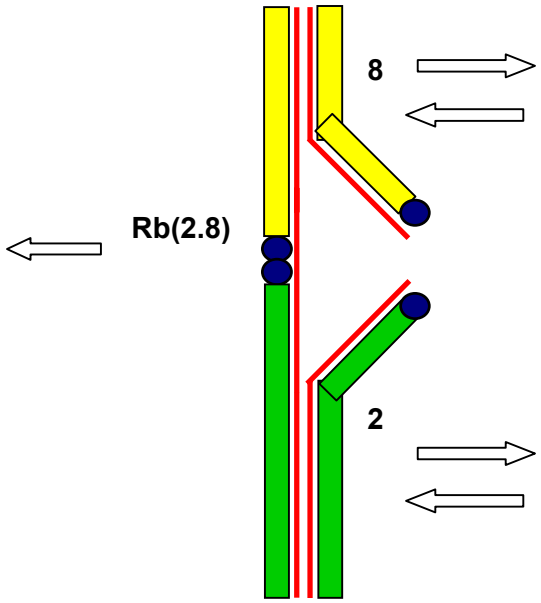
Little is known about the checkpoints governing the meiotic divisions or their similarity to mechanisms that act in mitosis. The first meiotic division differs markedly from mitosis. In the first meiotic division, homologous chromosome pairs are separated from each other in a reductional division, while in the second mitotic-like equational division, sister chromatids are separated from each other. The information governing the mode of meiotic anaphase separation is apparently contained within the chromosome and is not a property of the spindle (Paliulis and Nicklas, 2000). Checkpoint mechanisms signaling error in the two distinct division processes might also be intrinsic to the meiotic chromosomes. Investigations using model organisms have confirmed localization of checkpoint protein BUB1 in *Drosophila* spermatocytes (Basu et al., 1998), and MAD2 in maize gametocytes (Yu et al., 1999) and mouse spermatocytes (Kallio et al., 2000). CENP-E is localized on the kinetochores in metaphase mouse spermatocytes (Kallio et al., 1998), in pig oocytes during both meiotic divisions (Lee et al., 2000), and has been implicated as essential for MII arrest of mouse oocytes (Duesbery et al., 1997). Whether these proteins act singly or in concert as a spindle checkpoint mechanism during meiotic divisions is not known, nor is it known what the consequences of the checkpoint might be. One likely consequence of checkpoint-detected error might be apoptosis, which plays

an important role in male germ cell development and regulation (Print and Loveland, 2000; Sinha Hikim and Swerdloff, 1999).

Interestingly, evidence suggests that mammalian female meiosis lacks stringent checkpoint control, which could explain high rates of aneuploidy, particularly in humans (Hunt and LeMaire-Adkins, 1998; LeMaire-Adkins et al., 1997). It has generally been assumed that there is more effective quality control during male meiosis, but this assumption has not been experimentally tested. Identifying division-phase mechanisms that might detect chromosomal abnormalities and eliminate defective gametes is not easy in normal males, where the number of abnormal cells is small by comparison to the vast numbers of normal gametes.

Checkpoint mechanisms might more readily be revealed in males where the potential for chromosomal error in alignment and segregation is elevated. The model used here is male mice heterozygous for Robertsonian (Rb) translocations. Rb chromosomes are metacentric, or sub-metacentric, chromosomes formed by the centric fusion of two acrocentric chromosomes (Robertson, 1916). During the first meiotic prophase in individuals heterozygous for Rb chromosomes, the Rb participates in a trivalent with the two homologous acrocentric chromosomes (Fig. 1). Pairing defects in this unusual configuration could give rise to the potential for error in either chromosome alignment at metaphase I (MI) or unbalanced segregation at anaphase I (Figure 1). We used mice simultaneously heterozygous (Rb/+) for four different Rb chromosomes, Rb(5.15)3Bnr, Rb(11.13)4Bnr, Rb(16.17)7Bnr, Rb(2,8)2Lub, produced by mating

Figure 1. Diagrammatic representation of a Rb chromosome meiotic pairing configuration involving chromosomes 2 (green) and 8 (yellow). The synaptonemal complex is diagrammed in red, centromeres in blue. Pairing errors could give rise to aberrant alignment at MI and/or unbalanced anaphase segregation, indicated by the arrows.


8
Rb(2.8)
2

individuals quadruply homozygous (RBJ/Dn) to chromosomally normal individuals. Two lines of previous evidence had suggested that these heterozygous mice could provide a model to test for meiotic checkpoints responding to chromosomal misalignment and malsegregation. First, heterozygotes for the single translocations Rb(5.15)3Bnr, Rb(11.13)4Bnr, and Rb(16.17)7Bnr have each been shown to be prone to nondisjunction of the involved chromosomes, both by assessment of metaphase II (MII) spermatocytes and by zygotic loss (Cattanach and Moseley, 1973; Nijhoff and de Boer, 1979). Elevation of sperm aneuploidy has been documented by fluorescence in situ hybridization (FISH) analysis of sperm from male mice carrying Rb(8.14), a Rb chromosome not present in the RBJ/Dn stock used in this study (Lowe et al., 1996). Second, heterozygosity for some of these Rb translocations is associated with abnormalities in pairing and recombination suppression (Cattanach and Moseley, 1973; Davisson and Akeson, 1993), both of which could lead to delays in synapsis and abnormalities during segregation (Koehler et al., 1996). However, extent of error appears to be chromosome-specific (Davisson and Akeson, 1993; Winking et al., 2000). Spindle abnormalities and lagging chromosomes have also been observed in oocytes of Rb-heterozygous mice (Eichenlaub-Ritter and Winking, 1990).

We provide new data on meiotic pairing abnormalities and nondisjunction leading to apoptosis and gametic aneuploidy in male Rb heterozygotes. Our observations indicate that the unusual chromosome constitution in Rb-heterozygous males leads to abnormalities during meiotic division, with concomitant cell death consistent with checkpoint surveillance of chromosome alignment on the spindle. Nonetheless,

aneuploid gametes are produced, suggesting that checkpoint mechanisms do not reliably eliminate all aneuploid germ cells.

CHAPTER II

MATERIALS AND METHODS

Animals

RBJ/Dn mice (The Jackson Laboratory, Bar Harbor, ME) were crossed with C57BL/6J (B6) mice (The Jackson Laboratory, Bar Harbor, ME) to produce F1 individuals heterozygous (Rb/+) for each of the four Rb chromosomes present in the Rb-homozygous parent (Rb(5.15)3Bnr, Rb(11.13)4Bnr, Rb(16.17)7Bnr, Rb(2,8)2Lub).

Three-color Fluorescence in Situ Hybridization (FISH)

For sperm FISH analysis, four Rb/+ and six B6 mice were killed by cervical dislocation and sperm from epididymides were collected in 2.2% citrate. Sperm were spread onto a slide and dried. The slides were soaked in DTT on ice for 30 min and placed immediately into LIS (diiodosalicyclic acid) for 1 hr. The slides were air dried and dehydrated in ethanol. Slides and probes were denatured at 78^{o} C in formamide, then dehydrated and air-dried. The probes were specific for chromosomes 8, X and Y (gifts from Terry Hassold, Case Western University, Cleveland, Ohio). Biotin was used to label 1 μg of the Y probe pERS-532 (Eicher et al., 1991); the chr. 8 probe, which was a mixture (2 μg total) of four subclones (Boyle and Ward, 1992), was labeled with digoxygenin; and 1 μg of the X chromosome-specific probe DXWas (Disteche et al., 1987) was labeled with both biotin and digoxygenin separately. Probes were labeled with digoxygenin and biotin using a nick translation kit (Roche Pharmaceutical) and purified over a Sephadex- G50 column. The probe mix was added to each slide and allowed to

incubate at 37° C overnight. The next day, the slides were washed in 50% formamide/2X SSC, in 2X SSC, and then in PN Buffer (0.1M NaH_2PO_4, 0.1M Na_2HPO_4, 0.05% NP-40, pH 8). Slides were incubated in a BSA-blocking buffer and the appropriate fluorochrome-conjugated detector, also in BSA, at 37° C for 30 min, then washed in PN buffer twice. After adding DAPI/Antifade (Molecular Probes), slides were viewed with an epifluorescent microscope at 100X. Estimates of sperm aneuploidy were deliberately conservative. Only hyperhaploidy, and not hypohaploidy, was scored; the aneuploidy frequency represents twice the hyperhaploidy frequency. Additionally, sperm were deemed suitable for scoring only when the following criteria were met: fluorescent signals were clearly within and not on the edge of the sperm nucleus, fluorescent signals were all in the same plane of focus, and any two signals scored as separate were separated by a distance equal or greater than one signal domain.

Chromosome painting was performed on testicular cells fixed in 3:1 ethanol:acetic acid and then air-dried onto slides (Evans et al., 1964). The slides were air-dried overnight and dehydrated in a 70%, 90%, 90% and 100% ethanol series, then air-dried again. The DNA of the cells was denatured by incubation in 70% formamide/2X SSC at 65° C for 2 min. The slides were then quenched in the ethanol series above and air-dried again. Chromosome paint probes, for chr. 2 and chr. 8 (Cambio Inc, Cambridge, UK), were warmed to 37° C, and denatured at 65° C for 10 min, then at 37° C for 60-90 min. Subsequently, 15µl of each chromosome paint probe was added to each slide and the cells were coverslipped, sealed and incubated overnight at 37° C in a humidified chamber. The slides were washed twice for 5 min at 45° C in 50% formamide/2X SSC and then twice in 0.1X SSC. Detection reagents 1 and 2, provided by

the manufacturer (Cambio, Inc.) for the chr. 2 probe, which required amplification, were made in a 3% BSA/4X SSC blocking solution and slides were incubated with the appropriate detection reagent for 40 min in a humidified chamber at 37^{o} C. The slides were then processed for visualization as above.

Testis Fixation and In Situ Apoptosis Detection

Mice were killed by cervical dislocation, testes removed, and fixed either in 4% paraformaldehyde overnight at 4^{o} C or in Bouin's solution overnight at room temperature. Testes from 3 Rb/+ mice and 3 B6 mice at ages 14, 18 and 23 days old, as well as adult, were fixed in this manner. The testes were dehydrated through an ethanol series and toluene, then embedded in paraffin. The tissue was sectioned at 3-6 μM, and the sections placed on slides to dry. After deparaffination in xylene and rehydration in a decreasing ethanol series, the slides were subjected to the TUNEL reaction for assessment of apoptosis (see below). For staging of tubule sections, periodic acid-Schiff (PAS) staining was performed following the manufacturer's (Sigma) protocol with some modifications. After the TUNEL reaction, slides were rinsed in phosphate-buffered saline (PBS), then placed in 0.5% periodic acid for 10 min. After a 10 min wash in dH_2O, followed by incubation for 1 hr in Schiff reagent in the dark, the slides were placed in 1% potassium metabisulfite for 2 min. The slides were then washed in dH_2O, stained with hematoxylin for 2 min, rinsed with tap water, and placed in lithium carbonate (1.38g/100ml dH_2O saturated) for 3 sec. Following washes in an increasing ethanol series and xylene, the slides were mounted with Permount (Fisher).

Apoptosis assays were performed using the In Situ Cell Death Detection Kit (Roche/Boehringer Mannheim), employing the TUNEL reaction following the manufacturer's protocol, with the exception that the enzyme incubation was for 15 min. Scoring of apoptosis frequency was performed by counting alkaline phosphatase-positive (brown) cells in tubule sections. Tubule cross-sections were scored as apoptotic when three or more apoptotic meiotic cells were observed per tubule cross-section.

Fixation and Immunofluorescent Labeling of Tubule Segments and Isolated Germ Cells

To obtain cytological preparations enriched in meiotically dividing spermatocytes (stage XII of the mouse seminiferous epithelium) a variation of the transillumination procedure (Parvinen et al., 1993) was used. Testes from adult mice (3 B6 males and 3 Rb/+ males) were detunicated, then digested with collagenase for 8 min at 33^{o} C in Krebs-Ringer bicarbonate (KRB) buffered media. Transillumination patterns were observed using a dissecting microscope and the desired stage XII segments (visualized as 3 mm beyond the site of transition from optically dense to light) were excised and transferred onto a microscope slide in KRB. For fixation, a coverslip was placed on top of the segment, then the entire slide was frozen in liquid N_2 for 30 sec. The coverslip was removed, and the slide was fixed in 3:1 ethanol/acetic acid. Prior to incubation with antibody, the slide was placed in PBS/0.2% Triton X-100 (Sigma) for 5 min, then placed in blocking solution (PBS/10% goat serum) for 30 min.

Cell preparations enriched in germ cells were prepared as previously described (Cobb et al., 1999a). Briefly, testes were detunicated and digested in 0.5 mg/ml

collagenase (Sigma) in Krebs-Ringer buffer for 20 min at 32^{o} C and then in 0.5 mg/ml trypsin (Sigma) for 13 min, followed by filtering through 80 μm mesh and washing in buffer. To make surface-spread preparations for visualization of nuclei, cells were fixed in 2% paraformaldehyde with 0.03% SDS (Cobb et al., 1999a). Spermatocytes from germ cell preparations were also embedded in a fibrin clot using modifications to a previously published protocol (LeMaire-Adkins et al., 1997). Germ cells were isolated as mentioned above, and brought to a concentration of 25 X 10^{6} cells/ml. Onto a slide, 3 μl of fibrinogen (Calbiochem, 10mg/ml fresh) and 1.5 μl of the cell suspension were mixed. Then 2.5 μl of thrombin (Sigma, 250 units) was added, and allowed to clot for 5 min. The slide was fixed in 4% paraformaldehyde, washed in 0.2% Triton X-100, then processed for immunofluorescence.

The antisera used were 1) polyclonal anti-SYCP3, 2) anti-β-tubulin (Amersham), 3) anti-phosphorylated histone H3-Ser10 (Upstate Biotech), 4) anti-CENP-E (Schaar et al., 1997) and anti-CENP-F (Liao et al., 1995), generously provided by T. Yen, and 5) anti-MPM-2 (Upstate Biotech). The polyclonal antibody recognizing SYCP3 was prepared by Covance Research Products (Richmond, CA) against recombinant his-tagged protein expressed in *E. coli*. The *Sycp3* cDNA was synthesized by RT-PCR from testicular RNA, cloned into the pPROExHta expression vector (GibcoBRL) and the sequence verified by direct sequencing. Rats were injected intramuscularly with 0.5 mg of purified SYCP3 protein in 6M urea followed by booster injections of 0.25 mg protein at three-week intervals. Serum was collected at three-week intervals beginning one month after the initial injection. All sera collected after the injections contained specific antibodies that recognized the SYCP3 protein. The specificity of the antiserum was

determined by immunoblotting using extracts from pachytene spermatocytes, known to contain SYCP3 protein. Preimmune serum did not recognize any proteins in extracts from pachytene spermatocytes and did not stain cells. Serum collected after antigen injection recognized only protein of the appropriate molecular weight and stained axial elements and synaptonemal complexes in spermatocytes. Following overnight incubation in primary antibody, slides were incubated with rhodamine- or fluorescein-conjugated secondary antibodies (Pierce), followed by mounting with Prolong Antifade (Molecular Probes) containing DAPI (Molecular Probes) to stain DNA. Control slides were stained with either secondary antibodies only, or pre-immune sera as a primary antibody. Staining was observed with an Olympus epifluorescence microscope and images were captured and transferred to Adobe PhotoShop with a Hamamatsu color 3CCD camera. Confocal imaging was performed using a Leica TC SP2 laser-scanning confocal microscope.

CHAPTER III

RESULTS

Rb-Heterozygous Mice Exhibit Elevated Levels of Sperm Aneuploidy

Analysis of sperm by three-color fluorescence *in situ* hybridization (FISH) was used to seek evidence that Rb/+ mice are models for error-prone meiosis. This analysis revealed elevated levels of sperm aneuploidy in Rb/+ males by comparison to age-matched control males (Table 1). Disomy for chromosomes 8, X and Y was determined using probes specific for each chromosome, and sperm from 6 Rb/+ males were scored. The combined hyperhaploidy frequency for chromosomes 8, X and Y was 4.57% in sperm from Rb/+ males compared to 0.25% in sperm from B6 males (Figure 2 and Table 1). The hyperhaploidy frequency for chromosome 8 was 4.38% among sperm from Rb/+ males compared to 0.075% among sperm from B6 males. Since nullisomic sperm (those lacking signals) were not scored, the estimated overall aneuploidy frequency for chromosome 8 is twice the disomy frequency, or approximately 9%. Moreover, sperm from Rb/+ males were characterized by a significantly elevated level of chr. 8 aneuploidy, compared to sex-chromosome aneuploidy. This is an important point, as chr. 8 is involved in Rb(2.8)Lub in the Rb/+ males, while chromosomes X and Y are not a member of any of the translocation chromosomes. Since strict criteria were used for scoring sperm aneuploidy (see Materials and Methods), this estimate is a conservative one. Although probes were not used to detect aneuploidy of the chromosomes involved in the other Rb translocations in this RBJ/Dn stock, it can be assumed that a frequency

Figure 2. Illustrations of sperm stained by the three-color FISH method. A) A chromosomally normal sperm from a B6 mouse containing a single Y chromosome (green) and a single 8 chromosome (red). B) An aneuploid sperm from a Rb/+ mouse containing a single Y chromosome (green) and two 8 chromosomes (red). Scale bar = 5 μm.

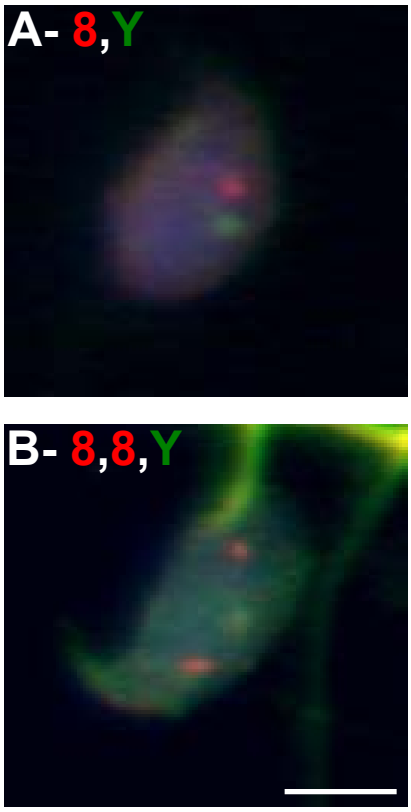

A- 8,Y
B- 8,8,Y

Table 1. Sperm FISH analysis of frequencies of aneuploid sperm from B6 and Rb-heterozygous mice. *Dis = disomy, values are percent of total sperm counted.

Mouse #	Dis8*	DisX*	DisY*	XY	Total	Total Sperm Counted
B6 201	0	0	0	0	0	1000
B6 202	0	0.1	0.2	0.1	0.4	1000
B6 203	0.1	0.1	0.1	0	0.3	1000
B6 204	0.2	0	0	0.1	0.3	1000
Avg%	0.075+/-0.1	0.05+/-0.06	0.075+/-0.1	0.05+/-0.06	**0.25+/-0.18**	
Rb/+ 197	4.3	0.1	0	0.2	4.5	1013
Rb/+ 198	3.9	0.1	0.1	0.1	4.1	1000
Rb/+ 199	5.5	0	0	0.09	5.6	1001
Rb/+ 200	4.5	0.09	0.09	0	4.7	1001
Rb/+ 204	3.8	0	0.2	0	4	1000
Rb/+ 205	4.3	0	0	0.2	4.5	1025
Avg%	**4.38+/-0.61**	0.048+/-0.05	0.065+/-0.08	0.098+/-0.09	**4.57+/-0.57**	

of 9% sperm aneuploidy is a minimal estimate of the overall frequency and that Rb/+ mice are a model for meiosis with errors in chromosome segregation.

Spermatocytes from Rb-Heterozygous Mice Exhibit Meiotic Pairing Abnormalities and Chromosome Misalignment

Since failure to maintain normal bivalent chromosomes could cause the observed gamete aneuploidy, metaphase chromosome pairing was examined from air-dried chromosome preparations. FISH with chromosome-specific paint probes was used to examine MI pairing configurations of the Rb(2.8)Lub and its homologs, the acrocentric chromosomes 2 and 8. Fig. 3A shows among spermatocytes from B6 control males, the signals for chromosomes 2 and 8 are combined, suggesting maintenance of homologous pairing at MI. In contrast, typical images of spermatocyte nuclei from the Rb/+ males revealed two types of signal configurations: those suggesting apparent homologous pairing (Fig. 3B) and those with apparent pairing disruption, where signals for homologous chromosomes are separated and sometimes one of the painted chromosomes (either chr. 2 or chr. 8) is juxtaposed with an unpainted DAPI-stained chromosome (Fig. 3C). Among the 5 individual males scored, the overall frequency of spermatocytes with apparently unpaired chromosomes 2 and/or 8 was 28.18% compared to 0% for B6 control spermatocytes (Table 2).

In addition to the univalence and pairing abnormalities illustrated in Fig. 3, earlier prophase pairing abnormalities were seen in surface-spread spermatocyte nuclei stained with antiserum against mouse SYCP3 for visualization of the synaptonemal complex.

Figure 3. Air-dried meiotic metaphase I (MI) chromosome spreads labeled with chromosome paint probes (2: green, 8: red). A) MI from a B6 mouse displaying proper pairing of homologs. B) Homologous pairing in an MI spermatocyte from a Rb/+ male. C) Failure in homologous chromosome pairing in an MI spermatocyte from a Rb/+ mouse. Scale bar = 5 μm.

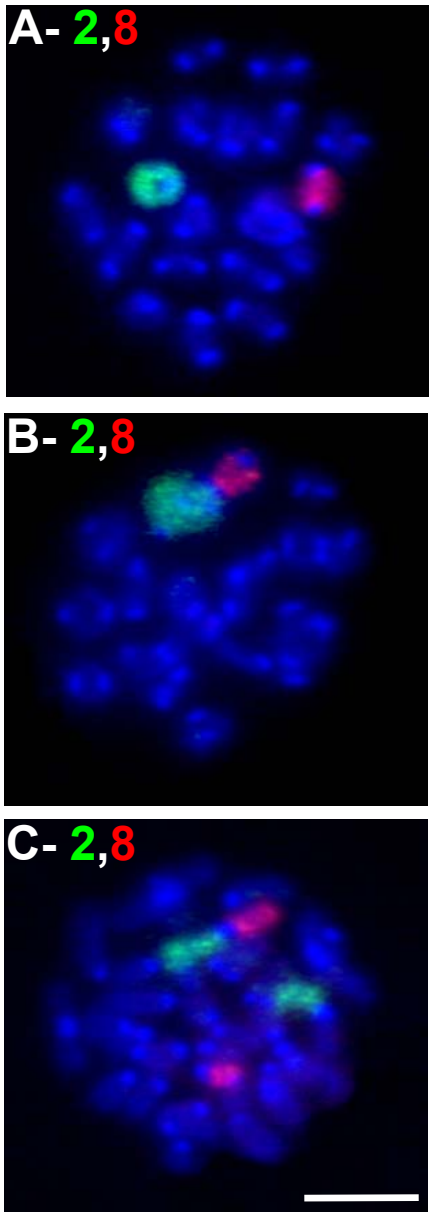

A- 2,8
B- 2,8
C- 2,8

Table 2. Frequencies of unpaired chromosomes (chromosomes 2 and 8) in MI spermatocytes of Rb-heterozygous mice.

Mouse	Unpaired/Total	% Unpaired
Rb/+ 201	35/102	34.3
Rb/+ 202	16/64	25
Rb/+ 203	14/48	29.2
Rb/+ 204	14/54	25.9
Rb/+ 205	9/34	26.5
	Avg.	**28.18**
	STDEV	**3.76**

These pairing abnormalities consisted primarily of incompletely paired regions, sometimes seen as pairing "protrusions" at the centromeric regions (Fig. 4). Additionally, unaligned chromosomes were seen on meiotic MI spindles, which could be a consequence of the observed pairing abnormalities. In order to retain the three-dimensional configuration of division-phase spermatocytes, germ cells were fixed and embedded in a fibrin clot and visualized by confocal microscopy. When scoring these cells, prometaphase cells were identified as having condensed chromosomes, loss of nuclear envelope and a unipolar spindle. Metaphase cells exhibit bipolar spindles and aligned chromosomes. Metaphase I cells retain SYCP3 epitopes, while metaphase II cells are spatially close to their sister cell and do not retain SYCP3 epitopes. These criteria allowed us to determine that cells with unaligned chromosomes were in metaphase (not prometaphase). Additionally, all frequencies of abnormalities were compared to control B6 spermatocytes. Spermatocytes from B6 mice consistently exhibited a "compact" MI configuration of chromosomes, with all chromosomes congressed to the meiotic spindle equator (Fig. 5A), revealed by immunofluorescence with antibodies against the phosphorylated form of histone H3-Ser10 and β-tubulin. Phosphorylation of histone H3 on Ser10 is correlated with chromosome condensation at G2/M in spermatocytes (Cobb et al., 1999b) and thus antibody staining provides a marker for cells in the division phase. In contrast to chromosomally normal spermatocytes, MI spermatocytes from Rb/+ mice frequently exhibited chromosomes that were unaligned or malattached at a distance from the metaphase equator (Fig. 5B). This pattern of misalignment was seen after establishment of the bipolar and elongated spindle,

Figure 4. Pairing abnormalities in surface-spread spermatocytes from Rb/+ mice. A) A nucleus showing the pairing abnormalities (arrowheads) in an Rb/+ spermatocyte stained with antiserum against the synaptonemal complex protein SYCP3 (red). B) A protrusion in the pairing regions (arrowhead). Scale bars = 10 μm (A) and 1 μm (B).

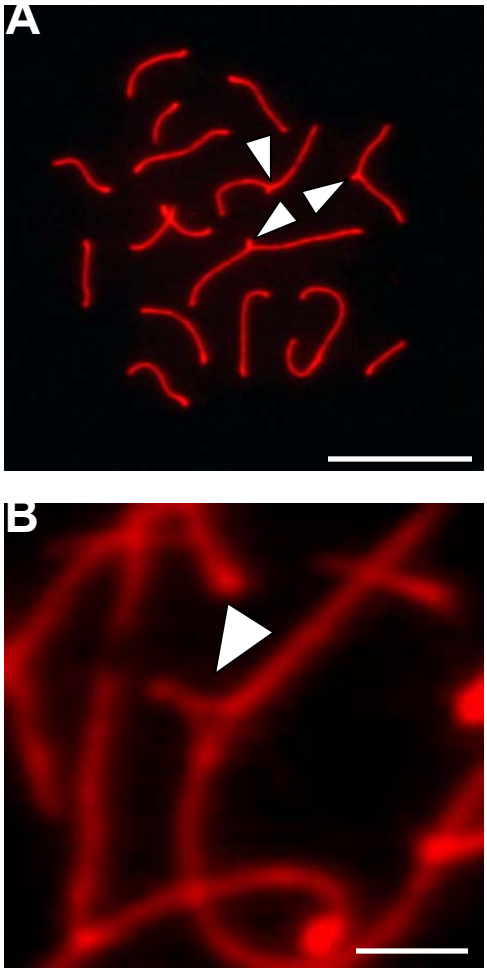
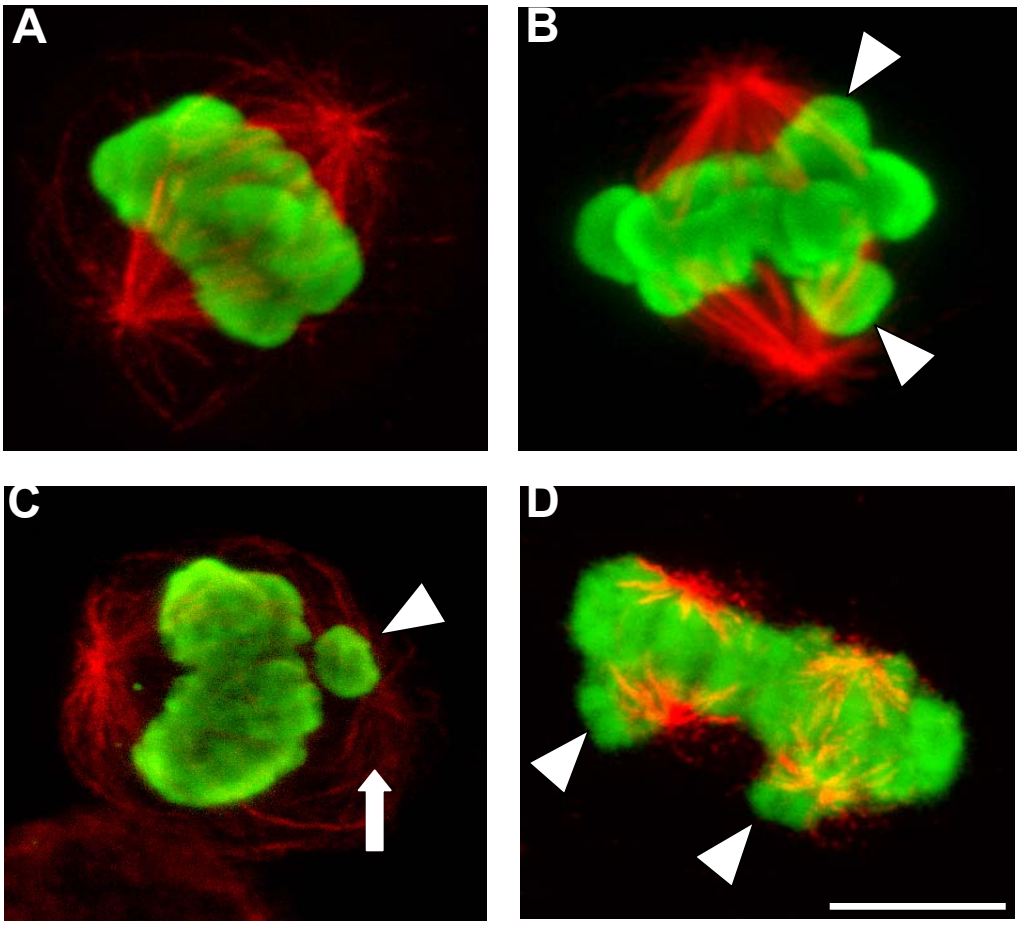

A
B

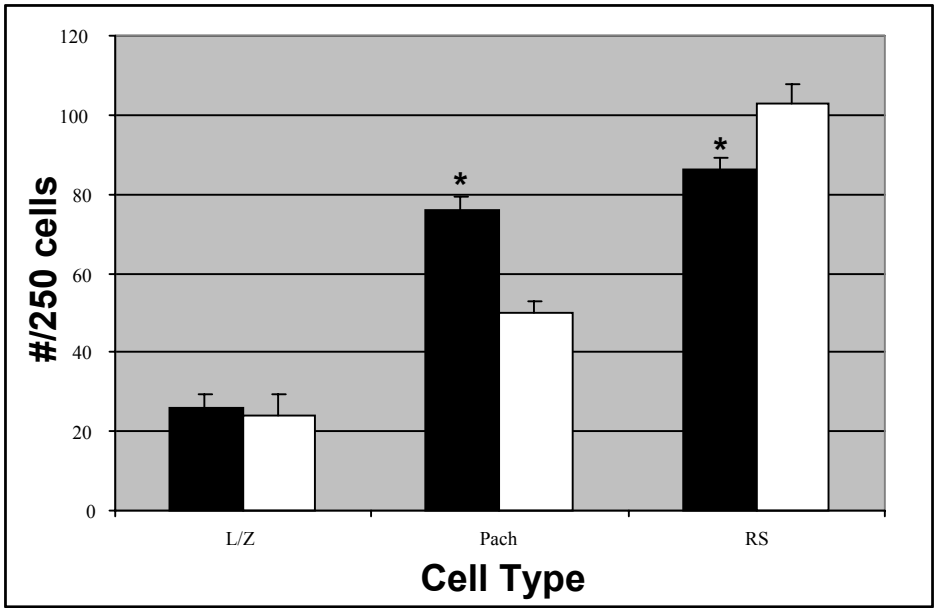
Figure 5. Confocal imaging of MI chromosomes and spindles from B6 and Rb/+ spermatocytes (β-tubulin in red, phospho-histone H3 in green). A) A MI spermatocyte from a control B6 mouse in which all chromosomes are found to be properly aligned on the metaphase plate. B) A MI spermatocyte from a Rb/+ mouse, illustrating unaligned chromosomes (arrowheads). C) A MI spermatocyte from a Rb/+ mouse displaying a misaligned chromosome (arrowhead) and an abnormal spindle, in which one pole is undeveloped (arrow). D) Rb/+ MII spermatocytes depicting chromosomes lagging behind the spindle poles (arrowheads). Scale bar = 10 μm.


A
B
C
D

which in rodents occurs during prometaphase (Kallio et al., 1998). This configuration was sometimes accompanied by abnormalities in spindle structure; for example, in Fig. 5C, note that one spindle pole is not developed, while the microtubule arrays radiate away from the metaphase plate. Such spindle abnormalities may be an early step in apoptosis (see below). Although spindle abnormalities were less frequent, nonaligned chromosomes were found in 23% of the 500 phospho-histone H3-positive MI spermatocytes scored in each of 3 Rb/+ mice, whereas unaligned chromosomes were seen in only 4.8% of 500 MI spermatocytes from each of 3 B6 males. In addition to the MI abnormalities, some MII spermatocytes from Rb/+ mice also exhibited aberrant chromosome configurations, for example, chromosomes that are positioned behind rather than between the spindle poles (Fig. 5D).

The frequency of spermatogenic cell stages was determined to test the hypothesis that these pairing and metaphase alignment abnormalities could cause a loss of cells and/or delay in the normal progression of spermatogenesis. Germ cells were isolated and the frequency of cell types was obtained from nuclei spreads (Fig. 6). The frequency of post-meiotic round spermatids, relative to the frequency of leptotene/zygotene spermatocytes, was decreased in the germ cell population from Rb/+ compared to that from B6 mice, and a concomitant increased frequency of pachytene spermatocytes, but not of leptotene/zygotene spermatocytes, was found among germ cells from Rb/+ mice compared to germ cells from the control B6 mice (Fig. 6). Additionally, when sectioned material was analyzed, the frequencies of stage XII, and VII-IX, tubule sections in Rb/+ testes were found to be greater than those in control B6 testes, while the frequency

Figure 6. The frequencies of spermatogenic cell stages from B6 (white bars) and Rb/+ (black bars) adult mice. Germ cells were isolated as an enriched population from testes of 3 adult mice, and the number of leptotene/zygotene spermatocytes (L/Z), pachytene spermatocytes (Pach), and round spermatids (RS) were determined in a total of 250 cells per mouse. These cells represented most but not all of the cell types in the population, which also included somatic cells and elongated spermatids. Asterisks represent paired values that differ significantly (Student's t test; $p = 0.001$ for difference in frequency of pachytene spermatocytes and $p = 0.008$ for difference in frequency of round spermatids).


120
100
80
60
40
20
0
#/250 cells
*
*
L/Z
Pach
RS
Cell Type

of the other stages did not differ statistically between the two (Fig. 7). Taken together, these data suggest loss of cells and possible delay in progress of spermatogenesis in Rb/+ mice.

Spermatocytes from Rb-Heterozygous Males with Misaligned Chromosomes Exhibit Elevated Frequency of Apoptosis in Meiotic Division Phase

To test the hypothesis that chromosome abnormalities might activate a meiotic checkpoint leading to apoptosis, apoptotic cells in tissue sections were identified and enumerated using the TUNEL reaction and periodic acid-Schiff reagent to stage tubule sections. The criterion for identifying individual cross-sections as apoptotic was the presence of three or more apoptotic cells per tubule section. Relatively few cells were found to be apoptotic in testes of control B6 males (Figs. 7 and 8). However, in testes of Rb/+ males, apoptosis was found to be elevated among MI spermatocytes in seminiferous epithelium stage XII. In a developmental analysis of the onset of apoptosis, testes from 3 Rb/+ and 3 control B6 mice were examined on days 14, 18 and 23 after birth. These time points were chosen to precede (days 14 and 18) and coincide with (day 23) appearance of significant numbers of MI cells. An elevated number of apoptotic meiotic germ cells were found in testes from Rb/+ mice only after 23 days of age (Fig. 8), with a frequency of 15.8 +/-2.8 apoptotic cells/stage XII tubule cross-section (data not shown).

In order to determine if the apoptotic cells seen in stage XII cross sections were due to MI spermatocytes with unaligned chromosomes, microdissected stage XII segments were analyzed for both apoptosis by the TUNEL reaction, for DNA by

Figure 7. Frequencies of seminiferous tubules at indicated stages and of apoptotic tubules (hatched bar) in B6 (white bars) and Rb/+ (black bars) adult mice. Sectioned material was staged with periodic acid-Schiff reagent and hematoxylin, and processed using the TUNEL method for detecting apoptotic cells. All stage XII tubules in Rb/+ mice were apoptotic (red). Asterisks represent paired values that differ significantly (Student's t test; $p = 0.035$ for difference in frequency of stage VII-IX tubules and $p = 0.033$ for difference in frequency of stage XII tubules).

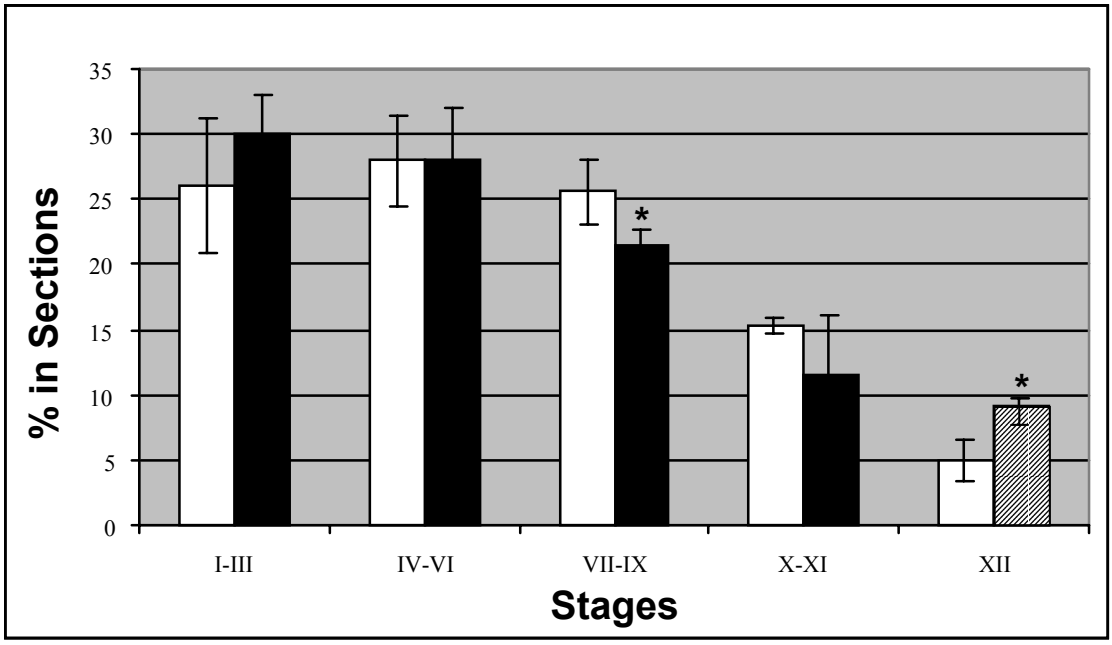
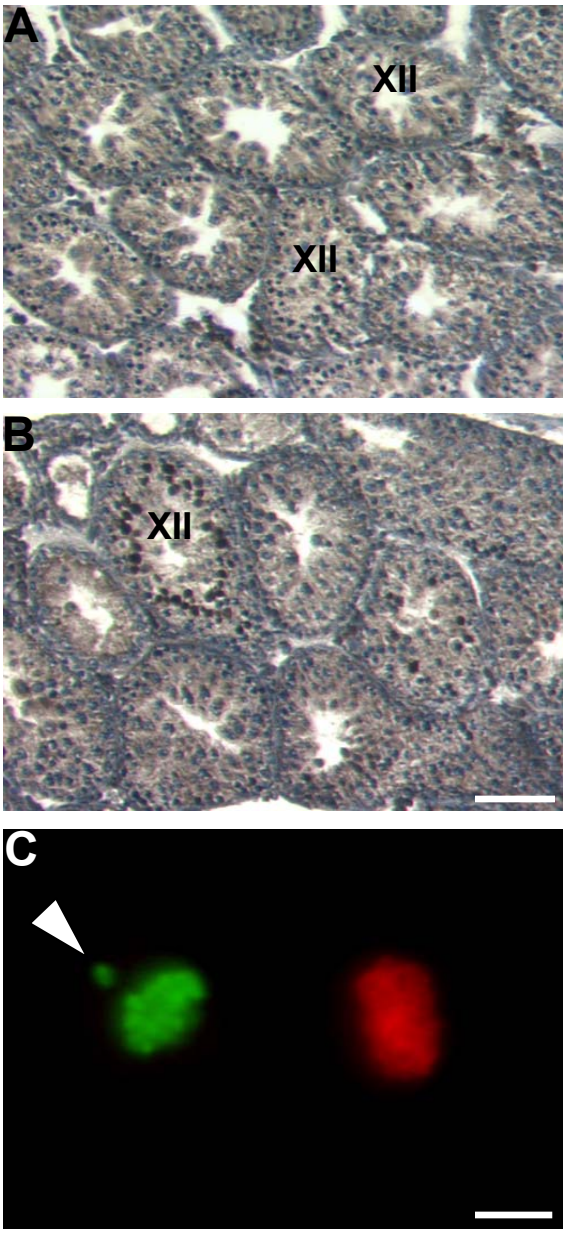

35
30
25
20
15
10
5
0
% in Sections
*
*
I-III
IV-VI
VII-IX
X-XI
XII
Stages

Figure 8. Apoptotic cells in stage-XII tubule sections of B6 (A) and Rb/+ (B) 23 day-old mice. Sections were stained with hematoxylin, periodic acid-Schiff reagent, and processed to observe apoptotic cells (brown cells) by the TUNEL reaction. C) Germ cells from a preparation of micro-dissected stage XII tubule from a Rb/+ mouse. The red staining represents antibody against phosphorylated histone H3 to visualize meiotic division-stage cells and the green staining denotes apoptosis (detected by the TUNEL method). Scale bars = 100 μm (A and B) or 10 μm (C).


A
XII
XII
B
XII
C

DAPI stain and by immunofluorescence with antibody against phosphorylated histone H3 to visualize chromosome alignment at MI. This analysis revealed that a significant proportion of the apoptotic MI spermatocytes exhibited a misaligned chromosome (Fig. 8C). A total of 1000 apoptotic MI spermatocytes were scored in tubules from 3 Rb/+ males and 79.8% contained chromosomes not properly aligned on the metaphase plate (Table 3). This observation directly links apoptosis to spermatocytes with unaligned chromosomes. Interestingly, it was observed that many of the apoptotic MI spermatocytes did not stain with the antibody against phospho-histone H3, suggesting loss of phosphorylation on Ser10 as part of the apoptotic process. This observation suggests that the previous estimate that 23% of MI spermatocytes in Rb/+ testes have misaligned chromosomes (above and Fig. 5) is low since this was derived only from MI spermatocytes that stained positively for phospho-histone H3. Taken together, these analyses show increased germ-cell apoptosis in testes of Rb/+ mice, provide evidence that the susceptible meiotic stage encompasses the division phases, and suggest that it is cells with chromosomal abnormalities that are undergoing apoptosis.

Meiotic Spermatocytes from Rb-Heterozygous Mice Exhibit Features of Normal G2/M but Also Abnormalities in Behavior of Putative Checkpoint Proteins

In spite of chromosome pairing abnormalities and apparent meiotic delay, many features of the meiotic prophase-metaphase (G2/M) transition were normal in spermatocytes from Rb/+ mice compared to those from B6 controls. In surface-

Table 3. Frequencies of apoptosis and chromosome misalignment in metaphase spermatocytes.

* UC= with unaligned chromosomes

** Data compiled across 3 B6 and 3 Rb/+ mice (250-500 cells scored per mouse)

*** Data compiled across 3 B6 mice (20-40 apoptotic MI's scored per mouse)

Strain	# MIs	# MIs Apop (%)	# Apop MIs	# Apop MIs-UC*
B6	1000**	89 (8.9)	100***	28 (28)
Rb/+	1000**	603 (60.3)	1000**	798 (79.8)

spread spermatocytes from both control and Rb/+ spermatocytes, we observed orderly disassembly of the synaptonemal complex, chromatin condensation and individualization, and appearance at MI of newly phosphorylated epitopes, detected by phospho-histone H3-Ser10 antibody (a marker for chromosome condensation) and MPM antibody (a marker for epitopes phosphorylated at division phase) (data not shown).

Because of evidence for spindle abnormalities in Rb/+ spermatocytes and for elimination of spermatocytes by apoptosis, attention was given to localization of proteins that might act directly or indirectly in checkpoint mechanisms. In mitotic HeLa cells, kinetochores on lagging chromosomes stain more intensely with antibodies against hBUBR1 and CENP-E, known spindle assembly checkpoint proteins, than do kinetochores on chromosomes that are properly aligned (Chan et al., 1999). Consequently, the pattern of localization and intensity of signal of CENP-E was monitored at kinetochores of chromosomes associated with spindles in Rb/+ spermatocytes, especially at the kinetochores of improperly attached or lagging chromosomes (such as in Figs. 5 and 8). In Fig. 9, the normal prometaphase (A and B) and metaphase (C and D) patterns of CENP-E staining of B6 spermatocytes from microdissected stage XII tubule sections is shown. This pattern of staining was also the predominant one in Rb/+ spermatocytes, with the important exception of kinetochores of chromosomes not aligned at the metaphase spindle equator (arrows in Fig. 9 E, F and G), where staining was more intense. Kinetochores on all of the malattached chromosomes stained more intensely with antibodies against CENP-E. A similar staining pattern was seen with antibodies against CENP-F (Fig. 10). The increase in fluorescence intensity in

Figure 9. CENP-E staining in prometaphase and metaphase spermatocytes from B6 and Rb/+ mice. CENP-E staining in B6 early prometaphase (A and B) and late prometaphase spermatocytes (C and D) (β-tubulin staining in red, CENP-E staining in green). A and C are overlays of CENP-E and β-tubulin staining, while B and D show CENP-E staining only. E-G) CENP-E (green) staining in a Rb/+ MI spermatocyte, containing misaligned chromosomes (arrows). E) CENP-E staining in green, F) DAPI (for DNA) in blue, and G) overlay of E and F with MPM-2 staining in orange. Scale bar = 10 μm.

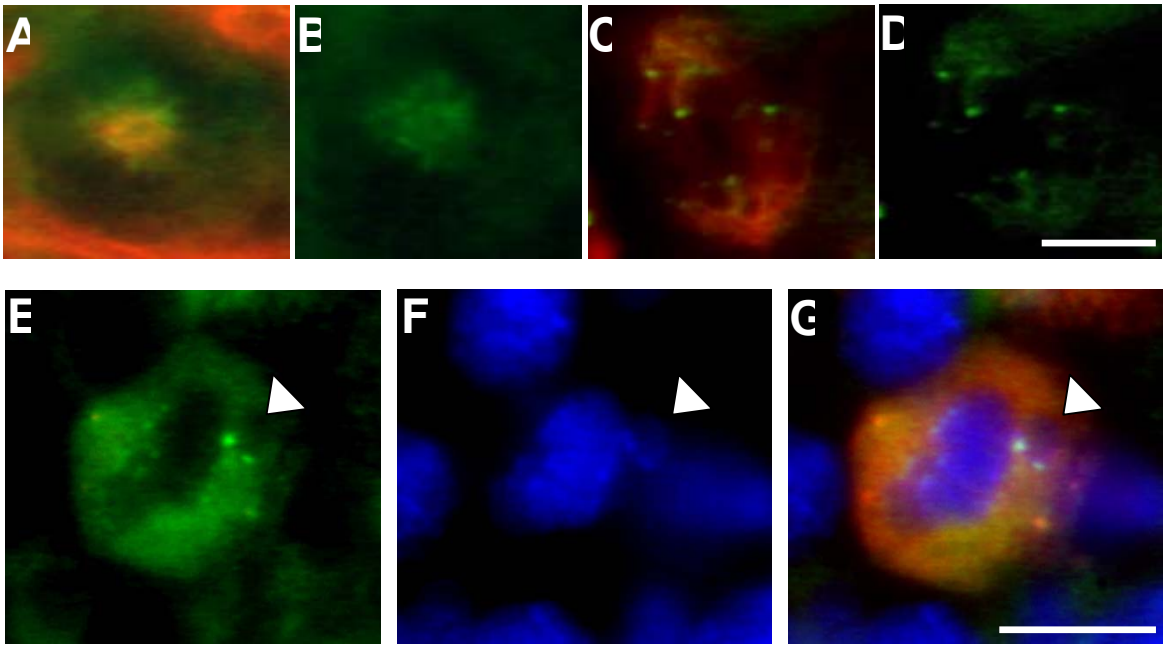
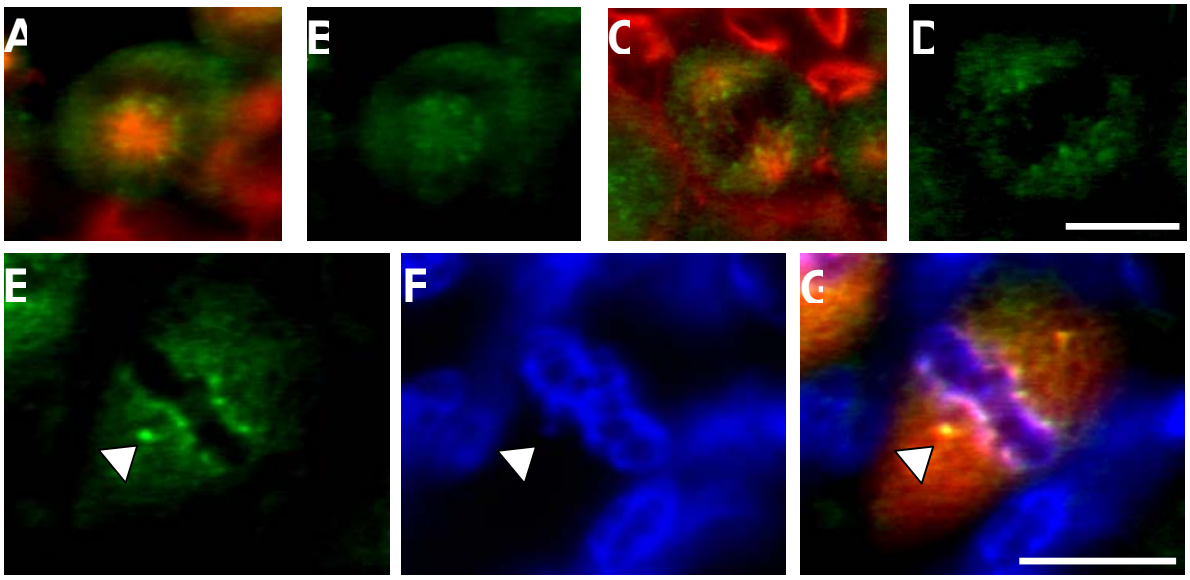

A
B
C
D
E
F
G

Figure 10: CENP-F staining in prometaphase and metaphase spermatocytes from B6 and Rb/+ mice. CENP-F staining in B6 prometaphase (A and B) and metaphase spermatocytes (C and D) (β-tubulin staining in red, CENP-F staining in green). A and C are overlays of CENP-F and β-tubulin staining, while B and D show CENP-F staining only. E-G) CENP-F (green) staining in a Rb/+ MI spermatocyte, containing misaligned chromosomes (arrows). E) CENP-F staining in green, F) DAPI (for DNA) in blue, and G) overlay of E and F with MPM-2 staining in orange. Scale bar = 10 μm.


A
E
C
D
E
F
G

detection of these proteins may be due to either an increase in the amount of protein at the kinetochore on unaligned chromosomes, or an increased accessibility of the epitope to the antibody, possibly due to a conformational alteration. Antibodies against the polo-like kinase PLK1 protein, MAD2 and SYCP3, as well as CREST antisera, were used to assess the possibility of an elevation in staining intensity of other proteins in centromeric regions, as well as to detect multiple kinetochores (data not shown). Staining with these antibodies revealed similar intensity on kinetochores of both properly aligned chromosomes and those that were not in Rb/+ spermatocytes. Although a role for PLK1 protein in both DNA repair and centrosome maturation has been suggested, it is not thought to be involved in a spindle checkpoint mechanism. While MAD2 is thought to play a role in the spindle assembly checkpoint, its function during mammalian meiosis has not been established. It was previously shown that MAD2 is present at most, but not all, kinetochores of mouse spermatocytes during the first metaphase of meiosis (Kallio et al., 2000). When we stained mouse metaphase I spermatocytes using antibodies against MAD2, we also observed variability in kinetochore staining within and amongst spermatocytes. This suggests that MAD2 may not be required for the first meiotic division during mammalian meiosis. The exact role of MAD2 during a possible spindle assembly checkpoint mechanism during meiosis awaits further experimental evidence.

CHAPTER IV

DISCUSSION

This study was conducted to seek evidence for how male germ cells cope with error in meiotic division. Mice heterozygous for Rb chromosome translocations have previously been shown to produce aneuploid gametes, and it is not clear if there are any correction mechanisms that might diminish the overall level of gamete aneuploidy. The results show that mice heterozygous for four different Rb chromosomes derived from RBJ/Dn are a good model in that they produce sperm characterized by a higher than normal frequency of aneuploidy. Abnormalities of chromosome pairing at metaphase of the first meiotic division were demonstrated by use of whole-chromosome FISH paint probes. Additionally, MI spermatocytes from Rb heterozygotes were characterized by an elevated frequency of chromosomes misaligned and failing to congress on the spindle. Evidence that there is ensuing cell death, delay and arrest, which could be mediated by a checkpoint mechanism, includes detection of increased apoptosis of meiotic division-phase spermatocytes, predominantly those with misaligned chromosomes, as well as changes in the kinetics of spermatogenesis and presence of putative checkpoint signals on misaligned chromosomes at metaphase. Nonetheless, the relatively high frequency of gametic aneuploidy suggests that the checkpoint mechanism might not be an efficient block to meiotic progress in cells faced with multiple chromosomal abnormalities.

Meiotic Division of Spermatocytes from Rb-Heterozygous Mice Is Error-Prone

There are three lines of evidence from this work suggesting that gametic aneuploidy is a characteristic of Rb/+ mice. The first, and most direct, derives from assessment of sperm aneuploidy by FISH. Sperm aneuploidy for chromosome 8, participating in a Rb chromosome, was 8.8%, compared to 0.15% for control sperm. Similarly increased aneuploidy has been observed previously. Specifically, a ten-fold increase in the sperm aneuploidy frequency was found for males heterozygous for the Rb(8.14)16Rma translocation, although hyperhaploidy in the sex chromosomes did not differ from control values (Lowe et al., 1996). It is highly likely that most of the sperm aneuploidy we have observed derives from unbalanced segregation of metacentric Rb chromosomes and their acrocentric homologs at anaphase I. Since chromosome 8 is involved in only one of the four Rb chromosomes (Rb(2,8)2Lub), 9% is likely to be a minimum estimate of the total sperm aneuploidy. The overall aneuploidy frequency could be as high as 72% if sperm FISH probes for all the other seven chromosomes involved in Rb translocations (chromosomes 2, 5, 11, 13, 15, 16 and 17) had been used. However, most probably aneuploidy frequencies are chromosome-specific (Winking et al., 2000) and thus the multiplicative estimate of 72% could be inaccurate. Previous observations also suggest that heterozygotes for the single translocations Rb(5.15)3Bnr, Rb(11.13)4Bnr, and Rb(16.17)7Bnr are prone to nondisjunction, as assessed both by metaphase II (MII) chromosome analysis and by zygotic loss (Cattanach and Moseley, 1973). Additionally, other data derived from scoring chromosome arms in MII spermatocytes suggests malsegregation of chromosomes in heterozygotes for Rb(11.13)4Bnr (Everett et al., 1996). Thus, Rb/+ mice are a model for production of

aneuploid sperm, and, furthermore, the aneuploidy appears to be restricted to the chromosomes involved in the Rb translocations.

The second line of evidence provides clues to what could be an origin of meiotic error in spermatocytes of Rb/+ mice. Spermatocytes scored at MI with whole-chromosome paint probes for chromosomes 2 and 8 (forming Rb(2,8)2Lub) displayed an abnormally high level (28%) of apparent univalence or nonhomologous pairings for these two chromosomes. This observation suggests that homolog pairing is diminished or that chiasmata are lacking or are prematurely resolved. Reduced chiasmata formation is also suggested by observations of pachytene spermatocytes showing abnormalities of chromosome pairing. Other studies have also shown that mispairing and recombination suppression occurs in Rb/+ spermatocytes, (Davisson and Akeson, 1993; Everett et al., 1996). However, this is the first study where mispaired chromosomes have been positively identified at MI by the use of chromosome-specific paint probes.

The third line of evidence also provides insight to a possible mechanism of aneuploidy. Spermatocytes scored at MI for misaligned or malattached chromosomes or for failure in congression showed an abnormally high frequency (23%) of these errors. The lagging chromosomes were seen after establishment and elongation of the bipolar spindle in prometaphase (Kallio et al., 1998). Careful comparison was made to the frequency of lagging chromosomes in control (B6) spermatocytes with elongated spindles to ensure that we were observing metaphase and not a stage in prometaphase congression. Although scoring was based on a sensitive immunofluorescence detection of MI chromosomes with phosphorylated histone H3, specific chromosomes could not be identified since the preparative techniques for visualization of spindles were not

compatible with chromosome FISH. Furthermore, the estimate of misaligned chromosomes derived by using antibody to phosphorylated histone H3 may be low, because further analysis showed that many MI spermatocytes with misaligned chromosomes were apoptotic and did not stain with antibody against phospho-histone H3 (Fig. 8C and Table 3). These observations are consistent with a previous finding of lagging chromosomes in anaphase mouse oocytes containing Rb translocations (Eichenlaub-Ritter and Winking, 1990). We assume, but do not know, that univalent or mispaired Rb trivalents contributed to the majority of misaligned chromosomes detected at MI. Taken together, these observations imply that there was premature separation of chromosome homologs and that univalent or non-homologously-paired chromosomes were delayed in spindle attachment and/or congression.

These three lines of evidence lend support to the hypothesis that meiosis in Rb/+ mice is fraught with an increased level of error. The common effect is malsegregation leading to gametic aneuploidy, but the causes can lie in diminished chromosome pairing leading to univalence or misaligned chromosomes as well as unbalanced segregation of paired trivalents involving Rb chromosomes. These errors undoubtedly contribute to germ cell aneuploidy and embryo death. Since roughly 9% of sperm from these quadruple Rb/+ mice were aneuploid for chromosome 8, we estimated (above) that the total of the four translocations involving eight chromosomes events could produce an aneuploidy frequency as high as 72%. Nonetheless, somewhat amazingly, male mice heterozygous for 4 different Rb chromosomes are fertile in spite of seemingly great potential for chromosomal disaster.

Apoptosis May Serve as an Elimination Mechanism for Abnormal Germ Cells

Evidence for a testicular mechanism for elimination of chromosomally aberrant germ cells was found in the elevated frequency of stage-specific apoptosis observed in testes of Rb/+ mice compared to both chromosomally normal B6 mice and Rb homozygotes. Apoptosis is a known mechanism for control of germ-cell number and elimination of abnormal and/or damaged germ cells in the testis (Print and Loveland, 2000); however, normally background levels of apoptosis are low. For example, previous observations documented a mean value of 1.9+/-0.2 apoptotic cells per tubule in testes of B6 mice (Kon et al., 1999) and this is consistent with our values for apoptosis frequency in control B6 mice (Figs. 7 and 8). In contrast, germ cell apoptosis was elevated in Rb/+ mice. Most apoptosis was seen in spermatocytes of stage XII tubules where spermatocytes undergo meiotic divisions. Moreover, apoptosis was not detected in Rb/+ mice until 23 days after birth, a time point coinciding with an increase in MI spermatocytes. Most significantly, apoptosis was found predominantly among MI spermatocytes that exhibited misaligned chromosomes (Fig. 8 and Table 3). Previously, correlations have been made between induced chromosome damage or genetic abnormalities and increased apoptosis. Now, these data directly link apoptosis to the presence of misaligned chromosomes at MI, thereby suggesting that the presence of a misaligned chromosome triggers a spindle checkpoint mechanism leading to cell death. Analysis of apoptosis in testes of mice homozygous for the Rb chromosomes revealed more frequent cell death in stage XII tubules than detected in B6 mice, but the frequency was not as high as found in the testes of Rb/+ mice (data not shown). Importantly, apoptosis was not detected during pachynema, even though Rb/+ mice exhibited an

elevated frequency of pachytene spermatocytes compared to B6 mice (Fig. 6). Thus there was no evidence for a "pachytene checkpoint," one that might monitor success in pairing of homologous chromosomes. Such a checkpoint might be expected to lead to apoptotic cells at a stage earlier than stage XII, although the more convoluted scenario of detection of error in pachytene leading to elimination at MI cannot be excluded.

The fact that Rb/+ testes contain an increased frequency of stage XII sections compared to B6 testes (Figure 8), in spite of the fact that there was no significant variation in frequency for any other stage between the two strains, is also suggestive of an arrest, or delay, in meiosis. This was also observed in various other Rb/+ strains (Hansmann et al., 1988) and suggests that some consequence of heterozygosity for Rb chromosomes, most likely a checkpoint-mediated mechanism detecting misaligned chromosomes, activates developmental arrest and elimination by apoptosis. Elimination of division-phase spermatocytes was also reflected in a reduced number of round spermatids among germ cells from testes of Rb/+ mice compared to B6 controls (Fig. 6), in spite of the fact that no differences were ascertained in frequencies of early prophase, leptotene and zygotene, spermatocytes. The elevated frequency of pachytene spermatocytes and reduced frequency of round spermatids in Rb heterozygotes compared to controls (Fig. 6) suggests that there was a delay in entry into division phase. Similar conclusions were reached from different kinds of analyses of mice carrying fewer and different Rb translocations (Nijhoff and de Boer, 1979; Speed and de Boer, 1983).

Surprisingly, the concurrent analysis of TUNEL reaction and phosphorylated histone H3 (Fig. 8C) revealed that most apoptotic MI spermatocytes do not react with the antibody to phosphorylated histone H3, suggesting that the epitope may be

dephosphorylated or no longer accessible. Antibody to another protein, SYCP3, also did not react with many apoptotic cells, suggesting changes in either antibody penetration or accessibility of epitopes in apoptotic cells. Although it has previously been determined that phosphorylation of histone H3 is not involved in apoptosis-induced condensation of interphase chromatin (Hendzel et al., 1998), this is, to our knowledge, the first suggestion that phosphorylated histone H3 could be dephosphorylated as part of apoptosis.

Taken together, these data suggest a delay in completion of MI and elimination of spermatocytes by apoptosis in Rb/+ mice. If this is checkpoint mediated, the important biological problem is to determine the checkpoint signal. The main events culminating in the first metaphase are chromosome condensation, spindle morphogenesis and alignment of chromosomes onto the spindle at the equator. In our observations, no differences were detected between Rb/+ and B6 mice with respect to timing of chromosome condensation and spindle formation. Thus, if a checkpoint is present, we hypothesized that the signal is improper alignment of chromosomes at metaphase.

Altered Staining Intensity of CENP-E and CENP-F Proteins on Improperly Aligned Kinetochores May Reveal an Element of a Meiotic Spindle Checkpoint Mechanism

Evidence for a spindle checkpoint mechanism responding to improperly attached chromosomes in Rb/+ spermatocytes stems from differences between properly attached and malaligned chromosomes in the staining intensity of proteins known to localize to kinetochores and to be components of a spindle assembly checkpoint mechanism. Among metaphase spermatocytes identified by anti-phospho-histone H3 staining from Rb/+ mice, 23% contain unaligned chromosomes (Figure 5B). All of the unaligned

kinetochores assessed stained more intensely with antibodies against CENP-E and CENP-F than did kinetochores of chromosomes that were properly positioned on the spindle. However, antibodies against proteins that are unrelated to the spindle assembly checkpoint (PLK1, CREST and SYCP3) yielded equal staining signal on aligned compared to unaligned chromosomes in Rb/+ metaphase spermatocytes. This observation suggests that the increased signal of CENP-E and CENP-F on unaligned chromosomes is specific and signals the state of chromosome alignment or attachment on the spindle.

Similar observations have been made of mitotic cells, where it was shown that kinetochores on lagging chromosomes stained more intensely with antibodies against CENP-E than did chromosomes aligned on the metaphase plate (Chan et al., 1999). Dynein has been shown to relocate onto kinetochores of chromosomes mechanically detached from spindle microtubules in grasshopper spermatocytes (King et al., 2000), where the relocation of dynein is a transient interaction, and not caused by structural alterations of the dynein protein itself, affecting antibody binding. Comparable results have been obtained for *Drosophila* mitotic and meiotic cells (Basu et al., 1998) using antibodies recognizing the BUB1 spindle checkpoint protein. CENP-E is a kinesin-like motor protein whose function in kinetochore-microtubule attachments has been proposed to be monitored by the hBUBR1 checkpoint kinase (Chan et al., 1999). During mitosis, this mechano-sensor complex relays signals from the kinetochore to inhibit the anaphase-promoting complex (APC) from ubiquitinating proteins whose destruction is required for entry into anaphase. We hypothesize that the increase in staining intensity for CENP-E and CENP-F on malattached meiotic chromosomes in Rb/+ spermatocytes may initiate a

signal either to correct the attachment problem, or, if the error cannot be corrected, to initiate apoptotic elimination of a spermatocyte likely to give rise to aneuploid gametes.

Abnormalities of Meiotic Chromosome Behavior May Activate a Checkpoint Leading to Elimination of Aberrant Germ Cells

Good gamete quality in males with increased potential for gametic aneuploidy could be maintained by the operation of checkpoint mechanisms. Indeed, this study provided data consistent with the hypothesis that chromosomal abnormalities, specifically misalignment, are detected in the meiotic division phase and lead to elimination of aberrant germ cells by apoptosis. These data suggest that mechanisms ensure the elimination of germ cells with abnormal chromosomal configurations or behavior. Similar mechanisms have been implicated by the MI arrest of male mice with a single sex chromosome, the XO*Sxr* male (Kot and Handel, 1990; Sutcliffe et al., 1991) and the improvement of gametogenic progress resulting from providing a partner for the X*Sxr* chromosome (Burgoyne et al., 1992). These examples are in contrast to the situation of mammalian female meiosis, where data suggest that checkpoint mechanisms may be inefficient or absent. For example, a single unpaired sex chromosome (in the XO female) does not trigger a meiotic arrest (LeMaire-Adkins et al., 1997), suggesting lack of apparent checkpoint control. Arrest in the female does occur when the oocyte is faced with massive chromosome univalency, as in the *Mlh1*-null female. Here spindle assembly fails, suggesting a role for the chromosomes in the morphogenesis of the oocyte's MI spindle. Surprisingly however, it is not clear how much improvement in gamete quality is brought about by elimination of aberrant MI germ cells. From FISH

analysis of MI spermatocytes it can be extrapolated that the frequency in the sperm population of sperm disomic or nullisomic for chromosome 8 would be 10-11% if there were no elimination of chromosomally aberrant germ cells. This frequency is not greatly different from the observed frequency of 9%. However, the potential frequency of aneuploidy deriving from adjacent segregation of the trivalent is not known, and it might increase the predicted aneuploidy for chromosome 8. Thus, at this point, it is not known if the frequency of 9% sperm scored as aneuploid for chromosome 8 represents a reduction from the expected frequency.

Taken together, the results from this study provide evidence for a meiotic spindle checkpoint mechanism in male gametogenic cells, but one that may not be totally efficient in eliminating germ cells destined to form aneuploid gametes. First, data on meiotic pairing abnormalities and nondisjunction leading to gametic aneuploidy in Rb/+ spermatocytes validate Rb/+ mice as a model for error-prone meiotic chromosome segregation. Second, abnormalities of chromosome attachment to and alignment on the meiotic spindle were prevalent in Rb/+ spermatocytes. Third, staining patterns for candidate checkpoint proteins differed between properly attached and malaligned chromosomes in meiotic metaphase spermatocytes. Fourth, an increased frequency of post-prophase meiotic germ cell death was seen in testes of Rb/+ mice, as well as developmental delays consistent with checkpoint surveillance. Most significantly, the data show that cells with misaligned chromosomes account for the apoptotic cells, providing a direct link between chromosome error and elimination by apoptosis. However, when aneuploidy for chromosome 8 was considered, the frequency of chromosomally unbalanced sperm was not substantially less than the frequency estimated

from observed meiotic abnormalities. Thus, considered in toto, these observations provide indirect but compelling evidence, for detection of meiotic chromosome error leading to subsequent elimination of spermatocytes. What is not yet known is how effective the checkpoint is. Clearly, aneuploid sperm are produced and this undoubtedly can lead to reduction of reproductive efficiency. Further insight into the role and efficacy of the spindle checkpoint mechanism in male gametes is sorely needed, and will derive, in part, from mutation of putative checkpoint genes and analysis of the phenotypic effects in models for meiotic error, such as Rb/+ mice.

ACKNOWLEDGEMENTS

This work was supported by a grant from the NIH, HD33816 to MAH. We are grateful to Debby Andreadis, Sally Fridge and Trisha Smith for maintenance of mice, to Dr. John Dunlap for his generosity in assistance with confocal imaging, to Dr. Terry Hassold for initial instruction in procedures for FISH as well as for providing FISH probes, to Dr. Tim Yen for generously providing antibodies recognizing CENP-E and CENP-F, and to Dr. Marko Kallio for instruction in procedures for microdissection by transillumination. We are indebted to Drs. John Eppig and Bruce McKee, Tim Yen, members of the Handel laboratory, and two anonymous reviewers for critical comments on the manuscript and discussions.

LIST OF REFERENCES

Abrieu, A., J.A. Kahana, K.W. Wood, and D.W. Cleveland. (2000). CENP-E as an essential component of the mitotic checkpoint in vitro. *Cell*. 102:817-826.

Basu, J., E. Logarinho, S. Herrmann, H. Bousbaa, Z.X. Li, G.K.T. Chan, T.J. Yen, C.E. Sunkel, and M.L. Goldberg. (1998). Localization of the *Drosophila* checkpoint control protein Bub3 to the kinetochore requires Bub1 but not Zw10 or Rod. *Chromosoma*. 107:376-385.

Boyle, A.L., and D.C. Ward. (1992). Isolation and initial characterization of a large repeat sequence element specific to mouse chromosome 8. *Genomics*. 12:517-525.

Burgoyne, P.S., S.K. Mahadevaiah, M.J. Sutcliffe, and S.J. Palmer. (1992). Fertility in mice requires X-Y pairing and a Y-chromosomal "spermiogenesis" gene mapping to the long arm. *Cell*. 71:391-398.

Burke, D.J. (2000). Complexity in the spindle checkpoint. *Curr Opin Genet Develop*. 10:26-31.

Cattanach, B.M., and H. Moseley. (1973). Nondisjunction and reduced fertility caused by the tobacco mouse metacentric chromosomes. *Cytogenet. Cell Genet.* 12:264-287.

Chan, G.K.T., S.A. Jablonski, V. Sudakin, J.C. Hittle, and T.J. Yen. (1999). Human BUBR1 is a mitotic checkpoint kinase that monitors CENP-E functions at kinetochores and binds the cyclosome/APC. *J Cell Biol*. 146:941-954.

Cobb, J., B. Cargile, and M.A. Handel. (1999a). Acquisition of competence to condense metaphase I chromosomes during spermatogenesis. *Develop Biol*. 205:49-64.

Cobb, J., M. Miyaike, A. Kikuchi, and M.A. Handel. (1999b). Meiotic events at the centromeric heterochromatin: histone H3 phosphorylation, topoisomerase II alpha localization and chromosome condensation. *Chromosoma*. 108:412-425.

Davisson, M.T., and E.C. Akeson. (1993). Recombination suppression by heterozygous Robertsonian chromosomes in the mouse. *Genetics*. 133:649-667.

Disteche, C.M., S.L. Gandy, and D.A. Adler. (1987). Translocation and amplification of an X-chromosome DNA repeat in inbred strains of mice. *Nucl. Acids Res.* 15:4393-4401.

Duesbery, N.S., T.S. Choi, K.D. Brown, K.W. Wood, J. Resau, K. Fukasawa, D.W. Cleveland, and G.F. Vande Woude. (1997). CENP-E is an essential kinetochore motor in maturing oocytes and is masked during Mos-dependent, cell cycle arrest at metaphase II. *Proc Natl Acad Sci USA*. 94:9165-9170.

Eichenlaub-Ritter, U., and H. Winking. (1990). Nondisjunction, disturbances in spindle structure, and characteristics of chromosome alignment in maturing oocytes of mice heterozygous for Robertsonian translocations. *Cytogenet. Cell Genet.* 54:47-54.

Eicher, E.M., D.W. Hale, P.A. Hunt, B.K. Lee, P.K. Tucker, T.R. King, J.T. Eppig, and L.L. Washburn. (1991). The mouse Y* chromosome involves a complex rearrangement, including interstitial positioning of the pseudoautosomal region. *Cytogenet. Cell Genet.* 57:221-230.

Evans, E.P., G. Breckon, and C.E. Ford. (1964). An air-drying method for meiotic preparations from mammalian testes. *Cytogenetics*. 3:289-294.

Everett, C.A., J.B. Searle, and B.M.N. Wallace. (1996). A study of meiotic pairing, nondisjunction and germ cell death in laboratory mice carrying Robertsonian translocations. *Genet Res*. 67:239-247.

Gardner, R.D., and D.J. Burke. (2000). The spindle checkpoint: two transitions, two pathways. *Trends Cell Biol*. 10:154-158.

Gorbsky, G.J., M. Kallio, J.R. Daum, and L.M. Topper. (1999). Protein dynamics at the kinetochore: cell cycle regulation of the metaphase to anaphase transition. *FASEB J.* 13:S231-S234.

Hansmann, I., P. de Boer, and R.M. Speed. (1988). Aneuploidy-related delay of meiotic development in the mouse and the Djungarian hamster. *In* The Cytogenetics of Mammalian Autosomal Rearrangements. A. Daniel, editor. Alan R. Liss, Inc., New York. 295-314.

Hendzel, M.J., W.K. Nishiokas, Y. Raymond, C.D. Allis, D.P. Bazett-Jones, and J.P. Th'ng. (1998). Chromatin condensation is not associated with apoptosis. *J. Biol. Chem.* 273:24470-24478.

Hunt, P.A., and R. LeMaire-Adkins. (1998). Genetic control of mammalian female meiosis. *In* Meiosis and Gametogenesis. Vol. 37. M.A. Handel, editor. Academic Press Inc, 525 B Street, Suite 1900, San Diego, CA 92101-4495. 359-381.

Kallio, M., J.E. Eriksson, and G.J. Gorbsky. (2000). Differences in spindle association of the mitotic checkpoint protein Mad2 in mammalian spermatogenesis and oogenesis. *Develop Biol*. 225:112-123.

Kallio, M., T. Mustalahti, T.J. Yen, and J. Lahdetie. (1998). Immunolocalization of alpha-tubulin, gamma-tubulin, and CENP-E in male rat and male mouse meiotic divisions: Pathway of meiosis I spindle formation in mammalian spermatocytes. *Dev Biol*. 195:29-37.

King, J.M., T.S. Hays, and R.B. Nicklas. (2000). Dynein is a transient kinetochore

component whose binding is regulated by microtubule attachment, not tension. *J Cell Biol*. 151:739-748.

Koehler, K.E., R.S. Hawley, S. Sherman, and T. Hassold. (1996). Recombination and nondisjunction in humans and flies. *Hum. Molec. Genet.* 5:1495-1504.

Kon, Y., H. Horikoshi, and D. Endoh. (1999). Metaphase-specific cell death in meiotic spermatocytes in mice. *Cell Tissue Res*. 296:359-369.

Kot, M.C., and M.A. Handel. (1990). Spermatogenesis in XO*Sxr* mice: Role of the Y chromosome. *J. Exp. Zool.* 256:92-105.

Lee, J., T. Miyano, Y.F. Dai, P. Wooding, T.J. Yen, and R.M. Moor. (2000). Specific regulation of CENP-E and kinetochores during meiosis I/meiosis II transition in pig oocytes. *Mol Reprod Dev*. 56:51-62.

LeMaire-Adkins, R., K. Radke, and P.A. Hunt. (1997). Lack of checkpoint control at the metaphase/anaphase transition: A mechanism of meiotic nondisjunction in mammalian females. *J Cell Biol*. 139:1611-1619.

Li, X., and R.B. Nicklas. (1995). Mitotic forces control a cell-cycle checkpoint. *Nature*. 373:630-632.

Li, X.T., and R.B. Nicklas. (1997). Tension-sensitive kinetochore phosphorylation and the chromosome distribution checkpoint in praying mantid spermatocytes. *J Cell Sci*. 110:537-545.

Liao, H., R.J. Winkfein, G. Mack, J.B. Rattner, and T.J. Yen. (1995). CENP-F is a protein of the nuclear matrix that assembles onto kinetochores at late G2 and is rapidly degraded after mitosis. *J Cell Biol*. 130:507-518.

Lowe, X., S. O'Hogan, D. Moore, J. Bishop, and A. Wyrobek. (1996). Aneuploid epididymal sperm detected in chromosomally normal and Robertsonian translocation-bearing mice using a new three-chromosome FISH method. *Chromosoma*. 105:204-210.

Nicklas, R.B., S.C. Ward, and G.J. Gorbsky. (1995). Kinetochore chemistry is sensitive to tension and may link mitotic forces to a cell cycle checkpoint. *J Cell Biol*. 130:929-939.

Nijhoff, J.H., and P. de Boer. (1979). A first exploration of a Robertsonian translocation heterozygote in the mouse for its usefulness in cytological evaluation of radiation-induced meiotic autosomal non-disjunction. *Muta. Res.* 61:77-86.

Paliulis, L.V., and R.B. Nicklas. (2000). The reduction of chromosome number in meiosis is determined by properties built into the chromosomes. *J Cell Biol*. 150:1223-1231.

Parvinen, M., J. Toppari, and J. Lahdetie. (1993). Transillumination phase contrast microscope techniques for evaluation of male germ cell toxicity and mutagenicity. *In* Methods in Toxicology. Vol. 3, part A. R.E. Chapin and J.J. Heindel, editors. Academic Press, San Diego. 142-165.

Print, C.G., and K.L. Loveland. (2000). Germ cell suicide: new insights into apoptosis during spermatogenesis. *BioEssays*. 22:423-430.

Robertson, W.R.B. (1916). Chromosome studies I. Taxonomic relationships shown in the chromosomes of *Tettigidae* and *Acrididae*: V-shaped chromosomes and their significance in *Acrididae*, *Locustidae*, and *Gryllidae*: Chromosomes and variation. *J. Morphol.* 27:179-331.

Schaar, B.T., G.K.T. Chan, P. Maddox, E.D. Salmon, and T.J. Yen. (1997). CENP-E function at kinetochores is essential for chromosome alignment. *J Cell Biol*. 139:1373-1382.

Sinha Hikim, A.P., and R.S. Swerdloff. (1999). Hormonal and genetic control of germ cell apoptosis in the testis. *Rev Reprod*. 4:38-47.

Speed, R.M., and P. de Boer. (1983). Delayed meiotic development and correlated death of spermatocyes in male mice with chromosome abnormalities. *Cytogenet. Cell Genet.* 35:257-262.

Sutcliffe, M.J., S.M. Darling, and P.S. Burgoyne. (1991). Spermatogenesis in XY, XY*Sxr*^{b} and XO*Sxr*^{a} mice: A quantitative analysis of spermatogenesis throughout puberty. *Mol. Reprod. Dev.* 30:81-89.

Waters, J.C., R.H. Chen, A.W. Murray, G.J. Gorbsky, E.D. Salmon, and R.B. Nicklas. (1999). Mad2 binding by phosphorylated kinetochores links error detection and checkpoint action in mitosis. *Curr Biol*. 9:649-652.

Winking, H., C. Reuter, and H. Bostelmann. 2000. Unequal nondisjunction frequencies of trivalent chromosomes in male mice heterozygous for two Robertsonian translocations. *Cytogenet. Cell Genet.* 91:303-306.

Yen, T.J., G. Li, B.T. Schaar, I. Szilak, and D.W. Cleveland. (1992). CENP-E is a putative kinetochore motor that accumulates just before mitosis. *Nature*. 359:536-539.

Yu, H.G., M.G. Muszynski, and R.K. Dawe. (1999). The maize homologue of the cell cycle checkpoint protein MAD2 reveals kinetochore substructure and contrasting mitotic and meiotic localization patterns. *J Cell Biol*. 145:425-435.

PART IV

MEIOTIC PROPHASE ABNORMALITIES AND METAPHASE CELL DEATH IN MLH1-DEFICIENT SPERMATOCYTES: INSIGHTS INTO REGULATION OF SPERMATOGENIC PROCESS*

*The work for this part was accomplished by efforts of April Pyle, Shannon Eaker, John Cobb and Mary Ann Handel. Part IV has been submitted to *Dev Biol*. Part IV also appeared in the Ph.D. dissertation of Dr. Shannon Eaker.

ABSTRACT

The MLH1 protein is required for normal meiosis in mice and its absence leads to failure in maintenance of pairing between bivalent chromosomes, abnormal meiotic division and ensuing sterility in both sexes. In this study we investigated whether failure to develop foci of MLH1 protein on chromosomes in prophase would lead to elimination of prophase spermatocytes, and, if not, whether univalent chromosomes could align normally on the meiotic spindle and whether metaphase spermatocytes would be delayed and/or eliminated. In spite of the absence of MLH1 foci, no apoptosis of spermatocytes in prophase was detected. In fact, chromosomes of pachytene spermatocytes from *Mlh1*$^{-/-}$ mice were competent to condense metaphase chromosomes, both *in vivo* and *in vitro*. Most condensed chromosomes were univalents with spatially distinct FISH signals. Typical metaphase events, such as synaptonemal complex breakdown and the phosphorylation of Ser10 on histone H3, occurred in *Mlh1*$^{-/-}$ spermatocytes, suggesting that there is no inhibition of onset of meiotic metaphase in the face of massive chromosomal abnormalities. However, the condensed univalent chromosomes did not align correctly onto the spindle apparatus in *Mlh1*$^{-/-}$ spermatocytes. Most meiotic metaphase spermatocytes were characterized with bipolar spindles, but chromosomes radiated away from the microtubule-organizing centers in a prometaphase-like pattern rather than achieving a bipolar orientation. Apoptosis was not observed until after the onset of meiotic metaphase. Thus spermatocytes are not eliminated in direct response to

the initial meiotic defect, but are eliminated later. Taken together, these observations suggest that a spindle assembly checkpoint, rather than a recombination or chiasmata checkpoint, may be activated in response to meiotic errors, thereby ensuring elimination of chromosomally abnormal gamete precursors.

CHAPTER I

INTRODUCTION

Making a genetically complete and normal gamete is essential for reproduction and continuity of the species. The process of meiosis ensures that gametes receive a haploid, 1N, complement of chromosomes and the 1C complement of DNA. The stage is set for accurate segregation of chromosomes by the events of meiotic prophase, principally pairing and synapsis of homologous chromosomes and recombination between them. Recombination results in the formation of physical links, chiasmata, between homologous chromosomes. These are required for proper chromosome alignment and segregation in the first meiotic division (Carpenter, 1994; Koehler *et al.*, 1996).

Since recombination is a prerequisite for faithful segregation of chromosomes, it is important to understand not only the molecular events of recombination but also the consequences of error and whether error is monitored in order to ensure gamete quality. Meiotic recombination is a complex series of steps, mediated by a large number of proteins that likely act together in complexes (Cohen and Pollard, 2001; Smith and Nicolas, 1998). The events of recombination include DNA double-strand breaks, strand invasion, formation of Holliday junctions and heteroduplex DNA, and processing of recombination intermediates by reactions that include DNA mismatch repair. A significant number of proteins have been implicated, directly or indirectly, in the events comprising recombination in mammals (Cohen and Pollard, 2001). While much is already known about the molecular processes of meiotic recombination, virtually nothing

is known about the mechanisms in mammalian gametogenesis that might monitor the progress of meiosis and ensure gamete quality.

In the apparent absence of mutations affecting mammalian meiotic checkpoint mechanisms, evidence for such processes can be gleaned from experimental investigation of mutants with errors in meiotic processes. Null, or knockout mutations have been particularly useful to test possible downstream effects, perhaps checkpoint mediated, of failure in specific meiotic processes. However, there is an important caveat: failure in progress of gametogenesis in the absence of a specific gene product can be explained in at least two ways. It could be due either to a requirement for the gene product in order to progress to the subsequent step in meiosis or due to checkpoint monitoring of a failed event and subsequent elimination by apoptosis of germ cells that are otherwise progressing in differentiation. Nonetheless, mutations or conditions interfering with the events of meiosis can be informative about specific requirements and possibly provide indirect evidence for the existence of meiotic checkpoint mechanisms. Here we study the effects on meiotic progress in spermatogenesis of absence of the MLH1 protein. The MLH1 protein promotes crossing over in budding yeast (Hunter and Borts, 1997), and in mice and humans, the MLH1 protein localizes with meiotic crossover sites, corresponding to the number and distribution of chiasmata (Anderson *et al.*, 1999; Barlow and Hulten, 1998). Mice that are homozygous for a knockout of the *Mlh1* gene are sterile, exhibiting a failure either to form or to maintain chiasmata, revealed by presence of univalent chromosomes at meiotic metaphase (Baker *et al.*, 1996; Edelmann *et al.*, 1996). In mutant female mice, oocytes clearly progress to metaphase, at which time they exhibit abnormalities of chromosome alignment and spindle assembly (Woods

et al., 1999). In mutant male mice, data about loss of spermatocytes is a bit more ambiguous, but apparently occurs in either late meiotic prophase (Edelmann *et al.*, 1996) or in the division phase (Baker *et al.*, 1996); the difference could be due to different mutations or differing interpretation of the phenotype. We analyzed the consequences of chiasmata failure for survival and progress of spermatocytes. In spite of absence of MLH1 protein, spermatocytes are not arrested or eliminated during the pachytene stage when MLH1 foci are first assembled onto chromosomes. Instead, there is an apparently normal transition from prophase to prometaphase, with the majority of spermatocytes dying at metaphase. Thus, if cell death is induced by a meiotic checkpoint, the checkpoint seemingly detects abnormalities at the stage of spindle assembly and chromosome alignment, well after the manifestation of the first meiotic abnormality in mutant spermatocytes.

CHAPTER II

MATERIALS AND METHODS

Mice

Mice carrying the *Mlh1* targeted mutation were generously provided by Sean Baker (Baker *et al.*, 1996). Briefly this mutation was generated as described below. A portion of the human MLH1 cDNA was used as a probe to isolate the mouse *Mlh1* cDNA. To generate mice with a null mutation in *Mlh1*, a replacement vector was transfected into mouse ES cells to delete by homologous recombination an exon encoding a highly conserved region of the mouse Mlh1 protein. Targeted ES cells were identified and injected into host blastocysts to generate chimeric animals that transmitted the *Mlh1* mutant allele to the F1 offspring. Offspring were genotyped by PCR reactions for the normal and targeted alleles of the *Mlh1* gene from DNA obtained from tail tips. Mice were housed under 14 hour light /10 hour dark photoperiods at constant temperature (21^{o} C), with free access to standard laboratory chow and water.

Cell and Tissue Preparation

Male mice were killed by cervical dislocation. Testes were removed and fixed by overnight immersion in cold 4% paraformaldehyde (Sigma) at 4^{o} C. After fixation and dehydration, testes were embedded in paraffin and sectioned at 3 μm. The deparaffinized sections were microwaved (10 min at power 3) to unmask antigens before reaction with antibody.

To obtain isolated germ cells, testes were detunicated, digested in 0.5 mg/ml collagenase (Sigma) in Krebs-Ringer bicarbonate (KRB) at 32° C for 20 min, then digested in 0.5 mg/ml trypsin (Sigma) in KRB at 32° C for 13 min. After filtration through 80 μM mesh and 3 washes in KRB, spermatocytes were either fixed in a fibrin clot (see below) or enriched for isolation of pachytene spermatocytes by sedimentation on a bovine serum albumin (BSA) gradient at unit gravity (Bellve, 1993).

After isolation of pachytene spermatocytes, the cells were cultured in MEM medium/5% fetal bovine serum (GibcoBRL). After overnight culture at 32° C with 5% CO_2, cells were treated for six hours with 5 μM okadaic acid (OA) or the ethanol solvent (Cobb *et al.*, 1999a). Chromatin configurations were visualized by Giemsa-staining of air-dried preparations of the treated cells (Evans *et al.*, 1964; Wiltshire *et al.*, 1995). Surface-spread chromatin preparations for synaptonemal complex visualization were performed as previously described (Cobb *et al.*, 1999a). Briefly, germ cells were fixed in 2% paraformaldehyde, and allowed to dry onto slides. The slides were fixed in 2% paraformaldehyde/0.03% SDS, then in 2% paraformaldehyde, then blocked in 10% goat serum/3% BSA in phosphate-buffered saline (PBS) prior to processing for immunofluorescence.

To obtain a preparation enriched in meiotically dividing spermatocytes, a variation of the transillumination procedure (Parvinen *et al.*, 1993) was used (Eaker *et al.*, 2001). Testes from adult mice were detunicated, and then digested with 0.5 mg/ml collagenase for 8 min at 33° C. Tubule segments were excised and transferred onto microscope slides in KRB. A coverslip was then placed on top of the segment, allowing the tubules to spread onto the slide. The entire slide was then frozen in liquid N_2 for 30

sec, the coverslip was removed, and the slide fixed in 3:1 ethanol/acetic acid. Prior to incubation with antibodies, the slide was blocked in PBS/10% goat serum for 30 min.

Spermatocytes from germ cell preparations were embedded in fibrin clots as previously described (Eaker *et al.*, 2001). Germ cells were isolated as described above, and brought to a concentration of 25 x 10^6 cells/ml. A 3 µl aliquot of fibrinogen (Calbiochem, 10 mg/ml fresh) and 1.5 µl of the cell suspension were pipetted onto a slide. Then 2.5 µl of thrombin (Sigma, 250 units) was added, and the slide was allowed to clot for 2 min. The slide was then fixed in 4% paraformaldehyde (Sigma) for 15 min, washed in 0.2% Triton X-100 (Sigma) for 5 min, then processed for immunofluorescence.

Chromosome painting, using fluorescence in situ hybridization (FISH), was performed as previously described (Eaker *et al.*, 2001). Briefly, spermatocytes were fixed in 3:1 ethanol: acetic acid, then dropped onto slides and allowed to dry. After dehydration in an increasing ethanol series, cells were denatured by incubation in 70% formamide/2X SSC at 65^o C for 2 min, followed by another dehydration series. Chromosome paint probes, for chromosome 2 and chromosome 8 (Cambio Inc, Cambridge, UK) were warmed to 37^o C, denatured at 65^o C, then cooled to 37^o C for 1 hr. A 15 µl aliquot of each chromosome paint probe was added to the slides. The slides were coverslipped, sealed, and incubated overnight at 37^o C in a humidified chamber. After two washes at 45^o C for 5 min in 50% formamide/2X SSC, followed by two washes in 0.1X SSC, detection reagents from the manufacturer (Cambio, Inc.) were added to each slide. The slides were then processed for fluorescent visualization as described below.

Apoptosis Analysis

Apoptosis assays were performed using the In Situ Cell Death Detection Kit (Roche Pharmaceuticals), utilizing the end-labeling TUNEL reaction on testes fixed and sectioned as described above. The TUNEL reaction was performed according to the manufacturer's protocol, with the exception of a 15 min incubation with the enzyme on the slides. After deparaffinization in xylene and rehydration, the slides were incubated in 80 µl of the reaction mix at 37^{o} C in a humidified chamber. After two 5 min washes in PBS, the slides were processed for immunofluorescence.

Immunolocalization

Antisera used were polyclonal anti-SYCP3 (Eaker *et al.*, 2001), anti-tubulin (Amersham), anti-phosphorylated histone H3 (Upstate Biotech.) and anti-MPM-2 (Upstate Biotech). Following overnight incubation in primary antibody, slides were incubated with rhodamine- or fluorescein-conjugated secondary antibodies (Pierce), and mounted with Prolong Antifade (Molecular Probes) containing DAPI (Molecular Probes) to stain DNA. Antibody localization was observed using an Olympus epifluorescence microscope, and images were captured to Adobe PhotoShop with a Hamamatsu color CCD camera. Confocal images were collected using a Leica TC SP2 laser-scanning confocal microscope.

CHAPTER III

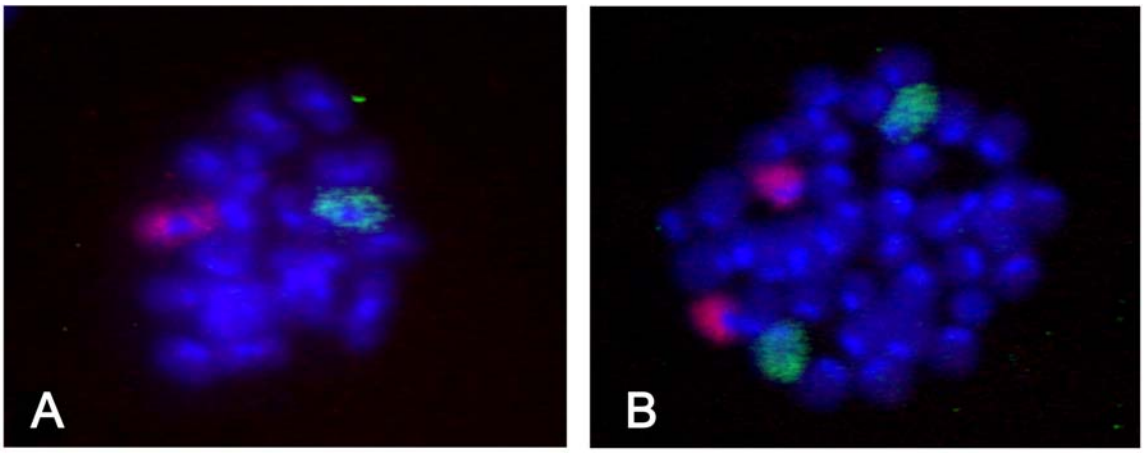
RESULTS

Chromosome Univalence and Events of the G2/M Transition in Mlh1$^{-/-}$ Spermatocytes

Previous findings of lack of MLH1 protein foci in *Mlh1*$^{-/-}$ spermatocytes and meiotic chromosome univalence (Baker *et al.*, 1996; Edelmann *et al.*, 1996) were confirmed. Chromosome behavior in *Mlh1*$^{-/-}$ spermatocytes was studied using FISH with chromosome-specific (Chrs. 2 and 8) paint probes on surface-spread chromosome preparations. This analysis was carried out on metaphase I (MI) spermatocytes retrieved from testes as well as on pachytene spermatocytes induced to reach MI by treatment with the phosphatase inhibitor OA (Wiltshire *et al.*, 1995), a protocol providing a larger number of MI spermatocytes for statistical purposes. Appropriate chromosome pairing, indicated by juxtaposed FISH signals, was observed for Chrs. 2 and 8 in control (*Mlh1*$^{+/+}$) spermatocytes, with 0% mispairing both *in vivo* and *in vitro* after treatment with OA (Fig. 1A). Among *Mlh1*$^{-/-}$spermatocytes, the majority (90%) of Chrs. 2 and 8 were neither homologously paired nor in physical proximity; that is, they were separated by more than one FISH signal domain (Fig. 1B). Since surface-spread chromosomes were scored, it is not known if homologous chromosomes could be in closer physical proximity in vivo. Nonetheless, this analysis reveals a clear difference in proximity of homologs when mutant and control spermatocytes were compared.

Incubation of pachytene spermatocytes with OA is an assay that allowed assessment of competence of the MLH1-deficient spermatocytes to undergo various

Figure 1. Chromosome pairing is defective in *Mlh1*$^{-/-}$ spermatocytes as revealed by FISH analysis of MI spermatocytes from *Mlh1*$^{+/+}$ (A) and *Mlh1*$^{-/-}$ (B) mice with chromosome paint probes (for chromosomes 2 , green, and 8, red, with DAPI-stained chromatin in blue). In A, signals of the same color are juxtaposed in a single bivalent, indicating paired homologous chromosomes in control spermatocytes. In B, univalent chromosomes are identified by 2 separate signals per chromosome in mutant spermatocytes.


A
B

events of the G2/M transition (Cobb *et al.*, 1999a). In these analyses, characteristic processes of the G2/M were monitored. These included disassembly of the axes of the synaptonemal complex recognized by the antibody to mouse SYCP3, condensation and individualization of chromosomes, the phosphorylation of histone H3, a characteristic marker of the transition into metaphase in both mitotic and meiotic cells (Cobb *et al.*, 1999b), and presence of division-phase phosphorylated epitopes recognized by the MPM-2 antiserum. In both control and mutant *Mlh1*$^{-/-}$ spermatocytes, treatment with OA led to chromosome condensation and other events of the G2/M transition (Figs. 2 and 3). Analysis of MI chromosomes in standard Giemsa-stained chromosome preparations (Fig. 2) not only revealed almost complete absence of chiasmata in mutant *Mlh1*$^{-/-}$ spermatocytes, but also showed competence to condense chromosomes in response to OA treatment (Fig. 2B). Both histone H3 phosphorylation and disassembly of the synaptonemal complex (SC), events consistent with metaphase entry, were also observed in OA-treated *Mlh1*$^{-/-}$ spermatocytes (Fig. 3). These events occur in a temporally normal manner in MLH1-deficient spermatocytes (Figs. 3B and D), with histone H3 phosphorylation originating in the centromeric heterochromatin in diplotene spermatocytes and pervasive throughout the chromatin in MI spermatocytes (Figs. 3A and B). These data show that although bivalent chromosomes are rarely formed, the entry into metaphase in *Mlh1*$^{-/-}$ spermatocytes is similar to that of *Mlh1*$^{+/+}$ spermatocytes, implying that although the MLH1 protein may be required for chiasmata formation or maintenance, chiasmata are not part of the signal machinery enabling either the normal or precocious, OA-induced, G2/M transition.

Figure 2. Pachytene spermatocytes from *Mlh1*$^{-/-}$ mice are competent to condense chromosomes in response to OA treatment. A. Control *Mlh1*$^{+/+}$ spermatocytes treated with OA for 6 hrs. B. *Mlh1*$^{-/-}$ spermatocytes treated with OA for 6 hrs. Condensed chromosomes are usually univalents, assessed by chromosome number, morphology and absence of visible chiasmata. C. *Mlh1*$^{-/-}$ spermatocytes treated with OA for 6 hrs., showing occasional chiasmate bivalents (arrow).

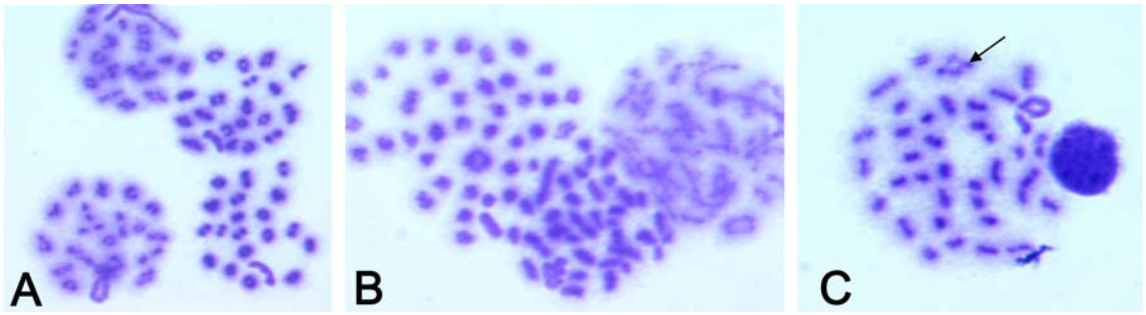
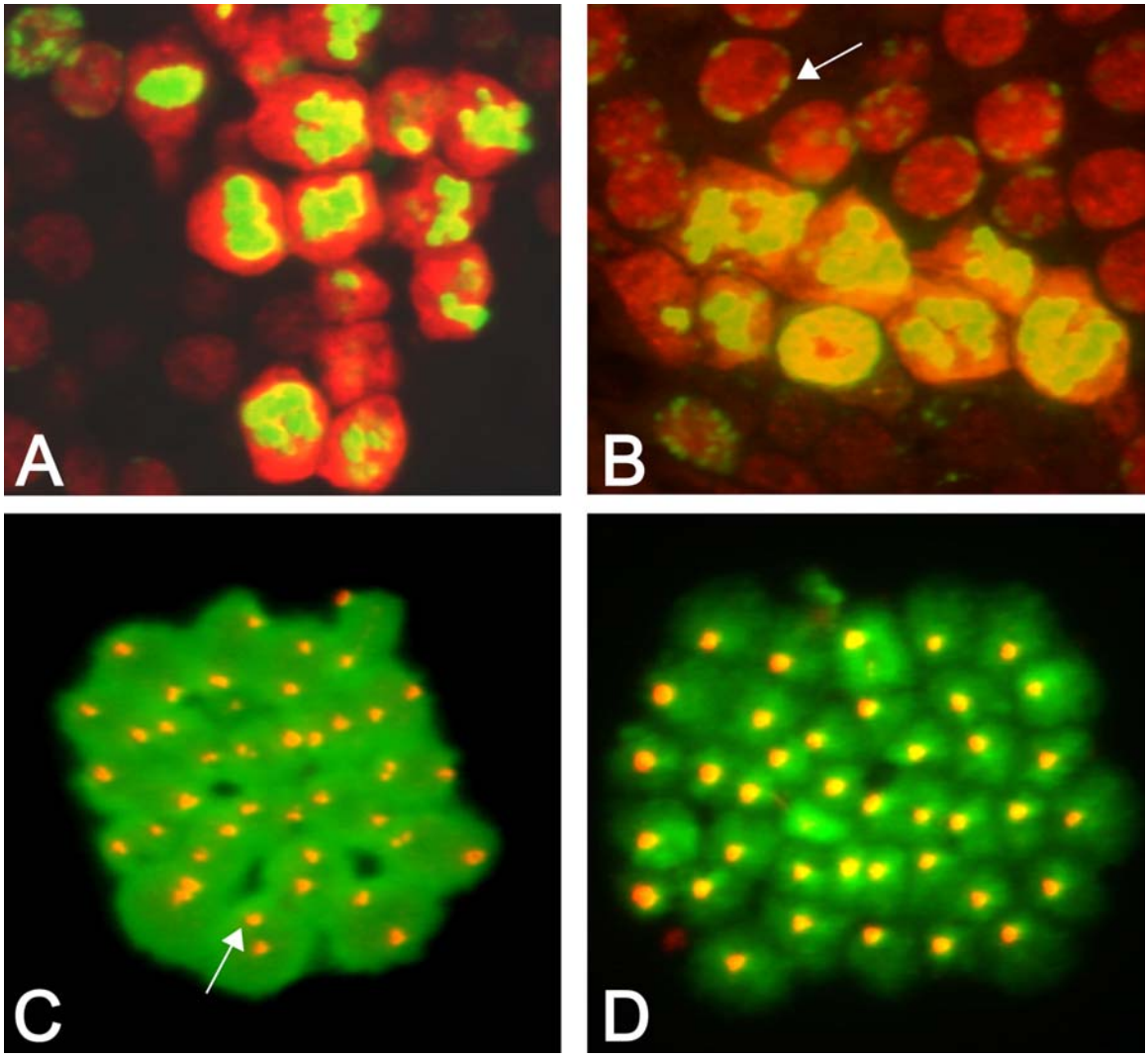

A
B
C

Figure 3. Events of the OA-induced G2/M occur in normal temporal order in *Mlh1*$^{-/-}$ spermatocytes. A. Section of stage XI-XII tubule from control *Mlh1*$^{+/-}$ testis, stained with antibodies for division-phase MPM-2 epitopes (red) and phosphorylated histone H3 (green), showing MI spermatocytes with aligned chromosomes. B. Section of stage XI-XII tubule from testis of an *Mlh1*$^{-/-}$ mouse, stained as in Fig. 1A. Note that diplotene spermatocytes show "speckled" staining for phosphorylated histone H3 at the centromeric heterochromatin located near the nuclear envelope (arrow) and that MI spermatocytes with heavily phosphorylated histone H3 do not have neatly aligned chromosomes. C. This image of a surface-spread control MI spermatocyte, stained with antibodies against SYCP3 (red) and phosphorylated histone H3 (green), shows typical residual SYCP3 staining at the paired metaphase centromeres (arrow). D. This *Mlh1*$^{-/-}$ spermatocyte, prepared as in Fig. 3C, shows that histone H3 is phosphorylated at MI, but that homologous centromeres are not paired.

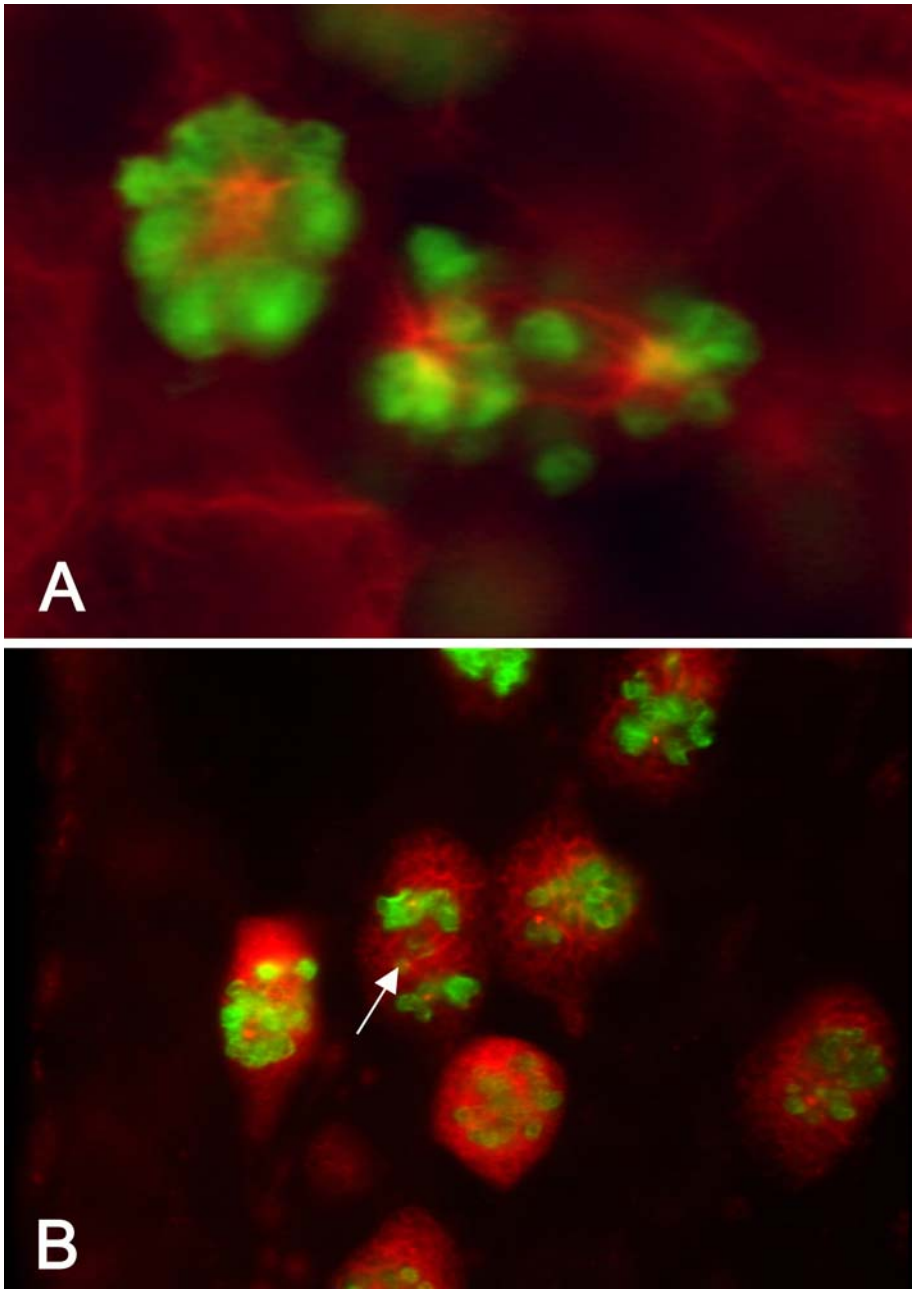

A
B
C
D

Spermatocytes of Mlh1$^{-/-}$ Mice Exhibit Metaphase Abnormalities and Apoptosis

Although *Mlh1*$^{-/-}$ spermatocytes show many characteristics of normal prophase to metaphase transition, their progress is halted soon after. In order to observe details of metaphase spindle dynamics in *Mlh1*$^{-/-}$ spermatocytes, we monitored spindle formation and chromosome behavior using immunofluorescence with antibodies against βeta-tubulin (to detect the spindle) and phospho-histone H3 (to visualize metaphase chromosomes). Confocal imaging was important to facilitate determination of whether chromosomes were misaligned on the MI spindle. Bipolar spindle formation, revealed by staining with anti-tubulin, does occur in the presence of univalent chromosomes. However, the univalent chromosomes of *Mlh1*$^{-/-}$ MI spermatocytes do not regularly achieve alignment and bipolar orientation on the spindle equator (Fig. 4A). Anaphase was only rarely observed among *Mlh1*$^{-/-}$ spermatocytes; it was characterized by lagging chromosomes in the spindle midzone (Fig. 4B). No metaphase II (MII) spermatocytes or round spermatids were seen in *Mlh1*$^{-/-}$ mice, evidence for elimination of spermatocytes at MI.

Since it was previously shown that metaphase spermatocytes with unaligned chromosomes frequently undergo apoptosis (Eaker *et al.*, 2001), the TUNEL assay was utilized to determine if apoptotic spermatocytes were present in testes of *Mlh1*$^{-/-}$ mice. To determine the relationship between germ-cell stage and cell death, apoptosis was scored in cross-sections of seminiferous tubules from mice 16, 18, 20, 22 and 24 days old, as well as from adults. Three control and three mutant mice from each age were used. Tubules with more than three apoptotic cells were scored as apoptotic, consistent with previously established criteria (Kon *et al.*, 1999). An increased frequency of tubules

Figure 4. Abnormalities characterize chromosome alignment and segregation in *Mlh1*$^{-/-}$ spermatocytes, revealed by confocal microscopy. A. Two *Mlh1*$^{-/-}$ MI spermatocytes stained with antibody to phosphorylated histone H3 (green) and to beta-tubulin (red). In the spermatocyte on the right chromosomes are scattered throughout the cell and not aligned on the spindle. The spermatocyte on the left is in a prometaphase configuration. B. An anaphase I *Mlh1*$^{-/-}$ spermatocyte stained with antibodies against MPM-2 antigens (red) and phosphorylated histone H3 (green) is shown, with lagging chromosomes (arrow) in the central zone of the spindle.


A
B

with apoptosis was detected in *Mlh1*$^{-/-}$ testes compared to control testes (Fig. 5A). Although the incidence of apoptosis was statistically different between most ages, the largest increase in the number of apoptotic tubules appeared at 22 days of age in tubules from *Mlh1*$^{-/-}$ mice (Figs. 5A). This age coincides with the appearance of significant numbers of MI spermatocytes, detected by staining of spermatocytes with antibody against phosphorylated histone H3, in both *Mlh1*$^{+/+}$ and *Mlh1*$^{-/-}$ mice (Fig. 5B). Although the incidence of apoptosis was significantly different at this age, there was no difference between *Mlh1*$^{+/+}$ and *Mlh1*$^{-/-}$ testes in the frequency of tubules with metaphase spermatocytes (Fig. 5B).

These observations suggested that *Mlh1*$^{-/-}$ spermatocytes undergo apoptosis after reaching MI, but in order to determine the timing of apoptosis relative to metaphase entry, carefully staged seminiferous tubule cross-sections were examined after staining for apoptosis with the TUNEL method and with antibodies against SYCP3 or phosphorylated histone H3 to recognize diplotene and MI spermatocytes. In both sectioned tubules from adults (Fig. 6) and fibrin clot-embedded spermatocytes (not shown), apoptosis was not detected in the diplotene spermatocytes, recognized as those with a "speckled" pattern of staining with antibody recognizing phosphorylated histone H3 (Fig. 6) and initial disassembly of the synaptonemal complex. Apoptosis was detected in spermatocytes deduced to be metaphase from tubule staging (stage XII) and chromatin patterns (Fig. 6). Interestingly, the majority of apoptotic cells lacked staining for phosphorylated histone H3, although some metaphase spermatocytes stained for both apoptosis and phosphorylated histone H3. The disappearance of reactivity for phosphorylated histone H3 in apoptotic spermatocytes may be due to its degradation in

Figure 5. There is a developmental increase in the frequency of apoptotic seminiferous tubule cross-sections in testes of *Mlh1*$^{-/-}$ mice. A. The frequency of tubules with apoptotic cells in *Mlh1*$^{-/-}$ (black bars) mice relative to control mice (white bars) increases dramatically at 22 days of age. B. The frequency of tubules with MI spermatocytes, recognized by antibody to phosphorylated histone H3 cells does not differ between *Mlh1*$^{+/+}$ (white bars) and *Mlh1*$^{-/-}$ (black bars) testes. Asterisks represent paired values that differ significantly from each other.

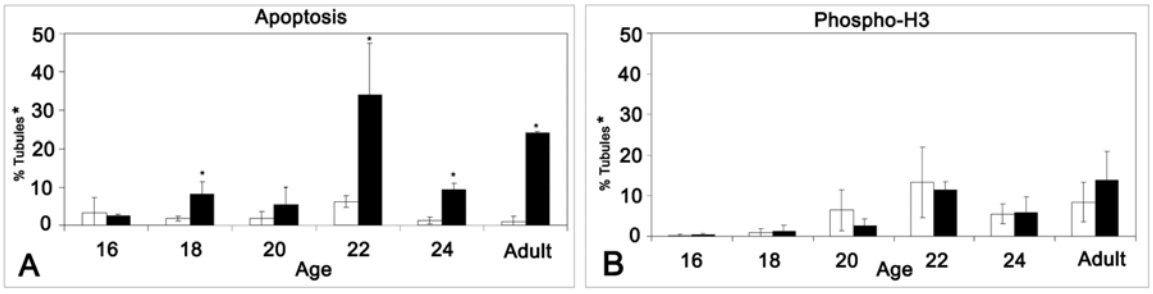
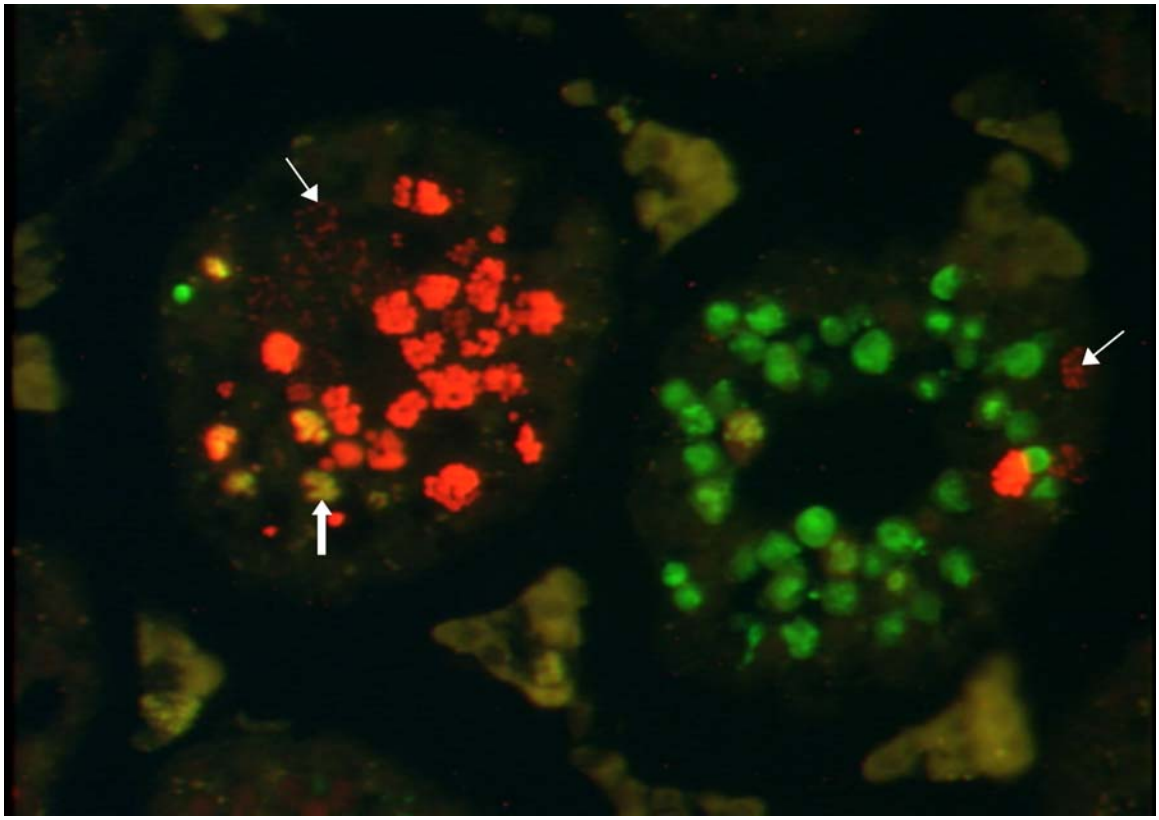

Apoptosis
% Tubules*
50
40
30
20
10
0
16
18
20
22
24
Adult
Age
A
Phospho-H3
% Tubules*
50
40
30
20
10
0
16
18
20
22
24
Adult
Age
B

Figure 6. Apoptosis of *Mlh1*$^{-/-}$ spermatocytes occurs at MI. This section from the testis of an Mlh1-/- male is stained for apoptosis by the TUNEL reaction (green) and with antibody against phosphorylated histone H3 (red) to detect division-phase spermatocytes. The tubule cross-section on the left is at the stage XI-XII transition, with both diplotene and MI cells visible. The diplotene spermatocytes (thin arrow) are recognized by patches of phosphorylated histone H3 and show no TUNEL staining. Many MI spermatocytes are intensely stained red by the antibody to phosphorylated histone H3, but are not apoptotic. Other MI spermatocytes have become apoptotic, staining yellow (thick arrow). The tubule cross-section on the right is stage XII, identified by two MI spermatocytes staining positively (red) for phosphorylated histone H3. Only two diplotene spermatocytes are present (thin arrow) and the vast majority of MI spermatocytes are stained positively (green) for apoptosis.



apoptotic cells, or to dephosphorylation. This phenomenon has been previously observed by us (Eaker et al., 2001). Taken together, these analyses showed that large numbers of apoptotic cells were first detected in the testes of *Mlh1*$^{-/-}$ mice at 22 days of age, coinciding with the first appearance of metaphase spermatocytes, and that apoptosis occurs after metaphase entry and chromosome condensation, and not in pachytene or diplotene spermatocytes.

CHAPTER IV

DISCUSSION

The progress of meiosis was analyzed in spermatocytes from *Mlh1*-knockout mice to determine the response to absence of the MLH1 protein. Of particular interest was whether impairment of meiotic and spermatogenic progress would be initiated during meiotic prophase when MLH1 foci normally first appear, or later. Absence of chiasmata in *Mlh1*$^{-/-}$ spermatocytes as previously described (Baker *et al.*, 1996; Edelmann *et al.*, 1996) was confirmed. Additionally, use of chromosome paint probes revealed that 90% of the Chrs. 2 and 8 were not closely associated with their homologous partners. Nonetheless, exit from meiotic prophase and entry into meiotic metaphase occurred in mutant spermatocytes and had many hallmarks of the normal process. Additionally, the induction *in vitro* of metaphase by OA suggests that mutant spermatocytes acquire metaphase competence on a normal schedule in spite of absence of MLH1 protein. Although a bipolar spindle was assembled in MI spermatocytes from *Mlh1*$^{-/-}$ mice, the univalent chromosomes failed to achieve alignment and bipolar orientation at the spindle equator and further progress of meiosis and spermatogenesis was not observed. Mutant spermatocytes exhibited features of apoptosis at metaphase, but not before, in either the pachytene or diplotene stages of meiotic prophase. Thus, although MLH1 protein first accumulates in foci at the mid-pachytene stage of meiotic prophase (Anderson *et al.*, 1999; Ashley and Plug, 1998; Baker *et al.*, 1996; Barlow and Hulten, 1998), apparent defects in the progress of spermatogenesis do not arise until metaphase of the first meiotic division.

The precise function of the MLH1 protein in mammalian meiotic recombination is not completely understood. In yeast, MLH1 protein promotes resolution of recombination events as crossovers (Hunter and Borts, 1997), suggesting a role in resolution of recombination events and/or crossovers. Indeed, in both mice and humans, the distribution of MLH1 foci in spermatocytes is highly correlated with both frequency and distribution of crossovers (Anderson *et al.*, 1999; Barlow and Hulten, 1998), and other members of the complex of mismatch repair proteins are also implicated in recombination (Cohen and Pollard, 2001). If MLH1 does resolve recombination in mammals, one would think that bivalents lacking MLH1 might get "stuck" in its absence, unable to resolve recombination intermediates. The presence of univalent chromosomes in knockout gametocytes means that somehow the bivalents were able to resolve chromosomes in the absence of MLH1 protein. Normally, MLH1 foci begin to accumulate on meiotic chromosome cores in the pachytene stage, primarily at mid-pachynema (Baker *et al.*, 1996; Tarsounas and Moens, 2001). However, the immunologically detectable foci are transient, rising from none at early pachynema, to a peak at mid to late pachynema, and declining to none by late pachynema (Anderson *et al.*, 1999). Thus, the prophase localization of MLH1 foci and the post-synaptic (metaphase) univalency pose an enigma about both the nature and the precise time of MLH1 function in mammalian meiotic cells.

A striking aspect of MLH1 deficiency is that both spermatocytes and oocytes arrest well after accumulation of MLH1 protein in nuclei. Interestingly, the phenotype of absence of two other proteins whose function may be involved in DNA mismatch repair, MSH4 and MSH5, is arrest at the time the proteins begin to accumulate. MSH4 protein

forms discrete foci along chromosomes early in meiotic prophase and spermatocytes lacking the protein are arrested and undergo apoptosis in early meiotic prophase (Kneitz *et al.*, 2000). Spermatocytes lacking MSH5 protein likewise undergo arrest early in meiotic prophase (de Vries *et al.*, 1999; Edelmann *et al.*, 1999). Similar observations of spermatogenic arrest at the time of accumulation of the relevant protein have been made with respect to spermatocytes lacking other proteins whose role in meiosis is implied, such as DMC1 (Pittman *et al.*, 1998; Yoshida *et al.*, 1998) and ATM (Barlow *et al.*, 1996; Xu *et al.*, 1996). In marked contrast, mice deficient in MLH1 protein do not undergo arrest and apoptosis of gametocytes until considerably after the protein accumulates, as documented here and elsewhere (Baker *et al.*, 1996; Edelmann *et al.*, 1996; Woods *et al.*, 1999). Although it might be that arrest and apoptosis could initiate at the time MLH1 protein accumulates in nuclei of spermatocytes, with progressive elimination until the time of metaphase, our developmental analysis shows that spermatocytes progress normally into MI. Thus there does not appear to be a gradual developmental accumulation of apoptotic cells throughout prophase, culminating at metaphase. Instead, arrest and apoptosis were detectable only after assembly of a bipolar spindle and misalignment of chromosomes on the spindle.

Our observations have several interesting implications with respect to the role of MLH1 in both progress of spermatogenesis and checkpoint control. All *Mlh1*$^{-/-}$ spermatocytes are characterized at MI by a very high frequency of univalent chromosomes, indicating massive, although not complete, failure in either formation or maintenance of chiasmata. Yet both in vivo and in vitro, mutant spermatocytes are competent to enter MI, doing so with many normal features of the G2/M transition. This

implies that stable chiasmata are neither required nor monitored for the transition from prophase to metaphase. Yet both in yeast (Bailis and Roeder, 2000; Bailis *et al.*, 2000; Leu and Roeder, 1999; Lydall *et al.*, 1996; McKee and Kleckner, 1997; Roeder and Bailis, 2000; San-Segundo and Roeder, 1999; San-Segundo and Roeder, 2000; Tung *et al.*, 2000; Xu *et al.*, 1997; Xu *et al.*, 1995) and, to a lesser extent, in mammals (Mahadevaiah *et al.*, 2000; Odorisio *et al.*, 1998; Rodriguez and Burgoyne, 2000) there is genetic evidence for checkpoints operating to monitor progress through meiotic prophase. Such checkpoints might effectively monitor pairing, synapsis, recombination or chiasmata, as well as acquisition of competence to undergo the meiotic division phase, and perhaps even competence for postmeiotic differentiation (sporulation or spermiogenesis). Checkpoints monitoring the progress of recombination in yeast link these events to the unfolding of the cell cycle and transition out of prophase. Thus cells with incomplete recombination do not enter the division phase; downstream effectors of the checkpoint include cell cycle regulators and involve phosphorylation events (Roeder and Bailis, 2000). Interestingly, in mammalian spermatocytes, defective synapsis seemingly can lead either to pachytene-stage germ cell loss or to MI arrest and apoptosis (Odorisio *et al.*, 1998). Importantly, in absence of mutations in checkpoint sensors and effectors, it is not yet known with certainty if arrest in these conditions is due to a checkpoint-mediated process or to a mechanical requirement for a previously occurring event that allows progress of spermatogenesis. Taken together, various analyses of spermatocytes lacking MLH1 suggest that MLH1 foci are not required for cell-cycle progress, nor is there a checkpoint-mediated arrest that signals a halt during prophase in their absence. Instead, the vast majority of MLH1-deficient spermatocytes arrest at

metaphase, not in the pachytene stage of prophase, much later than when MLH1 is first assembled onto chromosomes.

Metaphase arrest may be because chromosomes of mutant spermatocytes do not align correctly on the spindle during prometaphase, as was also observed for chromosomes in MLH1-deficient oocytes (Woods *et al.*, 1999). This observation implies that either MLH1 protein or, more likely, the physical links between homologs stabilized by a mechanism involving MLH1, are required for appropriate congression at the equator of the MI spindle. It is well known that tension is required for chromosome alignment and onset of anaphase (Li and Nicklas, 1995), and MLH1-deficient spermatocyte chromosomes cannot develop tension at MI because of lack of chiasmata. Thus metaphase arrest and apoptosis of MLH1-deficient spermatocytes could be a function of a checkpoint sensing that chromosomes are not attached or developing tension on the spindle. However, it is likely that this issue cannot be resolved until relevant checkpoint proteins and effectors are identified by mutation analysis.

The spermatocyte's assembly of an organized bipolar spindle despite univalent chromosomes is in contrast to abnormal spindle morphogenesis in *Mlh1*$^{-/-}$ oocytes (Woods *et al.*, 1999). Thus, although bivalent chromosomes and normal congression are apparently prerequisites for normal spindle morphogenesis in the oocyte, they do not appear to be required in spermatocytes. This may well be a reflection of the fact that, unlike the spindle in mammalian oocytes, the meiotic spindle in spermatocytes is nucleated by two centrosomes, even before its association with chromosomes (Kallio *et al.*, 1998).

Although MLH1-deficient spermatocytes clearly die by apoptosis, the executioner is not yet known. Since the genetic defect is intrinsic to the germ cells, one might presume that the signal for apoptosis is likewise germ cell-autonomous. However, in the absence of experimental information, it cannot be excluded that defective germ cells might influence Sertoli cells to initiate the apoptotic process.

ACKNOWLEDGEMENTS

This work was supported by a grant from the NIH, HD33816, to MAH. Sean Baker is gratefully acknowledged for providing mice to establish a colony segregating the *Mlh1* null allele. We are indebted to Brent Bowker, Debby Andreadis and Lori Kellam for able technical assistance, including maintenance and genotyping of the mice. We owe thanks to members of the Handel laboratory for frequent discussions and to Drs. John Eppig and Bruce McKee for thoughtful comments on the manuscript.

LIST OF REFERENCES

Anderson, L. K., Reeves, A., Webb, L. M., and Ashley, T. (1999). Distribution of crossing over on mouse synaptonemal complexes using immunofluorescent localization of MLH1 protein. *Genetics* 151, 1569-1579.

Ashley, T., and Plug, A. (1998). Caught in the act: Deducing meiotic function from protein immunolocalization. *In* "Meiosis and Gametogenesis" (M. A. Handel, Ed.), Vol. 37, pp. 201. Academic Press Inc, 525 B Street, Suite 1900, San Diego, CA 92101-4495.

Bailis, J. M., and Roeder, G. S. (2000). Pachytene exit controlled by reversal of Mek1-dependent phosphorylation. *Cell* 101, 211-221.

Bailis, J. M., Smith, A. V., and Roeder, G. S. (2000). Bypass of a meiotic checkpoint by overproduction of meiotic chromosomal proteins. *Mol Cell Biol* 20, 4838-4848.

Baker, S. M., Plug, A. W., Prolla, T. A., Bronner, C. E., Harris, A. C., Yao, X., Christie, D. M., Monell, C., Arnheim, N., Bradley, A., Ashley, T., and Liskay, R. M. (1996). Involvement of mouse *Mlh1* in DNA mismatch repair and meiotic crossing over. *Nat Genet* 13, 336-342.

Barlow, A. L., and Hulten, M. A. (1998). Crossing over analysis at pachytene in man. *Eur J Human Genet* 6, 350-358.

Barlow, C., Hirotsune, S., Paylor, R., Liyanage, M., Eckhaus, M., Collins, F., Shiloh, Y., Crawley, J. N., Ried, T., Tagle, D., and Wynshaw-Boris, A. (1996). *Atm*-deficient mice: a paradigm of ataxia telangiectasia. *Cell* 86, 159-171.

Bellve, A. R. (1993). Purification, culture and fractionation of spermatogenic cells. *Methods in Enzymology* 225, 84-113.

Carpenter, A. T. C. (1994). Chiasma function. *Cell* 77, 959-962.

Cobb, J., Cargile, B., and Handel, M. A. (1999a). Acquisition of competence to condense metaphase I chromosomes during spermatogenesis. *Develop Biol* 205, 49-64.

Cobb, J., Miyaike, M., Kikuchi, A., and Handel, M. A. (1999b). Meiotic events at the centromeric heterochromatin: histone H3 phosphorylation, topoisomerase II alpha localization and chromosome condensation. *Chromosoma* 108, 412-425.

Cohen, P., and Pollard, J. W. (2001). Regulation of meiotic recombination and prophase I progression in mammals. *BioEssays* 23, 996-109.

de Vries, S. S., Baart, E. B., Dekker, M., Siezen, A., de Rooij, D. G., de Boer, P., and te Riele, H. (1999). Mouse MutS-like protein Msh5 is required for proper chromosome synapsis in male and female meiosis. *Gene Develop* 13, 523-531.

Eaker, S., Pyle, A., Cobb, J., and Handel, M. A. (2001). Evidence for meiotic spindle checkpoint from analysis of spermatocytes from Robertsonian-chromosome heterozygous mice. *J Cell Sci* 114, 2953-2965.

Edelmann, W., Cohen, P. E., Kane, M., Lau, K., Morrow, B., Bennett, S., Umar, A., Kunkel, T., Cattoretti, G., Chaganti, R., Pollard, J. W., Kolodner, R. D., and Kucherlapati, R. (1996). Meiotic pachytene arrest in MLH1-deficient mice. *Cell* 85, 1125-1134.

Edelmann, W., Cohen, P. E., Kneitz, B., Winand, N., Lia, M., Heyer, J., Kolodner, R., Pollard, J. W., and Kucherlapati, R. (1999). Mammalian MutS homologue 5 is required for chromosome pairing in meiosis. *Nat Genet* 21, 123-127.

Evans, E. P., Breckon, G., and Ford, C. E. (1964). An air-drying method for meiotic preparations from mammalian testes. *Cytogenetics* 3, 289-294.

Hunter, N., and Borts, R. H. (1997). Mlh1 is unique among mismatch repair proteins in its ability to promote crossing-over during meiosis. *Gene Develop* 11, 1573-1582.

Kallio, M., Mustalahti, T., Yen, T. J., and Lahdetie, J. (1998). Immunolocalization of alpha-tubulin, gamma-tubulin, and CENP-E in male rat and male mouse meiotic divisions: Pathway of meiosis I spindle formation in mammalian spermatocytes. *Dev Biol* 195, 29-37.

Kneitz, B., Cohen, P. E., Avdievich, E., Zhu, L. Y., Kane, M. F., Hou, H., Kolodner, R. D., Kucherlapati, R., Pollard, J. W., and Edelmann, W. (2000). MutS homolog 4 localization to meiotic chromosomes is required for chromosome pairing during meiosis in male and female mice. *Gene Develop* 14, 1085-1097.

Koehler, K. E., Hawley, R. S., Sherman, S., and Hassold, T. (1996). Recombination and nondisjunction in humans and flies. *Hum. Molec. Genet.* 5, 1495-1504.

Kon, Y., Horikoshi, H., and Endoh, D. (1999). Metaphase-specific cell death in meiotic spermatocytes in mice. *Cell Tissue Res* 296, 359-369.

Leu, J. Y., and Roeder, G. S. (1999). The pachytene checkpoint in *S. cerevisiae* depends on Swe1-mediated phosphorylation of the cyclin-dependent kinase Cdc28. *Mol Cell* 4, 805-814.

Li, X., and Nicklas, R. B. (1995). Mitotic forces control a cell-cycle checkpoint. *Nature* 373, 630-632.

Lydall, D., Nikolsky, Y., Bishop, D. K., and Weinert, T. (1996). A meiotic recombination checkpoint controlled by mitotic checkpoint genes. *Nature* 383, 840-843.

Mahadevaiah, S. K., Evans, E. P., and Burgoyne, P. S. (2000). An analysis of meiotic impairment and of sex chromosome associations throughout meiosis in XYY mice. *Cytogenet Cell Genet* 89, 29-37.

McKee, A. H. Z., and Kleckner, N. (1997). Mutations in *Saccharomyces cerevisiae* that block meiotic prophase chromosome metabolism and confer cell cycle arrest at pachytene identify two new meiosis-specific genes *SAE1* and *SAE3*. *Genetics* 146, 817-834.

Odorisio, T., Rodriguez, T. A., Evans, E. P., Clarke, A. R., and Burgoyne, P. S. (1998). The meiotic checkpoint monitoring synapsis eliminates spermatocytes via p53-independent apoptosis. *Nat Genet* 18, 257-261.

Parvinen, M., Toppari, J., and Lahdetie, J. (1993). Transillumination phase contrast microscope techniques for evaluation of male germ cell toxicity and mutagenicity. *In* "Methods in Toxicology" (R. E. Chapin and J. J. Heindel, Eds.), Vol. 3, part A, pp. 142-165. Academic Press, San Diego.

Pittman, D. L., Cobb, J., Schimenti, K. J., Wilson, L. A., Cooper, D. M., Brignull, E., Handel, M. A., and Schimenti, J. C. (1998). Meiotic prophase arrest with failure of chromosome synapsis in mice deficient for *Dmc1*, a germline-specific RecA homolog. *Mol Cell* 1, 697-705.

Rodriguez, T. A., and Burgoyne, P. S. (2000). Evidence that sex chromosome asynapsis, rather than excess Y gene dosage, is responsible for the meiotic impairment of XYY mice. *Cytogenet Cell Genet* 89, 38-43.

Roeder, G. S., and Bailis, J. M. (2000). The pachytene checkpoint. *Trends Genet* 16, 395-403.

San-Segundo, P. A., and Roeder, G. S. (1999). Pch2 links chromatin silencing to meiotic checkpoint control. *Cell* 97, 313-324.

San-Segundo, P. A., and Roeder, G. S. (2000). Role for the silencing protein Dot1 in meiotic checkpoint control. *Mol Biol Cell* 11, 3601-3615.

Smith, K. N., and Nicolas, A. (1998). Recombination at work for meiosis. *Curr Opin Genet Develop* 8, 200-211.

Tarsounas, M., and Moens, P. B. (2001). Checkpoint and DNA-repair proteins are associated with the cores of mammalian meiotic chromosomes. *In* "Current Topics In Development" (G. P. Schatten, Ed.), Vol. 51, pp. 109-134. Academic Press Inc, 525 B Street, Suite 1900, San Diego, CA 92101-4495, USA.

Tung, K. S., Hong, E. J. E., and Roeder, G. S. (2000). The pachytene checkpoint prevents accumulation and phosphorylation of the meiosis-specific transcription factor Ndt80. *Proc Nat Acad Sci USA* 97, 12187-12192.

Wiltshire, T., Park, C., Caldwell, K. A., and Handel, M. A. (1995). Induced premature G2/M transition in pachytene spermatocytes includes events unique to meiosis. *Dev. Biol.* 169, 557-567.

Woods, L. M., Hodges, C. A., Baart, E., Baker, S. M., Liskay, M., and Hunt, P. A. (1999). Chromosomal influence on meiotic spindle assembly: Abnormal meiosis I in female *Mlh1* mutant mice. *J Cell Biol* 145, 1395-1406.

Xu, L. H., Weiner, B. M., and Kleckner, N. (1997). Meiotic cells monitor the status of the interhomolog recombination complex. *Gene Develop* 11, 106-118.

Xu, L. Z., Ajimura, M., Padmore, R., Klein, C., and Kleckner, N. (1995). NDT80, a meiosis-specific gene required for exit from pachytene in *Saccharomyces cerevisiae*. *Mol Cell Biol* 15, 6572-6581.

Xu, Y., Ashley, T., Brainerd, E. E., Bronson, R. T., Meyn, M. S., and Baltimore, D. (1996). Targeted disruption of *ATM* leads to growth retardation, chromosomal fragmentation during meiosis, immune defects, and thymic lymphoma. *Gene Develop* 10, 2411-2422.

Yoshida, K., Kondoh, G., Matsuda, Y., Habu, T., Nishimune, Y., and Morita, T. (1998). The mouse RecA-like gene *Dmc1* is required for homologous chromosome synapsis during meiosis. *Mol Cell* 1, 707-718.

PART V

PARTIAL COMPLEMENTATION OF *Brca2* MUTATION IN MICE BY THE HUMAN *BRCA2* GENE SHOWS A SEXUALLY DIMORPHIC MEIOTIC PHENOTYPE*

* The work for this part was accomplished by efforts of April Pyle, Shyam Sharan, Jamie Benedict, Vinenzo Coppola, Betty K. Martin, Lino Tessarollo, Jodi Flaws, and Mary Ann Handel.

ABSTRACT

The role of *Brca2* in gametogenesis is poorly understood. Although the protein has been detected in gonads, analysis of its precise function has not been possible due to the embryonic lethality of the knockout mice. We report here the rescue of the embryonic lethality by using a bacterial artificial chromosomal (BAC) containing the human *BRCA2* gene. The rescued BAC transgenic mice are phenotypically indistinguishable from their wild type littermates but they are sterile as the human transgene is poorly expressed in the gonads. Thus, the rescued *Brca2* mutant mice, in effect, represent a conditional or "severely repressed" knockout with respect to the gonads. The morphology of the testes of these mice at three weeks of age revealed both germ cell depletion and arrest of spermatogenesis at an early prophase stage. Arrest in zygonema was confirmed by analysis of surface spread spermatocytes by immunostaining using antibodies against the synaptonemal complex protein SYCP3 and the male germ-cell specific histone H1t. Approximately 0.5% of the spermatocytes progress to early-pachytene stage and none were positive for histone H1t, a marker for mid-pachytene. Additionally, the number of Rad51 foci localized to the chromatin was drastically reduced in rescued spermatocytes compared to wild-type. In contrast to the germ-cell deficient testes, there were no significant differences in the appearance of wild-type and *Brca2*-deficient ovaries harvested on postnatal days (PNDs) 2 and 21 (ovarian studies not presented in dissertation). At PND2, both classes of ovaries contained

morphologically normal and similar number of primodial and primary follicles. At PND21, both wild-type and rescued ovaries contained morphologically normal follicles in all stages of development and corpus lutea suggesting that unlike the spermatocytes, the primary oocytes are not arrested early in meiotic prophase. Although there were a similar number of antral follicles in the ovaries of PN21 wild type and rescued females, there was a significant reduction in the number of primodial and primary follicles in the rescued females. The ovarian follicles of adult females, which are mostly sterile, shows marked degeneration. Taken together these data reveal a sexually dimorphic response for *Brca2* in gametogenesis.

CHAPTER I

INTRODUCTION

Efforts to identify the genetic basis of familial breast cancer reached fruition, when the breast-cancer-susceptibility genes *BRCA1* and *BRCA2* were identified through positional cloning. Germline mutations in either of these genes account for 20-60% of breast cancer cases in families where multiple individuals are affected (2-6% of all cases) (Nathanson et al., 2001). The majority of mutations found in *BRCA1* and *BRCA2* are small insertions or deletions distributed throughout the genes, which are predicted to result in truncation of the encoded protein (Venkitaraman, 2001). Attempts to determine a correlation between the inheritance of a particular mutation and the resulting disease phenotype have proven largely unsuccessful. In part, this is because the prevalence of specific mutations is so small, but mostly because the associated-cancer risk is modified my additional factors (Gayther et al., 1997). Identification of genetic or environmental factors that modify the phenotypic effects of mutations in these genes is needed to provide important new insights into inherited cancer predisposition.

Despite the apparent dissimilarity in protein sequence and structure, there is considerable evidence that BRCA1 and BRCA2 have common biological functions. They are expressed in many tissues in a cell-cycle-dependent manner, and both are localized to the nucleus in somatic cells, where they co-exist in subnuclear foci that redistribute following DNA damage (Sharan and Bradley, 1997). In meiotic cells, both proteins co-localize to the synaptonemal complexes of the developing axial elements (Chen et al., 1998a). In addition, both gene products interact with hRAD51 in vivo

(Scully et al., 1997; Sharan et al., 1997). This is important, as RAD51 plays a key role in homologous recombination and double-strand break (DSB) repair. BRCA1, BRCA2, and RAD51 nullizygous mice are all embryonic lethals, for review and specific stage of embryonic arrest, see (Chen et al., 1998a).

There is evidence that BRCA2 is essential for DSB repair by homologous recombination. Cells with truncated *Brca2* accumulate aberrations in chromosome structure during passage in culture. In addition, the formation of nuclear foci containing RAD51 after exposure to DNA damage, putative sites for recombination repair, is compromised by BRCA2 deficiency (Chen et al., 1999). BRCA2 is also thought to control the intracellular transport and function of RAD51. In BRCA2-deficient cells, RAD51 is inefficiently transported into the nucleus, which suggests one function of BRCA2 is to move RAD51 from its site of synthesis to its site of activity (Davies et al., 2001).

Since BRCA2 $^{-/-}$ mice result in embryonic lethality, other mechanisms for study of the resulting phenotype need to be developed. Due to the lethality, studies of the role of this protein during meiosis are greatly hindered. This chapter describes a study in which the embryonic lethality is rescued, by using a bacterial artificial chromosomal (BAC) containing the human *BRCA2* gene. This study provides insight into what happens during meiosis, when BRCA2 is eliminated, and possibly a role for this protein in RAD51 function. In addition, this study has revealed a sexually dimorphic phenotype in the *Brca2* knockout mice (data not shown in dissertation).

CHAPTER II
MATERIALS AND METHODS

Mice

Brca2 $^{-/-}$ mice carrying the human *BRCA2* transgene (tg) were generously provided by Dr. Shyam Sharan from the National Cancer Institute at Frederick. Knockout (*Brca2* $^{-/-}$, tg +) and control mice, (*Brca2* $^{+/+}$, tg +) were examined at 3, 6 and > than 6 weeks of age as described below. Mice were housed under 14 hour light /10 hour dark photoperiods at constant temperature (21^{o} C), with free access to standard laboratory chow and water.

Cell and Tissue Preparation

To obtain mixed germ cells, testes were detunicated, digested in 0.5 mg/ml collagenase (Sigma) in Krebs-Ringer bicarbonate (KRB) at 32^{o} C for 20 min, then digested in 0.5 mg/ml trypsin (Sigma) in KRB at 32^{o} C for 13 min. Spermatocytes were then filtered through 80 μM mesh and 3 washes in KRB. Surface-spread chromatin preparations for synaptonemal complex visualization were performed as previously described (Cobb *et al.*, 1999a). Briefly, germ cells were fixed in 2% paraformaldehyde, and allowed to dry onto slides. The slides were fixed in 2% paraformaldehyde/0.03% SDS, then in 2% paraformaldehyde, then blocked in 10% goat serum/3% BSA in phosphate-buffered saline (PBS) prior to processing for immunofluorescence.

Immunofluorescence

Antisera used were polyclonal anti-SYCP3, anti-H1t (Eaker *et al.*, 2001), anti-RAD51 (Oncogene), anti-BRCA2 (gift from Shyam Sharan) and anti-phospho-H2AX (Upstate Biotech). Following overnight incubation in primary antibody, slides were incubated with rhodamine- or fluorescein-conjugated secondary antibodies (Pierce), and mounted with Prolong Antifade (Molecular Probes) containing DAPI (Molecular Probes) to stain DNA. Antibody localization was observed using an Olympus epifluorescence microscope, and images were captured to Adobe PhotoShop with a Hamamatsu color CCD camera.

CHAPTER III

RESULTS

Brca2 $^{-/-}$ lethality was rescued by using a bacterial artificial chromosomal (BAC) containing the human *BRCA2* gene. These mice are phenotypically indistinguishable from wild type mice, however they are sterile because the human transgene is poorly expressed in the gonads (data not shown). The morphology of the testes of these mice at three weeks of age revealed germ cell depletion and at this point, we received the mice for analysis of spermatogenesis. In this chapter, only a part of the results will be presented since the experiments are still in progress here at UT and in Dr. Shyam Sharan's lab at the NCI, Frederick. Therefore, results in this dissertation will present phenotypic abnormalities examined thus far during spermatogenesis.

Antibody staining was performed on C57BL/6J mice with BRCA2 to determine the normal localization pattern of this protein during spermatogenesis. Fig. 1 depicts examples of the staining pattern of BRCA2 during spermatogenesis. Fig. 1A depicts zygotene spermatocytes and the staining pattern appears to cover the entire cell. However, some areas appear to have increased staining around chromosome-specific regions (significance as yet unknown). In Fig. 1B, both early pachytene and late pachytene cells are shown, with localization of BRCA2 disappearing at mid to late pachytene (see bottom spermatocyte with little BRCA2 staining).

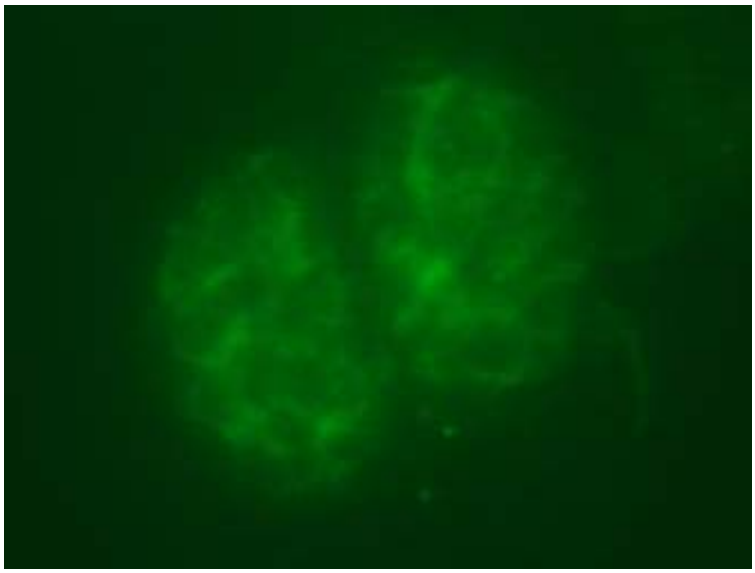
The *Brca2* knockout mice (tg +) were examined for specific stage of arrest during spermatogenesis. Arrest in zygonema was confirmed by analysis of surface spread spermatocytes by immunostaining using antibodies against the synaptonemal complex protein SYCP3 and the male germ-cell specific histone H1t. Only around 0.5% of the

spermatocytes progress to early-pachytene stage and none were positive for histone H1t, a marker for mid-pachytene, shown in Fig.2.

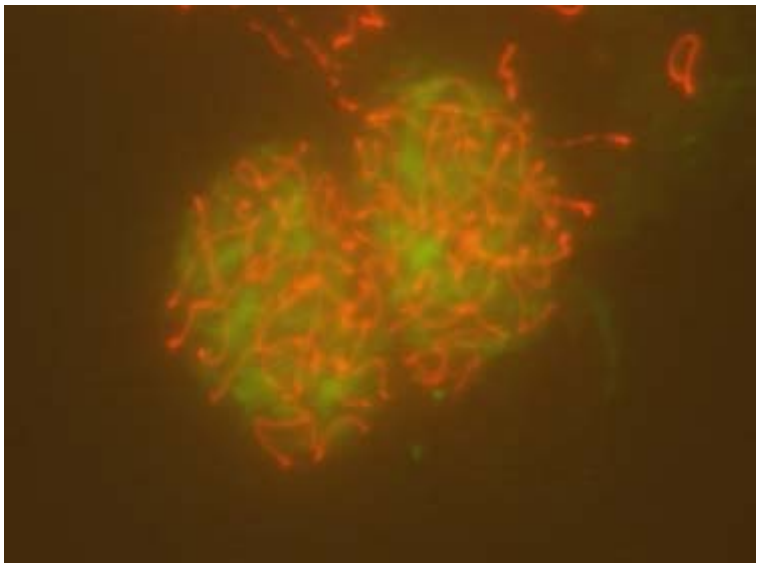
Therefore, since few spermatocytes progressed into pachytene, traditional markers for normal progression in meiosis during leptotene and zygotene were examined. One such marker, RAD51, was frequently absent in leptotene and zygotene spermatocytes. Fig. 3 shows a control leptotene spermatocyte with RAD51 foci (top left) and the bottom is a *Brca2* $^{-/-}$ leptotene spermatocyte with little or no RAD51 foci A total of 98.6 % of 8-week old spermatocytes were abnormal with respect to RAD51 foci in *Brca2* $^{-/-}$ mice (Figures 4 and 5). Of these, 57.1% had no foci during leptotene/zygotene and 41.5% had less than 100 RAD51 foci during leptotene/zygotene. Examination of 6-week old knockout mice revealed similar results (Figures 4 and 5). 93% of 6-week old mice had abnormal numbers of RAD51 foci. Of these, 56.1% had no foci, and 36.9% of spermatocytes had less than 100 RAD51 foci.

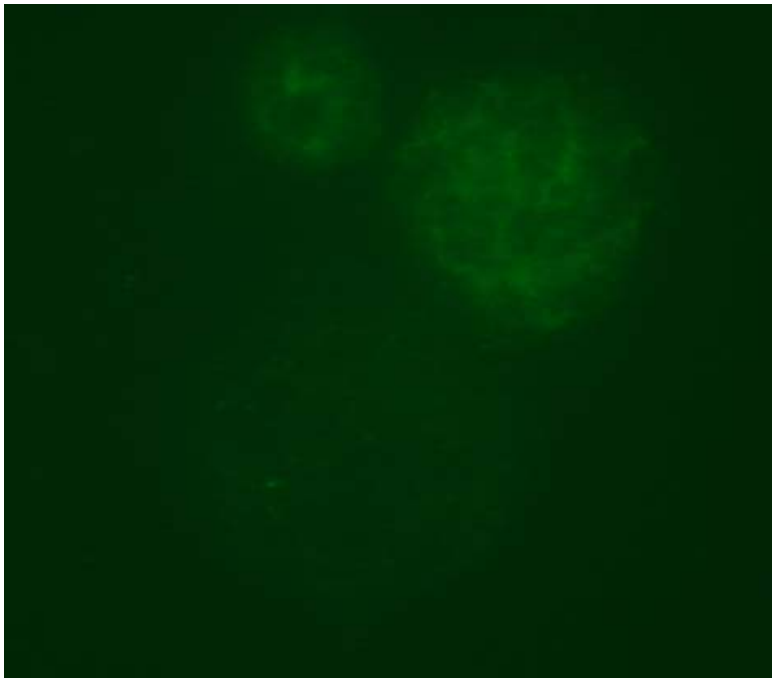
In addition, appearance of gamma-H2AX, which localizes to regions of double-strand breaks (Mahadevaiah et al. 2001), was also examined in control and *Brca2* $^{-/-}$ mice. Brca2 $^{-/-}$ mice have a normal staining pattern with gamma-H2AX. Specifically, the leptotene and zygotene cells have a punctate staining pattern and the few cells that may be starting early pachytene lose most of the gamma-H2AX staining as expected (Fig.6). However, in the knockout, the few early pachytene cells, also appear to lose gamma-H2AX staining on the sex body, whereas the controls have normal sex-body staining with gamma-H2AX.

Figure 1. Localization pattern of BRCA2 during spermatogenesis. Fig. 1A depicts zygotene spermatocytes stained with antibodies against BRCA2 (green) and SYCP3 (red). Fig. 1B depicts both a zygotene and pachytene spermatocyte stained with antibodies against BRCA2 (green) and SYCP3 (red). Note that staining disappears in pachytene-stage spermatocytes.



A





B

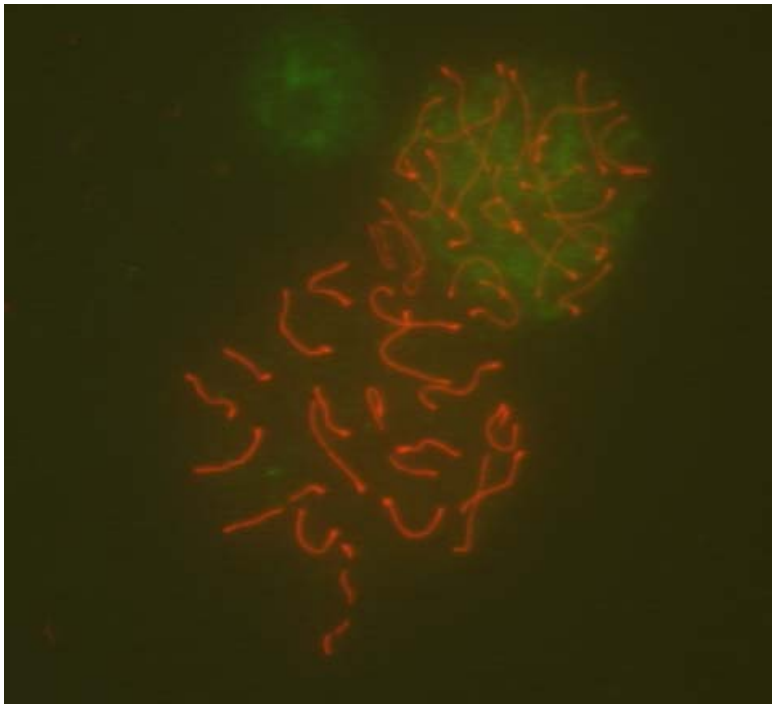
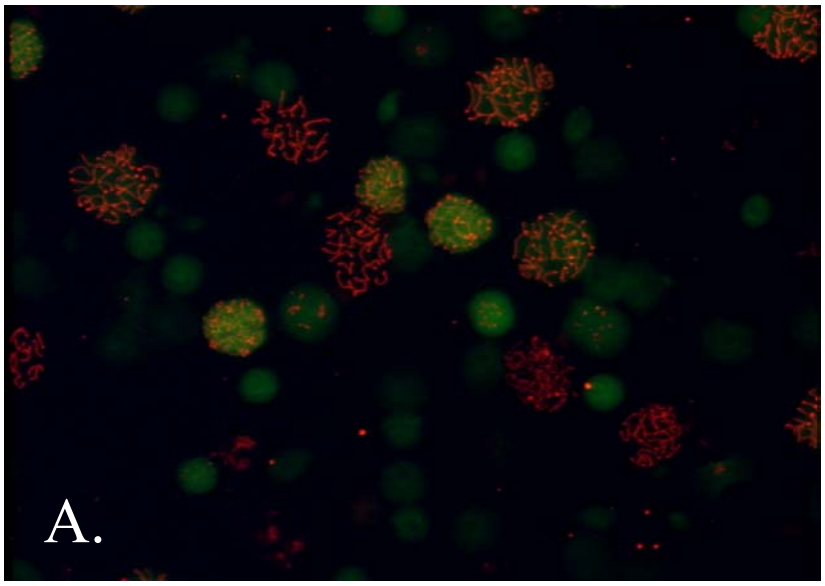


Figure 2. BRCA2 KO/+, tg+ spermatocytes are normal. Spermatocytes stain positively for H1t (green) and SYCP3 (red), as shown in A. BRCA2 KO/KO, tg+ spermatocytes arrest at zygotene and do not stain positive for H1t, therefore few if any spermatocytes make it into pachytene, as shown in B. SYCP3 staining in the BRCA2 KO/KO, tg+ reveals that most spermatocytes are leptotene or zygotene cells.


A.

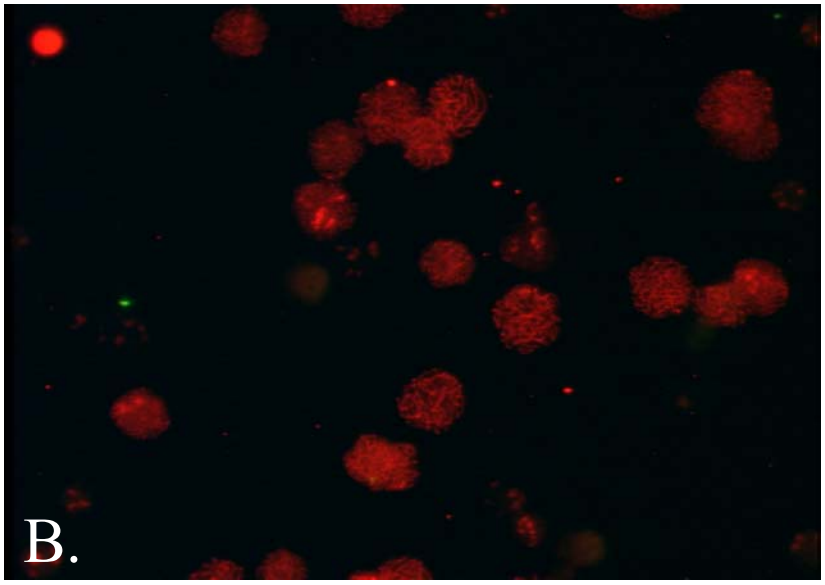

B.

Figure 3. Localization of RAD51 foci in *Brca2* knockout mice. BRCA2 KO/+, tg+ spermatocytes stain positive for RAD51 (green) and SYCP3 (red), as shown in A and B. RAD51 localization is decreased or absent in a high frequency of BRCA2 KO/KO, tg+ spermatocytes, shown in C and D.

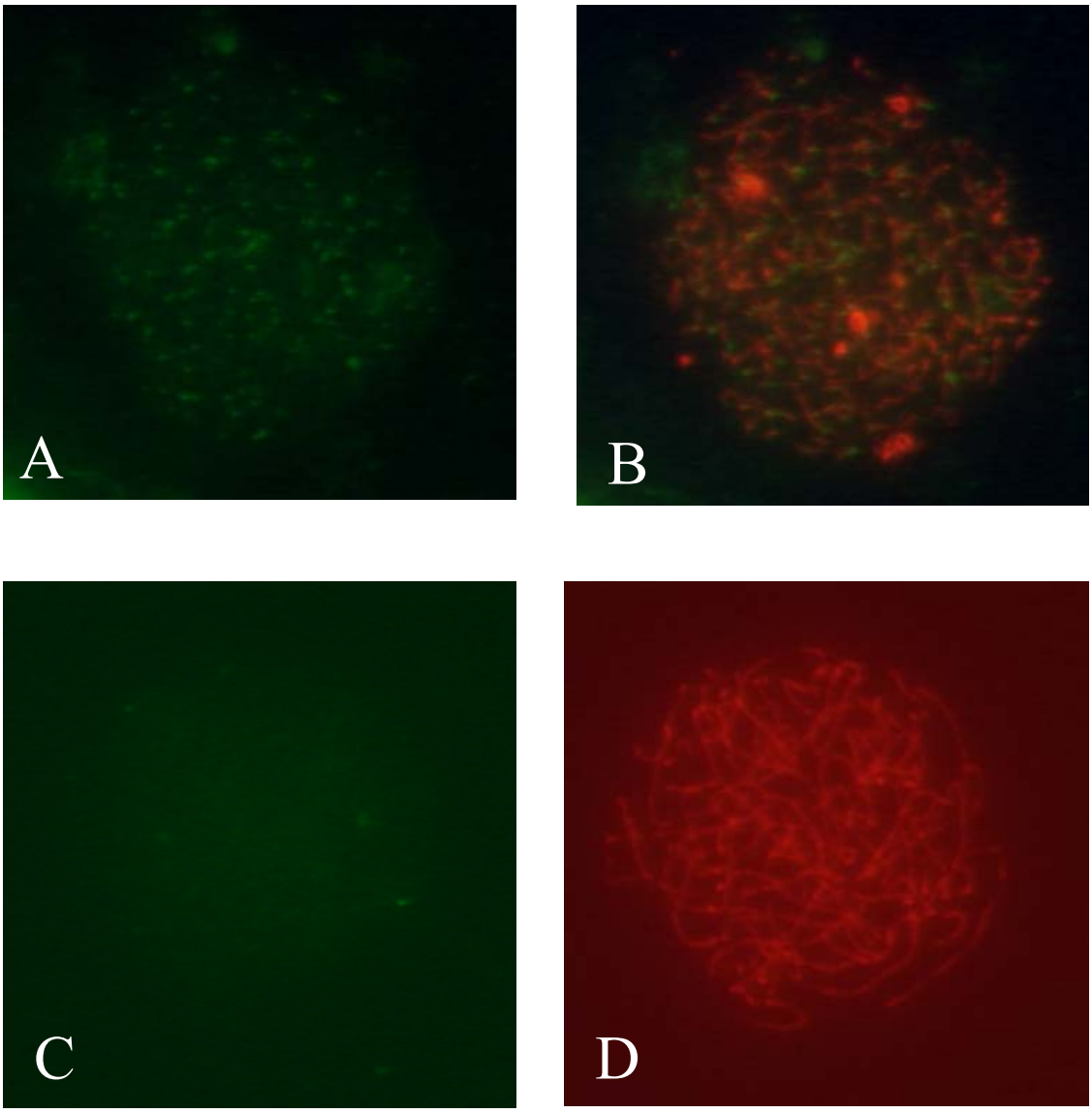

A
B
C
D

Figure 4. Overall % of L/Z spermatocytes with reduced numbers of RAD51 foci in BRCA2 KO/KO, tg/+ compared to KO/+, tg/+ in mice 6 and 8 weeks of age.

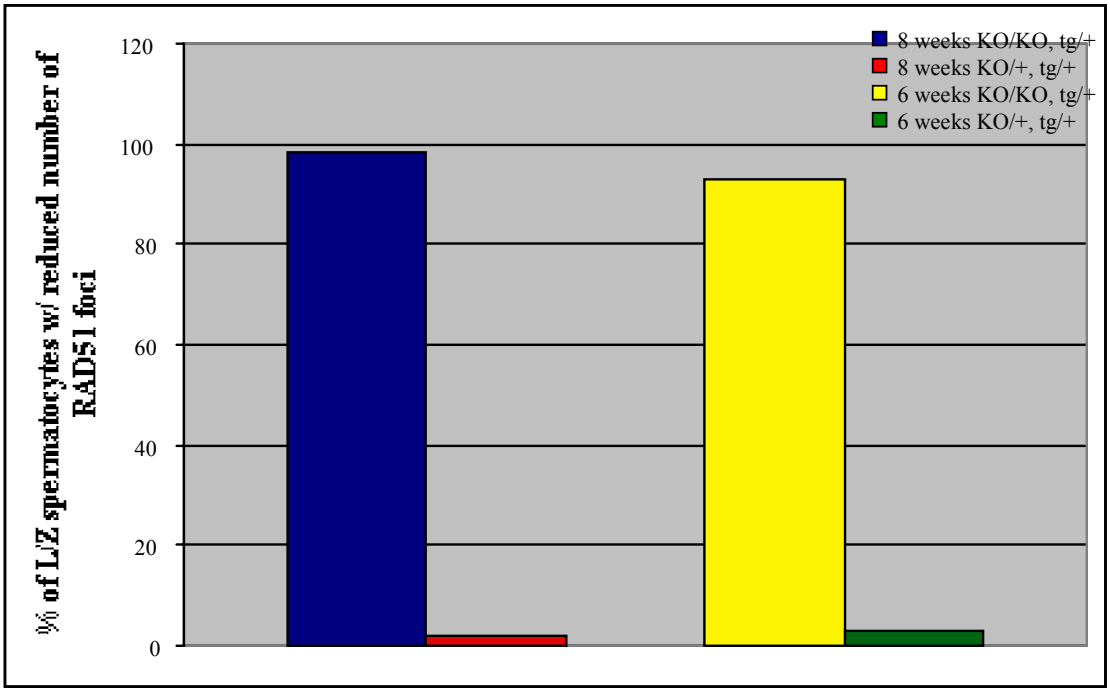

% of L/Z spermatocytes w/ reduced number of RAD51 foci
120
100
80
60
40
20
0
8 weeks KO/KO, tg/+
8 weeks KO/+, tg/+
6 weeks KO/KO, tg/+
6 weeks KO/+, tg/+

Figure 5. Number of RAD51 foci in BRCA2 KO/KO, tg/+ compared to KO/+, tg/+ in mice 6 and 8 weeks of age.

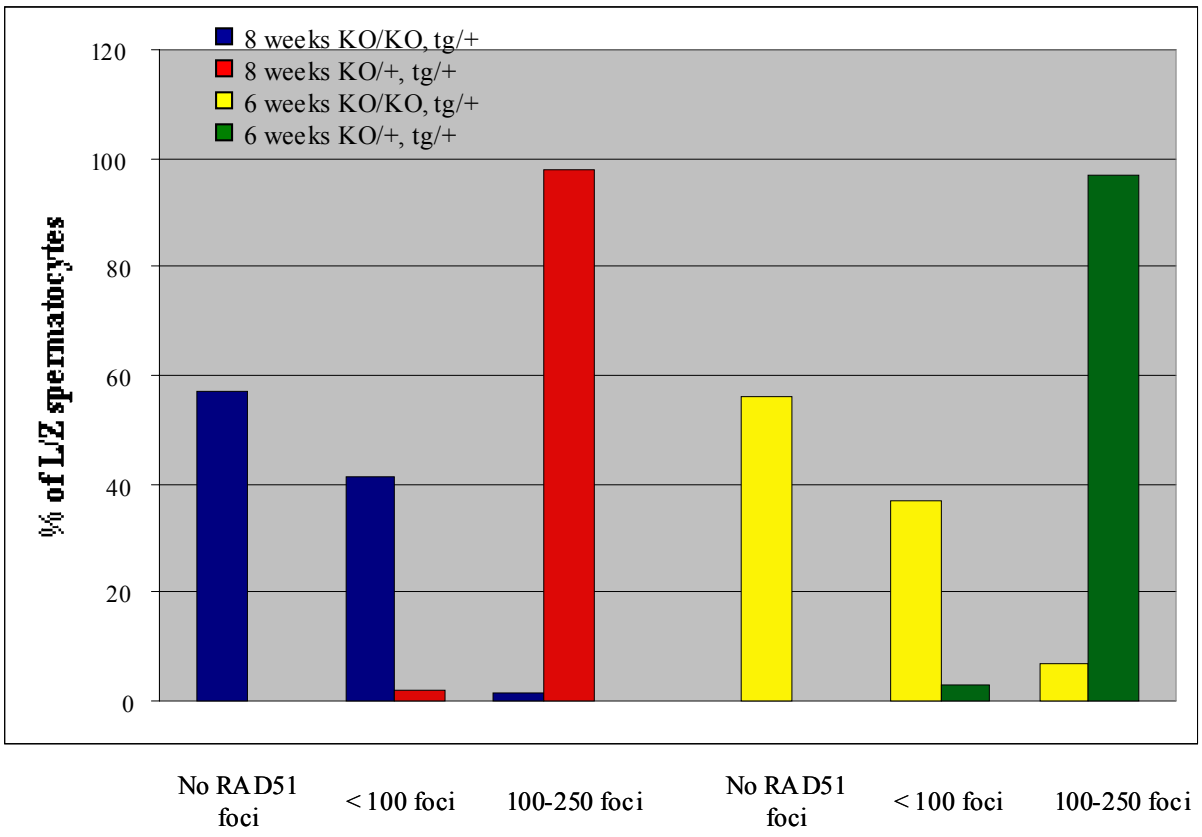
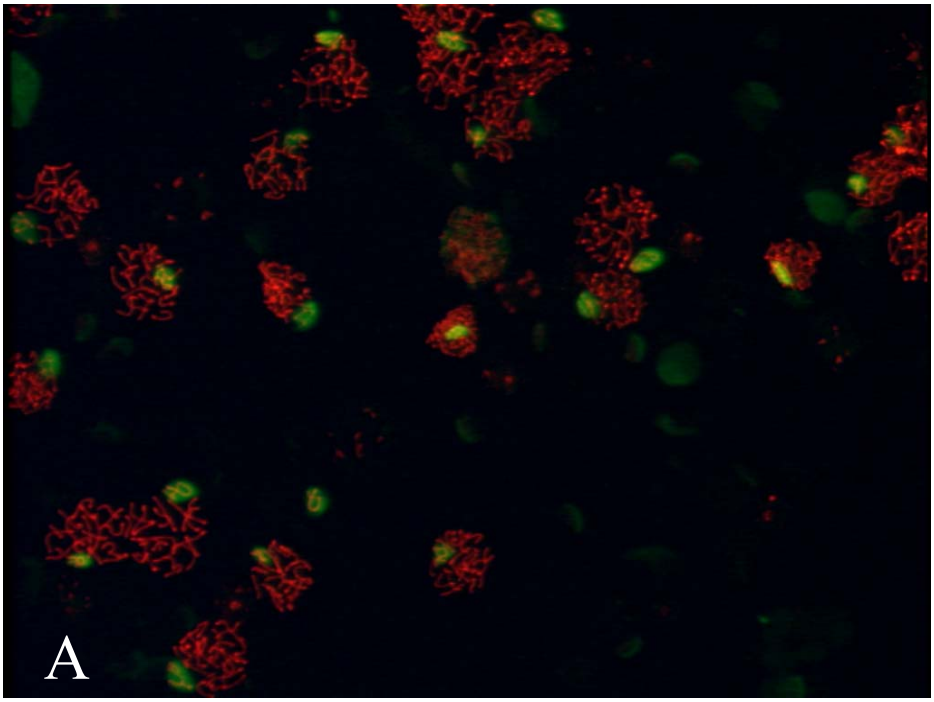
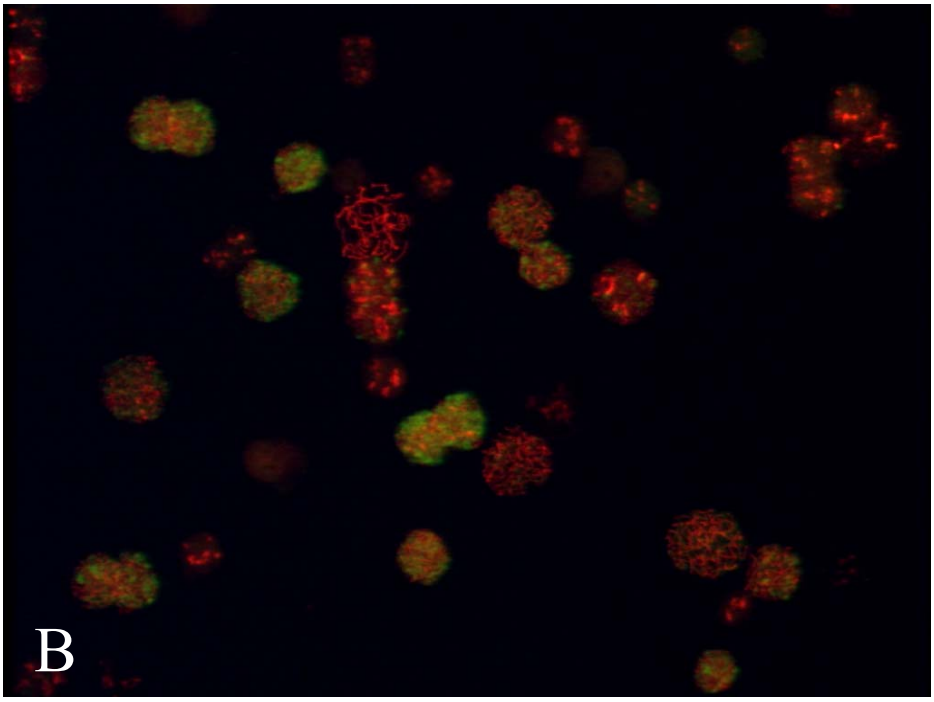

8 weeks KO/KO, tg/+
8 weeks KO/+, tg/+
6 weeks KO/KO, tg/+
6 weeks KO/+, tg/+
% of L/Z spermatocytes
120
100
80
60
40
20
0
No RAD51 foci
< 100 foci
100-250 foci
No RAD51 foci
< 100 foci
100-250 foci

Figure 6. *Brca2* $^{+/+}$ (tg+) and *Brca2* $^{-/-}$ (tg+) spermatocytes have regions of double-strand breaks, as measured by staining with an antibody against gamma-H2AX (green) and SYCP3 (red).


A


B

CHAPTER IV

DISCUSSION

This study has shown that the embryonic-lethality phenotype seen in *Brca2* knockout mice can be rescued by using a bacterial artificial chromosomal (BAC) containing the human *BRCA2* gene. However, the transgene is only expressed transiently in the gonads and this leads to sterility. Spermatogenesis in the knockout mice was halted at zygotene as measured by staining with an antibody against a synaptonemal component, SYCP3 and a marker for mid-pachytene, testis-specific H1t. This revealed that only around 0.5% of spermatocytes make it into early pachytene.

Further characterization of the *Brca2* $^{-/-}$ mice revealed that these mice have abnormal numbers of RAD51 foci. Previous studies have shown that leptotene/zygotene spermatocytes should have 100-250 RAD51 foci (Moens et al., 1997). Approximately 90% of leptotene/zygotene spermatocytes in the knockout mice have abnormal numbers of RAD51 foci, either no RAD51 foci or less than the normal 100. Therefore, elimination of BRCA2 causes loss or a decreased amount of RAD51 localization.

RAD51 is required for homologous recombination and DNA repair, including promoting joint molecule formation and DNA strand exchange between homologous DNA molecules (Benson et al., 1994; Baumann et al., 1996). RAD51 and BRCA2 have been shown to have a direct interaction in vitro with recombinant protein fragments (Chen et al., 1998b), by yeast-two hybrid (Sharan et al., 1997); and also by immunofluorescence co-localization (Chen et al., 1998a). Both BRCA2 and RAD51 are involved in response pathways to DNA damage (Sharan et al., 1997; Conner et al., 1997).

Therefore it is interesting that RAD51 localization is disrupted in the *Brca2* $^{-/-}$ mice. This suggests that the presence of BRCA2 may be required for RAD51 localization and possibly function during spermatogenesis. It has been shown that the formation of RAD51 foci is impaired in BRCA2-deficient cell lines, where reduced numbers of RAD51 foci are observed (Yuan et al., 1999). Another study showed that truncation of BRCA2 is associated with a defect in the normal nuclear localization of RAD51 (Davies et al., 2001). Therefore, during spermatogenesis RAD51 function may also be dependent on BRCA2. Future studies need to be performed to address the requirement of BRCA2 for RAD51 function. It will also be essential to determine the role of BRCA2 and RAD51 in repair after induction of DNA damage during spermatogenesis.

In contrast to loss of RAD51 foci, an antibody against gamma-H2AX was used to show that double-strand breaks do still occur in leptotene/zygotene cells in the *Brca2* $^{-/-}$ mice. Therefore, loss of RAD51 foci is not due to loss of double-strand breaks, but more likely due to loss of BRCA2. Further analysis needs to be performed to determine if the elimination of the spermatocytes in the knockout are by apoptosis. This would indicate a checkpoint in these mice that detect loss of BRCA2 or lack of proper resolution of DNA double-strand breaks. However previous studies have shown that in contrast to *Brca1*, disruption of *Brca2* does not appear to have a marked effect on cell cycle checkpoint enforcement (Patel et al., 1998). Future analysis is required before a greater understanding is reached regarding the role of BRCA2 in cell cycle progression during meiosis.

In conclusion, this study has proven that a BAC containing a human BRCA2 transgene can partially restore BRCA2 function. However, spermatocytes in the

knockout are arrested early in meiotic prophase. It has also been shown that BRCA2 may be required for RAD51 localization and possibly proper function. Experiments will continue to be performed to determine the specific role of BRCA2 during meiotic progression and its role in DNA repair during spermatogenesis. Future experiments include analysis of the localization patterns of other proteins involved in the double-strand break pathway during meiosis, such as SPO11 and DMC1.

LIST OF REFERENCES

Baumann P, Benson FE, West SC. 1996. Human Rad51 protein promotes ATP-dependent homologous pairing and strand transfer reactions in vitro. Cell 87:757-766.

Benson FE, Stasiak A, West SC. 1994. Purification and characterization of the human rad51 protein, an analogue of e-coli RecA. EMBO J 13:5764-5771.

Chen CF, Chen PL, Zhong Q, Sharp ZD, Lee WH. 1999. Expression of BRC repeats in breast cancer cells disrupts the BRCA2-Rad51 complex and leads to radiation hypersensitivity and loss of G2/M checkpoint control. J BiolChem 274:32931-32935.

Chen JJ, Silver DP, Walpita D, Cantor SB, Gazdar AF, Tomlinson G, Couch FJ, Weber BL, Ashley T, Livingston DM, Scully R. 1998a. Stable interaction between the products of the BRCA1 and BRCA2 tumor suppressor genes in mitotic and meiotic cells. Mol Cell 2:317-328.

Chen PL, Chen CF, Chen YM, Xiao J, Sharp ZD, Lee WH. 1998b. The BRC repeats in BRCA2 are critical for RAD51 binding and resistance to methyl methanesulfonate treatment. Proc Natl Acad Sci USA 95:5287-5292.

Conner F, Bertwistle D, Mee PJ, Ross GM, Swift S, Grigorieva E, Tybulewicz VL, Ashworth A. 1997. Tumorigenesis and a DNA repair defect in mice with a truncating Brca2 mutation. Nat Genet 17:423-30.

Davies AA, Masson JY, McIlwraith MJ, Stasiak AZ, Stasiak A, Benkitaraman AR, West SC. 2001. Role of BRCA2 in control of the RAD51 recombination and DNA repair protein. Mol Cell 7:273-282.

Gayther SA, Mangion J, Russell P, Seal S, Barfoot R, Ponder BA, Stratton MR, Easton D. 1997. Variation of risks of breast and ovarian cancer associated with different germline mutations of the BRCA2 gene. Nat Genet 15:103-105.

Mahadevaiah SK, Turner JMA, Baudat F, Rogakou EP, de Boer P, Blanco-Rodriguez J, Jasin M, Keeney S, Bonner WM, Burgoyne PS. 2001. Recombinational DNA double-strand breaks in mice precede synapsis. Nat Genet 27: 271-276.

Moens PB, Chen DJ, Shen ZY, Kolas N, Tarsounas M, Heng HHQ, Spyropoulos B. 1997. Rad51 immunocytology in rat and mouse spermatocytes and oocytes. Chromosoma 106:207-215.

Nathanson NK, Wooster R, Weber BL. 2001. Breast cancer genetics: what we know and what we need. Nat Med 7:552-556.

Patel KJ, Yu VPCC, Lee HS, Corcoran A, Thistlethwaite FC, Evans MJ, Colledge WH, Friedman LS, Ponder BAJ, Venkitaraman AR. 1998. Involvement of Brca2 in DNA repair. Mol Cell 1:347-357.

Scully R, Chen JJ, Plug A, Xiao YH, Weaver D, Feunteun J, Ashley T, Livingston DM. 1997. Association of BRCA1 with Rad51 in mitotic and meiotic cells. Cell 88:265-275.

Sharan SK, Bradley A. 1997. Murine BRCA2: sequence, map position, and expression pattern. Genomics 40:234-241.

Sharan SK, Morimatsu M, Albrecht U, Lim D-S, Regel E, Dinh C, Sands A, Eichele G, Bradley A. 1997. Embryonic lethality and radiation hypersensitivity mediated by Rad51 in mice lacking *Brca2*. Nature 386:804-810.

Venkitaraman AR. 2001. Functions of BRCA1 and BRCA2 in the biological response to DNA damage. Journal of Cell Science 114:3591-3598.

Yuan SSF, Lee SY, Chen G, Song MH, Tomlinson GE, Lee EYHP. 1999. BRCA2 is required for ionizing radiation-induced assembly of rad51 complex in vivo. Cancer Res 59:3547-3551.

PART VI

ETOPOSIDE: ENVIRONMENTAL INDUCTION OF GAMETIC ANEUPLOIDY*

* The work for this part was accomplished by efforts of April Pyle, Liane B. Russell, and Mary Ann Handel.

CHAPTER I

INTRODUCTION

Aneuploidy is the most prevalent type of human genetic abnormality. Most studies of aneuploidy have focused on the effects of its causative agents. However, information is needed on mechanisms and cellular targets associated with the occurrence of aneuploidy. In this respect, the ability of certain chemicals to increase the frequency of aneuploidy in spermatocytes and oocytes and the mechanism of action has been examined (Yin et al., 1998; Baumgartner et al., 2001; Schmid et al., 1999). However most of the chemicals studied cause chromosome breaks, rearrangements, or single base-pair changes in germ cells (Mailhes, 1995). Therefore, in order to understand the mechanism of nondisjunction, chemicals that attack specific aspects of meiosis, such as chromosome pairing, synapsis, and recombination are needed. This study focuses on using etoposide, a topoisomerase-type II inhibitor, to determine if this chemical can induce nondisjunction during spermatogenesis.

Etoposide has been shown to induce damage in somatic chromosomes. Specifically, etoposide was positive in the *in vivo* bone-marrow micronucleus test on mice, and induced numerical and structural chromosome aberrations (Ashby et al., 1994). In addition, male germ cells of rats exposed to etoposide both *in vitro* and *in vivo* yielded micronucleated spermatids (Sjoblom et al., 1994; Lahdetie et al., 1994). Etoposide is unique among chemical germline mutagens, in that it produces peak mutagenicity in

primary spermatocytes of the mouse (Russell et al., 1998). In this study, mice aged 10.5-15.5 weeks were injected intraperitoneally with etoposide or control (DMSO only), mated, and offspring were examined at days 21-42 days of age for mutations at specific loci. Etoposide induced differential effects in various male germ-cell stages. Stem-cell spermatogonia were not sensitive, but matings made weeks 4 through 6 post-injection with etoposide yielded mutations. The peak of mutagenicity was found during weeks 4 or 5, or days 22-35 post-injection. This corresponds to the appearance of mature spermatozoa in the ejaculate; whose antecedents had been exposed as diplotene-diakinesis primary spermatocytes 22-23 days earlier, late pachytene at 23-27 days earlier, or preleptotene at 33-35 days earlier (Oakberg, 1984). For example, if mating was performed at week 4 post-injection, then the diplotene-diakineses spermatocytes were the ones treated with etoposide since it will take approximately 22-23 days for the appearance of these spermatozoa in the ejaculate. Therefore, the crucial time points in meiosis I are affected by etoposide.

Although these data showed that etoposide induces specific locus mutations and dominant lethality in early and late meiotic stages (Russell et al., 1998), it is also a weak inducer of heritable translocations, suggesting that it can induce both stable and unstable chromosome aberrations in male germ cells (Shelby et al., 2001). It preferentially causes both recessive and dominant mutations in meiotic prophase, a period with high topoisomerase-II (topo-II) expression. It has also been shown that structurally similar chemicals, teniposide and ICRF-193, have a dramatic effect on male meiosis, specifically interfering with a proper pachytene to metaphase I transition (Cobb et al., 1997).

Etoposide has been shown to have the largest effect on the intervals that correspond to a period of topoisomerase-II activity during spermatogenesis (Kallio and Lahdetie, 1996). Topoisomerase-II is an endonuclease that removes torsional stress in DNA. The enzyme works by creating double-strand breaks in which the DNA duplex passes through. This allows for the chromosomes to disentangle after pairing and recombination. Etoposide forms a ternary complex composed of topo-II, etoposide, and DNA, thereby inhibiting proper topo-II function. Because type-II topoisomerases normally catalyze the transient formation and religation of DNA double-strand breaks, thereby helping to prevent supercoils and tangles during DNA replication or chromosome segregation (Kallio and Lahdetie, 1996), it appears likely that inhibition of this activity by etoposide would lead to abnormalities in resolution of crossovers. This leads to the question of whether there may be aberrant recombination after treatment with etoposide.

This was tested in a study in which genetic cross-overs were examined in the p-Tyr interval of mouse chromosome 7. Crossing over was significantly reduced when male germ cells were exposed to etoposide in early to mid-pachytene stages of meiosis (Russell et al., 2000). Cytological studies did not reveal a decrease in MLH1 foci, but there were changes in the appearance of RAD51 and RPA proteins (involved in formation of double-strand breaks and repair), suggesting that the mode of action of etoposide may be after MLH1 foci appear. Specifically, in etoposide-treated spermatocytes, in contrast to nontreated, both RAD51 and RPA foci were evident in late pachynema and throughout diplonema where they are normally not present in large numbers. In addition, the foci tended to be larger and more variable in shape. Since etoposide blocks religation of the cuts made by topo-II, repair of the DNA damage may

result in rejoining of the original DNA strands. In the process, this could undo the exchange that occurred and lead to a decrease in crossing-over (Russell et al., 2000).

Since recombination is altered after treatment with etoposide, it becomes important to determine whether aberrant recombination can lead to abnormalities during meiosis and chromosome segregation. A recent study showed that etoposide can induce both heritable chromosome aberrations and aneuploidy during male meiosis in the mouse (Marchetti et al., 2001). Specifically, high frequencies of chromosomal aberrations and aneuploidy were found in zygotic metaphases and spermatocytes after treatment during preleptotene and pachytene spermatocytes. Experiments, as described in this chapter, were also performed to determine if etoposide can induce aneuploidy in sperm as detected by sperm FISH.

CHAPTER II

MATERIALS AND METHODS

Chemical and mice used

Etoposide (Sigma, St. Louis) was dissolved in dimethyl sulfoxide (DMSO) at a concentration of 21 mg/ml and administered by i.p. injection at an exposure of 70 mg etoposide/kg, with controls receiving equivalent volumes of DMSO alone. Mice used were C3H/RI males, except for a portion of the pilot experiment in which they were (BALB/c RI X C3H/RI) F1. In the first experiment, the mice were sacrificed at days 26, 29, 32, and 34 days after treatment with etoposide or control, and sperm collected for sperm FISH analysis. In the second experiment, mice were sacrificed at days 27, 29, 32, and 34 after treatment with etoposide or solvent and sperm used as described below.

Three-color Fluorescence in Situ Hybridization (FISH)

For sperm FISH analysis, males were killed by cervical dislocation and sperm from epididymides were collected in 2.2% Na citrate. Sperm were spread onto a slide and dried. The slides were soaked in 10 mM dithithreitol (DTT) on ice for 30 min and placed immediately into 4 mM diiodosalicyclic acid (LIS) for 1 hr. The slides were air dried and dehydrated in ethanol. Slides and probes were denatured at 78°C in formamide, then dehydrated and air-dried. Probes specific for chromosomes 8, X and Y were a generous gift from Dr.Terry Hassold, Case Western University, Cleveland, Ohio. Biotin was used to label 1 µg of the Y probe pERS-532 (Eicher et al., 1991); the Chr. 8 probe, which was a mixture (2 µg total) of four subclones (Boyle and Ward, 1992), was

labeled with digoxygenin; and 1 μg of the X-chromosome-specific probe DXWas (Disteche et al., 1987) was labeled with both biotin and digoxygenin separately. Probes were labeled using a nick translation kit (Roche Pharmaceutical) and purified over a Sephadex- G50 column. The probe mix was added to each slide; which was then incubated at 37°C overnight. The next day, slides were washed in 50% formamide/2X SSC, in 2X SSC, and then in PN Buffer (0.1M NaH_2PO_4, 0.1M Na_2HPO_4, 0.05% NP-40, pH 8). Slides were incubated in a BSA-blocking buffer and the appropriate fluorochrome-conjugated detector, also in BSA, at 37°C for 30 min, then washed in PN buffer twice. After adding DAPI/Antifade (Molecular Probes), slides were viewed with an Olympus epifluorescent microscope at 100X. Estimates of sperm aneuploidy were deliberately conservative. Only hyperhaploidy, and not hypohaploidy, was scored; the aneuploidy frequency represents twice the hyperhaploidy frequency. Additionally, sperm were deemed suitable for scoring only when the following criteria were met: fluorescent signals were clearly within and not on the edge of the sperm nucleus, fluorescent signals were all in the same plane of focus, and any two signals scored as separate were separated by a distance equal or greater than one signal domain. "Blind" scoring was also performed to ensure no bias between treatment and solvent (control) samples.

CHAPTER III

RESULTS

In order to determine if etoposide induces aneuploidy, male mice were injected intraperitoneally with etoposide in DMSO or with DMSO only. Their sperm were collected at various intervals post-injection and examined by sperm FISH (Fig. 1). Two series of experiments were performed. The first was a small initial test to determine if etoposide induces aneuploidy and if so, when during meiosis the highest frequency of aneuploidy is induced. Sperm was collected from one etoposide-treated and one control mouse on each of days 26, 29, 32, and 34 after injection. Control frequencies ranged from 0.0 to 0.3%, and experimental frequencies from 0.2 to 0.8% (Table 1), with the highest being in the sperm that were collected 32 days after injection of etoposide, at 0.8% hyperhaploidy. Combined hyperhaploidy frequency for the four treated mice differed significantly from combined results for the four control mice for hyperhaploidy frequency, ($p < .02$, Fisher exact test). In comparison of the sum of four control mice versus the mouse treated day 32 prior to sperm collection, there was also a statistically significant difference at $p < .004$.

Since preliminary results from this pilot experiment indicated that etoposide does induce aneuploidy, the next experiment (with increased n value; see Table 2) was designed to see if the aneuploidy frequency was repeatable, and to possibly find the time of peak yield. In the second experiment, there were a total of five control mice and fourteen mice treated with etoposide. Sperm FISH was again performed from each group, 27, 29, 32, and 34 days after injection. Although the frequency of hyperhaploid

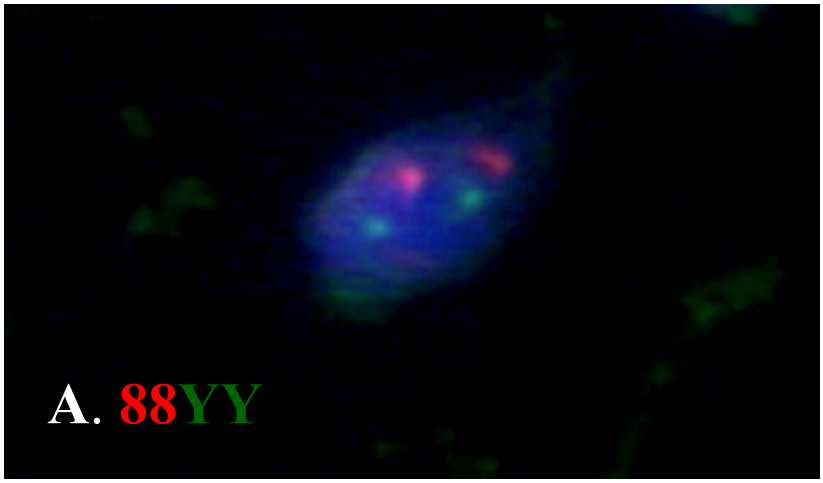
sperm summed for all etoposide-treated males (0.34%) was greater than that for controls (0.22%), the difference was not significant (P = 0.12, by Fischer Exact test). When the comparison was restricted to XX and YY sperm only, the experimental frequency (0.14%) was significantly greater (at P = 0.018) than control frequency (0.02%). However, there is insufficient evidence for identifying a peak sensitive stage.

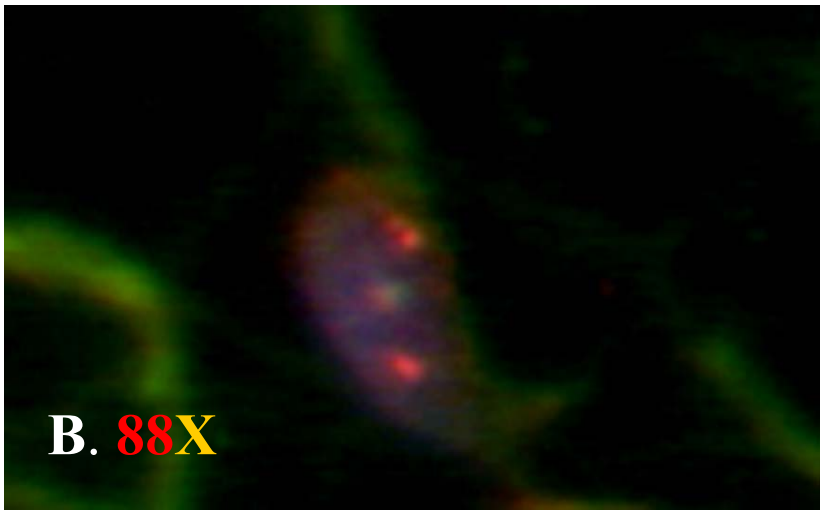
When data for the first and second experiment were combined, significant increases were found both in total frequency of disomic sperm (P = 0.012) and in the frequency of XX + YY sperm (P = 0.0083). The frequencies of disomic sperm were 0.37% and 0.20% for experimental and control sperm, respectively, and the frequencies of XX and YY sperm were 0.13 and 0.03%, respectively. It therefore appears that while etoposide increases nondisjunction events overall, MII nondisjunction is increased more than MI nondisjunction. Unfortunately, disomy-8 is noninformative as to whether it was caused by MI or MII nondisjunction.

Table 1. The frequency of hyperhaploidy (experiment #1) reveals an increase in hyperhaploidy in sperm for etoposide-treated males compared to non-treated control males. The chromosome-specific rates of aneuploidy are shown.

Day after injection	Treatment	XX	YY	XY	88	# aneuploid/ total counted	% aneuploidy
26	Control	0.0	0.0	0.0	0.1	1/1001	0.1
	Etop	0.0	0.0	0.3	0.2	5/1005	0.5
29	Control	0.1	0.1	0.0	0.1	3/1001	0.3
	Etop	0.1	0.0	0.0	0.1	2/1006	0.2
32	Control	0.0	0.0	0.0	0.0	0/1008	0.0
	Etop	0.1	0.2	0.2	0.3	8/1003	0.8
34	Control	0.0	0.1	0.0	0.2	3/1001	0.3
	Etop	0.0	0.0	0.2	0.1	3/1002	0.3

Figure 1. Representative sperm FISH images from etoposide-treated mice. A. (88YY) and B. (88X) represent sperm collected 32 days after etoposide treatment and C. (8YY) is from sperm collected 27 days after treatment, see Table 2.


A. 88YY


B. 88X

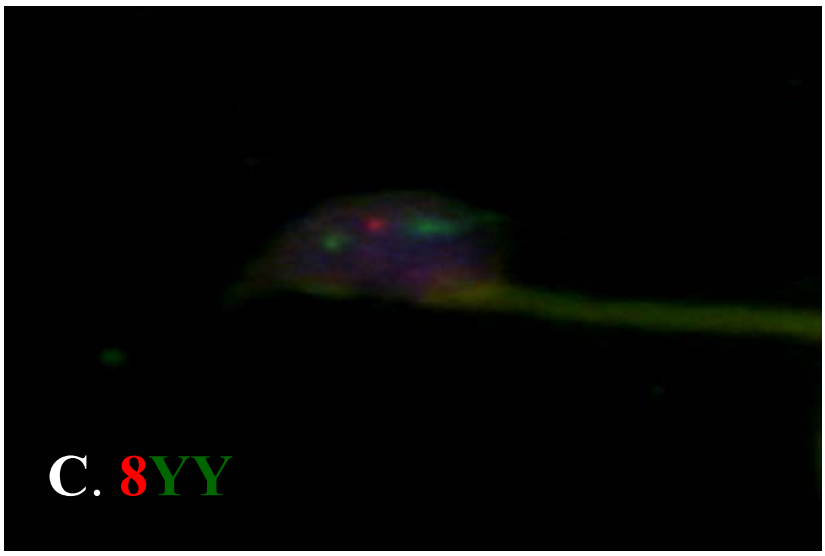

C. 8YY

Table 2. The frequency of sperm hyperhaploidy is shown for control vs. etoposide treated-males (experiment # 2). The chromosome-specific rates of aneuploidy are also shown.

Mouse/trt	Injection-to-collection interval	disomy 8	disomy XX	disomy XY	disomy YY	diploid	Total counted	% Hyperhaploidy
83902/contr	27	0.1	0.0	0.0	0.0	0.0	1001.0	0.1
83997/etop	27	0.2	0.2	0.0	0.2	0.0	1003.0	0.6
83907/etop	27	0.0	0.0	0.1	0.1	0.0	1009.0	0.2
84290/etop	27	0.1	0.0	0.2	0.2	0.0	1000.0	0.5
83954/contr	29	0.4	0.0	0.3	0.0	0.0	1000.0	0.7
83945/etop	29	0.2	0.0	0.1	0.0	0.0	1000.0	0.3
83429/etop	29	0.3	0.1	0.0	0.1	0.0	1000.0	0.5
83998/etop	29	0.0	0.0	0.0	0.1	0.0	1000.0	0.1
84363/contr	32	0.0	0.0	0.0	0.0	0.0	1000.0	0.0
84008/contr	32	0.1	0.0	0.1	0.0	0.0	1007.0	0.2
84304/etop	32	0.1	0.0	0.1	0.1	0.0	1006.0	0.3
84199/etop	32	0.0	0.0	0.2	0.0	0.0	1000.0	0.2
83957/etop	32	0.1	0.0	0.1	0.0	0.0	1002.0	0.2
83946/etop	32	0.2	0.3	0.0	0.1	0.1	1041.0	0.7
84007/etop	32	0.2	0.1	0.1	0.1	0.1	1001.0	0.6
84204/contr	34	0.0	0.0	0.0	0.1	0.0	1000.0	0.1
84358/etop	34	0.1	0.2	0.0	0.0	0.0	1000.0	0.3
83953/etop	34	0.1	0.0	0.2	0.0	0.0	1004.0	0.3
84197/etop	34	0.0	0.0	0.2	0.0	0.0	1002.0	0.2

CHAPTER IV

DISCUSSION

The mechanism of chemically-induced aneuploidy is not well understood. However, the mechanism of etoposide action is beginning to be understood, which makes it a valuable agent for study of induction of aneuploidy. The chemotherapeutic agent, etoposide, induced the largest mutagenic effect during prophase of meiosis (Russell et al., 1998), with most mutations being deletions. It was subsequently shown to decrease recombination in male mice (Russell et al., 2000) when treatment was applied to the same stages. The timing of etoposide action is critical, since this is when the most crucial events occur during meiosis, such as pairing of homologous chromosomes and recombination.

Many studies have focused on decreased recombination as a causative factor associated with nondisjunction (Hassold and Sherman, 2000; Hassold et al., 2000; Lamb et al., 1997; Savage et al., 1998). This is important, because etoposide is a topoisomerase-type II inhibitor and abnormalities during topoisomerase-II function could possibly lead to chromosome nondisjunction. Topoisomerase-II plays an essential role during meiosis. Type-II topoisomerases create a double-stranded nick, thereby allowing DNA to pass through the gap. This function is required for DNA replication, transcription, for condensing meiotic chromosomes at metaphase and anaphase and may also be required for recombination (Wang, 1985). One study showed that inhibition of topo-II by teniposide in cultured pachytene spermatocytes altered chromatin condensation and formation of meiotic metaphase chromosomes (Cobb et al., 1997).

Topoisomerase-II may then function to disentangle chromosomes that have become interlocked during the processes of homolog pairing and recombination. Etoposide prevents religation of double strand breaks by forming a ternary complex with topo-II/DNA/etoposide. If repair is initiated at this site, that could result in rejoining of the original strands, thus altering recombination. Altered recombination could then lead to aneuploidy (Hassold et al., 2000).

The present study showed that etoposide does in fact induce meiotic aneuploidy. In the first experiment, sperm FISH analysis revealed an increase of 0.8% hyperhaploidy at 32 days after treatment and 0.5% hyperhaploidy at 26 days after treatment. This was expected because previous results have shown that etoposide produced the highest rate of mutation at weeks 4 and 5 after injection, corresponding to days 22-35 (Russell et al., 1998). However, since only one animal was examined at each stage, this is insufficient evidence for assuming days 26 and 32 are, in fact, peak days. Etoposide is therefore capable of inducing production of aneuploid sperm, but more evidence is needed to determine when the peak affects occur.

A second, larger experiment was performed to test specifically when in the 26-34 day period the nondisjunction occurs, and if nondisjunction is during meiosis I or II or both. After treatment with etoposide, aneuploid sperm were again produced. However, when all of the nondisjunction was summed, values of treated and non-treated were not significantly different, at $p = 0.12$. When only the XX and YY sperm were compared, the etoposide treated frequency of hyperhaploidy was significantly greater, at $p = .018$. But there is still not enough evidence to indicate a peak sensitive stage to aneuploidy. Combining the first and second experiment, there was again a significant increase in both

the total frequency of disomic sperm ($p = 0.012$) and in the frequency of XX and YY sperm ($p = 0.0083$). Thus etoposide does induce nondisjunction overall, but MII nondisjunction was significant over MI nondisjunction.

It is important to understand why nondisjunction is the highest at MII. There are several possibilities for this result. Etoposide inhibits topo-II by forming a ternary complex consisting of topo-II, etoposide, and DNA. It is possible that this could have a downstream effect and result in MII nondisjunction. Etoposide could inhibit proper resolution of chiasmata, thereby leaving unresolved tangles in the sister chromatids if they were also somehow involved in the recombination event, affecting proper segregation at anaphase of MII. It is also possible that sister chromatid cohesion was disrupted after treatment with etoposide. It is not known whether inhibition of topo-II can also have an effect on improper segregation of sister chromatids. Several studies have suggested that nondisjunction events can be associated with premature sister chromatid separation (PSSC) (Angell, 1997; Angell, 1991). It is possible that etoposide can induce PSSC. How this would occur is difficult to ascertain. It is possible that pericentromeric exchanges could disrupt sister chromatid cohesion, resulting in premature separation of sisters at MII. It is also possible that extremely proximal exchanges could lead to entanglement that may not be resolved if topoisomerase-II function is disrupted. In this case the bivalent would remain intact until positioned on the MII plate and abnormal segregation could occur at MII. Etoposide could also cause MII nondisjunction by inhibiting resolution of intersister tangles during chromosome condensation. During replication, tangles between sister chromatids are formed, and inhibition of topo-II function may then inhibit proper resolution. Further studies are

needed to determine if either of these cases could lead to MII nondisjunction after treatment with etoposide.

This study showed that treatment of male mice with etoposide, a topo-II inhibitor induced meiotic nondisjunction. However, the data are preliminary and need to be repeated to confirm the ability of etoposide to induce nondisjunction during spermatogenesis. The possibility that etoposide can induce meiotic nondisjunction is especially interesting, since etoposide is used as a chemotherapeutic agent and could be detrimental to reproductive success as well. Further studies are needed to determine precisely how the nondisjunction is occurring and why MII nondisjunction predominates after treatment with etoposide.

LIST OF REFERENCES

Angell R. 1997. First-meiotic-division nondisjunction in human oocytes. Am J Hum Genet 61:23-32.

Angell RR. 1991. Predivision in human oocytes at meiosis I: a mechanism for trisomy formation in man. Human Genetics 86:383-387.

Ashby J, Tinwell H, Glover P, Poorman-Allen P, Krehl R, Callander RD, Clive D. 1994. Potent clastogenicity of the human carcinogen etoposide to the mouse bone marrow and mouse lymphoma L5178Y cells: comparison to Salmonella responses. Environ Mol Mutagen 24:51-60.

Baumgartner A, Schmid TE, Schuetz CG, Adler ID. 2001. Detection of aneuploidy in rodent and human sperm by multicolor FISH after chronic exposure to diazepam. Mutat Res Genet Toxicol E M 490:11-19.

Boyle AL, Ward DC. 1992. Isolation and initial characterization of a large repeat sequence element specific to mouse chromosome 8. Genomics 12:517-525.

Cobb J, Reddy RK, Park C, Handel MA. 1997. Analysis of expression and function of topoisomerase I and II during meiosis in male mice. Mol Reprod Dev 46:489-498.

Disteche CM, Gandy SL, Adler DA. 1987. Translocation and amplification of an X-chromosome DNA repeat in inbred strains of mice. Nucl Acids Res 15:4393-4401.

Eicher EM, Hale DW, Hunt PA, Lee BK, Tucker PK, King TR, Eppig JT, Washburn LL. 1991. The mouse Y* chromosome involves a complex rearrangement, including interstitial positioning of the pseudoautosomal region. Cytogenet Cell Genet 57:221-230.

Hassold T, Sherman S. 2000. Down syndrome: genetic recombination and the origin of the extra chromosome 21. Clin Genet 57:95-100.

Hassold T, Sherman S, Hunt P. 2000. Counting cross-overs: characterizing meiotic recombination in mammals. Hum Mol Genet 9:2409-2419.

Hassold TJ, Sherman SL, Pettay D, Page DC, Jacobs PA. 1991. XY chromosome nondisjunction in man is associated with diminished recombination in the pseudoautosomal region. Am J Hum Genet 49:253-260.

Kallio M, Lahdetie J. 1996. Fragmentation of centromeric DNA and prevention of homologous chromosome separation in male mouse meiosis in vivo by the topoisomerase II inhibitor etoposide. Mutagenesis 11:435-443.

Lahdetie J, Keiski A, Suutari A, Toppari J. 1994. Etoposide (VP-16) is a potent inducer of micronuclei in male rat meiosis: Spermatid micronucleus test and DNA flow cytometry after etoposide treatment. Environ Molec Mutagenesis 24:192-202.

Lamb NE, Feingold E, Savage A, Avramopoulos D, Freeman S, Gu Y, Hallberg A, Hersey J, Karadima G, Pettay D, Saker D, Shen J, Taft L, Mikkelsen M, Petersen MB, Hassold T, Sherman SL. 1997. Characterization of susceptible chiasma configurations that increase the risk for maternal nondisjunction of chromosome 21. Hum Mol Genet 6:1391-1399.

Mailhes JB. 1995. Important biological variables that can influence the degree of chemical-induced aneuploidy in mammalian oocyte and zygotes. Mutat Res 339:155-176.

Marchetti F, Bishop JB, Lowe X, Generoso WM, Hozier J, Wyrobek AJ. 2001. Etoposide induces heritable chromosomal aberrations and aneuploidy during male meiosis in the mouse. Proc Nat Acad Sci Usa 98:3952-3957.

Oakberg EF. 1984. Germ cell toxicity: Significance in genetic and fertility effects of radiation and chemicals. In EHY Chu and WM Generoso (ed): "Mutation, Cancer, and Malformation," New York City: Plenum Publishing Corporation, pp 549-590.

Russell LB, Hunsicker PR, Hack AM, Ashley T. 2000. Effect of the topoisomerase-II inhibitor etoposide on meiotic recombination in male mice. Mutat Res Genet Toxicol E M 464:201-212.

Russell LB, Hunsicker PR, Johnson DK, Shelby MD. 1998. Unlike other chemicals, etoposide (a topoisomerase-II inhibitor) produces peak mutagenicity in primary spermatocytes of the mouse. Mutat Res Fundam Mol Mech Mut 400:279-286.

Savage AR, Petersen MB, Pettay D, Taft L, Allran K, Freeman SB, Karadima G, Avramopoulos D, Torfs C, Mikkelsen M, Hassold TJ, Sherman SL. 1998. Elucidating the mechanisms of paternal non-disjunction of chromosome 21 in humans. Hum Mol Genet 7:1221-1227.

Schmid TE, Xu W, Adler ID. 1999. Detection of aneuploidy by multicolor FISH in mouse sperm after in vivo treatment with acrylamide, colchicine, diazepam or thiabendazole. Mutagenesis 14:173-179.

Shelby MD, Bishop JB, Hughes L, Morris RW, Generoso WM. 2001. in press:

Sjoblom T, Parvinen M, Lahdetie J. 1994. Germ-cell mutagenicity of etoposide: induction of meiotic micronulcei in cultured rat seminiferous tubules. Mutation Res 323:41-45.

Wang JC. 1985. DNA topoisomerases. Ann Rev Biochem 54:665-697.

Yin H, Cukurcam S, Betzendahl I, Adler ID, Eichenlaub-Ritter U. 1998. Trichlorfon exposure, spindle aberrations and nondisjunction in mammalian oocytes. Chromosoma 107:514-522.

PART VII

MUTAGENESIS AND A PHENOTYPE SCREEN FOR GAMETIC ANEUPLOIDY*

*The work for this part was accomplished by efforts of April Pyle, Irina Pinn, Eugene M. Rinchik, and Mary Ann Handel.

CHAPTER I

INTRODUCTION

Current studies of meiosis are hindered by the lack of knowledge about both the genes and the fundamental mechanisms involved in ensuring the fidelity of proper chromosome segregation. The outcome of malsegregation of chromosomes is aneuploidy, the causes of which are still poorly understood. This lack of information is due in part to the fact that not many mutations are known to affect the process of meiosis. It is an understatement to say that in order to study gene function, mutations are needed. For example, *Drosophila* geneticists have used mutants as a major tool to establish how the basic body plan is established (Nusslein-Volhard and Wieschaus, 1980). In this study, chemical mutagenesis produced hundreds of mutant flies with specific phenotypes of interest.

With respect to meiosis, important insights have come from analysis of yeast meiosis mutants. Many of these mutations were identified by screens for spore inviability, where inviability is due to aneuploidy and consequent failure of a spore to germinate (Kleckner, 1996; Lichten and Goldman, 1995; Roeder, 1997). In addition, one study by Chu et. al., 1998, used DNA microarrays with ~6200 protein-encoding genes to look at temporal patterns of gene expression during meiosis and spore formation. Microscopy was used to monitor morphological changes. Changes in mRNA transcripts from each gene were measured at hours 0,.5,2,5,7,9,11 after transfer of diploid cells to a nitrogen-deficient medium that induces sporulation. More than 1000 showed significant

changes in mRNA during sporulation, 1/2 induced,1/2 repressed. Genes were classified into temporal classes based on timepoint of expression (early-middle-mid-late-late). This study provided a wealth of information on sporulation-specific patterns of gene experession.

Studies have also shown the usefulness of mutations in increasing understanding of meiosis in the mouse. In one example, a knockout mutation in the *Mlh1* gene causes sterility and meiotic abnormalities (Baker et al., 1996). In addition, PMS2-deficient males were found to be infertile and this mouse model revealed a role for this protein in mismatch repair, and chromosome synapsis (Baker et al., 1995). However, studies of gametogenesis would be greatly strengthened with more meiosis-specific mutant models. One approach for uncovering new genes in meiosis is through mutagenesis.

Elucidating organismal function of DNA sequence and proteins requires heritable mutations, which can alter the quality and quantity of the protein. Successes over the past ten years have been due, in large part, to systematic identification of genes defined by a mutant allele or by creation of a mutation in a gene of known sequence by embryonic stem (ES)-cell knockout technology. Using embryonic stem cell technology, the function of virtually any gene can be disrupted, as long as information is available for the gene of interest. In most cases, null mutations are created and often result in embryonic lethality. Therefore, it is important that more subtle mutations can also be produced. This is possible through use of *N*-ethyl-*N*-nitrosourea (ENU) where a full range of gene function can be examined. ENU can induce mutations in coding regions or regulatory elements that can yield vastly different phenotypes (Justice et al., 1999). ENU mutagenesis is beneficial because it can be used to obtain a multiallelic series of single

genes to further define function; to dissect biochemical and developmental pathways; to obtain new recessive mutations on a single chromosome or genome-wide; and to saturate regions of the mouse genome that are uncovered by deletions (Justice and Bode, 1986; Kasarskis et al., 1998; Rinchik et al., 1995; Rinchik and Carpenter, 1999).

ENU is a point mutagen. The mechanism of action of ENU is through transfer of its ethyl group to oxygen or nitrogen radicals in DNA, resulting in mispairing and base pair substitution if not repaired. The highest mutation rates occur in pre-meiotic spermatogonial stem cells, with a single gene mutation occurring in one out of every 175-655 gametes screened (Hitotsumachi et al., 1985). ENU primarily modifies A/T base pairs, with 64% being missense mutations, 10% nonsense mutations, and 26% splicing errors (Justice et al., 1999).

There are two approaches for systematic generation of mutation across the mouse genome: genotype-driven and phenotype-driven. Genotype-driven approaches are sequence-driven and usually involve targeted mutations engineered through homologous recombination in embryonic stem cells. However, this does not allow recovery of large numbers of mutations. Gene-trap strategies are an alternative. In this strategy, an appropriate selectable marker construct is introduced into ES cells and large numbers of lines carrying disrupted transcription units can be obtained to maintain an ES cell mutation bank (Evans et al., 1997). One disadvantage is that prior assumptions have to be made about the role and importance of the gene trap sequence. The alternative approach, phenotype-driven, is based on using random mutagenesis systems to derive novel phenotypes to discover new genes and pathways. This is powerful, however, phenotype-driven screens require the application of appropriate screens.

ENU can be used in phenotype-driven screens to detect dominant and recessive mutations. ENU is usually administered intraperitoneally to male inbred mice, acting on spermatogonial stem cells. A variable period of sterility follows (10-15 weeks) while surviving mutagenized stem cell spermatogonia repopulate the testis (Russell et al., 1979). A typical ENU experiment involves mating of ENU-treated males to wild-type females and then scoring of the F1 progeny for dominant or semi-dominant mutations. This is the general scheme used in this study to identify novel genes involved in meiosis. Several groups have recovered dominant mutations in this manner, such as the dominant *Clock* mutation involved in circadian rhythms (King et al., 1997), and several biochemical abnormalities (Peters et al., 1986). Genome-wide recessive screens have also been successfully performed, but this can be time-consuming. For example, recovering recessive-induced mutations involves a minimum of three crosses. However, mouse mutants causing hyperphenylalaninaemia were recovered using a three-generation screen, including mutations in the gene for phenylalanine hydroxylase (Bode et al., 1988; McDonald et al., 1990).

In this chapter, ENU mutagenesis was used in a pilot study to induce mutations in genes whose function is essential in proper chromosome segregation. The phenotype screen consisted of sperm FISH to detect aneuploidy and examination of sperm-head morphology. Sperm FISH is used routinely to assess aneuploidy in humans (Martin et al., 1993; Williams et al., 1993; Spriggs et al., 1995) and mice (Wyrobek et al., 1995; Lowe et al., 1996; Adler et al., 1996). Its success in human clinical assays suggested the technique could be used to detect aneuploid sperm in this mutagenesis project. The payoff for this project could have been extremely high, especially if any newly

discovered mutations could have been maintained and used for functional analysis. However, success of the project depended on the efficacy of the phenotype screen. This was ultimately determined to be neither robust nor practical.

CHAPTER II

MATERIALS AND METHODS

ENU Mutagenesis and Mice

BALB/cByJ males of 10-12 weeks old were mutagenized with a standard dose of ENU (4 weekly doses of 100 mg/kg), and after their return to fertility, were mated to C3Hf/R1 females. Inbred strains were used to establish a baseline frequency of sperm aneuploidy in normal (C3Hf/R1 X BALB/c) F1 males. Additionally, they can be used to map any recovered mutations by standard genome-scanning techniques with simple-sequence length polymorphisms identified between the two parental strains.

Control males were killed by cervical dislocation to obtain sperm. Sperm from G1 males (bearing putative mutations) were obtained by hemicastration, thereby maintaining their ability to mate and pass on any mutations of interest. The G1 males were anesthetized with Avertin and subjected to hemicastration through a 2-5 mm lateral incision made into the scrotal region. The testis, epididymis and a portion of the vas deferens were pulled through the incision hole and clipped. The scrotal skin flaps were then closed with a suture. Testes were placed in fixative for subsequent examination of histology in cases of azoospermia. The epididymis and vas deferens were placed in PBS for removal of adherent fat, then transferred to 500 µl of 2.2% sodium citrate, minced in a 1.5 ml tube and incubated for 5 min. at 32ºC. The supernatant was then collected and stored indefinitely at 4ºC.

Sperm FISH

An aliquot of 5 µl from the sperm suspension was spread onto a slide and dried. The slides were soaked in 10 mM dithithreitol (DTT) on ice for 30 min and placed immediately into 4 mM diiodosalicyclic acid (LIS) for 1 hr. The slides were air dried and dehydrated in ethanol. Slides and probes were denatured at 78°C in formamide, then dehydrated and air-dried. Probes specific for chromosomes 8, X and Y were a generous gift from Dr.Terry Hassold, Case Western University, Cleveland, Ohio. Biotin was used to label 1 µg of the Y probe pERS-532 (Eicher et al., 1991); the Chr. 8 probe, which was a mixture (2 µg total) of four subclones (Boyle and Ward, 1992), was labeled with digoxygenin; and 1 µg of the X chromosome-specific probe DXWas (Disteche et al., 1987) was labeled with both biotin and digoxygenin separately. Probes were labeled using a nick translation kit (Roche Pharmaceutical) and purified over a Sephadex- G50 column. The probe mix was added to each slide; which was then incubated at 37°C overnight. The next day, slides were washed in 50% formamide/2X SSC, in 2X SSC, and then in PN Buffer (0.1M NaH_2PO_4, 0.1M Na_2HPO_4, 0.05% NP-40, pH 8). Slides were incubated in a BSA-blocking buffer and the appropriate fluorochrome-conjugated detector, also in BSA, at 37°C for 30 min, then washed in PN buffer twice. After adding DAPI/Antifade (Molecular Probes), slides were viewed with an Olympus epifluorescent microscope at 100X. Scoring of sperm aneuploidy was by deliberately conservative criteria. Only hyperhaploidy, and not hypohaploidy, was scored; thus the aneuploidy frequency is calculated as twice the hyperhaploidy frequency. Additionally, sperm were deemed suitable for scoring only when the following criteria were met: fluorescent signals were clearly within and not on the edge of the sperm nucleus, fluorescent signals

were all in the same plane of focus, and any two signals scored as separate were separated by a distance equal or greater than one signal domain. 1000 sperm per male were scored for aneuploidy and sperm-head morphology.

CHAPTER III

RESULTS

For control data, seven F1 males from a mating of untreated BALB/cBy males with C3H females were scored to obtain background sperm aneuploidy frequencies (Table 1). The overall frequency of sperm aneuploidy for the F1 control males was 0.17%.

An analysis of sperm aneuploidy was then performed for the F1 progeny (G1) from treated G_0 males in order to detect dominant mutations affecting this phenotype. 25 males were screened by sperm FISH for aneuploidy (Fig. 1). Of these, one male exhibited sperm aneuploidy that was approximately four-fold elevated over control frequencies (Table 2) at 0.8%.

In order to determine if the trait of sperm aneuploidy is transmitted, the F1 (# 13) male was mated to C3H/RI females, and sperm of his sons were scored by FISH. 28 males were scored, and of these, only four (see Table 3) were found to have as high a frequency as the F1 male. Since only 4 out of 28 exhibited increased hyperhaploidy, the trait does not appear to be inherited in a simple mendelian dominant manner and therefore mapping experiments were not performed.

Screening by sperm FISH was found not to be a high-throughput phenotype screen. For example, each FISH screen takes two days to complete if probe hybridization is efficient. However, efficient hybridization and visible probe signal could take several attempts. Scoring 1000 sperm on each slide for aneuploidy also could take 2-5 hours.

Unfortunately, this is not the most efficient phenotype screen. Other screening methods for discovery of meiotic mutations continue to be explored.

Table 1. Frequency of hyperhaploidy in the seven (C3Hf/R1 X BALB/c) F1 males scored. The average frequency of hyperhaploidy was at 0.17 % +/- .08.

Animal ID number	% Hyperhaploidy
401-10.21.99	0.3
403-10.21.99	0.1
404-10.21.99	0.2
405-10.21.99	0.2
409-10.21.99	0.1
410-10.21.99	0.2
411-10.21.99	0.1
Average %	**0.17 +/- .08**

Figure 1. A representative sperm with hyperhaploidy from a son of a G_0 treated male is shown. This sperm is diploid, with an 8,X,X,Y chromosome constitution.

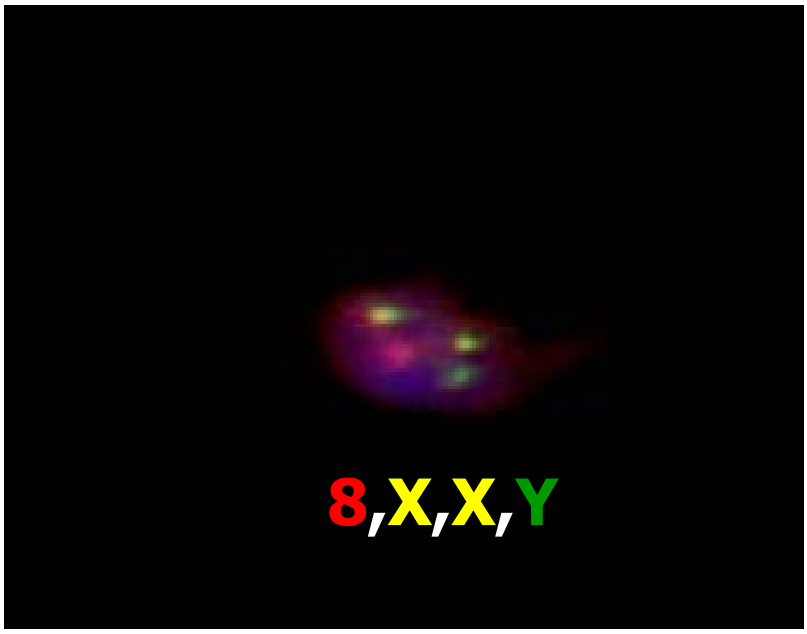

8,X,X,Y

Table 2. Frequency of hyperhaploidy in twenty-five (C3Hf/R1 X BALB/c) F1 sons of G_0 treated males. One male** exhibited a four-fold increase in hyperhaploidy over control, at 0.8%.

F1 ENU	
Animal ID number	% Hyperhaploidy
1-9-11-99	0
3-10-6-99	0.2
4-10-4-99	0.1
5-10-4-99	0.1
6-10-4-99	0.2
7-10-7-99	0.3
8-10-12-99	0.1
10-10-13-99	0.3
11-10-13-99	0.3
12-10-16-99	0.3
13-10-16-99	0.8**
14-10-16-99	0.1
15-10-16-99	0.3
16-10-17-99	0.1
17-10-17-99	0.1
18-10-17-99	0.2
19-10-17-99	0.3
21-10-23-99	0.5
22-10-24-99	0.1
23-10-30-99	0
24-10-30-99	0.2
24-10-30-99	0.2
32-11-16-99	0.1
36-10-24-99	0.1
37-11-23-99	0.1

Table 3. Frequency of hyperhaploid sperm from twenty-eight G2 sons of the one male (#13 from the F1 progeny with an increase in hyperhaploidy of 0.8%). Of the twenty-eight males scored for hyperhaploidy, only four** exhibited hyperhaploidy frequency as high as the F1 (#13).

F2 ENU	
Animal ID number	% Hyperhaploidy
13 MAH 2	0.25
13 MAH 3	0.10
13 MAH 4	0.30
13 MAH 5	0.00
13 MAH 6	0.67
13 MAH 7	0.30
13 MAH 8	0.85**
13 MAH 13	0.30
13 MAH 14	0.30
13 MAH 15	0.70
13 MAH 16	0.20
13 MAH 17	0.30
13 MAH 18	0.30
13 MAH 19	0.00
13 MAH 24	0.20
13 MAH 25	0.80**
13 MAH 26	0.30
13 MAH 27	0.20
13 MAH 28	0.20
13 MAH 29	0.00
13 MAH 34	0.10
13 MAH 165	0.00
13 MAH 166	0.20
13 MAH 167	0.90**
13 MAH 168	1.25**
13 MAH 169	0.30
13 MAH 170	0.30
13 MAH 171	0.30

CHAPTER IV

DISCUSSION

This chapter describes a pilot project to detect new meiotic mutations by screening for dominant mutations causing sperm aneuploidy, assessed by sperm FISH. Studies of meiosis are greatly hindered by lack of meiosis-specific mutations. One approach to obtaining new meiotic mutations is ENU mutagenesis. ENU mutagenesis is valuable because it can induce subtle changes in gene expression in addition to generating nulls. This is important because gene knockouts can often be embryonic lethals. Another relevant aspect is the potential for ENU to induce dominant mutations; especially shape changes in structural proteins due to amino acid substitutions (Justice, 2000). This could help identify proteins involved in meiosis, possibly ones involved in multi-protein complexes. Therefore, ENU mutagenesis is a very promising technique for increasing our understanding of gametogenesis.

What was unique to this project was the screen used to identify new meiotic mutations. Sperm FISH was used to identify gametes with aneuploidy for chromosomes 8,X and Y. We did identify one variant animal with a hyperhaploidy frequency of 0.8% out of 25 males screened. Although this is not an extremely high frequency, it is still possible that following the trait of hyperhaploid sperm could have lead to an important gene whose role in meiosis is not known. With this in mind, the male was bred to determine if the pattern of inheritance could be followed. Unfortunately, there was no clear pattern of dominant inheritance and seemed to rather be inherited in a complex manner. An additional possibility is that there could be a bimodal pattern of inheritance.

Since 6/28 have atleast a .67% of hyperhaploidy or higher, there could be two genes controlling the trait of aneuploidy in the F2 progeny. However, this would need to be further explored with additional F2 progeny.

In addition to the complexity found in the inheritance pattern of the mutant male, what we slowly discovered is that although screening for gametic aneuploidy by sperm FISH is feasible, it is not practical as a primary screen when large numbers of animals are involved. For example, in the entire project period (approximately 1.5 years) only 25 G1 males were able to be scored. In addition, scoring signals by very stringent criteria (see Methods) is also time-consuming.

Since sperm aneuploidy is not a feasible screen for detection of new meiotic mutations, it is important to determine what could be used as an efficient screen. Typically, sterility is detected by failure to breed. This approach could be taken, although it is both costly and time-consuming not to mention the fact that dominant sterility models could not be maintained. More appropriate screens may be to look for indicators of infertility, such as reduced testis weight (size), sperm-head morphology, and sperm count. This is a rapid approach that could lead to meiosis-specific genes. In addition, sectioned testis can be examined for missing cell types or abnormalities during spermatogenesis. However, this method would likely not detect small increases in aneuploidy as has been seen in sperm FISH analysis of hyperhaploidy. Other types of screens that might not initially be apparent, would be to monitor biochemical and enzyme levels in the G1 males to look for abnormalities during spermatogenesis. Although this screen has not been performed in germ cells, mutagenized mice have been analyzed

successfully for changes in activity of several metabolic enzymes (ex. LDH, GP-6-DH) in the blood (Charles and Pretsch, 1987).

Another approach would be to mutagenize embryonic stem (ES) cells. Breeding schemes, such as the one used in this project can be time consuming. The capacity to induce, characterize, and maintain mutations in cell culture of ES cells circumvents many of the problems of whole-animal mutagenesis (Chen et al., 2000b). Another advantage of ES cell mutagenesis is the ability to conduct screens directly in ES cells (Chen et al., 2000a). For example, genotype screens can be performed by examining the mutation frequency and spectrum at several different loci. Mutagenizing EG (embryonic germ) cells may also prove beneficial in screening for meiotic mutations. Sensitized screens, such as screens for UV-sensitive mutations have also been used successfully to detect DNA damage repair genes (Busch et al., 1989). Therefore, sensitized screens may also be a possibility for detecting meiosis-specific mutations. However using ES cells in a gene-driven approach would only give information about previously known genes, and therefore may not be useful in finding new meiotic genes.

In addition to ENU screens, bioinformatic approaches for identification of genes can also be used. Yeast and *Drosophila* screens have been used to identify new genes (Nusslein-Volhard and Wieschaus, 1980; Kleckner, 1996; Lichten and Goldman, 1995; Roeder, 1997), and it is now possible to search for homologues in higher eukaryotes. One approach can be through microarray analysis of genes expressed during meiosis. For example, one study used DNA microarrays with ~6200 protein-encoding genes to look at temporal patterns of gene expression during meiosis and spore formation (Chu et.al., 1998). This is a rapid approach for finding homologues, but will often not lead to new

genes. Another option is through enhancer-, gene- and promoter-trap screens. Gene-trap screens can be used in large-scale mutagenesis, by primarily disrupting an endogenous coding sequence but often can lead to unpredictable phenotypes (Stanford et al., 2001). In addition, the success has been limited by the appropriate vector design to use for gene-trap insertions and also the appropriate phenotype screen.

The appropriate screen for meiotic mutants is still needed. Therefore, new phenotype or genotype screens that are rapid and reliable still need to be developed for discovering new genes in the mouse. The combination of ENU or other mutagenesis strategies, with the appropriate screen will be a very powerful tool for the study of gametogenesis. Further advancements in mutagenesis and genomic-based approaches may lead to new insights into gene discovery, and greatly strengthen our understanding of factors associated with abnormal meiosis leading to nondisjunction.

LIST OF REFERENCES

Adler ID, Bishop J, Lowe X, Schmid TE, Schriever-Schwemmer G, Xu W, Wyrobek AJ. 1996. Spontaneous rates of sex chromosomal aneuploidies in sperm and offspring of mice: A validation of the detection of aneuploid sperm by fluorescence in situ hybridization. Mutat Res Fundam Mol Mech Mut 372:259-268.

Baker SM, Bronner CE, Zhang L, Plug AW, Robatzek M, Warren G, Elliott EA, Yu JA, Ashley T, Arnheim N, Flavell RA, Liskay RM. 1995. Male mice defective in the DNA mismatch repair gene *PMS2* exhibit abnormal chromosome synapsis in meiosis. Cell 82:309-319.

Baker SM, Plug AW, Prolla TA, Bronner CE, Harris AC, Yao X, Christie DM, Monell C, Arnheim N, Bradley A, Ashley T, Liskay RM. 1996. Involvement of mouse *Mlh1* in DNA mismatch repair and meiotic crossing over. Nat Genet 13:336-342.

Bode VC, McDonald JD, Guenet JL, Simon D. 1988. hph-1: a mouse mutant with hereditary hyperphenylalaninemia induced by ethylnitrosourea mutagenesis. Genetics 118:299-305.

Boyle AL, Ward DC. 1992. Isolation and initial characterization of a large repeat sequence element specific to mouse chromosome 8. Genomics 12:517-525.

Brown SDM, Nolan PM. 1998. Mouse mutagenesis - systematic studies of mammalian gene function. Hum Mol Genet 7:1627-1633.

Busch D, Greiner C, Lewis K, Ford R, Adair G. 1989. Summary of complementation groups of UV-sensitive CHO cell mutants isolated by large-scale screening. Mutagenesis 4:349-354.

Charles DJ, Pretsch W. 1987. Linear dose-relationship of erythrocyte enzyme-activity mutations in offspring of ethylnitrosourea-treated mice. Mutat Res 176:81-91.

Chen YJ, Schimenti J, Magnuson T. 2000a. Toward the yeastification of mouse genetics: chemical mutagenesis of embryonic stem cells. Mamm Genome 11:598-602.

Chen YJ, Yee D, Dains K, Chatterjee A, Cavalcoli J, Schneider E, Om J, Woychik RP, Magnuson T. 2000b. Genotype-based screen for ENU-induced mutations in mouse embryonic stem cells. Nat Genet 24:314-317.

Chu S, DeRisi J, Eisen M, Mulholland J, Botstein D, Brown PO, Herskowitz I. 1998. The transcriptional program of sporulation in budding yeast. Science 282 (5393):699-705.

Disteche CM, Gandy SL, Adler DA. 1987. Translocation and amplification of an X-chromosome DNA repeat in inbred strains of mice. Nucl Acids Res 15:4393-4401.

Eicher EM, Hale DW, Hunt PA, Lee BK, Tucker PK, King TR, Eppig JT, Washburn LL. 1991. The mouse Y* chromosome involves a complex rearrangement, including interstitial positioning of the pseudoautosomal region. Cytogenet Cell Genet 57:221-230.

Evans MJ, Carlton MBL, Russ AP. 1997. Gene trapping and functional genomics. Trends Genet 13:370-374.

Hitotsumachi S, Carpenter DA, Russell WL. 1985. Dose-repetition increases the mutagenic effectiveness of N-ethyl-N-nitrosourea in mouse spermatogonia. Proceedings of the National Academy of Science USA 82:6619-6621.

Justice MJ. 2000. Capitalizing on large-scale mouse mutagenesis screens. Nat Rev Genet 1:109-115.

Justice MJ, Bode VC. 1986. Induction of new mutations in a mouse t-haplotype using ethylnitrosourea mutagenesis. Genet Res 47:187-192.

Justice MJ, Noveroske JK, Weber JS, Zheng BH, Bradley A. 1999. Mouse ENU mutagenesis. Hum Mol Genet 8:1955-1963.

Kasarskis A, Manova K, Anderson KV. 1998. A phenotype-based screen for embryonic lethal mutations in the mouse. Proc Natl Acad Sci USA 95:7485-7490.

King DP, Zhao Y, Sangoram AM, Wilsbacher LD, Tanaka M, Antoch MP, Steeves TDL, Vitaterna MH, Kornhauser JM, Lowery PL, Turek FW, Takahashi JS. 1997. Positional cloning of the mouse circadian Clock gene. Cell 89:641-653.

Kleckner N. 1996. Meiosis: how could it work? Proc Natl Acad Sci USA 93:8167-8174.

Lichten M, Goldman ASH. 1995. Meiotic recombination hotspots. Annu Rev Genet 29:423-444.

Lowe X, O'Hogan S, Moore D, Bishop J, Wyrobek A. 1996. Aneuploid epididymal sperm detected in chromosomally normal and Robertsonian translocation-bearing mice using a new three-chromosome FISH method. Chromosoma 105:204-210.

Martin RH, Ko E, Chan K. 1993. Detection of aneuploidy in human interphase spermatozoa by fluorescence *in situ* hybridization (FISH). Cytogenet Cell Genet 64:23-26.

McDonald JD, Bode VC, Dove WF, Shedlovsky A. 1990. Pahhph-5: a mouse mutant deficient in phenylalanine hydroxylase. Proceedings of the National Academy of Science USA 87:1965-1967.

Nusslein-Volhard C, Wieschaus E. 1980. Mutations affecting segment number and polarity in Drosophila. Nature 287:795-801.

Peters J, Ball ST, Andrews SJ. 1986. The detection of mutations by electrophoresis and their analysis. In C Ramel, B Lambert and J Magnusson (ed): "Genetic Toxicology of Environmental Chemicals, Part B: Genetic Effects and Applied Mutagenesis," New York: A.R. Liss, pp 367-374.

Rinchik EM, Carpenter DA. 1999. N-ethyl-N-nitrosourea mutagenesis of a 6- to 11-cM subregion of the Fah-Hbb interval of mouse chromosome 7: completed testing of 4.557 gametes and deletion mapping and complementation analysis of 31 mutations. Genetics 152:373-382.

Rinchik EM, Carpenter DA, Handel MA. 1995. Pleiotropy in microdeletion syndromes: Neurologic and spermatogenic abnormalities in mice homozygous for the p^{6H} deletion are likely due to dysfunction of a single gene. Proc Natl Acad Sci USA 92:6394-6398.

Roeder GS. 1997. Meiotic chromosomes: it takes two to tango. Gene Develop 11:2600-2621.

Russell LB, Kelly EM, Hunsicker PR, Bangham JW, Maddux SC, Phipps EL. 1979. Specific-locus test shows ethylnitrosourea to be the most potent mutagen in the mouse. PNAS 76 (11):5818-9.

Spriggs EL, Rademaker AW, Martin RH. 1995. Aneuploidy in human sperm: results of two- and three-color fluorescence in situ hybridization using centromeric probes for chromosomes 1, 12, 15, 18, X, and Y. Cytogenet Cell Genet 71:47-53.

Stanford WL, Cohn JB, Sabine PC. 2001. Gene-trap mutagenesis: past, present, and beyond. Nat Rev Genet 2:756-768.

Williams BJ, Ballenger CA, Malter HE, Bishop F, Tucker M, Zwingman TA, Hassold TJ. 1993. Non-disjunction in human sperm: Results of fluorescence *in situ* hybridization studies using two and three probes. Hum Mol Genet 11:1929-1936.

Wyrobek A, Lowe X, Pinkel D, Bishop J. 1995. Aneuploidy in late-step spermatids of mice detected by two-chromosome fluorescence in situ hybridization. Mol Reprod Dev 40:259-266.

PART VIII

CONCLUSION

CHAPTER I

SUMMARY

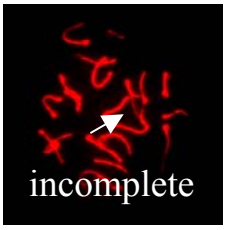
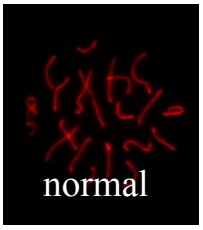
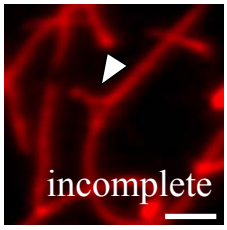
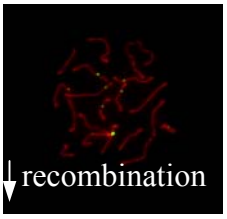
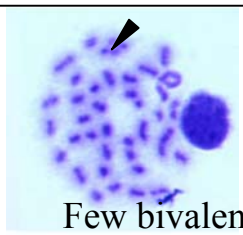
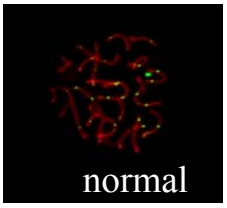
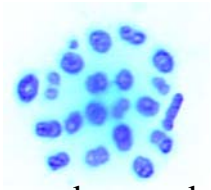
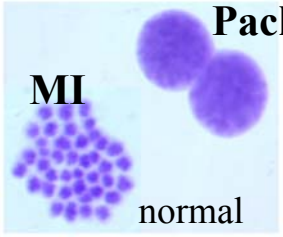
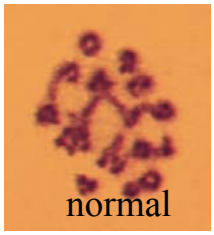
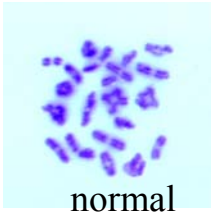
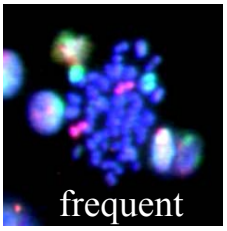
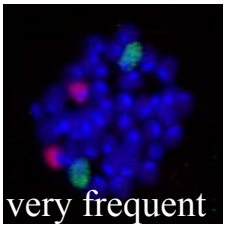
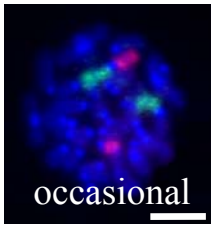
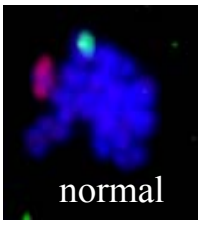
Meiotic progress in genetic models associated with aneuploidy has been the main focus of the research in this dissertation. Although several mouse models have been analyzed, many questions remain; thus it cannot be stated strongly enough that more genetic models are needed! Research reported here on four mouse models, has shown that, while there is no one outstanding feature that may lead to production of aneuploid conceptuses, several characteristics are shared among the models (Fig. 1). The next few sections will compare these models around a framework of meiotic events, pointing out common and disparate features. There will then be a discussion on what I think the next research directions should be in order to promote further understanding of what causes meiotic processes to go awry, leading to aneuploidy.

Prophase of meiosis: the role of pairing and recombination

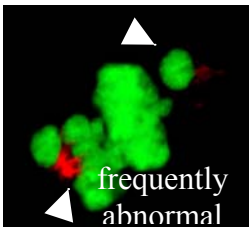
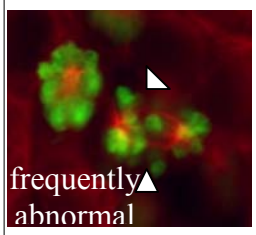
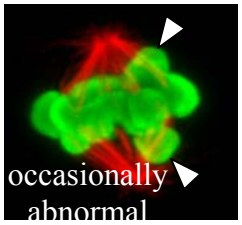
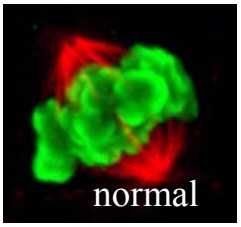
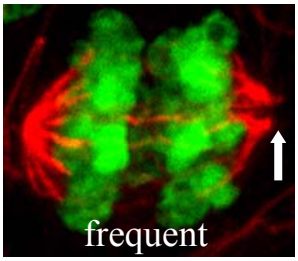
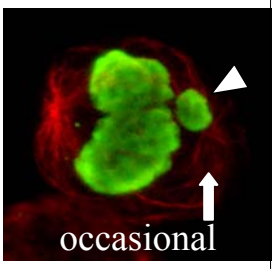
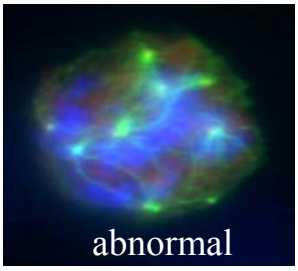
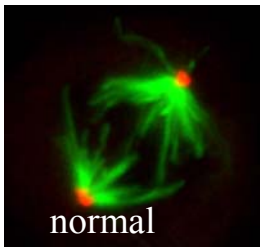
One of the most lengthy and significant stages of meiosis is prophase of meiosis I. Recombination is initiated during prophase, and is thought to be mediated by a cohort of proteins that accumulate at the site of recombination in the recombination nodule. The events of recombination occur within the framework of a proteinaceous structure known as the synaptonemal complex (SC). Studies of mammalian meiosis have been informed by recent advances in understanding yeast meiosis. Examples include analysis of

Figure 1. Comparison of each mouse model (PL/J, Mlh1 $^{-/-}$, Rb/+, and Wild type (B6)), for abnormalities in prophase, metaphase and arrest. Abnormal characteristics shared in at least three models are indicated (***).

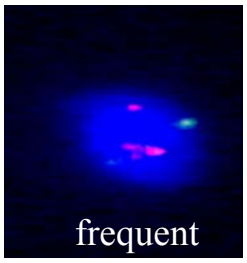
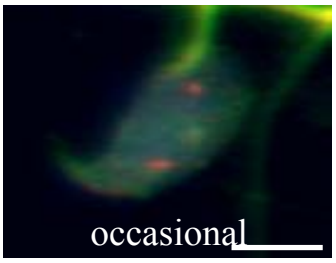
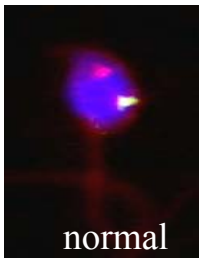
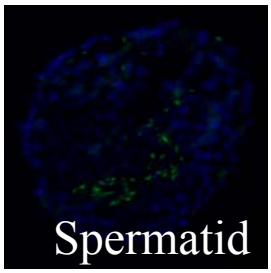
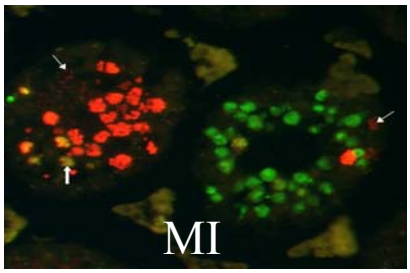
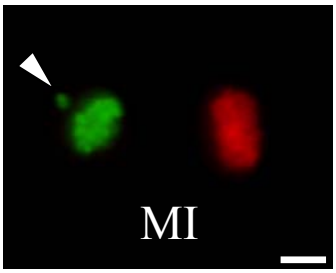
Prophase and Metaphase Comparisons in Each Model

	PL/J	*Mlh1* $^{-/-}$	Rb/+	Wild type B6
Synapsis	 incomplete	 normal	 incomplete	 normal
Recombination ***	 recombination	 Few bivalents	recomb. near centromeric ends??	 normal
Chromosome Condensation	 abnormal	 Pach MI normal	 normal	 normal
Univalents ***	 frequent	 very frequent	 occasional	 normal

Chromosome and Spindle-Associated Abnormalites

	PL/J	*Mlh1* $^{-/-}$	Rb/+	Wild type B6
Chromosome Alignment ***				
Spindle Abnormalities		Normal Spindles		Normal Spindles
Abnormal Centrosome #'s		Normal: 2 Centrosomes	Normal: 2 Centrosomes	

Comparison of Aneuploidy or Arrest in Each Model

	PL/J	*Mlh1* $^{-/-}$	Rb/+	Wild type B6
Sperm Aneuploidy		No sperm		
Apoptosis ***				normal
Stage of Arrest	No Arrest	Metaphase I	No Arrest	No

recombination outcomes by tetrad analysis and recombination hotspots as target sites for proteins of interest (Paques and Haber, 1999; Zickler and Kleckner, 1999). These studies have revealed that formation and processing of double-strand breaks (DSBs) and Holliday junction intermediates in *S. cerevisiae* requires the products of at least eleven different genes, including SPO11, MEI3, MER2, RAD50, MRE11, REC102, REC104, and XRS2. Moreover, in yeast, the formation of the SC is also dependent on recombination, unlike *Drosophila* and *C.elegans*, in which SC formation appears to precede recombination events (McKim et al., 1998; Page and Hawley, 2001; Dernberg et al., 1998) and to be required for recombination. In contrast, meiosis in *Schizosaccharomyces pombe* occurs in the absence of the SC (Kohli and Bahler, 1994).

Recombination in mammals has been studied primarily by a select few mutants whose phenotypes exhibit meiosis I defects. Examples include mouse knockouts of *Dmc1*, *Spo11*, *Msh4*, *Msh5*, *Mlh1*, and *Pms2*. MSH4, MSH5, SPO11 and DMC1 appear to function prior to synapsis, in leptonema and zygonema, while PMS2 and MLH1 are involved in post-synaptic functions at pachynema and beyond (Cohen and Pollard, 2001). Therefore it is important to underrstand, which proteins are involved prior to synapsis and which ones are required for proper metaphase entry. Studies in this dissertation have helped to dissect further the consequences of absence of two proteins during meiosis, MLH1 and BRCA2. Absence of the *Mlh1* gene causes univalence and sterility in both males and females (Baker et al., 1996; Woods et al., 1999). As shown in Part IV, although homologous chromosomes are univalent and not spatially near one another during the metaphase transition, MLH1-deficient spermatocytes condense chromosomes, form bipolar spindles, and undergo synaptonemal complex breakdown, all events

indicative of metaphase entry. Therefore, we have learned that MLH1 is not required for spermatocytes to enter metaphase, although they are arrested shortly thereafter.

BRCA2 is another protein whose presence is required for completion of meiosis. Homozygous *Brca2* $^{-/-}$ mice die as embryos (Conner et al., 1997). In a recent study, the embryonic lethality was rescued by using a bacterial artificial chromosomal (BAC) containing the human *BRCA2* gene. Only 0.5% of the spermatocytes in the transgene-rescued *Brca2* knockout progress to early-pachytene stage, and none of these were positive for histone H1t, a marker for mid-pachytene. Additionally, the number of RAD51 foci localized to the chromatin was drastically reduced in rescued spermatocytes compared to wild-type. Therefore, we have shown that BRCA2 is required for transition into pachytene and also may play a role in RAD51 localization or function. Many questions still remain in this study, which has not yet clarified the role BRCA2 plays in meiosis nor the nature of the requirement for BRCA2 in RAD51 localization.

The PL/J and Rb/+ mouse models have also increased our understanding of what processes during prophase are important for proper chromosome segregation. In PL/J mice, both asynapsis, decreased recombination and defects in condensation occur (Part II). Pairing abnormalities were also seen in Rb pachytene spermatocytes as shown by staining with SYCP3 (Part III-A). Previous studies have shown that there is reduced recombination near the centromeric ends in Rb/+ homologous chromosomes (Davisson and Akeson, 1993). The MLH1 protein has a role in recombination and DNA repair, and loss of the protein causes almost complete elimination of crossover as detected by chiasmata. Therefore in PL/J, Rb/+, and *Mlh1* $^{-/-}$ models, decreased recombination or proper resolution of recombination could be a factor associated with causing gamete

aneuploidy. Supporting evidence comes from PL/J mice that have decreased recombination, and possibly Rb/+ near centromeric ends, as well as loss of proper chiasmata formation in *Mlh1* $^{-/-}$ mice. Therefore, loss of chiasmata could cause some of the downstream abnormalities seen in these models, such as univalents and failure to align properly at the metaphase plate.

Pairing abnormalities in both Rb/+ and PL/J models could be a factor associated with decreased recombination. In each of these studies, regions of the SC were shown not to pair correctly, and perhaps there could be decreased recombination in these regions of abnormal pairing in both Rb/+ and PL/J. However, we have shown that the SC is formed correctly during pachytene in *Mlh1* $^{-/-}$ mice. Since SC formation is normal in *Mlh1* $^{-/-}$ mice, this suggests that SC formation is independent of MLH1 and possibly MLH1-mediated recombination, but not necessarily of other steps. However, incomplete or delayed synapsis in Rb/+ and PL/J could be a predisposing factor for the reduction in recombination seen.

Metaphase: entry and alignment of chromosomes

One of the most fundamental questions about meiosis, is what are the requirements for metaphase entry and exit. Studies in this dissertation have shown that even spermatocytes with altered chromosome states are capable of undergoing metaphase entry. After treatment with okadaic acid, PL/J spermatocytes do not fully condense chromosomes in a normal MI configuration. MI chromosomes are condensed in Rb/+ spermatocytes, but abnormal pairing configurations are seen due to the heterozygous translocations. In the *Mlh1* $^{-/-}$ mouse, chromosomes are condensed, but 90% are

univalents. Nonetheless, in each of these models (Rb/+, PL/J, and *Mlh1* $^{-/-}$), entry into metaphase occurs. Therefore, it does not appear that any of the abnormal chromosome configurations or ability to condense is an inhibitory factor in metaphase entry. However, once metaphase entry is reached, chromosomes in each model are not able to properly align at the spindle equator. In Fig. 1 there is an example in each model of unaligned chromosomes. Therefore, although entry is possible, proper exit into anaphase may not occur (discussed in next section).

Univalents are seen in PL/J, Rb/+, and MLH1. An important unanswered question is what causes the univalence in each model. This could be due to the reduction in recombination and proper chiasmata formation. The absence of chiasmata that hold homologous chromosomes together until proper orientation is achieved could cause the bivalents to fall apart. In the case of the Rb/+ model, this could stem from incomplete pairing due to the presence of the translocations.

It is also interesting, that in the BRCA2 mouse model, metaphase entry does not occur. Why is elimination of BRCA2 so detrimental? One explanation could be that BRCA2 is involved in one of the first processes of meiosis, perhaps processing of double-strand breaks. Therefore, spermatocytes may not be able to complete any of the requirements for metaphase entry, such as pairing, recombination, and chromosome condensation, without proper formation or resolution of double-strand breaks.

Spindle-associated abnormalities and progress into anaphase

To achieve accurate chromosome segregation, alignment of chromosomes on the metaphase plate, midway between the two spindle poles, must occur. In many cells, a

protective mechanism, known as the spindle checkpoint, inhibits entry into anaphase when chromosome alignment failure is detected (Gorbsky, 1995; Rudner and Murray, 1996; Nicklas et al., 1995). However some evidence contradicts the notion of a spindle assembly checkpoint in *Drosophila*. Analysis of mutants like *mei-S332* and *ord,* show that even in the face of precocious separation of sister chromatids, there is no inhibition of meiosis II progression (Goldstein, 1980). Studies have also shown that meiosis in *Drosophila* can be completed even in the presence of univalent chromosomes that rarely attain proper bi-oriented confirmation at the metaphase plate and that XY pairing failure does not prevent anaphase in *Drosophila* (Ashburner, 1989). However, more recent evidence suggests that a relatively high number of misaligned chromosomes, or a severe disruption of the meiotic spindle, results in significant delay in the time of entry into anaphase (Rebollo and Gonzalez, 2000). Therefore, more studies are needed to determine if a spindle assembly checkpoint mechanism exits, and if so, what is the mechanism of recognition of unaligned chromosomes during meiosis.

Genetic models studied in this dissertation provide some observations about a possible spindle checkpoint function in mammalian meiosis. Our observations on the Rb/+ and *Mlh1* $^{-/-}$ models suggest evidence of a checkpoint, possibly spindle assembly, that detects chromosomal misalignment and eliminates spermatocytes. However, even in the face of complexity and many abnormalities of spermatocytes, elimination of MI spermatocytes in PL/J does not occur. Does this mean there is a "faulty" checkpoint during spermatogenesis? Perhaps PL/J mice have a mutation in a protein involved in the checkpoint pathway. Furthermore, even though faulty Rb/+ spermatocytes undergo apoptosis, aneuploid sperm are still produced. Why? Is the checkpoint not efficient? Is

it not operational at all in PL/J? One method for answering these questions is to look for mutations in genes in PL/J that could lead to loss of checkpoint function. In addition, microarray analysis could be performed to determine if there are any abnormalities in gene expression that could contribute to the phenotypic and genetic complexity seen in PL/J males.

In addition to illuminating the complexity of checkpoints, studies in this dissertation have shown abnormal spindle formation in two mouse models for aneuploidy, PL/J and Rb/+. PL/J MI spermatocytes also have centrosomal abnormalities. It is possible that both the increased numbers of pericentrin foci and abnormal spindles could be associated with abnormal chromosome segregation. However, neither abnormal spindles nor centrosome numbers were seen in the *Mlh1* $^{-/-}$ mice. It is not well understood whether increased centrosome and abnormal spindles are a downstream consequence of unaligned chromosomes or if they are somehow a causative factor associated with aneuploidy.

Summary of mouse models for aneuploidy

From these studies is clear that no one factor is associated with aneuploidy, however several features are shared among the models, suggesting these factors could put cells at risk for nondisjunction (see Fig. 1). These include abnormal recombination, the presence of univalents and unaligned chromosomes. Apoptosis also appears to be a common downstream consequence. It has also been shown that loss of a critical protein, such as MLH1 or BRCA2, causes the most severe phenotype, arrest during meiosis.

More subtle mutations (in PL/J) or pairing abnormalities (in Rb/+) are not as detrimental and allow for progression through meiosis and production of aneuploid sperm.

Chemically-induced mouse models for aneuploidy

A different approach to study aneuploidy is to use chemicals that may cause chromosome malsegregation. In Part VI, the topoisomerase-II inhibitor, etoposide was chosen because previous results had shown a peak mutagenicity of etoposide during prophase of meiosis (Russell et al., 1998) as well as a decrease in recombination after treatment (Russell et al., 2000). Sperm FISH analysis showed that etoposide induces meiotic nondisjunction as well. However, MII, not MI, nondisjunction contributed most significantly to the aneuploidy. This was surprising since a function of topoisomerase-II is to untangle chromosomes prior to MI. Several questions still need to be explored. How does etoposide induce MII nondisjunction? Is sister chromatid cohesion affected? Thus studies of the mechanisms of chemically-induced aneuploidy could shed light on how nondisjunction arises.

What else can we do to explore mechanisms associated with nondisjunction?

An important resource for studying causes of aneuploidy would be new meiotic mutations causing gamete aneuploidy. Experiments in Part VII used ENU mutagenesis and a FISH-based phenotype screen to identify new meiosis-specific genes. Although, one male with a 4-fold increase in sperm aneuploidy was found, his phenotype was not inherited in a simple manner. A major problem with this mutagenesis approach was that the FISH screen used was extraordinarily time-consuming. Therefore, a more rapid

screen needs to be developed if detection of new meiotic genes is to become feasible. One possibility that we have considered is flow cytometry, or FACS sorting, of sperm to detect aneuploidy (Weissenberg et al., 1998; Baumgartner et al., 2001). One drawback with FACS sorting, is the possibility that the hyperhaploid population could not be detected efficiently. This would need to be validated using mouse models for aneuploidy, such as the ones in this dissertation. Instead of aneuploidy screens, it is also possible to screen for infertility by examining testes size and sperm count. Although in the infertility screens, the frequency of attaining a mutation that causes aneuploidy is lower, it is a much more feasible screen than sperm FISH. Therefore, it will continue to be a challenge to locate genes whose function is required for proper meiotic progression.

Conclusions

It is clear that the rules of proper meiotic chromosome segregation are just beginning to be revealed. Probably, many more meiotic mutations will be needed before we can determine specifically which factors are required for accurate chromosome segregation. The mouse models studied in this dissertation have revealed several factors associated with risk for production of aneuploid sperm. The challenge now remains to determine, both why some cells are caught and why other abnormal meiotic cells progress through divisions to produce aneuploid gametes. This will be essential to our understanding of how to prevent aneuploidy and associated birth defects.

LIST OF REFERENCES

Baker SM, Plug AW, Prolla TA, Bronner CE, Harris AC, Yao X, Christie DM, Monell C, Arnheim N, Bradley A, Ashley T, Liskay RM. 1996. Involvement of mouse *Mlh1* in DNA mismatch repair and meiotic crossing over. Nat Genet 13:336-342.

Baumgartner A, Schmid TE, Maerz HK, Adler ID, Tarnok A, Nuesse M. 2001. Automated evaluation of frequencies of aneuploid sperm by laser-scanning cytometry (LSC). Cytometry 44:156-60.

Cohen P, Pollard JW. 2001. Regulation of meiotic recombination and prophase I progression in mammals. BioEssays In press:

Conner F, Bertwistle D, Mee PJ, Ross GM, Swift S, Grigorieva E, Tybulewicz VL, Ashworth A. 1997. Tumorigenesis and a DNA repair defect in mice with a truncating Brca2 mutation. Nat Genet 17:423-30.

Davisson MT, Akeson EC. 1993. Recombination suppression by heterozygous Robertsonian chromosomes in the mouse. Genetics 133:649-667.

Dernburg AF, McDonald K, Moulder G, Barstead R, Dresser M, Villeneuve AM. Meiotic recombination in C.elegans initiates by a conserved mechanism and is dispensable for homologous chromosome synapsis. Cell 94(3):387-98.

Goldstein LSB. 1980. Mechanisms of chromosome orientation revealed by two meiotic mutants in *Drosophila melanogaster*. Chromosoma 78:79-111.

Gorbsky GJ. 1995. Kinetochores, microtubules and the metaphase checkpoint. Tr Cell Biol 5:143-148.

Kohli J, Bahler J. 1994. Homologous recombination in fission yeast: absence of crossover interference and synaptonemal complex. Experientia 50:295-306.

McKim KS, Green-Marroquin BL, Sekelsky JJ, Chin G, Steinberg C, Khodosh R, Hawley RS. 1998. Meiotic synapsis in the absence of recombination. Science 279:876-878.

Nicklas RB, Ward SC, Gorbsky GJ. 1995. Kinetochore chemistry is sensitive to tension and may link mitotic forces to a cell cycle checkpoint. J Cell Biol 130:929-939.

Page SL and Hawley RS. c(3)G encodes a Drosophila synaptonemal complex protein. Genes Dev 15(23):3130-43.

Paques F, Haber JE. 1999. Multiple pathways of recombination induced by double-strand breaks in *Saccharomyces cerevisiae*. Microbiol Mol Biol Rev 63:349+.

Rebollo E, Gonzalez C. 2000. Visualizing the spindle checkpoint in *Drosophila* spermatocytes. Embo Rep 1:65-70.

Rudner AD, Murray AW. 1996. The spindle assembly checkpoint. Curr Opin Cell Biol 8:773-780.

Russell LB, Hunsicker PR, Hack AM, Ashley T. 2000. Effect of the topoisomerase-II inhibitor etoposide on meiotic recombination in male mice. Mutat Res Genet Toxicol E M 464:201-212.

Russell LB, Hunsicker PR, Johnson DK, Shelby MD. 1998. Unlike other chemicals, etoposide (a topoisomerase-II inhibitor) produces peak mutagenicity in primary spermatocytes of the mouse. Mutat Res Fundam Mol Mech Mut 400:279-286.

Tsuzuki T, Fujii Y, Sakumi K, Tominaga Y, Nakao K, Sekiguchi M, Matsushiro A, Yoshimura Y, Morita T. 1996. Targeted disruption of the Rad51 gene leads to lethality in embryonic mice. Proc Natl Acad Sci USA 93:6236-6240.

Weissenberg R, Aviram A, Golan R, Lewin LM, Levron J, Madgar I, Dor J, Barkai G, Goldman B. 1998. Concurrent use of flow cytometry and fluorescence in-situ hybridization techniques for detecting faulty meiosis in a human sperm sample. Mol Hum Reprod 4:61-66.

Woods LM, Hodges CA, Baart E, Baker SM, Liskay M, Hunt PA. 1999. Chromosomal influence on meiotic spindle assembly: Abnormal meiosis I in female *Mlh1* mutant mice. J Cell Biol 145:1395-1406.

Zickler D, Kleckner N. 1999. Meiotic chromosomes: Integrating structure and function. Annu Rev Genet 33:603-754.

VITA

April Dawn Pyle was born on September 14th, 1974 in Memphis, Tennessee. She attended Bartlett High School in Memphis and graduated in 1992. She received her Bachelors of Science degree in Biology in 1996. As an undergraduate, she worked in several laboratories including Dr. Don Dougall at the University of Tennessee, Dr. Kevin Jones at the University of Colorado, and was first introduced to aspects of reproductive biology and cell cycle analysis from Dr. Pam McKenzie and Dr. Jay Wimalasena at the University of Tennessee Medical Center. After graduating in 1996, she worked for Genetic Systems Corporation in Seattle, Washington. In 1997, she became a graduate student in the Department of Biochemistry, Cellular and Molecular Biology at the University of Tennessee. There she joined the laboratory of Dr. Mary Ann Handel and received her Ph.D. degree in Biochemistry, Cellular and Molecular Biology in 2002.